THÈSE DE DOCTORAT DE L'ÉTABLISSEMENT UNIVERSITÉ BOURGOGNE FRANCHE-COMTÉ

PRÉPARÉE AU LABORATOIRE INTERDISCIPLINAIRE CARNOT DE BOURGOGNE

École doctorale n°553

Carnot Pasteur

Doctorat de Physique

Par

M. Maxime Federico

Spatio-temporal description of single photons: from cavity production to local detection

Thèse présentée et soutenue, le 23 Janvier 2024, à Dijon, France, en salle D115

Composition du Jury :

M. Gérard COLAS DES FRANCS	Professeur, Laboratoire ICB, Université de Bourgogne, France	Président
M. Stéphan DE BIÈVRE	Professeur, Laboratoire Paul Painlevé, Université de Lille, France	Rapporteur
Mme. Pérola MILMAN	Directrice de Recherche, Laboratoire MPQ, Université Paris cité, France	Rapporteure
M. Claude FABRE	Professeur Émérite, Laboratoire Kastler Brossel, Sorbonne Université, France	Examinateur
M. Axel KUHN	Professor, Clarendon Laboratory, University of Oxford, United Kingdom	Examinateur
M. Dominique SUGNY	Professeur, Laboratoire ICB, Université de Bourgogne, France	Examinateur
M. Stéphane GUÉRIN	Professeur, Laboratoire ICB, Université de Bourgogne, France	Invité
M. Hans-Rudolf JAUSLIN	Professeur, Laboratoire ICB, Université de Bourgogne, France	Directeur de thèse
M. Jonas LAMPART	Chargé de Recherche, Laboratoire ICB, Université de Bourgogne, France	Codirecteur de thèse

ECOLE DOCTORALE
CARNOT - PASTEUR

Titre : Description spatio-temporelle de photons uniques : de la production en cavité à la détection locale

Mots clés : photons uniques, propriétés spatio-temporelles, localisation de photons, représentations positions de Białynicki-Birula et Landau-Peierls, émission spontanée d'atomes d'Hydrogène, production adiabatique de photons uniques, modes quasinormaux

Résumé : Ce travail fournit une analyse des propriétés spatio-temporelles d'états à un photon. En commençant par une quantification directement réalisée en espace position, nous démontrons que deux formulations différentes de la théorie sont équivalentes : elles prédisent les mêmes résultats. L'équivalence est formulée sous forme d'un isomorphisme de leurs espaces de Hilbert respectifs. On utilise par la suite cette construction en espace position pour étudier la propagation des photons décrits par des impulsions. Nous démontrons que la dynamique de n'importe quel état du champ électromagnétique quantique est alors donnée par l'évolution temporelle de la représentation de l'état, telle que décrite par les équations de Maxwell classiques. Nous construisons également un modèle de détection locale de photons en utilisant l'opérateur densité d'énergie. Ce modèle nous permet de démontrer la non-localité de tout état à un photon grâce à la propriété d'anti-localité de l'opérateur fréquence $\Omega = c(-\Delta)^{1/2}$. Nous caractérisons ensuite cette non-localité pour un état à un photon produit par l'émission spontanée d'un atome d'Hydrogène et montrons que la décroissance de sa densité d'énergie se comporte asymptotiquement comme $1/r^6$ pour des distances r loin de l'atome. Enfin, nous nous intéressons à la production de photons en cavités pour laquelle nous démontrons au travers d'un argument topologique que, dans la limite adiabatique, l'approximation de l'onde tournante (rotating wave approximation) est justifiée et permet donc la production de photons très proches de photons uniques parfaits. Nous construisons aussi, comme résultat préliminaire, un modèle heuristique utilisant des modes quasinormaux pour décrire la production de photons dans des cavités ouvertes.

Title: Spatio-temporal description of single photons: from cavity production to local detection

Keywords: single photons, spatio-temporal properties, photon localization, Białynicki-Birula and Landau-Peierls position representations, spontaneous emission of Hydrogen atoms, adiabatic production of single photons, quasinormal modes

Abstract: This work provides an analysis of spatio-temporal properties of single-photon states. Starting with a direct quantization in position space representation, we show that two different formulations are equivalent, i.e., they give the same quantum theory. The equivalence is formulated in terms of isomorphisms of their respective Hilbert space of states. We then use this construction in position space to study the propagation of photons in terms of pulses, and we show that the dynamics of any state of the quantum electromagnetic field is given by the classical Maxwell equations for the classical pulse onto which the photons are defined. We also construct a model for local detection of photons using the energy density operator. This model allows us to show the nonlocality of all single-photon states using the anti-local property of the frequency operator $\Omega = c(-\Delta)^{1/2}$. We then characterize this nonlocal property for a single-photon state spontaneously emitted by a Hydrogen atom, and we show a radial decay of its energy density of $1/r^6$ in the asymptotic limit of large distances r from the atom. Finally, we consider the production of photons in cavities, where we show through topological arguments that in the adiabatic limit, the rotating wave approximation is justified, and thus the photons produced with these techniques can be very close to perfect single photons. We also construct, as a preliminary result, a heuristic model using quasinormal modes to describe the production of photons inside leaky cavities.

UBFC
UNIVERSITÉ
BOURGOGNE FRANCHE-COMTÉ

Université Bourgogne Franche-Comté
32, avenue de l'Observatoire
25000 Besançon

Is the world moving fast for you as well ? [...], I can't tell if it be only me.
Loyle Carner, *Speed of Plight*

Le souffleur à la lampe, Georges de la Tour ($\simeq$ 1640).

Contents

Abstract **ii**

Le souffleur à la lampe **vii**

Contents **ix**

Acknowledgments **xiii**

Résumé long **xv**

Introduction **1**

1 Theoretical background **7**
1.1 Maxwell's equations 8
1.1.1 Light propagation in a dielectric medium 8
1.1.2 Potentials and wave equation 11
1.2 Quantum description of matter 13
1.2.1 Quantum description of an atom 13
1.2.2 Semi-classical light-matter interaction 15
1.2.2.1 Atom in the electromagnetic field 15
1.2.2.2 Dipole approximation 16
1.2.2.3 Few-level approximation 17
1.2.2.4 Rotating wave approximation 19
1.3 Mathematical tools 20
1.3.1 Plane waves 20
1.3.2 Curl, frequency and helicity operators 22
1.3.3 Helicity spherical vector eigenfunctions of the Laplacian 25

2 Fock space quantization of the electromagnetic field in position space **27**
2.1 Fock space and quantization procedure 28

2.2 Quantization in the Coulomb gauge . . . 30
2.2.1 Hamiltonian formulation . . . 30
2.2.2 Complex representation — The Landau-Peierls field . . . 31
2.2.3 Momentum space formulation . . . 32
2.2.4 Correspondence principle . . . 33
2.2.4.1 Quantization in the momentum space $\mathscr{H}_M$ . . . 34
2.2.4.2 Quantization in the Landau-Peierls space $\mathscr{H}_{LP}$ . . . 34
2.2.5 Equivalence between the LP and momentum quantizations . . . 35
2.3 Białynicki-Birula's quantization . . . 36
2.3.1 Hamitonian structure . . . 36
2.3.2 The Riemann-Silberstein vector . . . 37
2.3.3 Alternative choice of canonical variables . . . 38
2.3.4 The Białynicki-Birula complex representation . . . 39
2.3.5 Quantization in the Białynicki-Birula representation . . . 40
2.4 Equivalence between the LP and the BB quantizations — Isomorphism . . . 42
2.5 Dynamics in the quantum models . . . 44

3 Propagation and local detection of photons **47**
3.1 Generalization of the Landau-Peierls quantization to dielectric media . . . 48
3.2 Evolution of the photon states determined from the dynamics of the classical modes . . . 50
3.2.1 Proof of the time evolution formulas . . . 51
3.2.2 Physical interpretation and application . . . 53
3.2.2.1 Propagation in an optical fiber — Space-to-time mapping . . . 54
3.2.2.2 Time-bin photon encoding . . . 54
3.3 Photons through beam-splitters . . . 56
3.3.1 One-photon state . . . 56
3.3.1.1 Initial classical mode and its time evolution . . . 56
3.3.1.2 Quantum dynamics of the one-photon state . . . 57
3.3.1.3 Alternative treatments of beam-splitters . . . 58
3.3.2 Two-photon state: The Hong-Ou-Mandel effect . . . 61
3.3.2.1 Initial classical modes and their time evolution . . . 61
3.3.2.2 Quantum dynamics of the two-photon state . . . 62
3.3.2.3 Detection model to interpret the dynamics . . . 63
3.3.2.4 Photons are not like classical waves nor like classical particles 64
3.4 Local detection of single-photon states . . . 65
3.4.1 Single-photon detectors . . . 65
3.4.2 Local observable for the detection . . . 65
3.4.3 Brief review on photon's nonlocality property . . . 68
3.4.4 Nonlocality of the energy density for single-photon states — Proof . . . 70
3.4.5 Illustration of the nonlocality . . . 72
3.4.6 Localization properties of other states of the quantum electromagnetic field . . . 74
3.4.6.1 N-photon states . . . 74
3.4.6.2 Coherent states . . . 75

3.4.7 Glauber's photodetection operator . . . 76
3.4.8 Nonlocality and causality . . . 77

4 Production of photons **79**
4.1 Spontaneous emission of a Hydrogen atom . . . 80
4.1.1 Model . . . 81
4.1.2 Weisskopf-Wigner equations . . . 83
4.1.3 Spatial distribution of the energy density . . . 85
4.1.4 Interpretation and multiphoton components . . . 89
4.2 Photon production in perfect cavities . . . 90
4.2.1 Hamiltonian and rotating wave approximation . . . 90
4.2.2 Floquet theory and adiabatic theorem . . . 93
4.2.3 Impact of the RWA on the production of single-photon states . . . 94
4.3 Perspectives for further developments: open cavities . . . 98
4.3.1 Normal modes vs quasinormal modes . . . 100
4.3.2 Truncated quasinormal modes — Leakage of single photons . . . 102
4.3.3 Quantum models using quasinormal modes . . . 103
4.3.3.1 Hybrid basis . . . 103
4.3.3.2 Interacting model . . . 105
4.3.4 Summary on the perspectives . . . 106

Conclusion and outlook **109**

A Positive and negative frequency parts of a field **113**

B Time evolution of a general N-photon state **117**

C Knight's theorem and equal-time correlation functions **121**

D Anti-locality of the frequency operator — Proof of Lemma 1 **125**

E Coherent states **129**

F Coupling coefficient for the single-photon spontaneous emission **133**

G Solution of the Friedrichs model **137**

H Asymptotic behavior of the radial integrals for spontaneous emission **141**

Bibliography **145**

Acknowledgments

I would first like to thank all the jury members who accepted to read my work. In particular, I deeply thank my supervisor Hans who taught me what being a devoted researcher means and from whom I realized that humility is an important skill to make good research. I am also grateful to Jonas who thoroughly helped me with his wide mathematical culture, network, and his precise advices. Finally, I am thankful to Gérard with whom I did my first internship as a student and who offered me an interesting teaching opportunity during this PhD.

In the lab, I had the opportunity to meet many other students whom I want to thank. Special dedications go to my office mates: Alberto, Benjamin, Georgii, and Siggi with whom my working environment was perfect. I am also very thankful to the rest of the Food gang who gave me that perfect amount of socialization I needed during these years: Astghik, Colm, Etienne, Gohar, Maria, Pierre, Rodolphe, and Xavier (the undying). Many thanks to Alix with whom I shared two nice years of Master as well as this PhD. I sincerely acknowledge all the people working here at the university without whom life in the lab would not be as pleasant as it is; especially administrative and cleaning agents. Outside the lab but still at the university, I have met many other PhD students within the Expérimentarium network; thank you all for showing me that research exists in so many fields, that it is done in so many different ways but that in the end we all are the same. A special thanks goes to Elise and Coralie from l'Expé who taught me how to tell people about what I do, and with whom I acquired much more confidence in myself.

I would also like to greatly thank people from Le Four, you had been there way before this thesis, you have been there during this thesis, and you will be there way after this thesis.

I am also very grateful to Antonio, Marie-José, and Marina, who regularly gave me support during these years and even before.

Last but not least, I dedicate this work to my family who has always been supportive since I was born. Maman, Papa, thank you for your love. Deb, I really doubt I would have made these long studies if you did not show me it was possible. Marjo, you will always be my little sister and this means a lot to me. Elisa, my love, the last 10 years would have been very empty without you; I owe you so much for what I have become; thank you for being there for me, you are my true light source.

Résumé long

De manière générale en optique quantique, les photons sont décrits dans l'espace de Fourier et représentés par des vecteurs $|\vec{k}, \lambda\rangle$ avec un vecteur d'onde et une polarisation donnés. L'état correspondant dans l'espace position est une onde plane complètement délocalisée et donc peu utile pour décrire les propriétés spatiales. De plus, les ondes planes ne sont pas physiques puisqu'elles possèdent une énergie infinie et servent donc uniquement à construire des paquets d'ondes qui eux ont une énergie finie. Dans cette thèse, nous utiliserons donc une construction de la théorie quantique du champ électromagnétique directement faite en termes d'impulsions bien définies et à partir desquelles les propriétés spatiales peuvent être analysées. Les photons uniques seront donc décrit par des vecteur $|\vec{\eta}\rangle$ où $\vec{\eta}$ est une condition initiale des équations de Maxwell formulée dans une représentation complexe. Plusieurs de ces représentations complexes existent, telles que les représentations dites de Landau-Peierls et de Białynicki-Birula. Après avoir rappelé comment elles sont construites, nous démontrons qu'elles sont en fait complètement équivalentes en formulant un isomorphisme reliant leurs espaces de Hilbert respectifs. Cette équivalence garantie que les deux théories ainsi construites sont identiques, c'est à dire qu'elles prédisent les mêmes résultats. La forme relativement simple de l'isomorphisme permet donc de passer de l'une à l'autre des représentations en fonctions des différents aspects de la théorie que l'on souhaite étudier. Nous démontrons également à travers l'étude des générateurs de la dynamique, que cette équivalence se préserve au cours du temps. Finalement, nous discutons de la généralisation de cette description sous forme d'impulsions au cas de la propagation de photons dans des milieux diélectriques passifs inhomogènes.

Un des avantages de la description en termes d'impulsion en espace position est ensuite illustré pour le calcul de la propagation d'états du champ quantifié. En effet, nous démontrons que l'évolution temporelle d'un état quelconque est déterminée par la dynamique prédite par les équations de Maxwell des fonctions classiques représentants l'état. La représentation en espace position fournit donc une approche simple pour traiter l'évolu-tion de n'importe quel état du champ quantique grâce à l'utilisation de l'évolution temporelle classique souvent bien connue. Cette propriétée est illustré avec l'exemple de la lame séparatrice, et permet notamment de retrouver les résultats observés dans l'effet

Hong-Ou-Mandel.

Puisque l'interprétation des phénomènes quantiques ne peut se faire que par une analyse conjointe des états et des observables, nous introduisons également un modèle permettant de discuter la détection locale de photons. En effet, l'existence de résultats expérimentaux utilisant des photons à priori plus grand que n'importe quel détecteur utilisé pour les mesurer, témoigne du besoin d'un tel modèle tenant compte de cette distribution spatiale. Pour cela, nous utilisons la densité d'énergie électromagnétique comme observable locale et calculons sa valeur moyenne pour différents états du champ. Ces résultats nous permettent ensuite de démontrer la non-localité des états à N photons en général, pour N fini. C'est à dire que pour ces états, il n'existe pas de volume de localisation à l'extérieur duquel la valeur moyenne de la densité d'énergie coïncide avec celle obtenue pour le vide. Ce résultat, déjà connu dans la littérature, est redémontré ici pour une observable locale concrète qui en principe peut représenter un détecteur réel utilisé dans une expérience. De plus, notre démonstration est valable pour tous les états à N photons, le plus général soient ils, et ne fait pas intervenir l'évolution temporelle de ces derniers. En revanche, les états cohérents, qui représentent ce qu'émet un laser par exemple, peuvent être localisés. Ce résultat vient du fait que leur état s'écrive comme une superposition d'états à n photons, pour n arbitrairement grand.

Concernant la production de photons, et au vu des résultats sur leur non-localité, nous caractérisons la distribution spatiale d'états à un photon produits par l'émission spontanée d'un atome d'Hydrogène. On trouve une décroissance algèbrique asymptotique de $1/r^6$, pour des distances r loin de l'atome. Afin de mieux comprendre la production expérimentale d'états très proche de photons uniques, nous considérons par la suite l'interaction entre un mode du champ et un atome à deux niveaux, dans une cavité parfaite. Ce modèle prédit la production d'états à un photon uniquement si l'on applique l'approximation de l'onde tournante (rotating wave approximation, RWA). En considérant l'interaction entre l'atome et le mode de cavité comme un champ de contrôle, et en ajoutant une interaction avec un laser classique externe, nous démontrons, grâce à la théorie de Floquet et dans la limite adiabatique, que les termes non résonants qui sont éliminés par l'approximation RWA, n'empêchent pas le contrôle du système vers l'état final cible : atome dans son état fondamental et un photon dans la cavité ; et ce, en conservant les mêmes champs de contrôle. Cette analyse est réalisée en utilisant un argument topologique, et indique que les photons produits par des méthodes de contrôle adiabatique seront très proches de photons uniques parfaits.

Pour terminer, et à titre de résultats préliminaires, nous introduisons le concept de modes quasinormaux (quasinormal modes, QNMs) qui sont des solutions de l'équation d'onde obtenues en appliquant une condition dite d'onde sortante. Elles permettent par exemple de décrire classiquement une cavité imparfaite, c'est à dire pour laquelle au moins un des miroirs n'est pas complètement réfléchissant. En utilisant un QNM tronqué spatialement, nous construisons une fonction pouvant représenter la sortie d'un photon initialement dans la cavité. Une telle approche est intrinsèquement dynamique et se fait en gardant la même structure pour la théorie quantique du champ. Seule la fonction représentant l'état est choisie de telle sorte que le photon, naturellement, sorte de la cavité. De plus, en construisant une base hybride composée de QNMs tronqués à l'intérieur de la cavité et d'une

base standard tronquée à l'extérieur, nous construisons un modèle quantique heuristique, similaire à celui construit généralement pour les cavités parfaites. L'originalité de cette approche réside dans l'utilisation d'opérateurs créations et annihilations directement construits sur des QNMs, de ce fait, on s'attend à ce que les photons produits suivant la dynamique de ce modèle se propagent naturellement vers l'extérieur de la cavité.

Introduction

Parts of the present work have led to the following articles:

[1] M. Federico, V. Dorier, S. Guérin and H. R. Jauslin. Space-time propagation of photon pulses in dielectric media, illustrations with beam splitters. *Journal of Physics B: Atomic, Molecular and Optical Physics*, 55(17):174002, 2022.

[2] M. Federico and H. R. Jauslin. Isomorphism between the Białynicki-Birula and the Landau-Peierls Fock space quantization of the electromagnetic field in position representation. *Journal of Physics A: Mathematical and Theoretical*, 56(23):235302, 2023.

[3] M. Federico and H. R. Jauslin. Nonlocality of the energy density for all single-photon states. *Physical Review A*, 108(4):043720, 2023.

[4] M. Federico and H. R. Jauslin. Nonlocality of the energy density of a spontaneously emitted single-photon from a Hydrogen atom. *arXiv:2403.13622v1*, 2024.

PHOTONS are the elementary excitations of the quantum electromagnetic field. Before being interpreted as such, they have been postulated and described within several different models [5] starting with the pioneering works of Planck [6] and Einstein [7, 8]. The transition from Planck's mathematical trick and Einstein's energy quanta to our current understanding of photons has involved many physicists but one of the starting works discussing electromagnetic radiations in a quantum field framework was done by Dirac [9]. The concept of photons, as described by Dirac, was originally a key tool for understanding subatomic interactions and, together with the relativistic description of electrons, they were the starting point towards the construction of the standard model of particle physics. In optics, all the light sources available at that time were far from the quantum regime and one had to wait until the construction of lasers to have the first optics experiments involving a small number of photons [10–13], giving birth to the field of quantum optics. Theoretically, the description of such experiments cannot be done with the models used in subatomic physics since in this context one needs to consider

much more particles of matter ranging from one single atom to a full solid medium. The description of matter is thus often non relativistic in quantum optics and it will be the case in the rest of this manuscript.
Over the past 50 years, the field has grown in an impressive manner and both experimental and theoretical techniques have been pushed forward in order to build light sources able to produce photons one-by-one and on-demand. There exists now many different platforms to do so, e.g., spontaneous parametric down conversion with nonlinear crystals, color centers in diamonds, quantum dots or single-atoms/ions in cavities. Moreover, the experimental controllability over these schemes allows now to select some properties of the emitted photons such as their spatial/temporal distribution, often refered to as the "shape of the photon". This notion, which seems to be relevant for the description of experimentally well-mastered techniques, was the starting point of this thesis, i.e., we want to have models taking into account the spatial properties of photons when describing current quantum optics experiments. To analyze the question, we will consider the three key elements in these experiments, namely the production, propagation, and detection of the photons.

*
* *

In many works, single photons are described in the momentum/Fourier space and represented as $|\vec{k}, \lambda\rangle$ with a given wavevector and polarization. The corresponding states in position space are associated to plane waves that are completely delocalized and therefore not useful to describe spatial properties. Additionally, plane wave photons are not physical since they have infinite energy and can be used only to construct wavepackets of finite energy. Following this line, we want to use a construction of the quantum theory of the electromagnetic field which explicitly makes use of these well-defined photons on pulses from which we can analyze the spatial properties directly. We will thus work beyond the standard notation $|n\rangle$ referring to the number of photons in the system, and use a more detailed notation $|\vec{\eta}\rangle$ where $\vec{\eta}$ will be a valid initial condition for Maxwell's equations written in a complex formulation. Several complex formulations of Maxwell's equations exist and we will discuss in this thesis two of them, showing that they are both a valid option to construct the quantum field theory in position space and that the two resulting theories are indeed equivalent. We will also provide an explicit formula linking the two formulations and allowing to pass from one to the other in a rather simple way. The use of one formulation or the other will thus be a matter of preferences, in particular depending on the aspect of the theory one wants to look at and in order to simplify the calculations as much as possible. We will also show that the description of photons with pulses is not valid only in the vacuum but can be generalized to the case of an inhomogeneous passive dielectric medium [1, 14], in particular to be able to discuss the propagation of photons through lenses, beam-splitters, dielectric mirrors or inside optical fibers.
This question of the description of photons in position space is historically closely related to that of the wavefunction of photons [15–27], however we will deliberately not use this terminology in our work for several reasons: (i) Wavefunctions in standard non-relativistic quantum mechanics, e.g., for electrons, are eigenfunctions of a position operator associated to the described particle. For photons, the concept of position operator has been widely debated and is certainly not as simple and intuitive as it can be for other systems. (ii)

Wavefunctions usually are associated to a Born probability rule, namely they provide the probability density of a certain measurement and its associated operator. The objects we will use for the photons do not yield the probability density but rather the expectation value of some associated operator. In that sense, we believe that the word wavefunction can be misleading in the context of photons and we will thus not use it for clarity reasons. Instead, we will only use the concept of states of the electromagnetic field.

The importance of Maxwell's equations in the quantum theory of the electromagnetic field is not reduced to its construction since the dynamics of free photons, i.e., without considering their sources, is in fact given by the classical dynamics of the associated pulse on which the photons have been created. This result, well-known for single-photon states [28], is true for any N-photon state and we will give an explicit proof of it. To illustrate this property, we will consider two examples starting with the passage of a single-photon state through a dielectric beam-splitter and recover the behavior that is observed in experiments. The particularity of our approach is that we will not use any creation-annihilation operator related to vacuum fluctuations as it is often done in quantum optics textbooks [28–35] since the description in terms of propagating pulses is enough to obtain the full picture. The second example is the Hong-Ou-Mandel effect which describes the passage of a two-photon state constructed on two disjoint pulses so that they simultaneously impinge on the two faces of a beam-splitter. The formulation of the theory in terms of propagating pulses gives consistent results for this setup and predicts the bunching property of photons. We will also discuss the semantics often used for photons since the Hong-Ou-Mandel effect gives a clear indication that photons do not behave as waves nor as particles.

An important feature of field theories is that looking at the state functions only does not give a full picture of the system. One has to consider the joint representation of the states and the observables to obtain the full information on a certain property of the system. In particular, we need to introduce an observable relevant for the discussion of the spatial properties of photons. Following the works of Białynicki-Birula [21, 25], we will use the energy density operator as the observable describing the local detection of photons as it can be done in experiments, e.g., using superconducting nanowires [36]. The interesting particularity of this detection model is that it allows one to probe photons described by a state function that is never fully inside the detector volume. It represents thus the local detection of photons. Such a model for local detection is needed since there exist on-demand single-photon sources that produce photons carried by $\Delta\tau \simeq 1$ μs pulses which correspond to a spatial extension of $\Delta x = c\Delta\tau \simeq 300$ m [37], and therefore cannot fully fit into any actual detector. Using this detection model, we will show that all single-photon states are nonlocal, i.e., the expectation value of the energy density observable is never zero for any open set of $\mathbb{R}^3$. Our result is an extension of the works by Białynicki-Birula [38,39], and a complementary approach to the results of Knight [40] and of Hegerfeldt [41–44], which is valid without using the time evolution of the states. The nonlocality of photons is thus not a consequence of their dynamics but a property already true for initial conditions.

Regarding the production of single photons, in view of the results obtained for the detection, we will first characterize the spatial distribution of single photons produced by the spontaneous emission of a Hydrogen atom. As expected, the nonlocality can be seen in the decrease of the expectation value of the energy density with respect to the position of

the atom. We find in the asymptotic limit of large distances from the atom, a $1/r^6$ fall-off. This result can be obtained only by considering a full $\vec{\hat{A}} \cdot \vec{p}$ coupling between the atom and the quantized electromagnetic field since the standard dipole approximation does not allow to compute the state of the emitted photon but only the decay of the atom [45–49]. The recent methods for the experimental production of single photons does not rely on spontaneous emission but on the control of generally a two- or three-level system by different control parameters. We will thus discuss how photons can be produced through the interaction of an atom with a laser field inside a perfect cavity. The key point to get as close as possible to the production of single-photon states relies on the validity of the rotating wave approximation. We will show using a topological argument constructed using the Floquet theory [50] that in the adiabatic limit [51], this approximation is valid all along the dynamics of production and this regime of control is thus well-suited for the production of single photons. In practice however, photons must be produced in leaky/open cavities if one wants to use them in the outside environment. The theoretical description of such leakage by the photons remains a crucial point in quantum optics and several techniques have been developed to address this question. We will try in this work to briefly sketch, as a preliminary result, how one could use the concept of quasinormal modes in this context. Quasinormal modes (QNM) are particular solutions of Maxwell's equations with outgoing boundary conditions [52–63]. They have the interesting property of being able to fully describe a resonant structure taking into account the leakage towards the outside. Nonetheless, they possess a drawback that is their divergence for positions infinitely far from the resonant structure, preventing to use them as a basis for the full space of study. We would like to use them as a state function describing the photon that is produced in a cavity and which will eventually leak out. To do so, we will show that it is possible to construct a dynamical function using a truncated QNM initially only inside the cavity but which will propagate to the outside at any later time. The importance of taking a truncated QNM is to avoid the divergence at infinite positions while keeping the intrinsic leaking property. Such a function can thus be normalized and used as state function for the photon. The last step in our preliminary construction will be to introduce a hybrid basis made of QNMs inside the cavity and any other basis for the outside. This basis can then be used to represent observables in the quantum model and to build a heuristic model similar to what one had for the perfect cavity case but taking into account the leakage towards the outside.

*
* *

To address all these questions, the manuscript will be divided in four main chapters. We will start in Chapter 1 by recalling the basic theoretical tools we will extensively use in the rest of the work, i.e., Maxwell's equations and their generalization for passive dielectric media, then the quantum description of atoms and the standard equations for light-matter interaction, including the most relevant approximations. We will conclude on this chapter with the definition of some operators that we will extensively use in the description of the quantum electromagnetic field, as well as some eigenfunctions of these operators which will be of interest to solve the models we will construct in the next chapters. Chapter 2 will be devoted to the quantization of the free electromagnetic field

in position space, and to the equivalence of the different position space representations. Chapter 3 will be divided into two parts with first the description of propagation, including the illustration with beam-splitters, and then with the construction of the model for local detection and the proof of nonlocality of all single-photon states. Finally Chapter 4 will be dedicated to the production of photons starting with the characterization of the spatial distribution of spontaneously emitted photons from a Hydrogen atom. We will then discuss the production of photons in a perfect cavity and show the relevance of the rotating wave approximation in the adiabatic limit. We will, in the last part, introduce the concept of quasinormal modes and briefly discuss, as a preliminary result, how one could use them to describe the production of photons in open cavities.

1

Theoretical background

This first chapter is dedicated to the introduction of the concepts that will be needed to understand the quantum description of the electromagnetic field in position space representations, as well as its interaction with matter.

We start by recalling the basics of classical electrodynamics, based on the microscopic Maxwell equations and then formulate the macroscopic Maxwell equations which allow to take into account the propagation of light in media. In order to prepare the quantization scheme, we introduce the notions of potentials for both formulations and explicitly write the theory in terms of wave equations. We also recall important results on the quantum description of atoms and their interaction with classical light. Particularly, we show how standard approximations are derived and construct semi-classical Hamiltonians to prepare the passage towards a full quantum description. Finally, we define mathematical tools which will be extensively used throughout this work, in particular the frequency and helicity operators and their associated eigenfunctions.

1.1 Maxwell's equations 8
1.1.1 Light propagation in a dielectric medium 8
1.1.2 Potentials and wave equation 11
1.2 Quantum description of matter 13
1.2.1 Quantum description of an atom 13
1.2.2 Semi-classical light-matter interaction 15
1.2.2.1 Atom in the electromagnetic field 15
1.2.2.2 Dipole approximation 16
1.2.2.3 Few-level approximation 17
1.2.2.4 Rotating wave approximation 19
1.3 Mathematical tools 20
1.3.1 Plane waves 20
1.3.2 Curl, frequency and helicity operators 22
1.3.3 Helicity spherical vector eigenfunctions of the Laplacian 25

1.1 Maxwell's equations

Any physical systems involving electromagnetic radiations, charges and currents are described by the microscopic Maxwell equations

$$\nabla \times \vec{B} = \mu_0 \vec{j} + \mu_0 \varepsilon_0 \frac{\partial \vec{E}}{\partial t}, \tag{1.1a}$$

$$\nabla \times \vec{E} = -\frac{\partial \vec{B}}{\partial t}, \tag{1.1b}$$

$$\nabla \cdot \vec{E} = \frac{\rho}{\varepsilon_0}, \tag{1.1c}$$

$$\nabla \cdot \vec{B} = 0, \tag{1.1d}$$

where $\vec{E}$ and $\vec{B}$ are the electric and magnetic fields, ρ and $\vec{j}$ the charge and current densities, ε_0 and μ_0 the vacuum permittivity and permeability, related to the speed of light in vacuum c by $\mu_0 \varepsilon_0 c^2 = 1$. We also used the notations $\nabla\cdot$ and $\nabla\times$ for the divergence and the curl operators.
This set of equations can be interpreted as follows:

- (1.1a) indicates that the presence of currents or time variations of the electric field, produce a magnetic field;
- (1.1b) indicates that time variations of the magnetic field produce an electric field;
- (1.1c) shows that electric charges create electric fields;
- (1.1d) expresses the non-existence of magnetic charges.

More information is contained in the set (1.1) such as the charge conservation which is obtained by combining the divergence of (1.1a) with (1.1c) yielding

$$\frac{\partial \rho}{\partial t} + \nabla \cdot \vec{j} = 0, \tag{1.2}$$

known as the continuity equation. This relation expresses that any variation of the density of charges is related to a variation of current.
So far, we have considered the microscopic Maxwell equations that are useful to describe systems having a small number of charges with some easily tracked motion (currents simple to describe) or in vacuum (without any charges nor current, $\rho = 0$, $\vec{j} = 0$). However, to describe light propagating in a medium, one uses macroscopic quantities which encompass the collective response of the medium, containing many charges.

1.1.1 Light propagation in a dielectric medium

To construct such a phenomenological model for matter, we split charges and currents into two categories: one bounded to the medium (ρ_m, $\vec{j}_\mathrm{m}$) and one external to the medium

(ρ_{ext}, $\vec{j}_{\text{ext}}$). The total charge and current densities that appear in the microscopic Maxwell equations (1.1) can thus be replaced by

$$\rho = \rho_{\text{m}} + \rho_{\text{ext}}, \tag{1.3a}$$
$$\vec{j} = \vec{j}_{\text{m}} + \vec{j}_{\text{ext}}. \tag{1.3b}$$

Using Poincaré's lemma [64] and the continuity equation, the total charge and current densities can be expressed as

$$\rho = -\nabla \cdot \vec{\mathfrak{P}}, \tag{1.4a}$$
$$\vec{j} = \nabla \times \vec{\mathfrak{M}} + \frac{\partial \vec{\mathfrak{P}}}{\partial t}, \tag{1.4b}$$

where the fields $\vec{\mathfrak{P}}$ and $\vec{\mathfrak{M}}$ are called polarization and magnetization densities, respectively. They sum up the collective information from charges and current on a macroscopic scale without needing to know the behavior of every single one of them.
In the following, we will only consider non magnetic media, i.e., $\vec{\mathfrak{M}} = 0$. Putting the new expressions for ρ and $\vec{j}$ inside (1.1), leads to the macroscopic Maxwell equations

$$\nabla \times \vec{B} = \mu_0 \frac{\partial \vec{\mathfrak{P}}}{\partial t} + \frac{1}{c^2} \frac{\partial \vec{E}}{\partial t}, \tag{1.5a}$$
$$\nabla \times \vec{E} = -\frac{\partial \vec{B}}{\partial t}, \tag{1.5b}$$
$$\nabla \cdot \vec{E} = -\frac{1}{\varepsilon_0} \nabla \cdot \vec{\mathfrak{P}}, \tag{1.5c}$$
$$\nabla \cdot \vec{B} = 0. \tag{1.5d}$$

We explained above that the polarization density arises from the collective behaviors of charges and currents both inside and outside the medium. We can thus divide its expression from three contributions:

$$\vec{\mathfrak{P}} = \vec{\mathfrak{P}}_{\text{ind}} + \vec{\mathfrak{P}}_{\text{sp}} + \vec{\mathfrak{P}}_{\text{ext}}, \tag{1.6}$$

where the last term describes the contribution from external charges (ρ_{ext}, $\vec{j}_{\text{ext}}$), the second describes spontaneous contribution generated by charges inside the medium and the first describes the contribution induced by the interaction between the medium and light. The first and second terms come from the medium charges and currents (ρ_{m}, $\vec{j}_{\text{m}}$).
The spontaneous polarization density is a difficult quantity to estimate (especially for experiments) which depends on the initial condition of the medium. Therefore, it is often treated theoretically as a random noise, or set to zero when its effect is known to be negligible. The latter is the option we will take in this work. Additionally, we will consider only systems which do not have any external charges nor current so that the polarization density — in our case — is identical to the induced one.
The media we will consider are neutral — before the interaction with an electromagnetic field — hence the induced polarization is created by the electric field which displaces electric charges inside the medium. Indeed, as one can see in Figure 1.1, an atom —

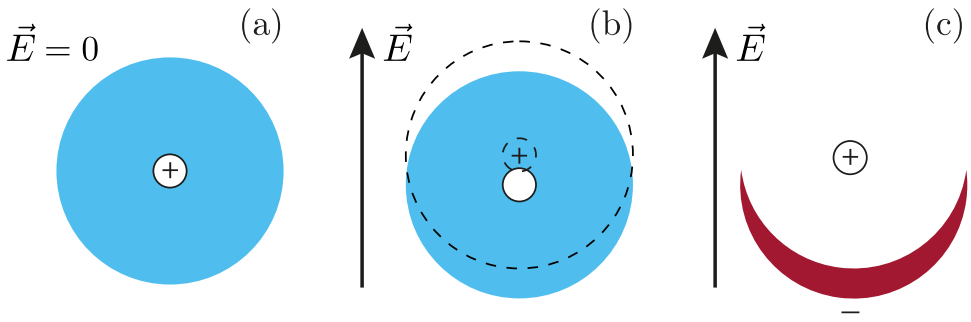

Figure 1.1: Sketch illustrating the electromagnetic response to an static electric field of a neutral medium. (a) Neutral case with zero electric field: the positive nuclear and negative electronic disributions compensate each other. (b) When an electric field is applied, nucleus and electronic density of charges are displaced in opposite directions, breaking the symmetry of the system. (c) The asymmetry brought by the static electric field creates a net charge distribution (in red) yielding the medium polarization density. (Illustration partially reproduced from [65])

considered in the vacuum — is neutral, so it does not give any polarization density, unless an electric field is applied to it resulting in a displacement in opposite direction of positive and negative charges. The net result is then proportional to the electric field and powers of it. In this thesis, we will only deal with linear optics. One can thus express the induced polarization density as

$$\vec{\mathfrak{P}}_{\text{ind}}(\vec{x},t) = \varepsilon_0 \int_{-\infty}^{+\infty} dt' \chi(\vec{x}, t-t') \vec{E}(\vec{x},t'), \tag{1.7}$$

where the dimensionless function χ is the linear response function of the medium. The expression (1.7) is so far too general since it would take into account the influence of the electric field from past time as well as future time which does not make sense from a causality point of view. However, one can choose a particular form for the response function χ which takes into account this requirement; two choices can be done and lead to two types of media that have different physical properties. We have:

- A retarded response function $\chi(\vec{x}, t-t') = \chi_{\text{m}}(\vec{x}, t-t')\Theta(t-t')$, where Θ stands for the Heaviside step function

$$\Theta(t-t') = \begin{cases} 1 & \text{if } t' \leq t \\ 0 & \text{if } t' > t \end{cases}, \tag{1.8}$$

  yielding for the polarization density

$$\vec{\mathfrak{P}}_{\text{ind}}(\vec{x},t) = \varepsilon_0 \int_{t}^{+\infty} dt' \chi_{\text{m}}(\vec{x}, t-t') \vec{E}(\vec{x},t'). \tag{1.9}$$

- An instantaneous response function $\chi(\vec{x}, t-t') = \chi_{\text{m}}(\vec{x})\delta(t-t')$, where $\delta(t-t')$ is the Dirac delta function so that the polarization density simply becomes

$$\vec{\mathfrak{P}}_{\text{ind}}(\vec{x},t) = \varepsilon_0 \chi_{\text{m}}(\vec{x}) \vec{E}(\vec{x},t). \tag{1.10}$$

The retarded response gives rise to Kramers-Kronig media which feature both dispersion and dissipation. The instantaneous response leads to passive media, for which refractive indices do not depend on the frequency and without absorption. In this thesis, we will consider only the latter since we are interested in describing the production of photons inside a cavity having dielectric mirrors and then propagating in a dielectric medium (optical fiber) over sufficiently short distances such that both dispersion and dissipation inside that medium will be neglected.
Inserting the expression (1.10) of the instantaneous response polarization into Maxwell's equation (1.5a) yields

$$\nabla \times \vec{B} = \frac{1}{c^2} \left(\chi_{\mathrm{m}}(\vec{x}) + 1\right) \frac{\partial \vec{E}}{\partial t}. \tag{1.11}$$

We consider media under sufficiently stable conditions compared to the interaction time scale such that their response do not change with time. We introduce the dielectric coefficient $\varepsilon_{\mathrm{m}}(\vec{x}) := \chi_{\mathrm{m}}(\vec{x}) + 1$, giving for Maxwell's equation (1.11)

$$\nabla \times \vec{B} = \frac{\varepsilon_{\mathrm{m}}(\vec{x})}{c^2} \frac{\partial \vec{E}}{\partial t}. \tag{1.12}$$

By doing the same for the constraint (1.5c), one can rewrite it as

$$\nabla \cdot \left(\varepsilon_{\mathrm{m}}(\vec{x}) \vec{E}\right) = 0. \tag{1.13}$$

1.1.2 Potentials and wave equation

For now, we have described Maxwell's equations inside a passive medium using the electric and magnetic fields. However, the set of equations we ended up with mixes the electric and magnetic fields which sometimes makes it harder to solve. To circumvent this difficulty, we are going to introduce the notion of potentials that are very useful in both classical and quantum electrodynamics as we will see later. Indeed, one can remark (using Poincaré's lemma) that equation (1.5d) implies the existence of a vector field $\vec{A}'$ such that

$$\vec{B} = \nabla \times \vec{A}'. \tag{1.14}$$

Inserting this new vector field into (1.5b) gives

$$\nabla \times \left(\vec{E} + \frac{\partial \vec{A}'}{\partial t}\right) = 0, \tag{1.15}$$

which implies the existence of a scalar potential U' such that

$$\vec{E} + \frac{\partial \vec{A}'}{\partial t} = -\nabla U'. \tag{1.16}$$

Maxwell's equations can then be expressed in terms of these potentials and become

$$\nabla \times \nabla \times \vec{A}' + \frac{\varepsilon_\mathrm{m}}{c^2}\frac{\partial}{\partial t}\nabla U' + \frac{\varepsilon_\mathrm{m}}{c^2}\frac{\partial^2 \vec{A}'}{\partial t^2} = 0, \tag{1.17a}$$

$$\nabla \cdot \left(\varepsilon_\mathrm{m}(\vec{x})\vec{E}\right) = 0, \tag{1.17b}$$

$$\vec{B} = \nabla \times \vec{A}', \tag{1.17c}$$

$$\vec{E} = -\nabla U' - \frac{\partial \vec{A}'}{\partial t}. \tag{1.17d}$$

The last two equations define the potentials, the second one (1.17b) is the generalized constraint taking the medium into account and the first one (1.17a) is a generalized form of a wave equation.
An advantage of using potentials to write Maxwell's equations is that they are not unique since for any field $f(\vec{x}, t)$, the new potentials defined as

$$\vec{A}'_\mathrm{g} = \vec{A}' + \nabla f, \tag{1.18a}$$

$$U'_\mathrm{g} = U' - \frac{\partial f}{\partial t}, \tag{1.18b}$$

will give rise to the same electromagnetic fields as $(\vec{A}', U')$. Such transformations are called gauge transformations and are used in practice to construct potentials which simplify the equations to be solved. In our case, the generalized wave equation can be drastically simplified by the choice of potentials in the generalized Coulomb gauge. It corresponds to the set of potential $(\vec{A}'_\mathrm{gC}, U'_\mathrm{gC})$ chosen (using an appropriate field f) such that they fulfill

$$\nabla \cdot \left(\varepsilon_\mathrm{m}\vec{A}'_\mathrm{gC}\right) = 0, \tag{1.19a}$$

$$U'_\mathrm{gC} = 0, \tag{1.19b}$$

and it simplifies the wave equation (1.17a) to

$$\nabla \times \nabla \times \vec{A}'_\mathrm{gC} + \frac{\varepsilon_\mathrm{m}}{c^2}\frac{\partial^2 \vec{A}'_\mathrm{gC}}{\partial t^2} = 0. \tag{1.20}$$

The set of Maxwell equations for a passive medium we will use in the rest of this thesis reads thus

$$\nabla \times \nabla \times \vec{A}'_\mathrm{gC} + \frac{\varepsilon_\mathrm{m}}{c^2}\frac{\partial^2 \vec{A}'_\mathrm{gC}}{\partial t^2} = 0, \tag{1.21a}$$

$$\nabla \cdot \left(\varepsilon_\mathrm{m}\vec{A}'_\mathrm{gC}\right) = 0, \tag{1.21b}$$

$$\vec{B} = \nabla \times \vec{A}'_\mathrm{gC}, \tag{1.21c}$$

$$\vec{E} = -\frac{\partial \vec{A}'_\mathrm{gC}}{\partial t}. \tag{1.21d}$$

In the particular case of the vacuum, i.e., $\varepsilon_{\mathrm{m}} = 1$, it simplifies to

$$\frac{\partial^2 \vec{A}'_{\mathrm{C}}}{\partial t^2} = c^2 \Delta \vec{A}'_{\mathrm{C}}, \tag{1.22a}$$

$$\nabla \cdot \vec{A}'_{\mathrm{C}} = 0, \tag{1.22b}$$

$$\vec{B} = \nabla \times \vec{A}'_{\mathrm{C}}, \tag{1.22c}$$

$$\vec{E} = -\frac{\partial \vec{A}'_{\mathrm{C}}}{\partial t}, \tag{1.22d}$$

where we have used $\nabla \times \nabla \times \vec{A}'_{\mathrm{C}} = -\Delta \vec{A}'_{\mathrm{C}} + \nabla(\nabla \cdot \vec{A}'_{\mathrm{C}}) = -\Delta \vec{A}'_{\mathrm{C}}$ which is valid since $\vec{A}'_{\mathrm{C}}$ is transverse (1.22b).

1.2 Quantum description of matter

To have a full description of the production and propagation of photons, we will need to consider the sources and the propagating media. These elements are composed of matter that we will have to describe from a quantum point of view. We will use two different approaches to treat on one hand the sources and on the other hand the propagation media. Indeed, we have seen already in the classical formulation of electrodynamics that the medium into which light propagates can be taken into account in a macroscopic effective model that gathers all the matter information and interaction with electromagnetic quantities into the dielectric function. Although this model does not contain the microscopic behavior of each element in the medium, it can be formulated with a Hamiltonian structure that is close to the one we will obtain for the vacuum, and therefore a quantum model can be constructed in a similar way with only few modifications. This approach will be detailed in Chapter 3 following the general procedure that we will develop in detail in Chapter 2.
Regarding the sources, the production of single photons relies heavily on the discretization of energy levels of the emitters. Indeed, it is the transition from of a higher to a lower energy level which is mostly responsible for the creation of photons. Before going into the details of this transition, and being able to understand how one can control such emission in order to have on demand single-photon sources, it is important to understand the internal structure of such emitters alone. In this work, for simplicity reasons, we will focus on the description of photons produced by atoms. However, we note that the description we will use to represent atoms, is applicable to many other sources like ions or quantum dots for example. In this section, we recall some basic results on the quantum description of atoms, explain how to describe classically their interaction with the electromagnetic field and introduce the most common approximations performed in that context.

1.2.1 Quantum description of an atom

For simplicity, we consider a Hydrogen atom which is composed of a proton of mass $\mathfrak{m}_{\mathrm{p}} = 1.7 \times 10^{-27}$ kg and charge $q = 1.6 \times 10^{-19}$ C; and of an electron of mass $\mathfrak{m} = 0.91 \times 10^{-30}$ kg

and charge $-q$ [66]. Since $\frac{\mathfrak{m}}{\mathfrak{m}_\mathrm{p}} \ll 1$, the center of mass of the system is close to the proton which we consider from now on fixed and placed at $\vec{x}_\mathrm{at} = 0$. The classical interaction between the two particles is electrostatic and described by the Coulomb potential

$$V_\mathrm{Coul} = -\frac{q^2}{4\pi\varepsilon_0|\vec{x}_\mathrm{at} - \vec{x}|} = -\frac{e^2}{r}, \tag{1.23}$$

where $\vec{x}$ denotes the position of the electron, $r = |\vec{x}|$ and $e^2 = {}^{q^2}/_{4\pi\varepsilon_0}$. The classical Hamiltonian of the system is thus given by

$$H_\mathrm{at} = \frac{\vec{p}^2}{2\mathfrak{m}} - \frac{e^2}{r}, \tag{1.24}$$

where $\vec{p}$ is the momentum vector associated to the electron. To obtain the quantum Hamiltonian, one applies the standard correspondence principle

$$\vec{p} \mapsto \vec{\hat{p}} = -i\hbar\nabla, \tag{1.25a}$$

$$\vec{x} \mapsto \vec{\hat{x}}, \tag{1.25b}$$

where the position operator $\vec{\hat{x}}$ acts on elements of the atomic Hilbert space, in position representation $\mathcal{H}_\mathrm{at} = L^2(\mathbb{R}^3)$, as the multiplication by $\vec{x}$. The quantum atomic Hamiltonian reads thus

$$\hat{H}_\mathrm{at} = \frac{\vec{\hat{p}}^2}{2\mathfrak{m}} - \frac{e^2}{\hat{r}}, \tag{1.26}$$

where in this central symmetric problem, the operator $\hat{r}$ acts on elements of $\mathcal{H}_\mathrm{at}$ as multiplication by r.
To characterize the system, one solves now the time-independent Schrödinger equation

$$\hat{H}_\mathrm{at}\varphi_{nlm}(\vec{x}) = E_n\varphi_{nlm}(\vec{x}), \tag{1.27}$$

where the eigenenergies are

$$E_n = -\frac{E_\mathrm{i}}{n^2}, \tag{1.28}$$

expressed in terms of the ionization energy $E_\mathrm{i} = {}^{\alpha^2\mathfrak{m}c^2}/_2$, with $\alpha \simeq {}^1/_{137}$ the fine-structure constant. The quantum numbers (n, l, m) label the different eigenfunctions and can take the following values:

$$n = 1, 2, 3, \ldots, \quad \text{i.e., } n \in \mathbb{N}^*; \tag{1.29a}$$

$$l = 0, 1, 2, \ldots, n-1; \tag{1.29b}$$

$$m = -l, -l+1, \ldots, l-1, l. \tag{1.29c}$$

For each l there is thus $2l+1$ different values of m and the total degeneracy of each E_n level is

$$g_n = \sum_{l=0}^{n-1}(2l+1) = n^2, \tag{1.30}$$

and should be multiplied by two to take into account the electron spin ${}^1/_2$ which we will not consider in this work.

The expression in spherical coordinates (r, ϑ, φ) of the eigenfunctions for $n = 1$ and $n = 2$ are

$$\varphi_{n=1,l=0,m=0}(r,\vartheta,\varphi) = \frac{1}{\sqrt{\pi r_{\mathrm{B}}^3}} e^{-r/r_{\mathrm{B}}}, \tag{1.31a}$$

$$\varphi_{n=2,l=0,m=0}(r,\vartheta,\varphi) = \frac{1}{\sqrt{8\pi r_{\mathrm{B}}^3}} \left(1 - \frac{r}{2r_{\mathrm{B}}}\right) e^{-r/2r_{\mathrm{B}}}, \tag{1.31b}$$

$$\varphi_{n=2,l=1,m=1}(r,\vartheta,\varphi) = -\frac{1}{8\sqrt{\pi r_{\mathrm{B}}^3}} \frac{r}{r_{\mathrm{B}}} e^{-r/2r_{\mathrm{B}}} \sin\vartheta \; e^{i\varphi}, \tag{1.31c}$$

$$\varphi_{n=2,l=1,m=0}(r,\vartheta,\varphi) = \frac{1}{4\sqrt{2\pi r_{\mathrm{B}}^3}} \frac{r}{r_{\mathrm{B}}} e^{-r/2r_{\mathrm{B}}} \cos\vartheta, \tag{1.31d}$$

$$\varphi_{n=2,l=1,m=-1}(r,\vartheta,\varphi) = \frac{1}{8\sqrt{\pi r_{\mathrm{B}}^3}} \frac{r}{r_{\mathrm{B}}} e^{-r/2r_{\mathrm{B}}} \sin\vartheta \; e^{-i\varphi}, \tag{1.31e}$$

where $r_{\mathrm{B}} = \hbar/\alpha \mathfrak{m} c$ is the Bohr radius.

1.2.2 Semi-classical light-matter interaction

The semi-classical approach of light-matter interaction consists in describing matter with a quantum model while the electromagnetic field remains classical. This is a first step which allows to account for many phenomena that cannot be understood properly in a fully classical model but which still fails for some other ones, e.g., spontaneous emission. In this section, we want to construct a semi-classical model in which a quantum Hydrogen atom interacts with the classical electromagnetic field.

1.2.2.1 Atom in the electromagnetic field

The central point to build such a model is to construct its Hamiltonian. Classically, the electron is subjected to the Lorentz force $\vec{F}_{\mathrm{L}} = q(\vec{E} + \dot{\vec{x}} \times \vec{B})$ so that the Newton equation of motion reads

$$\mathfrak{m}\ddot{\vec{x}} = q\left(\vec{E} + \dot{\vec{x}} \times \vec{B}\right). \tag{1.32}$$

Here, the notation $\dot{\vec{x}}$ refers to a time derivative of the variable $\vec{x}$ which gives the velocity of the electron, and $\ddot{\vec{x}}$ the acceleration. An equivalent formulation can be done using the classical Hamiltonian expressed for a pair of potentials $(\vec{A}, U)$

$$H = \frac{1}{2\mathfrak{m}} \left(\vec{p} - q\vec{A}(\vec{x})\right)^2 + qU(\vec{x}), \tag{1.33}$$

and the corresponding Hamilton equations for the j component

$$\dot{x}_j = \frac{\partial H}{\partial p_j} = \frac{1}{\mathfrak{m}} \left(p_j - qA_j\right), \tag{1.34a}$$

$$\dot{p}_j = -\frac{\partial H}{\partial x_j} = \frac{q}{\mathfrak{m}} \sum_{i=1}^{3} \left(\frac{\partial A_i}{\partial x_j} p_i - qA_i \frac{\partial A_i}{\partial x_j}\right) - q\frac{\partial U_j}{\partial x_j}. \tag{1.34b}$$

Indeed, by inserting (1.34a) in (1.34b) and using the relations

$$\frac{dA_j}{dt} = \frac{\partial A_j}{\partial t} + \left(\vec{\dot{x}} \cdot \nabla\right) A_j, \tag{1.35}$$

and

$$\left[\vec{\dot{x}} \times \left(\nabla \times \vec{A}\right)\right]_j = \sum_{i=1}^{3} \dot{x}_i \left(\frac{\partial A_i}{\partial x_j} - \frac{\partial A_j}{\partial x_i}\right), \tag{1.36}$$

as well as the definition of the potentials (1.14) and (1.16), equations (1.34) give back Newton's equation of motion (1.32). We emphasize here that throughout this work, the dot product will denote $\vec{u} \cdot \vec{v} = \sum_{i=1}^{3} u_i v_i$, i.e., without complex conjugation when applied to complex vectors.
The semi-classical Hamiltonian describing a Hydrogen atom in the electromagnetic field is thus obtained by applying the correspondence principle (1.25) to the atomic variables and yields

$$\hat{H} = \frac{1}{2\mathfrak{m}} \left(\vec{\hat{p}} - q\vec{A}(\vec{\hat{x}})\right)^2 + qU(\vec{\hat{x}}). \tag{1.37}$$

1.2.2.2 Dipole approximation

From the general classical Hamiltonian we have introduced in the preceding section, the dipole approximation for the interaction is often performed. It is constructed as follows: We start working in the Coulomb gauge which has the advantage that one can make a clear separtaration of the static field induced by the fixed nucleus and the time dependent external field applied to the atom [28]. Indeed, the vector potential is not affected by the static field produced by the nucleus while the scalar potential is equal to the static Coulomb potential $U_{\mathrm{C}} = V_{\mathrm{Coul}}/q$. The next step consists in applying a change of gauge which allows to get rid of the vector potential dependence and instead express the Hamiltonian in terms of the electric field. To do so, one defines the Göppert-Mayer gauge [67] which is constructed from the Coulomb gauge using the standard gauge transformation (1.18) with the auxiliary function f_{GM}

$$f_{\mathrm{GM}} = (\vec{x}_{\mathrm{at}} - \vec{x}) \cdot \vec{A}_{\mathrm{C}}(\vec{x}_{\mathrm{at}}), \tag{1.38}$$

yielding the potentials

$$\vec{A}_{\mathrm{GM}}(\vec{x}) = \vec{A}_{\mathrm{C}}(\vec{x}) - \vec{A}_{\mathrm{C}}(\vec{x}_{\mathrm{at}}), \tag{1.39a}$$

$$U_{\mathrm{GM}}(\vec{x}) = U_{\mathrm{C}}(\vec{x}) + (\vec{x} - \vec{x}_{\mathrm{at}}) \cdot \frac{\partial \vec{A}_{\mathrm{C}}(\vec{x}_{\mathrm{at}})}{\partial t} = \frac{1}{q} V_{\mathrm{Coul}}(\vec{x}) - (\vec{x} - \vec{x}_{\mathrm{at}}) \cdot \vec{E}(\vec{x}_{\mathrm{at}}). \tag{1.39b}$$

By inserting these potentials into (1.33) and defining the electric dipole function as $\vec{d}(\vec{x}) = q(\vec{x} - \vec{x}_{\mathrm{at}})$, we obtain

$$H = \frac{1}{2\mathfrak{m}} \left(\vec{\hat{p}} - q\vec{A}_{\mathrm{GM}}(\vec{x})\right)^2 - \frac{e^2}{|\vec{x} - \vec{x}_{\mathrm{at}}|} - \vec{d}(\vec{x}) \cdot \vec{E}(\vec{x}_{\mathrm{at}}). \tag{1.40}$$

So far, no approximation has been made, we only rewrote the Hamiltonian using another gauge that is well suited for the problem we want to analyze. To further simplify this Hamiltonian, we make the long wavelength approximation which states that for the type of interaction we will consider in this work, the wavelengths of the fields will be large compared to the atomic dimensions. As an example, the typical emission and absorption lines of a Hydrogen atom have a wavelength of at least 100 nm while atomic sizes are of the order of the Bohr radius $r_{\mathrm{B}} = 0.053$ nm. Fields amplitude are thus almost constant over the spatial extension of the atom so that we approximate them by their value at the position of the atom $\vec{x}_{\mathrm{at}}$. Applying this approximation for (1.40) means replacing $\vec{A}_{\mathrm{GM}}(\vec{x})$ by $\vec{A}_{\mathrm{GM}}(\vec{x}_{\mathrm{at}})$ which is zero according to (1.39a). We obtain finally the classical Hamiltonian in the dipole approximation

$$H = \frac{\vec{p}^2}{2\mathfrak{m}} - \frac{e^2}{|\vec{x} - \vec{x}_{\mathrm{at}}|} - \vec{d} \cdot \vec{E}(\vec{x}_{\mathrm{at}}) \tag{1.41a}$$

$$= H_{\mathrm{at}} - \vec{d} \cdot \vec{E}(\vec{x}_{\mathrm{at}}), \tag{1.41b}$$

which is the free atomic Hamiltonian plus the electric dipole interaction term. We note that although we have made several gauge transformations on the potentials to obtain this result, in the end it does not depend on the potentials anymore. The semi-classical Hamiltonian is again obtained by applying the correspondence principle (1.25) to the atomic variables:

$$\hat{H} = \frac{\hat{\vec{p}}^2}{2\mathfrak{m}} - \frac{e^2}{|\hat{\vec{x}} - \vec{x}_{\mathrm{at}}|} - \hat{\vec{d}} \cdot \vec{E}(\vec{x}_{\mathrm{at}}) \tag{1.42a}$$

$$= \hat{H}_{\mathrm{at}} - \hat{\vec{d}} \cdot \vec{E}(\vec{x}_{\mathrm{at}}). \tag{1.42b}$$

1.2.2.3 Few-level approximation

The model we have been constructing so far to describe the interaction between an atom and the classical electromagnetic field, contains the full free atomic Hamiltonian plus the dipole interaction term. According to the results of Section 1.2.1 of this chapter, the atomic part can be decomposed using the spectral theorem as

$$\hat{H}_{\mathrm{at}} = \sum_{n,l,m} E_n \left|n, m, l\right\rangle \left\langle n, m, l\right|, \tag{1.43}$$

where $|n, l, m\rangle \equiv \varphi_{nlm}$, and thus

$$\hat{H} = \sum_{n,l,m} E_n \left|n, m, l\right\rangle \left\langle n, m, l\right| - \hat{\vec{d}} \cdot \vec{E}(\vec{x}_{\mathrm{at}}). \tag{1.44}$$

To express the dipole operator, we use a trick [68] using the parity operator $\hat{\varpi}$ which flips the sign of the position operator $\hat{\vec{x}}$, i.e., $\hat{\varpi}\hat{\vec{x}}\hat{\varpi}^{-1} = -\hat{\vec{x}}$ and thus $\hat{\varpi}\hat{\vec{x}} = -\hat{\vec{x}}\hat{\varpi}$. The parity

operator $\hat{\varpi}$ is an involution, i.e., $\hat{\varpi}^{-1} = \hat{\varpi}$, $\hat{\varpi}^2 = \mathbb{1}$ and its spectrum is $\{\pm 1\}$. One can then conclude that for any atomic eigenstates

$$\langle n,l,m| \left(\hat{\varpi}\vec{\hat{d}} + \vec{\hat{d}}\hat{\varpi}\right) |n',l',m'\rangle = 0 \tag{1.45a}$$

$$\Leftrightarrow (\varpi_{nlm} + \varpi_{n'l'm'}) \langle n,l,m| \vec{\hat{d}} |n',l',m'\rangle = 0, \tag{1.45b}$$

where ϖ_{nlm} is the parity of the state $|n,l,m\rangle$, i.e., $\hat{\varpi}|n,l,m\rangle = \varpi_{nlm}|n,l,m\rangle$ with $\varpi_{nlm} = \pm 1$. A first consequence of (1.45) is that diagonal elements of $\vec{\hat{d}}$ are all zero since for any (n,l,m), $\varpi_{nlm} + \varpi_{nlm} = \pm 2 \neq 0$ and thus

$$\langle n,l,m| \vec{\hat{d}} |n,l,m\rangle = 0. \tag{1.46}$$

The dipole operator can be written in an abstract way as

$$\vec{\hat{d}} = \sum_{\substack{n,l,m \\ n',l',m'}} \langle n',l',m'| \vec{\hat{d}} |n,l,m\rangle |n',l',m'\rangle \langle n,l,m|, \tag{1.47}$$

where the sums over n and n' go until a given $n_{\max}$ which corresponds to the last state before the ionization of the atom. The full interaction term in the semi-classical light-matter interaction Hamiltonian in the dipole approximation reads thus

$$\hat{H}_{\text{int}} = -\sum_{\substack{n,l,m \\ n',l',m'}} \langle n',l',m'| \vec{\hat{d}} \cdot \vec{E}(\vec{x}_{\text{at}}) |n,l,m\rangle |n',l',m'\rangle \langle n,l,m|, \tag{1.48}$$

and depending on the type of electric field that is applied to the atom, this expression can be drastically simplified.
In Chapter 4, we will be interested in the control of atoms using lasers which can be considered as quasi-monochromatic with a central frequency ω_{L} that is resonant with a particular transition $|n_g,l_g,m_g\rangle \leftrightarrow |n_e,l_e,m_e\rangle$, i.e., which fulfill

$$\omega_{\text{L}} \simeq \frac{E_{n_e} - E_{n_g}}{\hbar}. \tag{1.49}$$

In that case, the matrix element $|\langle e| \vec{\hat{d}} \cdot \vec{E}(\vec{x}_{\text{at}}) |g\rangle|$, where $|e\rangle \equiv |n_e,l_e,m_e\rangle$ and $|g\rangle \equiv |n_g,l_g,m_g\rangle$, will be much bigger than any other and the interaction term can be rewritten as

$$\hat{H}_{\text{int}} \simeq -\langle e| \vec{\hat{d}} \cdot \vec{E}(\vec{x}_{\text{at}}) |g\rangle |e\rangle \langle g| - \langle g| \vec{\hat{d}} \cdot \vec{E}(\vec{x}_{\text{at}}) |e\rangle |g\rangle \langle e|. \tag{1.50}$$

Only two levels are thus concerned by the dynamics, and the full Hamiltonian can be rewritten as

$$\hat{H}_{\text{2-level}} = E_{n_g} |g\rangle \langle g| + E_{n_e} |e\rangle \langle e| - \langle e| \vec{\hat{d}} \cdot \vec{E}(\vec{x}_{\text{at}}) |g\rangle |e\rangle \langle g| - \langle g| \vec{\hat{d}} \cdot \vec{E}(\vec{x}_{\text{at}}) |e\rangle |g\rangle \langle e|, \tag{1.51}$$

which is the Hamiltonian of a 2-level atom interacting with a classical electric field in the dipole approximation. It can be notationally simplified by choosing without lost of

generality the zero energy to be E_{n_g} and by fixing the phase of $\langle e|\,\vec{\hat{d}}\cdot\vec{E}(\vec{x}_{\rm at})\,|g\rangle$ so that it is real, and one obtains

$$\hat{H}_{\text{2-level}} = E_{n_e}\,|e\rangle\langle e| - \langle e|\,\vec{\hat{d}}\cdot\vec{E}(\vec{x}_{\rm at})\,|g\rangle\,(|e\rangle\langle g| + |g\rangle\langle e|)\,. \tag{1.52}$$

In many experiments, two different lasers with different central frequencies are used to control the atom. In such situation, two transitions will be favored in the sum (1.48) and one can construct a 3-level Hamiltonian with the states $|1\rangle$, $|2\rangle$ and $|3\rangle$

$$\begin{aligned}\hat{H}_{\text{3-level}} = E_{n_2}\,|2\rangle\langle 2| + E_{n_3}\,|3\rangle\langle 3| - \langle 1|\,\vec{\hat{d}}\cdot\vec{E}_{12}(\vec{x}_{\rm at})\,|2\rangle\,(|1\rangle\langle 2| + |2\rangle\langle 1|)\\ - \langle 2|\,\vec{\hat{d}}\cdot\vec{E}_{23}(\vec{x}_{\rm at})\,|3\rangle\,(|2\rangle\langle 3| + |3\rangle\langle 2|)\,,\end{aligned} \tag{1.53}$$

where the zero of energy has been set for E_1. Here, we have chosen to couple the states $|1\rangle \leftrightarrow |2\rangle$ with one laser and the states $|2\rangle \leftrightarrow |3\rangle$ with another, but any other choice can be constructed in the same fashion.
The main advantage of such formulation, is that it can be obtained for many different systems and not only atoms. For instance, ions, quantum dots and superconducting circuits can be described with a finite number of discrete energy levels and thus a 2- or 3-level Hamiltonian with the same structure can be equivalently constructed for those systems. In Chapter 4 of the present work, we will show some results on how to control the dynamics of 2- level systems in general.

1.2.2.4 Rotating wave approximation

In the preceding section, we have constructed a model where a 2-level atom interact with the classical electromagnetic field under the electric dipole approximation coupling. This approach is general and in particular, we did not consider the time-dependence of the electric field that is applied on the atom. This is the purpose of this section and it will lead to a widely used approximation called the rotating wave approximation (RWA) and which will be of utmost importance in the description of the production of single photons in cavities. We will focus mostly on the 2-level case since the 3- or higher-level cases can be deduced from it. To construct the interacting 2-level Hamiltonian (1.52), we have assumed that the electric field is quasi-monochromatic, i.e., it can be written with the following form

$$\vec{E}(\vec{x},t) = \vec{E}_{\rm L}(\vec{x},t)\cos\Big(\vec{k}_{\rm L}\cdot\vec{x} - \omega_{\rm L}t\Big), \tag{1.54}$$

where $\omega_{\rm L} = c|\vec{k}_{\rm L}|$ is the central frequency which must be resonant with the transition frequency of the atom, and $\vec{E}_{\rm L}(\vec{x},t)$ is the polarization-amplitude vector. Since in the interaction, the field is taken at the position $\vec{x}_{\rm at} = 0$, one obtains

$$\vec{E}(\vec{x}_{\rm at},t) = \vec{E}_{\rm L}(\vec{x}_{\rm at},t)\cos(\omega_{\rm L}t) \tag{1.55a}$$

$$= \frac{\vec{E}_{\rm L}(\vec{x}_{\rm at},t)}{2}\left(e^{i\omega_{\rm L}t} + e^{-i\omega_{\rm L}t}\right), \tag{1.55b}$$

and the interacting part of (1.52) becomes

$$\hat{H}_{\text{int}} = -\frac{\langle e|\,\hat{\vec{d}}\cdot\vec{E}(\vec{x}_{\text{at}},t)\,|g\rangle}{2}\left(e^{i\omega_{\text{L}}t}+e^{-i\omega_{\text{L}}t}\right)\left(|e\rangle\langle g|+|g\rangle\langle e|\right) \tag{1.56a}$$

$$= \frac{\hbar\Omega_{eg}(t)}{2}\left(e^{i\omega_{\text{L}}t}+e^{-i\omega_{\text{L}}t}\right)\left(|e\rangle\langle g|+|g\rangle\langle e|\right), \tag{1.56b}$$

where $\Omega_{eg}(t) = -\langle e|\,\hat{\vec{d}}\cdot\vec{E}(\vec{x}_{\text{at}},t)\,|g\rangle/\hbar$ is the time-dependent Rabi frequency of the transition. If we fix a matrix representation for the states $|g\rangle = \begin{pmatrix}1 & 0\end{pmatrix}^T$ and $|e\rangle = \begin{pmatrix}0 & 1\end{pmatrix}^T$, the full 2-level Hamiltonian can be expressed as

$$\hat{H} = \frac{\hbar}{2}\begin{pmatrix} 0 & \Omega_{eg}(t)\left(e^{i\omega_{\text{L}}t}+e^{-i\omega_{\text{L}}t}\right) \\ \Omega_{eg}(t)\left(e^{i\omega_{\text{L}}t}+e^{-i\omega_{\text{L}}t}\right) & 2\omega_{\text{a}}\end{pmatrix}, \tag{1.57}$$

where we have introduced the Bohr frequency of the transition $\hbar\omega_{\text{a}} = E_{n_e} - E_{n_g}$. The Hamiltonian can be further analyzed by extracting the resonant contribution from the coupling, by applying the unitary resonant transformation

$$R = \begin{pmatrix}1 & 0\\ 0 & e^{i\omega_{\text{L}}t}\end{pmatrix} \tag{1.58}$$

to obtain

$$\hat{H}' = R^\dagger\hat{H}R = \frac{\hbar}{2}\begin{pmatrix}0 & \Omega_{eg}(t)\\ \Omega_{eg}(t) & 2\omega_0\end{pmatrix} + \frac{\hbar\Omega_{eg}(t)}{2}\begin{pmatrix}0 & e^{2i\omega_{\text{L}}t}\\ e^{-2i\omega_{\text{L}}t} & 0\end{pmatrix}. \tag{1.59}$$

The interaction part has been separated into two parts, a resonant one that we have put in the first term and a non resonant contribution in the second term. The RWA consists then to remove the second term. This procedure can be justified in several ways but what we want to emphasize here is that the second term can in fact be iteratively eliminated using KAM type transformations which allow to keep track of the non resonant terms. This procedure of quantum averaging using KAM transformations is more detailed in [50, 69]. In the end, if one puts aside the non-resonant term, and applies the inverse resonant transformation, we obtain the RWA Hamiltonian as

$$\hat{H}_{\text{2-level,rwa}} = \frac{\hbar}{2}\begin{pmatrix}0 & \Omega_{eg}(t)e^{-i\omega_{\text{L}}t}\\ \Omega_{eg}(t)e^{i\omega_{\text{L}}t} & 2\omega_0\end{pmatrix}. \tag{1.60}$$

1.3 Mathematical tools

Before getting into the main results of the present work, we need to introduce some mathematical tools which will be extensively used.

1.3.1 Plane waves

Even though plane waves have limitations when it comes to describe photons and their spatial properties, they still allow in many situations to perform calculations in a much

simpler way. The reason for their practicality will become clear later when we will use them to diagonalize some operators that are central for the description of the electromagnetic field.
We start by defining circularly polarized plane waves

$$\vec{\phi}_{\vec{k},\pm}(\vec{x}) = \frac{1}{(2\pi)^{3/2}}\vec{\epsilon}_{\pm}(\vec{k})e^{i\vec{k}\cdot\vec{x}}, \qquad \vec{k} \in \mathbb{R}^3, \tag{1.61}$$

where $^{+}/_{-}$ labels the $^{\text{left}}/_{\text{right}}$ circular polarization vectors with the following parametrization

$$\vec{\epsilon}_{+}(\vec{k}) = \frac{1}{\sqrt{2}|\vec{k}|\sqrt{k_x^2+k_y^2}}\begin{pmatrix} -k_xk_z + i|\vec{k}|k_y \\ -k_yk_z - i|\vec{k}|k_x \\ k_x^2+k_y^2 \end{pmatrix}, \quad \vec{\epsilon}_{-}(\vec{k}) = \vec{\epsilon}_{+}(\vec{k})^{\star}. \tag{1.62}$$

If the wave vector $\vec{k}$ is aligned with the z-axis, then one makes the following choice

$$\vec{\epsilon}_{+}(\vec{k}) = \frac{\text{sign}(k_z)}{\sqrt{2}}\begin{pmatrix} 1 \\ i \\ 0 \end{pmatrix}. \tag{1.63}$$

Other equivalent parametrizations exist with different global phase conventions but in the rest of the thesis, plane waves are to be understood with this particular choice. So far, the plane waves are transverse since $\nabla \cdot \vec{\epsilon}_{\pm}(\vec{k}) = 0$ but one can also define longitudinal plane waves with a polarization vector $\vec{\epsilon}_0(\vec{k}) = \vec{k}/|\vec{k}|$. In fact, the unit vectors $\vec{\epsilon}_\sigma(\vec{k})$ for $\sigma = \{0, \pm\}$ satisfies

$$\vec{n} \times \vec{\epsilon}_\sigma(\vec{k}) = -i\sigma\vec{\epsilon}_\sigma(\vec{k}), \tag{1.64}$$

with $\vec{n} = \vec{k}/|\vec{k}|$. In this section, for the sake of completeness, we will discuss the most general plane waves, including longitudinal ones, even though in the rest of the manuscript we will deal only with transverse fields.
Plane waves are useful to describe square integrable functions — which will be used to represent photon states — since they satisfy the following relations of orthonormality

$$\int_{\mathbb{R}^3} d^3x\ \vec{\phi}^{\star}_{\vec{k},\sigma}(\vec{x}) \cdot \vec{\phi}_{\vec{k}',\sigma'}(\vec{x}) = \delta(\vec{k}-\vec{k}')\delta_{\sigma,\sigma'}, \tag{1.65}$$

and completeness

$$\int_{\mathbb{R}^3} d^3k \sum_\sigma |\vec{\phi}_{\vec{k},\sigma}\rangle\ \langle\vec{\phi}_{\vec{k},\sigma}| = \int_{\mathbb{R}^3} d^3k \sum_\sigma \vec{\phi}_{\vec{k},\sigma}(\vec{x})\vec{\phi}^{\star}_{\vec{k},\sigma}(\vec{x}') = \delta(\vec{x}-\vec{x}'), \tag{1.66}$$

so that any square integrable vector field $\vec{v} \in L^2$ can be written as

$$\begin{aligned}
\vec{v}(\vec{x}) &= \int_{\mathbb{R}^3} d^3x'\ \delta(\vec{x}-\vec{x}')\vec{v}(\vec{x}') && \text{(1.67a)}\\
&= \int_{\mathbb{R}^3} d^3x' \int_{\mathbb{R}^3} d^3k \sum_\sigma \vec{\phi}_{\vec{k},\sigma}(\vec{x})\vec{\phi}^{\star}_{\vec{k},\sigma}(\vec{x}') \cdot \vec{v}(\vec{x}') && \text{(1.67b)}\\
&= \int_{\mathbb{R}^3} d^3k \sum_\sigma \left(\int_{\mathbb{R}^3} d^3x'\ \vec{\phi}^{\star}_{\vec{k},\sigma}(\vec{x}') \cdot \vec{v}(\vec{x}') \right) \vec{\phi}_{\vec{k},\sigma}(\vec{x}) && \text{(1.67c)}\\
&= \int_{\mathbb{R}^3} d^3k \sum_\sigma \langle\vec{\phi}_{\vec{k},\sigma}|\vec{v}\rangle\ \vec{\phi}_{\vec{k},\sigma}(\vec{x}), && \text{(1.67d)}
\end{aligned}$$

where $\langle\cdot|\cdot\rangle$ is the scalar product in L^2.
Since plane waves are not themselves square integrable, they are not in L^2 and should thus not be considered as a basis of the space. However, the denomination generalized basis is used to refer to such functions able to generate any element of a space, like in (1.67), even though they do not belong to that space. From now on, we will use the term basis without specifying whether it is a generalized basis or not.
If one wants to describe a general transverse field $\vec{u}$, i.e., $\nabla \cdot \vec{u} = 0$, the completeness relation for the subspace of transverse field $\mathcal{H}^\perp \subset \mathcal{H}$ reads

$$\int_{\mathbb{R}^3} d^3k \sum_{\lambda=\pm} |\vec{\phi}_{\vec{k},\lambda}\rangle \langle\vec{\phi}_{\vec{k},\lambda}| = \delta^\perp(\vec{x} - \vec{x}'), \tag{1.68}$$

where $\delta^\perp(\vec{x}-\vec{x}')$ is the transverse delta function defined for any field $\vec{v}$ with a decomposition in transverse and longitudinal part $\vec{v} = \vec{u} + \vec{w}$ with $\nabla \cdot \vec{u} = 0$ and $\nabla \times \vec{w} = 0$ as

$$\int_{\mathbb{R}^3} d^3x' \ \delta^\perp(\vec{x} - \vec{x}')\vec{v}(\vec{x}') = \vec{u}(\vec{x}). \tag{1.69}$$

The set of circularly polarized plane waves $\{\vec{\phi}_{\vec{k},\lambda}\}$, with $\lambda = \pm$ will thus be used as a basis for transverse fields.

1.3.2 Curl, frequency and helicity operators

We have seen in Maxwell's equations that vectorial differential operators are central for the description of the electromagnetic field. In particular, if one puts aside the divergence $\nabla\cdot$ which appears only for the constraints, and focuses on the dynamics, the curl operator $\nabla\times$ is of uttermost importance. It is a local differential operator for which the plane waves with circular polarization are eigenfunctions

$$\nabla \times \vec{\phi}_{\vec{k},\sigma}(\vec{x}) = \sigma|\vec{k}|\, \vec{\phi}_{\vec{k},\sigma}(\vec{x}), \tag{1.70}$$

and the operator can thus be written using the spectral decomposition as

$$\nabla\times = \int_{\mathbb{R}^3} d^3k \sum_{\sigma} \sigma|\vec{k}|\ |\vec{\phi}_{\vec{k},\sigma}\rangle \langle\vec{\phi}_{\vec{k},\sigma}|\,. \tag{1.71}$$

When Maxwell's equations are expressed in terms of a wave equation, the important operator becomes the double curl $\nabla \times \nabla\times$ for which plane waves are still eigenfunctions

$$\nabla \times \nabla \times \vec{\phi}_{\vec{k},\sigma}(\vec{x}) = |\vec{k}|^2\ \vec{\phi}_{\vec{k},\sigma}(\vec{x}), \tag{1.72}$$

and the operator can be written as

$$\nabla \times \nabla\times = \int_{\mathbb{R}^3} d^3k \sum_{\sigma} |\vec{k}|^2 |\vec{\phi}_{\vec{k},\sigma}\rangle \langle\vec{\phi}_{\vec{k},\sigma}|\,. \tag{1.73}$$

If one adds the transversality constraint, the double curl operator is then equal to $-\Delta$ which can be decomposed as

$$-\Delta = \int_{\mathbb{R}^3} d^3k \sum_{\lambda} |\vec{k}|^2 |\vec{\phi}_{\vec{k},\lambda}\rangle \langle\vec{\phi}_{\vec{k},\lambda}|\,. \tag{1.74}$$

The difference between (1.73) and (1.74) is that for the Laplacian, we have removed the contribution of longitudinal fields with index $\sigma = 0$.
To describe the Maxwell equations with a Hamiltonian structure, we will need to define an operator $\Omega^2 = -c^2\Delta$ and its positive square root, called frequency operator, using the spectral decomposition

$$\Omega = \int_{\mathbb{R}^3} d^3k \sum_\lambda \omega_{\vec{k}} \, |\vec{\phi}_{\vec{k},\lambda}\rangle \, \langle\vec{\phi}_{\vec{k},\lambda}| \,, \quad \text{with } \omega_{\vec{k}} = c|\vec{k}| > 0. \tag{1.75}$$

It is a real and selfadjoint operator since

$$(\Omega\vec{\phi}_{\vec{k},\lambda})^\star = (c|\vec{k}| \, \vec{\phi}_{\vec{k},\lambda})^\star = c|\vec{k}| \, \vec{\phi}^\star_{\vec{k},\lambda} = \Omega\vec{\phi}^\star_{\vec{k},\lambda}, \tag{1.76}$$

and

$$\langle\vec{u}|\Omega\vec{u}'\rangle = \int_{\mathbb{R}^3} d^3k \int_{\mathbb{R}^3} d^3k' \sum_\sigma \sum_{\sigma'} \omega_{\vec{k}} \, \langle\vec{\phi}_{\vec{k},\sigma}|\vec{u}\rangle \, \langle\vec{u}|\vec{\phi}_{\vec{k}',\sigma'}\rangle \, \langle\vec{\phi}_{\vec{k}',\sigma'}|\vec{\phi}_{\vec{k},\sigma}\rangle \tag{1.77a}$$

$$= \int_{\mathbb{R}^3} d^3k \sum_\sigma \omega_{\vec{k}} \, \langle\vec{\phi}_{\vec{k},\sigma}|\vec{u}\rangle \, \langle\vec{u}|\vec{\phi}_{\vec{k}',\sigma'}\rangle \tag{1.77b}$$

$$= \int_{\mathbb{R}^3} d^3k \int_{\mathbb{R}^3} d^3k' \sum_\sigma \sum_{\sigma'} \omega_{\vec{k}'} \, \langle\vec{\phi}_{\vec{k},\sigma}|\vec{u}\rangle \, \langle\vec{u}|\vec{\phi}_{\vec{k}',\sigma'}\rangle \, \langle\vec{\phi}_{\vec{k}',\sigma'}|\vec{\phi}_{\vec{k},\sigma}\rangle \tag{1.77c}$$

$$= \langle\Omega\vec{u}|\vec{u}'\rangle \, . \tag{1.77d}$$

Using the spectral theorem, one can also define any power Ω^p for a real p [70–73] by giving its action on the plane wave basis

$$\Omega^p\vec{\phi}_{\vec{k},\lambda} = \omega^p_{\vec{k}}\vec{\phi}_{\vec{k},\lambda}. \tag{1.78}$$

Another operator, called helicity, will be of great importance especially when we will discuss local detection and nonlocal properties of single photons. It is defined as a combination of the curl and frequency operator

$$\Lambda = c\Omega^{-1}\nabla\times \, . \tag{1.79}$$

Because $\nabla\times$ and Ω^p have common eigenfunctions the three operators commute $[\nabla\times, \Omega^p] = 0 = [\nabla\times, \Lambda] = [\Omega^p, \Lambda]$ and Λ fulfills the following eigenvalue equation

$$\Lambda\vec{\phi}_{\vec{k},\sigma} = \sigma\vec{\phi}_{\vec{k},\sigma}. \tag{1.80}$$

From this, one can remark that the Hilbert space generated by $\{\vec{\phi}_{\vec{k},\sigma}\}$ can be split into three subspaces according to the helicity

$$\mathcal{H} = \mathcal{H}^{(h+)} \oplus \mathcal{H}^{(h-)} \oplus \mathcal{H}^{(h0)}. \tag{1.81}$$

The zero-helicity subspace is identical to the subspace of longitudinal fields while the subspace of transverse fields is the sum of positive and negative helicity subspaces $\mathcal{H}^\perp =$

$\mathcal{H}^{(h+)} \oplus \mathcal{H}^{(h-)}$. It means that any transverse field $\vec{u}(\vec{x})$ can always be written as the sum of a positive and negative helicity components as

$$\vec{u}(\vec{x}) = \vec{u}^{(h+)}(\vec{x}) + \vec{u}^{(h-)}(\vec{x}), \tag{1.82}$$

with $\Lambda\vec{u}^{(h\pm)} = \pm\vec{u}^{(h\pm)}$. To construct helicity components, one defines the following projectors

$$\mathbb{P}^{(h\pm)} = \frac{\mathbb{P}^{\perp} \pm \Lambda}{2}, \tag{1.83}$$

where $\mathbb{P}^{\perp} = \int_{\mathbb{R}^3} d^3k \sum_{\lambda} |\vec{\phi}_{\vec{k},\sigma}\rangle \langle\vec{\phi}_{\vec{k},\sigma}|$ is the projector into the subspace of transverse fields. For the zero helicity component, one simply projects onto the subspace of longitudinal fields, i.e., using $\mathbb{P}^{\parallel} = \mathbb{1} - \mathbb{P}^{\perp}$.
This result of splitting into +/– helicity component will be central for the isomorphism linking the two position space representations of photons as well as for the description of local detection and will give an explanation for the nonlocal property of single photons.

Remarks:

- The concept of helicity is common in quantum field theory where it is defined as the projection of the spin onto the direction of motion. Here, we emphasize that the definition involves only a combination of operators which will naturally appear in some complex formulations of Maxwell's equations. However, one can make the link between the two descriptions by rewriting the curl operator in a matrix form as

$$\nabla\times = \begin{pmatrix} 0 & -\partial_3 & \partial_2 \\ \partial_3 & 0 & -\partial_1 \\ -\partial_2 & \partial_1 & 0 \end{pmatrix} \tag{1.84a}$$

$$= \vec{\hat{S}} \cdot \frac{\nabla}{i} = \vec{\hat{S}} \cdot \frac{\vec{\hat{p}}}{\hbar}, \tag{1.84b}$$

  where $\vec{\hat{p}} = -i\hbar\nabla$ is the standard quantum momentum operator and $\vec{\hat{S}} = \left(\hat{S}_1, \hat{S}_2, \hat{S}_3\right)^T$ are the spin-1 operators defined as $[\hat{S}_i]_{j,k} = -i\epsilon_{ijk}$, with ϵ_{ijk} the totally antisymmetric Levi-Civita tensor which gives in the matrix representation

$$\hat{S}_1 = \begin{pmatrix} 0 & 0 & 0 \\ 0 & 0 & -i \\ 0 & i & 0 \end{pmatrix}, \quad \hat{S}_2 = \begin{pmatrix} 0 & 0 & i \\ 0 & 0 & 0 \\ -i & 0 & 0 \end{pmatrix}, \quad \hat{S}_3 = \begin{pmatrix} 0 & -i & 0 \\ i & 0 & 0 \\ 0 & 0 & 0 \end{pmatrix}. \tag{1.85}$$

  Equation (1.84b) illustrates the standard interpretation of quantum field theory.

- The notation $^{(h\pm)}$ refers to positive/negative helicity parts of a field and should not be confused with the positive/negative frequency parts of a field. Indeed, in general the two concepts do not coincide, i.e., for a transverse field $\vec{u}$,

$$\vec{u}^{(h\pm)} \neq \vec{u}^{(f\pm)}. \tag{1.86}$$

  More details about the concept of positive/negative frequency parts are given in Appendix A.

1.3.3 Helicity spherical vector eigenfunctions of the Laplacian

In the last chapter of this thesis concerning the spontaneous emission by a Hydrogen atom, we will need another basis of eigenfunctions of the Laplacian which is not the plane waves basis. Indeed, to perform calculations for systems with a spherical symmetry, we will need a basis of vectors $|k, J, M, \lambda\rangle \equiv \vec{\psi}^{(\lambda)}_{k,J,M}(\vec{x})$ that are eigenfunctions of the following operators [45, 74, 75]

$$-\Delta\vec{\psi}^{(\lambda)}_{k,J,M} = k^2\vec{\psi}^{(\lambda)}_{k,J,M}, \qquad k \in (0,\infty), \tag{1.87a}$$

$$\hat{J}^2\vec{\psi}^{(\lambda)}_{k,J,M} = J(J+1)\vec{\psi}^{(\lambda)}_{k,J,M}, \quad J \in \{0,1,2,\dots\}, \tag{1.87b}$$

$$\hat{J}_3\vec{\psi}^{(\lambda)}_{k,J,M} = M\vec{\psi}^{(\lambda)}_{k,J,M}, \qquad M \in \{-J,\dots,J\}, \tag{1.87c}$$

$$\Lambda\vec{\psi}^{(\lambda)}_{k,J,M} = \lambda\vec{\psi}^{(\lambda)}_{k,J,M} \qquad \lambda = \pm 1, \tag{1.87d}$$

where

$$\vec{\hat{J}} = \vec{\hat{L}} + \vec{\hat{S}}, \tag{1.88a}$$

$$\vec{\hat{L}} = \nabla \times \vec{x} = \vec{x} \times \nabla, \tag{1.88b}$$

$$\vec{\hat{S}} = \left(\hat{S}_1, \hat{S}_2, \hat{S}_3\right)^T, \quad [\hat{S}_i]_{j,k} = -i\epsilon_{ijk}. \tag{1.88c}$$

The helicity vector spherical eigenfunctions can be written in spherical coordinates (r, ϑ, φ) as

$$\vec{\psi}^{(\lambda)}_{k,J,M}(r,\vartheta,\varphi) = \frac{i}{\sqrt{2}}\Bigg[\sqrt{\frac{J+1}{2J+1}}\vec{\psi}^{J-1}_{k,J,M}(r,\vartheta,\varphi) - \sqrt{\frac{J}{2J+1}}\vec{\psi}^{J+1}_{k,J,M}(r,\vartheta,\varphi) - i\lambda\vec{\psi}^{J}_{k,J,M}(r,\vartheta,\varphi)\Bigg], \tag{1.89}$$

where the functions $\vec{\psi}^{L}_{k,J,M}$ can be expressed in terms of vector spherical harmonics $\vec{Y}^{L}_{J,M}$, i.e., eigenfunctions of $\hat{J}^2$, $\hat{J}_3$, $\hat{L}^2$ and $\hat{S}^2$ but not of Λ, and spherical Bessel functions $j_L(kr)$ as

$$\vec{\psi}^{L}_{k,J,M}(r,\vartheta,\varphi) = \sqrt{\frac{2}{\pi}}k\; j_L(kr)\vec{Y}^{L}_{J,M}(\vartheta,\varphi). \tag{1.90}$$

We remark that by constructing the functions $\vec{\psi}^{(\lambda)}_{k,J,M}$ from $\vec{\psi}^{L}_{k,J,M}$ we obtain eigenfunctions of $-\Delta$, $\hat{J}^2$, $\hat{J}_3$ and Λ but not of $\hat{L}^2$ while $\vec{\psi}^{L}_{k,J,M}$ is an eigenfunction of $-\Delta$, $\hat{J}^2$, $\hat{J}_3$ and $\hat{L}^2$ but not of Λ.
The helicity spherical vector eigenfunctions $\{\vec{\psi}^{(\lambda)}_{k,J,M}\}$ are transverse, $\nabla \cdot \vec{\psi}^{(\lambda)}_{k,J,M} = 0$, orthonormal

$$\int_0^\infty dr\; r^2 \int_0^\pi d\vartheta\; \sin\vartheta \int_0^{2\pi} d\varphi\; \vec{\psi}^{\lambda\star}_{k,J,M}(r,\vartheta,\varphi)\cdot\vec{\psi}^{\lambda'}_{k',J',M'}(r,\vartheta,\varphi) = \delta(k-k')\delta_{J,J'}\delta_{M,M'}\delta_{\lambda,\lambda'}, \tag{1.91}$$

and form a complete set of the subspace of transverse field since the set of function $\{\vec{\psi}^{J-1}_{k,J,M}, \vec{\psi}^{J}_{k,J,M}, \vec{\psi}^{J+1}_{k,J,M}\}$ from which they are defined is a complete set with

$$\int_0^\infty d^3k \sum_{J=0}^{\infty} \sum_{M=-J}^{J} \sum_{L=J-1}^{J+1} \left[\vec{\psi}^{L}_{k,J,M}(r',\vartheta',\varphi')\right]_\mu \left[\vec{\psi}^{L\star}_{k,J,M}(r,\vartheta,\varphi)\right]_\nu = \frac{1}{r^2 \sin\vartheta}\delta_{\mu,\nu}\delta(r-r')\delta(\vartheta-\vartheta')\delta(\varphi-\varphi'). \tag{1.92}$$

The last equation is a consequence of the completeness of the Bessel functions $j_L(kr)$ and vector spherical harmonics $\vec{Y}^{L}_{J,M}$.

2

Fock space quantization of the electromagnetic field in position space

This chapter is dedicated to the quantization of the free electromagnetic field both in momentum and position space representations. The equivalence between the representations is shown using explicit isomorphims between their respective Hilbert spaces of states.

We start by recalling the construction of a Hamiltonian formulation of Maxwell's equations in the Coulomb gauge where canonical variables can be defined first in position space and then in momentum space. The quantization using a correspondence principle is then performed in momentum space since the Hamilton function in that representation takes the form of a set of uncoupled harmonic oscillators. A similar correspondence principle can be applied in position space and the two quantizations are equivalent since their Hilbert spaces are isomorphic. A similar procedure, called the Białynicki-Birula (BB) quantization, was put forward by taking directly the electromagnetic fields as canonical variables and defining in momentum space a correspondence principle. The central result of this chapter is to show that the BB quantization is also linked to the Coulomb gauge quantization through an isomorphism of their Hilbert spaces. This isomorphism, that we explicitly give, shows that the two constructions are equivalent and can be used to analyze spatial properties of photons. Finally, we look at the generator of the dynamics in each representation and show that the equivalence will be preserved at all times.
Most of the results in this chapter have been published in [2].

2.1 Fock space and quantization procedure 28
2.2 Quantization in the Coulomb gauge 30
2.2.1 Hamiltonian formulation 30
2.2.2 Complex representation — The Landau-Peierls field 31
2.2.3 Momentum space formulation 32
2.2.4 Correspondence principle 33
2.2.4.1 Quantization in the momentum space $\mathscr{H}_M$ 34
2.2.4.2 Quantization in the Landau-Peierls space $\mathscr{H}_{LP}$ 34

2.2.5 Equivalence between the LP and momentum quantizations 35
2.3 Białynicki-Birula's quantization 36
2.3.1 Hamitonian structure 36
2.3.2 The Riemann-Silberstein vector 37
2.3.3 Alternative choice of canonical variables 38
2.3.4 The Białynicki-Birula complex representation 39
2.3.5 Quantization in the Białynicki-Birula representation 40
2.4 Equivalence between the LP and the BB quantizations — Isomorphism . . 42
2.5 Dynamics in the quantum models 44

2.1 Fock space and quantization procedure

The major novelty brought by quantum field theory is to allow processes for which the number of quanta in the system is not fixed. To have a well-defined mathematical description of such processes, we introduce a new type of Hilbert space for the states called Fock space. Given a one-particle Hilbert space $\mathscr{H}$, the corresponding bosonic Fock space is defined as the direct sum of spaces of n quanta [76, 77]

$$\mathbb{F}^{\mathfrak{B}}(\mathscr{H}) = \bigoplus_{n=0}^{\infty} \mathscr{H}^{\otimes_S n}, \tag{2.1}$$

where $\mathscr{H}^{\otimes_S n}$ is the symmetrized n-times tensor product of $\mathscr{H}$ with itself. A similar construction using the anti-symmetrized tensor product could be done for fermions but in the following, we will use the Fock space only for photons that are known to be bosons[1]. Each subspace corresponds thus to a fixed number of quanta

$$\begin{aligned}
\mathscr{H}^{\otimes_S 0} &= \mathbb{C} \equiv \text{Hilbert space of the vaccum,}\\
\mathscr{H}^{\otimes_S 1} &= \mathscr{H} \equiv \text{Hilbert space of one-quantum states,}\\
\mathscr{H}^{\otimes_S 2} &= \mathscr{H} \otimes_S \mathscr{H} \equiv \text{Hilbert space of two-quanta states,}\\
&\vdots\\
\mathscr{H}^{\otimes_S n} &= \underbrace{\mathscr{H} \otimes_S \ldots \otimes_S \mathscr{H}}_{n \text{ times}} \equiv \text{Hilbert space of } n\text{-quanta states.}
\end{aligned}$$

The symmetrized tensor product formally represented by $\otimes_S$ hides in fact the following construction

$$\eta_1 \otimes_S \ldots \otimes_S \eta_n = \mathcal{S}_n \left(\eta_1 \otimes \ldots \otimes \eta_n\right), \tag{2.2}$$

$\{\eta_i\}$ being elements of $\mathscr{H}$ and $\mathcal{S}_n$ the projectors into the symmetric subspaces defined by

$$\mathcal{S}_n \left(\eta_1 \otimes \ldots \otimes \eta_n\right) = \frac{1}{n!} \sum_{\varsigma \in \mathscr{P}_n} \left(\eta_{\varsigma_1} \otimes \ldots \otimes \eta_{\varsigma_n}\right), \tag{2.3}$$

[1] Photons are known to be bosons and several arguments can support this claim: experimental evidences, e.g., Hong-Ou-Mandel effect with bunching property (see Chapter 3); but also theoretical one like the spin statistics theorem [78]. One can also remark that the quantum field theory of light emerges as a collection of independent harmonic oscillators which suggests the bosonic construction as we will later see in this chapter.

with a sum over every permutation ς in the permutation group $\mathscr{P}_n$ of order n.
A state $|\Phi\rangle$ of the Fock space can be labeled by a sequence

$$|\Phi\rangle = (|\phi_0\rangle, |\phi_1\rangle, |\phi_2\rangle, \dots), \tag{2.4}$$

where each $|\phi_m\rangle \in \mathscr{H}^{\otimes_S m}$ can be written as a linear combination of terms of the form

$$|\eta_1 \otimes_S \cdots \otimes_S \eta_m\rangle . \tag{2.5}$$

The construction we have done so far is general in the sense that it would be the same for any field whose quantum excitations are bosons. The only difference will appear from the choice of the one-quantum Hilbert space $\mathscr{H}$ that is made.
We construct then creation-annihilation operators allowing to go from one subspace with a fixed number of quanta to another built for any $\eta \in \mathscr{H}$ as

$$\hat{B}_\eta^\dagger : \mathscr{H}^{\otimes_S n} \to \mathscr{H}^{\otimes_S (n+1)}, \qquad \hat{B}_\eta : \mathscr{H}^{\otimes_S n} \to \mathscr{H}^{\otimes_S (n-1)}, \tag{2.6}$$

and defined on the tensor product monomials by

$$\hat{B}_\eta^\dagger |\eta_1 \otimes \ldots \otimes \eta_n\rangle = \sqrt{n+1}\, \mathcal{S}_{n+1} |\eta \otimes \eta_1 \otimes \ldots \otimes \eta_n\rangle , \tag{2.7a}$$

$$\hat{B}_\eta |\eta_1 \otimes \ldots \otimes \eta_n\rangle = \frac{1}{\sqrt{n}} \sum_{j=1}^{n} \langle \eta | \eta_j \rangle_{\mathscr{H}}\ \mathcal{S}_{n-1} |\eta_1 \otimes \ldots \otimes \not{\eta}_j \ldots \otimes \eta_n\rangle , \tag{2.7b}$$

where the notation $\not{\eta}_j$ indicates that this term is missing and $\langle \cdot | \cdot \rangle_{\mathscr{H}}$ refers to the scalar product in $\mathscr{H}$. They fulfill the standard bosonic commutation rules[2] [33, 80]

$$\left[\hat{B}_{\eta_1}, \hat{B}_{\eta_2}^\dagger\right] = \langle \eta_1 | \eta_2 \rangle_{\mathscr{H}} , \tag{2.8a}$$

$$\left[\hat{B}_{\eta_1}, \hat{B}_{\eta_2}\right] = 0 = \left[\hat{B}_{\eta_1}^\dagger, \hat{B}_{\eta_2}^\dagger\right] . \tag{2.8b}$$

The Fock space will be central in the construction of the quantum theory of the electromagnetic field as we will see in the coming sections.
As a quick reminder, we recall the quantization procedure we will extensively repeat in the next sections to construct the quantum theory of the electromagnetic field in several momentum and position space representations. It consists in the following steps:

- Formulate Maxwell's equations in a Hamiltonian form, identifying a pair of canonical variables, defining a phase space such that the corresponding Hamilton equations are equivalent to Maxwell's equations.
- Construct a complex Hilbert space $\mathscr{H}$ of classical configurations and a complex representation of the Hamiltonian structure.
- Build a bosonic Fock space by following the general procedure we have presented before.

[2] If the $\{\eta_i\}$ are orthonormal states, the commutation relation (2.8a) is thus equal to a Kronecker delta $\delta_{1,2}$ and it gives back the standard formulation in terms, e.g., of plane waves as it is often formulated in the quantum optics literature [29, 79].

- Construct quantum observables from their classical equivalent using a correspondence principle.
- Define the generator of the quantum dynamics in Fock space from the single-photon dynamics, which is determined by the classical Hamiltonian dynamics.

2.2 Quantization in the Coulomb gauge

The first step to construct a one-quantum Hilbert space which suitably represents the theory to quantize, is to find a Hamiltonian formulation of that specific theory. We will construct in the following, a real Hamiltonian formulation and then a complex version of it from which the one-quantum Hilbert space can be easily built. This construction will be done in both position and momentum representations and the explicit isomorphism linking the two representations will be introduced.

2.2.1 Hamiltonian formulation

We start by recalling Maxwell's equations in the form we introduced in Chapter 1 equations (1.14), (1.16), (1.19a) and (1.20) but now expressed for the particular case of the vacuum, i.e., $\varepsilon_{\mathrm{m}} = 1$:

$$\frac{\partial^2 \vec{A}}{\partial t^2} = c^2 \Delta \vec{A}, \tag{2.9a}$$

$$\nabla \cdot \vec{A} = 0, \tag{2.9b}$$

$$\vec{B} = \nabla \times \vec{A}, \tag{2.9c}$$

$$\vec{E} = -\frac{\partial \vec{A}}{\partial t}. \tag{2.9d}$$

We have also used $\nabla \times \nabla \times = -\Delta$ which can be deduced from $\nabla \cdot \vec{A} = 0$. By choosing as canonical variables $\vec{A}$ and its conjugate variable $\vec{\Pi} = \varepsilon_0 \frac{\partial \vec{A}}{\partial t} = -\varepsilon_0 \vec{E}$, the wave equation (2.9a) can be written in a Hamiltonian form[3]

$$\frac{\partial \vec{A}}{\partial t} = \frac{\delta H}{\delta \vec{\Pi}} = \frac{\vec{\Pi}}{\varepsilon_0}, \tag{2.10a}$$

$$\frac{\partial \vec{\Pi}}{\partial t} = -\frac{\delta H}{\delta \vec{A}} = \varepsilon_0 c^2 \Delta \vec{A} = -\varepsilon_0 \Omega^2 \vec{A}, \tag{2.10b}$$

where the Hamilton function H is given by

$$H = \int_{\mathbb{R}^3} d^3x \left(\frac{1}{2\varepsilon_0} \vec{\Pi} \cdot \vec{\Pi} + \frac{\varepsilon_0}{2} \vec{A} \cdot \Omega^2 \vec{A} \right). \tag{2.11}$$

The Hamilton equations (2.10) and the constraints

$$\nabla \cdot \vec{A} = 0, \tag{2.12a}$$

$$\nabla \cdot \vec{\Pi} = 0, \tag{2.12b}$$

are equivalent to Maxwell's equations (2.9).

[3] A detailed description of Hamiltonian mechanics can be found in the following references [81–83].

Remark: The Hamilton function H has a structure similar to a one-dimensional harmonic oscillator where ε_0 takes the place of the mass, and the operator Ω takes the place of the frequency. Because of this analogy, it has been stated that Maxwell's equations look like an infinite dimensional harmonic oscillator. This image can be used as a guideline for the construction of the quantized theory in terms of a bosonic Fock space for the states. The role of Ω also justifies a posteriori its denomination as frequency operator (see Chapter 1).

2.2.2 Complex representation — The Landau-Peierls field

To construct a complex Hilbert space with the Hamiltonian structure introduced before, we define the following complex field, called the Landau-Peierls (LP) field [15, 18, 19] as

$$\vec{\psi} = \frac{1}{\sqrt{2\hbar}} \left[(\varepsilon_0 \Omega)^{1/2} \vec{A} + i(\varepsilon_0 \Omega)^{-1/2} \vec{\Pi} \right], \tag{2.13}$$

from which we build the Hilbert space

$$\mathscr{H}_{LP} = \left\{ \vec{\psi}(\vec{x}) \middle| \nabla \cdot \vec{\psi} = 0, \ \ \langle \vec{\psi} | \vec{\psi} \rangle_{LP} < \infty \right\}, \tag{2.14}$$

with the scalar product

$$\langle \vec{\psi} | \vec{\psi}' \rangle_{LP} = \int_{\mathbb{R}^3} d^3x \ \vec{\psi}^\star(\vec{x}) \cdot \vec{\psi}'(\vec{x}). \tag{2.15}$$

Remark: The LP Hilbert space $\mathscr{H}_{LP}$ is a complex representation of pulse shaped electromagnetic fields. Therefore, it does not contain fields which carry infinite energy such as plane waves. Nevertheless, we will make an extensive use of fields that are not in $\mathscr{H}_{LP}$, e.g., circularly polarized plane waves $\vec{\phi}_{\vec{k},\lambda}$, as generalized eigenfunctions of selfadjoint differential operators.

The Hamilton function in terms of the LP complex variable takes the form

$$H = \hbar \int_{\mathbb{R}^3} d^3x \ \vec{\psi}^\star \cdot \Omega \vec{\psi}, \tag{2.16}$$

and the corresponding complex Hamilton equation is

$$i \frac{\partial \vec{\psi}}{\partial t} = \frac{1}{\hbar} \frac{\delta H}{\delta \vec{\psi}^\star} = \Omega \vec{\psi}. \tag{2.17}$$

Together with the transversality constraint $\nabla \cdot \vec{\psi} = 0$, they are equivalent to Maxwell's equations (2.9). We remark that (2.17) has the form of a Schrödinger equation where Ω is the generator of the dynamics. This result will be central when considering dynamics in the quantum model (Section 2.5).
Electromagnetic fields can be recovered from $\vec{\psi}$ by inverting (2.13),

$$\vec{A}(\vec{x}) = \sqrt{\frac{\hbar}{2\varepsilon_0}} \Omega^{-1/2} \left(\vec{\psi}(\vec{x}) + \vec{\psi}^\star(\vec{x}) \right), \tag{2.18a}$$

$$\vec{E}(\vec{x}) = i \sqrt{\frac{\hbar}{2\varepsilon_0}} \Omega^{1/2} \left(\vec{\psi}(\vec{x}) - \vec{\psi}^\star(\vec{x}) \right), \tag{2.18b}$$

$$\vec{B}(\vec{x}) = \sqrt{\frac{\hbar}{2\varepsilon_0}} \Omega^{-1/2} \nabla \times \left(\vec{\psi}(\vec{x}) + \vec{\psi}^\star(\vec{x}) \right). \tag{2.18c}$$

2.2.3 Momentum space formulation

A similar procedure can be done in the reciprocal momentum (or Fourier) space. In this section we will only give the main results of that description and the link with the position description. For a more detailed overview of this formulation, we refer to the standard quantization of the free electromagnetic field of the quantum optics literature [28, 29, 31–34, 67, 79].
We use the orthonormal basis of circular polarization plane waves (1.61) to decompose $\vec{\psi}$ as

$$\vec{\psi}(\vec{x}) = \int_{\mathbb{R}^3} d^3k \sum_{\lambda=\pm} \vec{\phi}_{\vec{k},\lambda}(\vec{x}) z(\vec{k},\lambda), \tag{2.19}$$

where $z(\vec{k},\lambda) = \langle \vec{\phi}_{\vec{k},\lambda} | \vec{\psi} \rangle_{LP} \in \mathbb{C}$. We define the momentum Hilbert space as

$$\mathscr{H}_M = \{ z(\vec{k},\lambda) \mid \langle z|z \rangle_M < \infty \}, \tag{2.20}$$

endowed with the scalar product

$$\langle z|z' \rangle_M = \int_{\mathbb{R}^3} d^3k \sum_{\lambda=\pm} z^\star(\vec{k},\lambda) z'(\vec{k},\lambda). \tag{2.21}$$

The denomination of this space as momentum space is anticipated from the quantized theory since in that context, the variable $\vec{k}$ is proportional to the momentum of monochromatic photons. It is sometimes also referred to as the Fourier space representation since it is related to the position space formulation by a decomposition into the circular plane waves basis which is very close to a Fourier transform. Indeed, one can pass from the position space description to the momentum description using the map

$$\begin{aligned} &\mathcal{M} : \mathscr{H}_{LP} \to \mathscr{H}_M \\ &\quad \vec{\psi}(\vec{x}) \mapsto z(\vec{k},\lambda) = \int_{\mathbb{R}^3} d^3x \ \vec{\phi}^\star_{\vec{k},\lambda}(\vec{x}) \cdot \vec{\psi}(\vec{x}), \end{aligned} \tag{2.22}$$

which is a unitary transformation providing an isomorphism between the two Hilbert spaces. The inverse map $\mathcal{M}^{-1}$ is given by (2.19), and the equivalence of the scalar products can be computed as

$$\langle z|z' \rangle_M = \int_{\mathbb{R}^3} d^3k \sum_{\lambda=\pm} z^\star(\vec{k},\lambda) z'(\vec{k},\lambda) \tag{2.23a}$$

$$= \int_{\mathbb{R}^3} d^3k \sum_{\lambda=\pm} \left(\int_{\mathbb{R}^3} d^3x \ \vec{\phi}_{\vec{k},\lambda}(\vec{x}) \cdot \vec{\psi}^\star(\vec{x}) \right) \left(\int_{\mathbb{R}^3} d^3y \ \vec{\phi}^\star_{\vec{k},\lambda}(\vec{y}) \cdot \vec{\psi}'(\vec{y}) \right) \tag{2.23b}$$

$$= \int_{\mathbb{R}^3} d^3x \int_{\mathbb{R}^3} d^3y \ \vec{\psi}^\star(\vec{x}) \cdot \left(\int_{\mathbb{R}^3} d^3k \sum_{\lambda=\pm} \vec{\phi}_{\vec{k},\lambda}(\vec{x}) \vec{\phi}^\star_{\vec{k},\lambda}(\vec{y}) \right) \cdot \vec{\psi}'(\vec{y}) \tag{2.23c}$$

$$= \int_{\mathbb{R}^3} d^3x \int_{\mathbb{R}^3} d^3y \ \vec{\psi}^\star(\vec{x}) \cdot \delta^T(\vec{x}-\vec{y}) \vec{\psi}'(\vec{y}) \tag{2.23d}$$

$$= \langle \psi | \vec{\psi}' \rangle_{LP}, \tag{2.23e}$$

where we have used the completeness (1.66) of the basis $\{\vec{\phi}_{\vec{k},\lambda}\}$. The Hamilton function expressed in the new variables takes the form

$$H = \int_{\mathbb{R}^3} d^3k \sum_{\lambda=\pm} \hbar\omega_{\vec{k}}\ z^\star(\vec{k},\lambda) z(\vec{k},\lambda), \tag{2.24}$$

and can be put in a harmonic oscillator form

$$H = \int_{\mathbb{R}^3} d^3k \sum_{\lambda=\pm} \left(\frac{1}{2\varepsilon_0} p^2_{\vec{k},\lambda} + \frac{1}{2}\varepsilon_0 \omega^2_{\vec{k}} q^2_{\vec{k},\lambda} \right), \tag{2.25}$$

by defining the real variables

$$p_{\vec{k},\lambda} = -i\sqrt{\frac{\hbar\varepsilon_0\omega_{\vec{k}}}{2}}(z - z^\star), \tag{2.26a}$$

$$q_{\vec{k},\lambda} = \sqrt{\frac{\hbar}{2\varepsilon_0\omega_{\vec{k}}}}(z + z^\star), \tag{2.26b}$$

$$z(\vec{k},\lambda) = \frac{1}{\sqrt{2\hbar}} \left((\varepsilon_0\omega_{\vec{k}})^{1/2} q_{\vec{k},\lambda} + i(\varepsilon_0\omega_{\vec{k}})^{-1/2} p_{\vec{k},\lambda} \right). \tag{2.26c}$$

The Hamilton equation for the complex and real variables can be written as

$$i\frac{\partial z}{\partial t} = \frac{1}{\hbar}\frac{\delta H}{\delta z^\star} = \omega_{\vec{k}} z, \tag{2.27}$$

and

$$\frac{\partial q_{\vec{k},\lambda}}{\partial t} = \frac{\delta H}{\delta p_{\vec{k},\lambda}} = \frac{p_{\vec{k},\lambda}}{\varepsilon_0}, \tag{2.28a}$$

$$\frac{\partial p_{\vec{k},\lambda}}{\partial t} = -\frac{\delta H}{\delta q_{\vec{k},\lambda}} = -\varepsilon_0\omega^2_{\vec{k}} q_{\vec{k},\lambda}. \tag{2.28b}$$

One of the advantages of the momentum representation for the quantization, is that the canonical variables $(q_{\vec{k},\lambda}, p_{\vec{k},\lambda})$ or $(z(\vec{k},\lambda), z(\vec{k},\lambda)^\star)$, are free of constraints and can thus be quantized by applying directly a correspondence principle as we will show in the following section.

2.2.4 Correspondence principle

Using the general construction presented in Section 2.1 for the bosonic Fock space, and the two classical Hilbert spaces of states constructed from the complex formulations of Maxwell's equations, we can build the quantum model. The next step now is to associate classical objects to the already constructed operators acting on the Fock space. For a system like the Maxwell field that has a quadratic Hamiltonian, it can be done through a principle of correspondence, suggested by the fact that in the momentum space, the classical Hamilton function (2.25) has the form of an infinite collection of independent harmonic oscillators.

2.2.4.1 Quantization in the momentum space $\mathscr{H}_M$

By this analogy, one postulates the following rule of correspondence, first defined in the momentum Fock space $\mathbb{F}^{\mathfrak{B}}(\mathscr{H}_M)$:

$$\text{Quantization map:} \qquad z(\vec{k},\lambda) \mapsto \hat{B}_{\varphi_{\vec{k},\lambda}}, \tag{2.29a}$$

$$z^\star(\vec{k},\lambda) \mapsto \hat{B}^\dagger_{\varphi_{\vec{k},\lambda}}, \tag{2.29b}$$

where $\varphi_{\vec{k},\lambda}$ are the generalized basis eigenfunctions in $\mathscr{H}_M$ given by

$$\varphi_{\vec{k},\lambda}(\vec{k}',\lambda') = \mathcal{M}\vec{\phi}_{\vec{k},\lambda} \tag{2.30a}$$

$$= \int_{\mathbb{R}^3} d^3x \ \vec{\phi}^\star_{\vec{k}',\lambda'}(\vec{x}) \cdot \vec{\phi}_{\vec{k},\lambda}(\vec{x}) \tag{2.30b}$$

$$= \delta_{\lambda,\lambda'}\delta(\vec{k}-\vec{k}'), \tag{2.30c}$$

which comes from the orthonormality of the functions $\vec{\phi}_{\vec{k},\lambda}$.

2.2.4.2 Quantization in the Landau-Peierls space $\mathscr{H}_{LP}$

By the isomorphism $\mathcal{M}$ (2.19), the correspondence rule can be translated to the position LP Fock space $\mathbb{F}^{\mathfrak{B}}(\mathscr{H}_{LP})$ and gives:

$$\text{Quantization map:} \qquad \vec{\psi}(\vec{x}) \mapsto \int_{\mathbb{R}^3} d^3k \sum_{\lambda=\pm} \vec{\phi}_{\vec{k},\lambda}(\vec{x})\hat{B}_{\vec{\phi}_{\vec{k},\lambda}} = \vec{\hat{\Psi}}(\vec{x}), \tag{2.31a}$$

$$\vec{\psi}^\star(\vec{x}) \mapsto \int_{\mathbb{R}^3} d^3k \sum_{\lambda=\pm} \vec{\phi}^\star_{\vec{k},\lambda}(\vec{x})\hat{B}^\dagger_{\vec{\phi}_{\vec{k},\lambda}} = \vec{\hat{\Psi}}^\dagger(\vec{x}), \tag{2.31b}$$

which defines the field operators $\vec{\hat{\Psi}}(\vec{x})$ and $\vec{\hat{\Psi}}^\dagger(\vec{x})$. From these maps, one can write the electromagnetic field operators following their classical expressions (2.18)

$$\vec{\hat{A}}(\vec{x}) = \sqrt{\frac{\hbar}{2\varepsilon_0}}\Omega^{-1/2}\left(\vec{\hat{\Psi}}(\vec{x}) + \vec{\hat{\Psi}}^\dagger(\vec{x})\right), \tag{2.32a}$$

$$\vec{\hat{E}}(\vec{x}) = i\sqrt{\frac{\hbar}{2\varepsilon_0}}\Omega^{1/2}\left(\vec{\hat{\Psi}}(\vec{x}) - \vec{\hat{\Psi}}^\dagger(\vec{x})\right), \tag{2.32b}$$

$$\vec{\hat{B}}(\vec{x}) = \sqrt{\frac{\hbar}{2\varepsilon_0}}\Omega^{-1/2}\nabla\times\left(\vec{\hat{\Psi}}(\vec{x}) + \vec{\hat{\Psi}}^\dagger(\vec{x})\right). \tag{2.32c}$$

Remark: We point out that the interpretation of the field operators $\vec{\hat{\Psi}}^\dagger$ and $\vec{\hat{\Psi}}$ is not to be confused with that of the creation-anihilation operators $\hat{B}^\dagger_{\vec{\psi}}$ and $\hat{B}_{\vec{\psi}}$ for $\vec{\psi} \in \mathscr{H}_{LP}$. Indeed, when applied to the vacuum state, $\hat{B}^\dagger_{\vec{\psi}}$ creates a photon carried by the classical solution $\vec{\psi}$ of Maxwell's equations, while each component $\hat{\Psi}^\dagger_j$ is an operator-valued distribution which has to be integrated over the whole space acting on a test function to properly create a state. For

instance, if we consider the j^{th} component at a given position $\vec{x}_0$, the field operator yields

$$\hat{\Psi}_j^\dagger(\vec{x}_0)\,|\varnothing\rangle = |\vec{\xi}_{\vec{x}_0,j}\rangle = \int_{\mathbb{R}^3} d^3k \sum_{\lambda=\pm} \phi^{(j)\star}_{\vec{k},\lambda}(\vec{x}_0)\hat{B}^\dagger_{\vec{\phi}_{\vec{k},\lambda}}\,|\varnothing\rangle \tag{2.33a}$$

$$= \int_{\mathbb{R}^3} d^3k \sum_{\lambda=\pm} \phi^{(j)\star}_{\vec{k},\lambda}(\vec{x}_0)\,|\vec{\phi}_{\vec{k},\lambda}\rangle\,, \tag{2.33b}$$

which is not a regular single-photon state since $|\vec{\phi}_{\vec{k},\lambda}\rangle$ are not in $\mathscr{H}_{LP}$ as we discussed before. Similarly, the use of the functions $\vec{\phi}_{\vec{k},\lambda}$ and $\varphi_{\vec{k},\lambda}$ as classical functions onto which photons are created, also yields a singular photon state. That is why we will use them only to decompose regular functions in the Hilbert space, mostly for calculation reasons.

2.2.5 Equivalence between the LP and momentum quantizations

In this section, we show that the isomorphism $\mathcal{M}$ given by equations (2.19), (2.22) and (2.23), provides a direct relation between the quantized theories we have constructed above. Indeed, since the central concept of bosonic creation-annihilation operators, which allows one to write any state and observable in the theory, are explicitly linked by the classical isomorphism $\mathcal{M}$, all physical predictions made with the two representations are the same.
If one considers, e.g., a single-photon state in the position space LP representation which reads

$$\hat{B}^\dagger_{\vec{\psi}}|\varnothing\rangle_{LP} = |\vec{\psi}\rangle_{LP}\,, \tag{2.34}$$

with $\vec{\psi} \in \mathscr{H}_{LP}$. One can use the isomorphism $\mathcal{M}$ to write it in terms of a creation operator in the momentum space as follows

$$|\vec{\psi}\rangle_{LP} = |\mathcal{M}^{-1}z\rangle_{LP} \tag{2.35a}$$

$$= \mathcal{M}^{-1}\,|z\rangle_M \tag{2.35b}$$

$$= \mathcal{M}^{-1}\hat{B}^\dagger_z\,|\varnothing\rangle_M \tag{2.35c}$$

$$= \mathcal{M}^{-1}\hat{B}^\dagger_z\mathcal{M}\,|\varnothing\rangle_{LP}\,, \tag{2.35d}$$

from which we deduce that $\hat{B}^\dagger_{\vec{\psi}} = \mathcal{M}^{-1}\hat{B}^\dagger_z\mathcal{M} = \mathcal{M}^{-1}\hat{B}^\dagger_{\mathcal{M}\vec{\psi}}\mathcal{M}$, where $\hat{B}^\dagger_z : \mathscr{H}_M^{\otimes_S l} \to \mathscr{H}_M^{\otimes_S (l+1)}$ is the creation operator acting on the momentum Fock space $\mathbb{F}^{\mathfrak{B}}(\mathscr{H}_M)$. We have extended here the isomorphism $\mathcal{M}$ to the whole Fock space by defining its action on the vacuum state: $\mathcal{M}\,|\varnothing\rangle_{LP} = |\varnothing\rangle_M$. The same state can then be described in one or the other representation without ambiguity.

Remark: Photon states $|z\rangle_M$ or $|\vec{\psi}\rangle_{LP}$ are well defined for any classical configuration z or $\vec{\psi}$, without any restriction about their normalization. However, for simplicity of their interpretation, they are often chosen to be normalized, i.e., $\langle z|z\rangle_M = \langle\vec{\psi}|\vec{\psi}\rangle_{LP} = 1$. If the state function is not normalized, it is anyway always possible to rewrite the photon state in terms of a normalized classical function for example: if $\langle\vec{\psi}'|\vec{\psi}'\rangle_{LP} \neq 1$, it can be rewritten as $\vec{\psi}' = \alpha\vec{\psi}$ for $\alpha \in \mathbb{C}$ and $\langle\vec{\psi}|\vec{\psi}\rangle_{LP} = 1$, which yields an unnormalized photon state of the form $|\vec{\psi}'\rangle = \hat{B}^\dagger_{\alpha\vec{\psi}}|\varnothing\rangle = \alpha\,|\vec{\psi}\rangle$. We will see in Chapter 3 that unnormalized states of this form

naturally appear through the dynamics.

Regarding the observables, one can for instance express the electric field in terms of creation-annihilation operators in the LP position representation as

$$\hat{\vec{E}}_{LP}(\vec{x}) = i\sqrt{\frac{\hbar}{2\varepsilon_0}}\Omega^{1/2}\left(\hat{\vec{\Psi}}(\vec{x}) - \hat{\vec{\Psi}}^\dagger(\vec{x})\right) \tag{2.36a}$$

$$= i\sqrt{\frac{\hbar}{2\varepsilon_0}}\int_{\mathbb{R}^3} d^3k \sum_{\lambda=\pm} \omega_{\vec{k}}^{1/2}\left(\vec{\phi}_{\vec{k},\lambda}(\vec{x})\hat{B}_{\vec{\phi}_{\vec{k},\lambda}} - \vec{\phi}^\star_{\vec{k},\lambda}(\vec{x})\hat{B}^\dagger_{\vec{\phi}_{\vec{k},\lambda}}\right), \tag{2.36b}$$

which is then expressed in the momentum representation by

$$\hat{\vec{E}}_M(\vec{x}) = \mathcal{M}\hat{\vec{E}}_{LP}\mathcal{M}^{-1} \tag{2.37a}$$

$$= i\sqrt{\frac{\hbar}{2\varepsilon_0}}\int_{\mathbb{R}^3} d^3k \sum_{\lambda=\pm} \omega_{\vec{k}}^{1/2}\left(\vec{\phi}_{\vec{k},\lambda}(\vec{x})\mathcal{M}\hat{B}_{\vec{\phi}_{\vec{k},\lambda}}\mathcal{M}^{-1} - \vec{\phi}^\star_{\vec{k},\lambda}(\vec{x})\mathcal{M}\hat{B}^\dagger_{\vec{\phi}_{\vec{k},\lambda}}\mathcal{M}^{-1}\right) \tag{2.37b}$$

$$= i\sqrt{\frac{\hbar}{2\varepsilon_0}}\int_{\mathbb{R}^3} d^3k \sum_{\lambda=\pm} \omega_{\vec{k}}^{1/2}\left(\vec{\phi}_{\vec{k},\lambda}(\vec{x})\hat{B}_{\varphi_{\vec{k},\lambda}} - \vec{\phi}^\star_{\vec{k},\lambda}(\vec{x})\hat{B}^\dagger_{\varphi_{\vec{k},\lambda}}\right) \tag{2.37c}$$

$$= i\sqrt{\frac{\hbar}{2\varepsilon_0}}\int_{\mathbb{R}^3} d^3k \sum_{\lambda=\pm} \omega_{\vec{k}}^{1/2}\left(\vec{\phi}_{\vec{k},\lambda}(\vec{x})\hat{a}_{\vec{k},\lambda} - \vec{\phi}^\star_{\vec{k},\lambda}(\vec{x})\hat{a}^\dagger_{\vec{k},\lambda}\right), \tag{2.37d}$$

where we have used in the last equality the usual notation $\hat{a}_{\vec{k},\lambda} = \hat{B}_{\delta_{\lambda,\lambda'}\delta(\vec{k}-\vec{k}')}$ and $\hat{a}^\dagger_{\vec{k},\lambda} = \hat{B}^\dagger_{\delta_{\lambda,\lambda'}\delta(\vec{k}-\vec{k}')}$. Furthermore, if one plugs in the expression of the circular plane wave eigenfunctions (1.61), we obtain the usual expression of the quantum optics literature [29, 31, 33, 67, 79]

$$\hat{\vec{E}}_M(\vec{x}) = i\sqrt{\frac{\hbar}{2\varepsilon_0(2\pi)^3}}\int_{\mathbb{R}^3} d^3k \sum_{\lambda=\pm} \omega_{\vec{k}}^{1/2}\left(\vec{\epsilon}_\lambda(\vec{k})e^{i\vec{k}\cdot\vec{x}}\hat{a}_{\vec{k},\lambda} - \vec{\epsilon}_\lambda(\vec{k})^\star e^{-i\vec{k}\cdot\vec{x}}\hat{a}^\dagger_{\vec{k},\lambda}\right). \tag{2.38}$$

With this example, we have shown how one can pass from one representation to the other using directly the classical isomorphism $\mathcal{M}$ in a standard way, i.e., directly applied to the states and through a similarity relation for creation-annihilation operators or observables. This simple relation guarantees that the predictions one can make with one theory is equal to what is obtained with the other.

2.3 Białynicki-Birula's quantization

2.3.1 Hamitonian structure

We consider now another approach for the quantization which has been developed mainly by Białynicki-Birula [21, 25, 38]. One of the advantages of this construction is that it does not require to choose any particular gauge since it starts by defining the canonical variables to be directly proportional to the electric and magnetic fields as

$$\vec{\mathcal{P}}_{RS} = \frac{\vec{B}}{\sqrt{\mu_0}}, \qquad \vec{\mathcal{Q}}_{RS} = \sqrt{\varepsilon_0}\vec{E}. \tag{2.39}$$

The Hamilton function is defined by

$$K_{RS} = \frac{c}{2}\int_{\mathbb{R}^3} d^3x \left(\vec{\mathcal{P}}_{RS}\cdot\nabla\times\vec{\mathcal{P}}_{RS} + \vec{\mathcal{Q}}_{RS}\cdot\nabla\times\vec{\mathcal{Q}}_{RS}\right) \tag{2.40a}$$

$$= \frac{c}{2}\int_{\mathbb{R}^3} d^3x \left(\varepsilon_0\vec{E}\cdot\nabla\times\vec{E} + \frac{1}{\mu_0}\vec{B}\cdot\nabla\times\vec{B}\right), \tag{2.40b}$$

yielding the following Hamilton equations

$$\frac{\partial\vec{\mathcal{P}}_{RS}}{\partial t} = -\frac{\delta K_{RS}}{\delta\vec{\mathcal{Q}}_{RS}} = -c\nabla\times\vec{\mathcal{Q}}_{RS}, \tag{2.41a}$$

$$\frac{\partial\vec{\mathcal{Q}}_{RS}}{\partial t} = \frac{\delta K_{RS}}{\delta\vec{\mathcal{P}}_{RS}} = c\nabla\times\vec{\mathcal{P}}_{RS}, \tag{2.41b}$$

that are equivalent to Maxwell's equations (1.1). We denote the Hamilton function by K_{RS} and not by H, to emphasize that it is not the total electromagnetic energy [67, 84], which reads

$$\mathcal{E}_{\text{tot}} = \frac{1}{2}\int_{\mathbb{R}^3} d^3x \left(\varepsilon_0\vec{E}\cdot\vec{E} + \frac{1}{\mu_0}\vec{B}\cdot\vec{B}\right) \tag{2.42a}$$

$$= \frac{1}{2}\int_{\mathbb{R}^3} d^3x \left(\vec{\mathcal{P}}_{RS}\cdot\vec{\mathcal{P}}_{RS} + \vec{\mathcal{Q}}_{RS}\cdot\vec{\mathcal{Q}}_{RS}\right). \tag{2.42b}$$

2.3.2 The Riemann-Silberstein vector

From the canonical variables defined above one can construct a complex representation of the field called the Riemann-Silberstein (RS) vector [85]

$$\vec{F}_{RS} = \frac{1}{\sqrt{2}}\left(\vec{\mathcal{Q}}_{RS} + i\vec{\mathcal{P}}_{RS}\right) = \sqrt{\frac{\varepsilon_0}{2}}\left(\vec{E} + ic\vec{B}\right). \tag{2.43}$$

Maxwell's equations can be written in the RS complex representation as

$$i\frac{\partial\vec{F}_{RS}}{\partial t} = -\frac{\delta K_{RS}}{\delta\vec{F}^{\star}_{RS}} = c\nabla\times\vec{F}_{RS}, \tag{2.44}$$

with

$$K_{RS} = c\int_{\mathbb{R}^3} d^3x\ \vec{F}^{\star}_{RS}\cdot\nabla\times\vec{F}_{RS}. \tag{2.45}$$

In analogy with what we did for the Coulomb gauge, we define the unitary map

$$\vec{F}_{RS} \mapsto z_{RS}(\vec{k},\lambda) = \int_{\mathbb{R}^3} d^3x\ \vec{\phi}^{\star}_{\vec{k},\lambda}(\vec{x})\cdot\vec{F}_{RS}(\vec{x}), \tag{2.46}$$

from which we deduce the Hamilton function in terms of the RS momentum variable z_{RS}

$$K_{RS} = \int_{\mathbb{R}^3} d^3k \left[\omega_{\vec{k}}\ z^{\star}_{RS}(\vec{k},+)z_{RS}(\vec{k},+) - \omega_{\vec{k}}\ z^{\star}_{RS}(\vec{k},-)z_{RS}(\vec{k},-)\right]. \tag{2.47}$$

Written in terms of the real variables defined as

$$p^{RS}_{\vec{k},\lambda} = -i\sqrt{\frac{\varepsilon_0\omega_{\vec{k}}}{2}}(z_{RS} - z^{\star}_{RS}), \tag{2.48a}$$

$$q^{RS}_{\vec{k},\lambda} = \sqrt{\frac{1}{2\varepsilon_0\omega_{\vec{k}}}}(z_{RS} + z^{\star}_{RS}), \tag{2.48b}$$

$$z_{RS}(\vec{k},\lambda) = \frac{1}{\sqrt{2}}\left((\varepsilon_0\omega_{\vec{k}})^{1/2}q^{RS}_{\vec{k},\lambda} + i(\varepsilon_0\omega_{\vec{k}})^{-1/2}p^{RS}_{\vec{k},\lambda}\right), \tag{2.48c}$$

the Hamilton function becomes

$$K_{RS} = \int_{\mathbb{R}^3} d^3k \left[\left(\frac{(p^{RS}_{\vec{k},+})^2}{2\varepsilon_0} + \frac{\varepsilon_0}{2}\omega^2_{\vec{k}}(q^{RS}_{\vec{k},+})^2\right) - \left(\frac{(p^{RS}_{\vec{k},-})^2}{2\varepsilon_0} + \frac{\varepsilon_0}{2}\omega^2_{\vec{k}}(q^{RS}_{\vec{k},-})^2\right)\right]. \tag{2.49}$$

We see here that it looks like two infinite collections of independent harmonic oscillators but the second one appears with a minus sign. This situation is similar to the one encountered with the Dirac equation, in which the electrons could have positive and negative energies. It poses a difficulty for the construction of the quantized model. However, this difficulty can be avoided by making a different choice for the canonical variables, as we describe in the next section. The construction we are going to introduce is strongly inspired by the work of Białynicki-Birula (BB) [21] which is the reason why we will call it the BB complex representation, although we formulate it in a slightly different form.

2.3.3 Alternative choice of canonical variables

To construct canonical variables that avoid the difficulty of the negative eigenvalues described above, we have to locate the variables that lead to negative contributions. This can be done using the notion of helicity (see Chapter 1) which allows us to decompose the RS vector into its positive and negative helicity parts $\vec{F}_{RS} = \vec{F}^{(h+)}_{RS} + \vec{F}^{(h-)}_{RS}$ or equivalently in terms of the real canonical variables $\vec{\mathcal{P}}_{RS} = \vec{\mathcal{P}}^{(h+)}_{RS} + \vec{\mathcal{P}}^{(h-)}_{RS}$ and $\vec{\mathcal{Q}}_{RS} = \vec{\mathcal{Q}}^{(h+)}_{RS} + \vec{\mathcal{Q}}^{(h-)}_{RS}$, from which the Hamilton function takes the form

$$\begin{aligned} K_{RS} &= \frac{c}{2}\int_{\mathbb{R}^3} d^3x \left[\left(\vec{\mathcal{P}}^{(h+)}_{RS}\cdot\nabla\times\vec{\mathcal{P}}^{(h+)}_{RS} + \vec{\mathcal{Q}}^{(h+)}_{RS}\cdot\nabla\times\vec{\mathcal{Q}}^{(h+)}_{RS}\right) + \right. \\ &\qquad \left.\left(\vec{\mathcal{P}}^{(h-)}_{RS}\cdot\nabla\times\vec{\mathcal{P}}^{(h-)} + \vec{\mathcal{Q}}^{(h-)}_{RS}\cdot\nabla\times\vec{\mathcal{Q}}^{(h-)}_{RS}\right)\right] \qquad (2.50a) \\ &= \frac{1}{2}\int_{\mathbb{R}^3} d^3x \left[\left(\vec{\mathcal{P}}^{(h+)}_{RS}\cdot\Omega\vec{\mathcal{P}}^{(h+)}_{RS} + \vec{\mathcal{Q}}^{(h+)}_{RS}\cdot\Omega\vec{\mathcal{Q}}^{(h+)}_{RS}\right) - \right. \\ &\qquad \left.\left(\vec{\mathcal{P}}^{(h-)}_{RS}\cdot\Omega\vec{\mathcal{P}}^{(h-)}_{RS} + \vec{\mathcal{Q}}^{(h-)}_{RS}\cdot\Omega\vec{\mathcal{Q}}^{(h-)}_{RS}\right)\right], \qquad (2.50b) \end{aligned}$$

where we have used $c\nabla\times = \Omega\Lambda$ to obtain the second expression and the fact that $\Lambda\vec{v}^{(h\pm)} = \pm\vec{v}^{(h\pm)}$. It shows that the negative contributions identified in the momentum representation come from the negative helicity part of the field. To circumvent this problem, one can define new canonical variables that we call the BB variables

$$\vec{\mathcal{Q}}_{BB} = \vec{\mathcal{Q}}_{RS}, \qquad \vec{\mathcal{P}}_{BB} = \Lambda\vec{\mathcal{P}}_{RS}, \tag{2.51}$$

and a new classical Hamilton function

$$K_{BB} = \frac{1}{2}\int_{\mathbb{R}^3} d^3x \left[\left(\vec{\mathcal{P}}_{BB}^{(h+)} \cdot \Omega\vec{\mathcal{P}}_{BB}^{(h+)} + \vec{\mathcal{Q}}_{BB}^{(h+)} \cdot \Omega\vec{\mathcal{Q}}_{BB}^{(h+)}\right) + \left(\vec{\mathcal{P}}_{BB}^{(h-)} \cdot \Omega\vec{\mathcal{P}}_{BB}^{(h-)} + \vec{\mathcal{Q}}_{BB}^{(h-)} \cdot \Omega\vec{\mathcal{Q}}_{BB}^{(h-)}\right)\right], \tag{2.52}$$

which is positive since Ω is a positive operator, as opposed to $\nabla\times$. This alternative choice of the canonical variables thus avoids the problem of negative eigenvalues. We emphasize that K_{BB} is not the Hamilton function K_{RS} expressed in the new variables since the relation (2.51) is not a canonical transformation.

2.3.4 The Białynicki-Birula complex representation

We have chosen with the BB variables a different Hamiltonian structure that gives the same classical Maxwell equations. For the complex representation, we define thus a modification of the RS vector adapted to the new canonical variables which we call the Białynicki-Birula vector

$$\vec{F} = \frac{1}{\sqrt{2}}\left(\vec{\mathcal{Q}}_{BB} + i\vec{\mathcal{P}}_{BB}\right) = \sqrt{\frac{\varepsilon_0}{2}}\left(\vec{E} + ic\Lambda\vec{B}\right), \tag{2.53}$$

which can be decomposed in the six-component field (bispinor) notation used originally in [21]

$$\Psi_{BB} = \begin{pmatrix} \vec{F}^{(h+)} \\ \vec{F}^{(h-)} \end{pmatrix} = \begin{pmatrix} \vec{F}_{RS}^{(h+)} \\ \vec{F}_{RS}^{(h-)\star} \end{pmatrix}. \tag{2.54}$$

The Hamilton function K_{BB} in the BB complex representation reads

$$K_{BB} = \int_{\mathbb{R}^3} d^3x\ \vec{F}^{\star} \cdot \Omega\vec{F}, \tag{2.55}$$

and the corresponding Hamilton equations can be written as

$$i\frac{\partial\vec{F}}{\partial t} = \frac{\delta K_{BB}}{\delta\vec{F}^{\star}} = \Omega\vec{F}. \tag{2.56}$$

Using the six-component notation Ψ_{BB} the last two equations are equivalent to

$$K_{BB} = \int_{\mathbb{R}^3} d^3x\ \Psi_{BB}^{\star} \cdot \Omega\Psi_{BB}, \tag{2.57}$$

and

$$i\frac{\partial\Psi_{BB}}{\partial t} = \frac{\delta K_{BB}}{\delta\Psi_{BB}^{\star}} = \Omega\Psi_{BB}. \tag{2.58}$$

Remarks:

- The BB vector $\vec{F}$ that we introduced here was not mentioned explicitly in [21,25] but is a completely equivalent formulation of the original formulation using the six-component field Ψ_{BB}. We prefer, however, to use $\vec{F}$ since it is a more compact notation which allows us to write simpler formulas especially when we will introduce the isomorphism with the LP field.
- In the original works of BB [21], the six-component field Ψ_{BB} was defined using the

positive and negative frequency parts of the RS field which we denote by $\vec{F}_{RS}^{(f\pm)}$, instead of the positive and negative helicity parts as we have done here. This difference does not change anything for the definition of Ψ_{BB} since $\vec{F}_{RS}^{(h\pm)} = \vec{F}_{RS}^{(f\pm)}$ (see Appendix A). However, we stress out that this property is in general not true, e.g., $\vec{\psi}^{(h\pm)} \neq \vec{\psi}^{(f\pm)}$ since $\vec{\psi}^{(f-)} = 0$ for any $\vec{\psi} \in \mathscr{H}_{LP}$ while $\vec{\psi}^{(h-)} \neq 0$ in general. Other examples are the electric and the magnetic fields for which $\vec{E}^{(h\pm)} \neq \vec{E}^{(f\pm)}$ and $\vec{B}^{(h\pm)} \neq \vec{B}^{(f\pm)}$. Explicit demonstrations of these relations are given in the Appendix A

- The construction introduced here is similar to what is done for the Dirac equation to remove the negative energy solutions and which led to the interpretation of anti-matter. However, in our case the negative contributions are not negative energies since K_{RS} is not the energy of the field. We remove them because it is more convenient for the quantization as we will see later, and it allows to make the link with the quantization in the Coulomb gauge explicit.
- The RS vector can be expressed in terms of the BB vector as

$$\vec{F}_{RS} = \sqrt{\frac{\varepsilon_0}{2}}\left(\vec{E} + ic\vec{B}\right) \tag{2.59a}$$

$$= \sqrt{\frac{\varepsilon_0}{2}}\left(\vec{E}^{(h+)} + ic\vec{B}^{(h+)}\right) + \sqrt{\frac{\varepsilon_0}{2}}\left(\vec{E}^{(h-)} + ic\vec{B}^{(h-)}\right) \tag{2.59b}$$

$$= \vec{F}^{(h+)} + \vec{F}^{(h-)\star}. \tag{2.59c}$$

- The BB vector is equal to the wave function proposed by Sipe [20].

2.3.5 Quantization in the Białynicki-Birula representation

Since we have now a well-defined Hamiltonian structure, we can proceed with the quantization, following the same procedure as what we did for the LP field. We associate thus to the BB vector, a classical Hilbert space $\mathscr{H}_{BB}$ defined as

$$\mathscr{H}_{BB} \quad = \left\{\vec{F}(\vec{x}) \middle| \nabla \cdot \vec{F} = 0, \;\; \langle \vec{F} | \vec{F} \rangle_{BB} < \infty \right\} \tag{2.60}$$

with the following weighted scalar product [21, 25, 38]

$$\langle \vec{F} | \vec{F}' \rangle_{BB} = \frac{1}{\hbar} \int_{\mathbb{R}^3} d^3x \;\; \vec{F}^{\star}(\vec{x}) \cdot \Omega^{-1} \vec{F}'(\vec{x}). \tag{2.61}$$

The main motivation for the choice of this weighted scalar product is that it is Lorentz invariant [21,23,24,26]. We will see that it is also an essential ingredient for the isomorphism with the standard quantization in the Coulomb gauge.
Classical electromagnetic fields can be expressed in terms of the BB vector by inverting (2.53) which gives

$$\vec{E}(\vec{x}) = \frac{1}{\sqrt{2\varepsilon_0}}\left(\vec{F}(\vec{x}) + \vec{F}^{\star}(\vec{x})\right), \tag{2.62a}$$

$$\vec{B}(\vec{x}) = \frac{-i}{\sqrt{2\varepsilon_0 c^2}}\Lambda\left(\vec{F}(\vec{x}) - \vec{F}^{\star}(\vec{x})\right). \tag{2.62b}$$

From this classical Hilbert space $\mathscr{H}_{BB}$, one can construct the bosonic Fock space $\mathbb{F}^{\mathfrak{B}}(\mathscr{H}_{BB})$ by the general procedure. The quantum observables associated to the classical physical

quantities are then obtained by a correspondence principle in analogy with what was done for the Coulomb gauge and with the harmonic oscillator structure of the Hamilton function. Indeed, one can develop the BB vector into

$$\vec{F}(\vec{x}) = \int_{\mathbb{R}^3} d^3k \sum_{\lambda=\pm} \vec{g}_{\vec{k},\lambda}(\vec{x}) z_{BB}(\vec{k},\lambda), \quad z_{BB}(\vec{k},\lambda) = \langle \vec{g}_{\vec{k},\lambda} | \vec{F} \rangle_{BB}\,, \tag{2.63a}$$

$$\vec{F}^\star(\vec{x}) = \int_{\mathbb{R}^3} d^3k \sum_{\lambda=\pm} \vec{g}^\star_{\vec{k},\lambda}(\vec{x}) z^\star_{BB}(\vec{k},\lambda), \tag{2.63b}$$

where the functions $\{\vec{g}_{\vec{k},\lambda}\}$ are a generalized orthonormal basis of $\mathscr{H}_{BB}$, which can be taken as $\vec{g}_{\vec{k},\lambda} = i\sqrt{\hbar\omega_{\vec{k}}}\vec{\phi}_{\vec{k},\lambda}$. The quantization map of the BB representation is thus defined by

$$z_{BB} \mapsto \hat{C}_{\vec{g}_{\vec{k},\lambda}}, \tag{2.64a}$$

$$z^\star_{BB} \mapsto \hat{C}^\dagger_{\vec{g}_{\vec{k},\lambda}}, \tag{2.64b}$$

where $\hat{C}^\dagger_{\vec{g}_{\vec{k},\lambda}}$ and $\hat{C}_{\vec{g}_{\vec{k},\lambda}}$ are creation-annihilation operators in the BB Fock space $\mathbb{F}^{\mathfrak{B}}(\mathscr{H}_{BB})$, defined by the general construction (2.7). We also introduce BB field operators as

$$\hat{\vec{\mathbf{F}}}(\vec{x}) = \int_{\mathbb{R}^3} d^3k \sum_{\lambda=\pm} \vec{g}_{\vec{k},\lambda}(\vec{x}) \hat{C}_{\vec{g}_{\vec{k},\lambda}}, \tag{2.65a}$$

$$\hat{\vec{\mathbf{F}}}^\dagger(\vec{x}) = \int_{\mathbb{R}^3} d^3k \sum_{\lambda=\pm} \vec{g}^\star_{\vec{k},\lambda}(\vec{x}) \hat{C}^\dagger_{\vec{g}_{\vec{k},\lambda}}. \tag{2.65b}$$

Quantized electromagnetic observables are given directly by the operators

$$\hat{\vec{E}}(\vec{x}) = \frac{1}{\sqrt{2\varepsilon_0}} \left(\hat{\vec{\mathbf{F}}}(\vec{x}) + \hat{\vec{\mathbf{F}}}^\dagger(\vec{x}) \right), \tag{2.66a}$$

$$\hat{\vec{B}}(\vec{x}) = \frac{-i}{\sqrt{2\varepsilon_0 c^2}} \Lambda \left(\hat{\vec{\mathbf{F}}}(\vec{x}) - \hat{\vec{\mathbf{F}}}^\dagger(\vec{x}) \right). \tag{2.66b}$$

One can check that it corresponds to the quantization proposed by BB, by computing the form of the RS field operator:

$$\hat{\vec{F}}_{RS} = \hat{\vec{\mathbf{F}}}^{(h+)} + \hat{\vec{\mathbf{F}}}^{(h-)\dagger} \tag{2.67a}$$

$$= \int d^3k \sum_{\lambda=\pm} \left[\mathbb{P}^{(h+)} \vec{g}_{\vec{k},\lambda}(\vec{x}) \hat{C}_{\vec{g}_{\vec{k},\lambda}} + \mathbb{P}^{(h-)} \vec{g}^\star_{\vec{k},\lambda}(\vec{x}) \hat{C}^\dagger_{\vec{g}_{\vec{k},\lambda}} \right] \tag{2.67b}$$

$$= \int d^3k \left[\vec{g}_{\vec{k},+}(\vec{x}) \hat{C}_{\vec{g}_{\vec{k},+}} + \vec{g}^\star_{\vec{k},-}(\vec{x}) \hat{C}^\dagger_{\vec{g}_{\vec{k},-}} \right] \tag{2.67c}$$

$$= \int d^3k \left[i\sqrt{\frac{\hbar\omega_{\vec{k}}}{(2\pi)^3}} \vec{\epsilon}_+(\vec{k}) e^{i\vec{k}\cdot\vec{x}} \hat{C}_{\vec{g}_{\vec{k},+}} + i\sqrt{\frac{\hbar\omega_{\vec{k}}}{(2\pi)^3}} \vec{\epsilon}_-(\vec{k})^\star e^{-i\vec{k}\cdot\vec{x}} \hat{C}^\dagger_{\vec{g}_{\vec{k},-}} \right] \tag{2.67d}$$

$$= \int d^3k \sqrt{\frac{\hbar\omega_{\vec{k}}}{(2\pi)^3}} \vec{e}(\vec{k}) \left[e^{i\vec{k}\cdot\vec{x}} \hat{a}(\vec{k}) + e^{-i\vec{k}\cdot\vec{x}} \hat{b}^\dagger(\vec{k}) \right], \tag{2.67e}$$

where we have used the notation $\vec{e}(\vec{k}) = \vec{\epsilon}_+(\vec{k}) = \vec{\epsilon}_-(\vec{k})^\star$ and the creation-annnihilation operators are linked through $\hat{a}(\vec{k}) = i\hat{C}_{\vec{g}_{\vec{k},+}}$ and $\hat{b}^\dagger(\vec{k}) = i\hat{C}^\dagger_{\vec{g}_{\vec{k},+}}$. The expression (2.67) coincides with [38, equation (7)] which confirms that the quantization we have defined in (2.64) coincides with the one used by BB, e.g., in [21, 25, 38, 86–89].

2.4 Equivalence between the LP and the BB quantizations — Isomorphism

In Section 2.2.5, we have shown that the Coulomb gauge quantizations in position and momentum representations are equivalent and linked through explicit relations given by the classical isomorphism $\mathcal{M}$. In the same spirit, we will now introduce a classical isomorphism $\mathcal{I}$ between the LP and the BB Hilbert spaces in order to show that the two constructed quantized theories are equivalent. We will also show how one can pass from one theory to the other through explicit transformations involving the classical isomorphism.
We start by defining the map

$$\begin{aligned} \mathcal{I} : \mathscr{H}_{LP} &\to \mathscr{H}_{BB} \\ \vec{\psi} &\mapsto \vec{F} = \mathcal{I}\vec{\psi} = i\sqrt{\hbar}\Omega^{1/2}\vec{\psi}, \end{aligned} \tag{2.68}$$

which is extended to the Fock space by also defining $\mathcal{I}\,|\varnothing\rangle_{LP} = |\varnothing\rangle_{BB}$. The inverse transformation is given by

$$\begin{aligned} \mathcal{I}^{-1} : \mathscr{H}_{BB} &\to \mathscr{H}_{LP} \\ \vec{F} &\mapsto \vec{\psi} = \mathcal{I}^{-1}\vec{F} = -\frac{i}{\sqrt{\hbar}}\Omega^{-1/2}\vec{F}. \end{aligned} \tag{2.69}$$

One can check that $\mathcal{I}$ indeed links the two representations by computing directly

$$i\sqrt{\hbar}\Omega^{1/2}\vec{\psi} = i\sqrt{\frac{\varepsilon_0}{2}}\left(\Omega\vec{A} - i\vec{E}\right) \tag{2.70a}$$

$$= \sqrt{\frac{\varepsilon_0}{2}}\left(ic\Lambda\nabla\times\vec{A} + \vec{E}\right) \tag{2.70b}$$

$$= \frac{1}{\sqrt{2}}\left(\sqrt{\varepsilon_0}\vec{E} + \frac{i}{\sqrt{\mu_0}}\Lambda\vec{B}\right) \tag{2.70c}$$

$$= \frac{1}{\sqrt{2}}\left(\vec{\mathcal{Q}}_{BB} + i\vec{\mathcal{P}}_{BB}\right) = \vec{F}, \tag{2.70d}$$

where we have used the relation $\Omega = c\Lambda\nabla\times$ and $\Lambda^{-1} = \Lambda$. The equivalence of their respective scalar products follows immediately from the definitions

$$\langle\vec{F}|\vec{F}'\rangle_{BB} = \langle\mathcal{I}\vec{\psi}|\mathcal{I}\vec{\psi}'\rangle_{BB} \tag{2.71a}$$

$$= \frac{1}{\hbar}\int_{\mathbb{R}^3} d^3x\ (\mathcal{I}\vec{\psi})^\star\cdot\Omega^{-1}\mathcal{I}\vec{\psi}' \tag{2.71b}$$

$$= \int_{\mathbb{R}^3} d^3x\ \Omega^{1/2}\vec{\psi}^\star\cdot\Omega^{-1}\Omega^{1/2}\vec{\psi}' \tag{2.71c}$$

$$= \int_{\mathbb{R}^3} d^3x\ \vec{\psi}^\star\cdot\vec{\psi}' = \langle\vec{\psi}|\vec{\psi}'\rangle_{LP}\,, \tag{2.71d}$$

where we have used the selfadjoint property of $\Omega^{1/2}$ to obtain (2.71d).
We can express the link between the creation-annihilation operators of both representations by starting, e.g., with a single-photon state in the LP representation

$$\hat{B}^\dagger_{\vec{\psi}} |\varnothing\rangle_{LP} = |\vec{\psi}\rangle_{LP}\,, \tag{2.72}$$

and by rewriting it using the isomorphism $\mathcal{I}$ as

$$\begin{aligned} |\vec{\psi}\rangle_{LP} &= |\mathcal{I}^{-1}\vec{F}\rangle_{LP} && (2.73a)\\ &= \mathcal{I}^{-1}\,|\vec{F}\rangle_{BB} && (2.73b)\\ &= \mathcal{I}^{-1}\hat{C}^\dagger_{\vec{F}}\,|\varnothing\rangle_{BB} && (2.73c)\\ &= \mathcal{I}^{-1}\hat{C}^\dagger_{\vec{F}}\mathcal{I}\,|\varnothing\rangle_{LP}\,. && (2.73d) \end{aligned}$$

From this one can identify

$$\hat{B}^\dagger_{\vec{\psi}} = \mathcal{I}^{-1}\hat{C}^\dagger_{\vec{F}}\mathcal{I} = \mathcal{I}^{-1}\hat{C}^\dagger_{\mathcal{I}\vec{\psi}}\mathcal{I}, \tag{2.74}$$

and therefore the other relations are

$$\hat{B}_{\vec{\psi}} = \mathcal{I}^{-1}\hat{C}_{\vec{F}}\mathcal{I}, \qquad \hat{C}^\dagger_{\vec{F}} = \mathcal{I}\hat{B}^\dagger_{\vec{\psi}}\mathcal{I}^{-1}, \qquad \hat{C}_{\vec{F}} = \mathcal{I}\hat{B}_{\vec{\psi}}\mathcal{I}^{-1}. \tag{2.75}$$

The equivalence of electromagnetic quantities can be verified for instance for the electric field

$$\begin{aligned} \mathcal{I}\hat{\vec{E}}_{LP}\mathcal{I}^{-1} &= i\sqrt{\frac{\hbar}{2\varepsilon_0}}\int_{\mathbb{R}^3} d^3k \sum_{\lambda=\pm}\omega_{\vec{k}}^{1/2}\left(\vec{\phi}_{\vec{k},\lambda}(\vec{x})\mathcal{I}\hat{B}_{\vec{\phi}_{\vec{k},\lambda}}\mathcal{I}^{-1} - \vec{\phi}^{\star}_{\vec{k},\lambda}(\vec{x})\mathcal{I}\hat{B}^\dagger_{\vec{\phi}_{\vec{k},\lambda}}\mathcal{I}^{-1}\right) && (2.76a)\\ &= i\sqrt{\frac{\hbar}{2\varepsilon_0}}\int_{\mathbb{R}^3} d^3k \sum_{\lambda=\pm}\omega_{\vec{k}}^{1/2}\left(\vec{\phi}_{\vec{k},\lambda}(\vec{x})\hat{C}_{\mathcal{I}\vec{\phi}_{\vec{k},\lambda}} - \vec{\phi}^{\star}_{\vec{k},\lambda}(\vec{x})\hat{C}^\dagger_{\mathcal{I}\vec{\phi}_{\vec{k},\lambda}}\right) && (2.76b)\\ &= \frac{1}{\sqrt{2\varepsilon_0}}\int_{\mathbb{R}^3} d^3k \sum_{\lambda=\pm}\left(\vec{g}_{\vec{k},\lambda}(\vec{x})\hat{C}_{\vec{g}_{\vec{k},\lambda}} - \vec{g}^{\star}_{\vec{k},\lambda}(\vec{x})\hat{C}^\dagger_{\vec{g}_{\vec{k},\lambda}}\right) && (2.76c)\\ &= \frac{1}{\sqrt{2\varepsilon_0}}\left(\vec{\hat{\mathbf{F}}}(\vec{x}) + \vec{\hat{\mathbf{F}}}^\dagger(\vec{x})\right) = \hat{\vec{E}}_{BB}(\vec{x}), && (2.76d) \end{aligned}$$

where we have used the basis $\vec{g}_{\vec{k},\lambda} = \mathcal{I}\vec{\phi}_{\vec{k},\lambda} = i\sqrt{\hbar\omega_{\vec{k}}}\vec{\phi}_{\vec{k},\lambda}$ of $\mathscr{H}_{BB}$ and we have identified $\vec{\hat{\mathbf{F}}}$ and $\vec{\hat{\mathbf{F}}}^\dagger$ by their definitions (2.65). This expression indeed coincides with (2.66a) for the electric field.

Remark: The key point to obtain the last result is to note that applying the isomorphism $\mathcal{I}$ to the electric field operator or any other set of three operators, e.g., the field operator $\hat{\vec{\Psi}}$, should be done component by components, i.e., for $i = 1, 2, 3$,

$$\begin{aligned} \mathcal{I}\hat{E}^{(i)}_{LP}\mathcal{I}^{-1} &= i\sqrt{\frac{\hbar}{2\varepsilon_0}}\int_{\mathbb{R}^3} d^3k \sum_{\lambda=\pm}\omega_{\vec{k}}^{1/2}\mathcal{I}\left(\phi^{(i)}_{\vec{k},\lambda}(\vec{x})\hat{B}_{\vec{\phi}_{\vec{k},\lambda}} - \phi^{(i)\star}_{\vec{k},\lambda}(\vec{x})\hat{B}^\dagger_{\vec{\phi}_{\vec{k},\lambda}}\right)\mathcal{I}^{-1} && (2.77a)\\ &= i\sqrt{\frac{\hbar}{2\varepsilon_0}}\int_{\mathbb{R}^3} d^3k \sum_{\lambda=\pm}\omega_{\vec{k}}^{1/2}\left(\phi^{(i)}_{\vec{k},\lambda}(\vec{x})\mathcal{I}\hat{B}_{\vec{\phi}_{\vec{k},\lambda}}\mathcal{I}^{-1} - \phi^{(i)\star}_{\vec{k},\lambda}(\vec{x})\mathcal{I}\hat{B}^\dagger_{\vec{\phi}_{\vec{k},\lambda}}\mathcal{I}^{-1}\right), && (2.77b) \end{aligned}$$

where $\mathcal{I}$ does not act on $\phi^{(i)}_{\vec{k},\lambda}(\vec{x})$ since it is not an element of the Fock space.

However, one has to be careful when transforming other objects like the field operators $\hat{\vec{\Psi}}$ and $\hat{\vec{\mathbf{F}}}$. Indeed, $\hat{\vec{\mathbf{F}}} \neq \mathcal{I}\hat{\vec{\Psi}}\mathcal{I}^{-1}$ since if one decomposes the LP field operator in terms of creation-annihilation operators, it yields

$$\mathcal{I}\hat{\vec{\Psi}}(\vec{x})\mathcal{I}^{-1} = \int_{\mathbb{R}^3} d^3k \sum_{\lambda=\pm} \vec{\phi}_{\vec{k},\lambda}(\vec{x})\mathcal{I}\hat{B}_{\vec{\phi}_{\vec{k},\lambda}}\mathcal{I}^{-1} \tag{2.78a}$$

$$= \int_{\mathbb{R}^3} d^3k \sum_{\lambda=\pm} \vec{\phi}_{\vec{k},\lambda}(\vec{x})\hat{C}_{\vec{g}_{\vec{k},\lambda}} \tag{2.78b}$$

$$= -i\int_{\mathbb{R}^3} d^3k \sum_{\lambda=\pm} (\hbar\omega_{\vec{k}})^{-1/2}\vec{g}_{\vec{k},\lambda}(\vec{x})\hat{C}_{\vec{g}_{\vec{k},\lambda}} \tag{2.78c}$$

$$= \frac{-i}{\sqrt{\hbar}}\Omega^{-1/2}\hat{\vec{\mathbf{F}}}. \tag{2.78d}$$

2.5 Dynamics in the quantum models

So far, we have constructed the quantum field theory of the free electromagnetic field using several representations and we have shown that they can all be related trough different isomorphisms of their respective Hilbert spaces. We have discussed how states and electromagnetic field operators are constructed in the quantum theory but we have on purpose put aside the particular case of the Hamiltonian. The aim of the present Section is to deal with the quantized Hamiltonian and discuss how the dynamics of the theory is defined. Indeed, the Hamiltonian in a quantum theory plays two roles: it is the operator associated to the total energy observable of the system and it is the generator of the dynamics of the states in the Schrödinger representation.

The construction of the dynamics within the Fock space formulation is done as follows: one starts with the one-quantum subspace, which coincides with the classical Hilbert space $\mathscr{H}$, and whose time evolution is given by the classical one. From this, a one-quantum operator is identified as the generator of the dynamics. For Maxwell's equations, the generator of the dynamics is $\hbar\Omega$ for all representations we discussed before (see equations (2.17), (2.27) and (2.56) or (2.58), where $\hbar$ has been added in order to match the dimensions required by a Schrödinger equation in the quantized model). The next step is to extend this operator $\hbar\Omega$, which is defined in the single-photon subspace, to the entire Fock space $\mathbb{F}^{\mathfrak{B}}(\mathscr{H})$. This can be done in general with the map denoted $\mathrm{d}\Gamma(\hbar\Omega)$ [77, 90] and defined by its action on the monomials $|\eta_1 \otimes_S \eta_2 \otimes_S \ldots \otimes_S \eta_n\rangle \in \mathscr{H}^{\otimes_S n}$:

$$\begin{aligned}\mathrm{d}\Gamma(\hbar\Omega)\,|\eta_1 \otimes_S \eta_2 \otimes_S \ldots \otimes_S \eta_n\rangle = {}& |\hbar\Omega\eta_1 \otimes_S \eta_2 \otimes_S \ldots \otimes_S \eta_n\rangle + |\eta_1 \otimes_S \hbar\Omega\eta_2 \otimes_S \ldots \otimes_S \eta_n\rangle \\ & + \cdots + |\eta_1 \otimes_S \ \eta_2 \otimes_S \ldots \otimes_S \hbar\Omega\eta_n\rangle\,.\end{aligned} \tag{2.79}$$

If $\{\phi_\kappa\} \in \mathscr{H}$ is an orthonormal basis, with respect to $\langle\cdot|\cdot\rangle_{\mathscr{H}}$, of eigenfunctions of Ω, i.e., $\Omega\phi_\kappa = \omega_\kappa\phi_\kappa$, the map $\mathrm{d}\Gamma(\hbar\Omega)$ can be expressed as [77, p. 440]

$$\mathrm{d}\Gamma(\hbar\Omega) = \sum_\kappa \hbar\omega_\kappa \hat{B}^\dagger_{\phi_\kappa}\hat{B}_{\phi_\kappa}. \tag{2.80}$$

We apply this procedure to the different Hilbert spaces defined in the preceding sections, starting with the LP representation

$$\mathrm{d}\Gamma_{LP}(\hbar\Omega) = \int_{\mathbb{R}^3} d^3k \sum_{\lambda=\pm} \hbar\omega_{\vec{k}} \hat{B}^\dagger_{\vec{\phi}_{\vec{k},\lambda}} \hat{B}_{\vec{\phi}_{\vec{k},\lambda}}. \tag{2.81}$$

We see that it is equal to the quantized total energy operator which can be written as

$$\hat{H}_{LP} = \hbar \int_{\mathbb{R}^3} d^3x \; \hat{\vec{\Psi}}^\dagger \cdot \Omega \hat{\vec{\Psi}} = \int_{\mathbb{R}^3} d^3k \sum_{\lambda=\pm} \hbar\omega_{\vec{k}} \hat{B}^\dagger_{\vec{\phi}_{\vec{k},\lambda}} \hat{B}_{\vec{\phi}_{\vec{k},\lambda}}, \tag{2.82}$$

showing that the total energy is the generator of the dynamics in the position space Coulomb gauge formulation of the quantized electromagnetic field. For the momentum representation, one has directly

$$\mathrm{d}\Gamma_M(\hbar\Omega) = \int_{\mathbb{R}^3} d^3k \sum_{\lambda=\pm} \hbar\omega_{\vec{k}} \hat{a}^\dagger_{\vec{k},\lambda} \hat{a}_{\vec{k},\lambda} = \hat{H}_M, \tag{2.83}$$

and finally for the BB formulation, using the basis $\{\vec{g}_{\vec{k},\lambda}\}$ one obtains

$$\mathrm{d}\Gamma_{BB}(\hbar\Omega) = \int_{\mathbb{R}^3} d^3k \sum_{\lambda=\pm} \hbar\omega_{\vec{k}} \hat{C}^\dagger_{\vec{g}_{\vec{k},\lambda}} \hat{C}_{\vec{g}_{\vec{k},\lambda}}, \tag{2.84}$$

which coincides with the total energy

$$\begin{aligned}
\hat{\mathcal{E}}_{\mathrm{tot}} &= \int_{\mathbb{R}^3} d^3x \; \hat{\vec{\mathbf{F}}}^\dagger \cdot \hat{\vec{\mathbf{F}}} && \text{(2.85a)}\\
&= \int_{\mathbb{R}^3} d^3k \int_{\mathbb{R}^3} d^3k' \sum_{\lambda,\lambda'} \left(\int_{\mathbb{R}^3} d^3x \; \vec{g}^\star_{\vec{k},\lambda}(\vec{x}) \cdot \vec{g}_{\vec{k}',\lambda'}(\vec{x}) \right) \hat{C}^\dagger_{\vec{g}_{\vec{k},\lambda}} \hat{C}_{\vec{g}_{\vec{k}',\lambda'}} && \text{(2.85b)}\\
&= \hbar \int_{\mathbb{R}^3} d^3k \int_{\mathbb{R}^3} d^3k' \sum_{\lambda,\lambda'} \langle \vec{g}_{\vec{k},\lambda} | \Omega \vec{g}_{\vec{k}',\lambda'} \rangle_{BB} \; \hat{C}^\dagger_{\vec{g}_{\vec{k},\lambda}} \hat{C}_{\vec{g}_{\vec{k}',\lambda'}} && \text{(2.85c)}\\
&= \hbar \int_{\mathbb{R}^3} d^3k \int_{\mathbb{R}^3} d^3k' \sum_{\lambda,\lambda'} \omega_{\vec{k}'} \langle \vec{g}_{\vec{k},\lambda} | \vec{g}_{\vec{k}',\lambda'} \rangle_{BB} \; \hat{C}^\dagger_{\vec{g}_{\vec{k},\lambda}} \hat{C}_{\vec{g}_{\vec{k}',\lambda'}} && \text{(2.85d)}\\
&= \int_{\mathbb{R}^3} d^3k \sum_{\lambda=\pm} \hbar\omega_{\vec{k}} \; \hat{C}^\dagger_{\vec{g}_{\vec{k},\lambda}} \hat{C}_{\vec{g}_{\vec{k},\lambda}} \equiv \hat{H}_{BB}. && \text{(2.85e)}
\end{aligned}$$

This confirms that in the quantized theory, the generator of the dynamics is the quantized operator of the total energy in the BB representation and not the quantization of the classical Hamilton function K_{BB}. The time evolution of the states is given by the unitary operator $\hat{U}_{BB}(t) = e^{-i\hat{H}_{BB}t}$, and it leads, e.g., when applied to single-photon states to the expressions given in the literature [21, equation (4.20)]. One can further check that the Hamiltonians written in their respective representations can be recovered from one to the

other using the isomorphisms, e.g., between the LP and BB field operators (2.78)

$$\mathcal{I}\hat{H}_{LP}\mathcal{I}^{-1} = \hbar \int_{\mathbb{R}^3} d^3x \; \mathcal{I}\vec{\hat{\Psi}}^\dagger \mathcal{I}^{-1} \cdot \Omega \mathcal{I}\vec{\hat{\Psi}}\mathcal{I}^{-1} \tag{2.86a}$$

$$= \int_{\mathbb{R}^3} d^3x \; \Omega^{-1/2}\vec{\hat{\mathbf{F}}}^\dagger \cdot \Omega^{1/2}\vec{\hat{\mathbf{F}}} \tag{2.86b}$$

$$= \int_{\mathbb{R}^3} d^3x \; \vec{\hat{\mathbf{F}}}^\dagger \cdot \vec{\hat{\mathbf{F}}} = \hat{H}_{BB}. \tag{2.86c}$$

The equivalence of the generators of the dynamics guarantees that the isomorphism is preserved during the time evolution and that the theories are completely equivalent at any time.

3

Propagation and local detection of photons

In this chapter, we focus on the dynamical properties of photons assumed to be already produced. We discuss their propagation in inhomogeneous dielectric media as well as their detection by detectors well localized in space and with a finite volume.

After recalling how one can generalize the free space Landau-Peierls quantization to inhomogeneous passive dielectric media, we show that the time evolution of any photon state is given by the time evolution of the associated classical configuration. To illustrate this property, we discuss the passage of a photon through a beam-splitter and show how one can describe the Hong-Ou-Mandel effect in a dynamical way. We then discuss the construction of a detection model in which the photon spatial distribution is taken into account. We use the energy density observable to characterize the nonlocal property of photons and show that any single-photon state is nonlocal. The demonstration is done using the anti-local property of the frequency operator and is a complementary approach to what was already in the literature so far since our proof does not involve the time evolution. Photons are thus nonlocal at any time including the initial condition.
The first part of this Chapter has led to the article [1] and the second part to [3]

3.1 Generalization of the Landau-Peierls quantization to dielectric media 48
3.2 Evolution of the photon states determined from the dynamics of the classical modes 50
3.2.1 Proof of the time evolution formulas 51
3.2.2 Physical interpretation and application 53
3.2.2.1 Propagation in an optical fiber — Space-to-time mapping . 54
3.2.2.2 Time-bin photon encoding 54
3.3 Photons through beam-splitters 56
3.3.1 One-photon state 56
3.3.1.1 Initial classical mode and its time evolution 56
3.3.1.2 Quantum dynamics of the one-photon state 57
3.3.1.3 Alternative treatments of beam-splitters 58
3.3.2 Two-photon state: The Hong-Ou-Mandel effect 61

3.3.2.1 Initial classical modes and their time evolution 61
3.3.2.2 Quantum dynamics of the two-photon state 62
3.3.2.3 Detection model to interpret the dynamics 63
3.3.2.4 Photons are not like classical waves nor like classical particles 64
3.4 Local detection of single-photon states 65
3.4.1 Single-photon detectors 65
3.4.2 Local observable for the detection 65
3.4.3 Brief review on photon's nonlocality property 68
3.4.4 Nonlocality of the energy density for single-photon states — Proof . 70
3.4.5 Illustration of the nonlocality 72
3.4.6 Localization properties of other states of the quantum electromagnetic field 74
3.4.6.1 N-photon states 74
3.4.6.2 Coherent states 75
3.4.7 Glauber's photodetection operator 76
3.4.8 Nonlocality and causality 77

3.1 Generalization of the Landau-Peierls quantization to dielectric media

In this Section, and following the pioneering work of Lewenstein and Glauber [14], we want to generalize the quantization we performed before to a case where the electromagnetic field is interacting with a linear inhomogeneous dielectric medium as we have classically described in Chapter 1. We start again with Maxwell's equations which read in this situation

$$\varepsilon(\vec{x})\frac{\partial^2 \vec{A}'}{\partial t^2} = -c^2 \nabla \times \nabla \times \vec{A}', \tag{3.1a}$$

$$\vec{E} = -\frac{\partial \vec{A}'}{\partial t}, \qquad \vec{B} = \nabla \times \vec{A}', \tag{3.1b}$$

where we use the potential vector $\vec{A}'$ in the generalized Coulomb gauge $\nabla \cdot (\varepsilon \vec{A}') = 0$. Here, $\varepsilon(\vec{x})$ is the position dependent dielectric function which describes the interaction of the fields with the surrounding medium. The medium is considered to be absorption free, dispersionless and linear, i.e., ε is real, frequency-independent and comes from a linear instantaneous response of the medium.
In the following, we will show how one can construct a generalization of the LP quantization for the dielectric medium case. By making the following change of variable

$$\vec{A} = \sqrt{\epsilon}\vec{A}', \tag{3.2}$$

the wave equation (3.1a) becomes

$$\frac{\partial^2 \vec{A}}{\partial t^2} = -\frac{1}{\sqrt{\varepsilon}} c^2 \nabla \times \nabla \times \frac{1}{\sqrt{\varepsilon}} \vec{A}. \tag{3.3}$$

The operator

$$\frac{c}{\sqrt{\varepsilon}}\nabla\times\nabla\times\frac{c}{\sqrt{\varepsilon}}=\Xi^\dagger\Xi,\qquad\text{with }\Xi=\nabla\times\frac{c}{\sqrt{\varepsilon}},\tag{3.4}$$

is positive, selfadjoint, and there is a unique positive operator $\Omega_{\rm m}$, such that

$$\Xi^\dagger\Xi=\Omega_{\rm m}^2,\qquad\text{i.e., }\Omega_{\rm m}=\left(\frac{c}{\sqrt{\varepsilon}}\nabla\times\nabla\times\frac{c}{\sqrt{\varepsilon}}\right)^{1/2}.\tag{3.5}$$

Thus Maxwell's equations in a passive dielectric medium can be written as

$$\frac{\partial^2\vec{A}}{\partial t^2}=-\Omega_{\rm m}^2\vec{A},\tag{3.6}$$

which has the same structure as in empty space, where $\Omega^2=-c^2\Delta$, but with the frequency operator $\Omega_{\rm m}$ defined in (3.5) and the generalized transversality constraint.
The LP construction in a medium can then be done in the exact same way by defining first

$$\vec{\psi}_{\rm m}=\frac{1}{\sqrt{2\hbar}}\left((\varepsilon_0\Omega_{\rm m})^{1/2}\vec{A}+i(\varepsilon_0\Omega_{\rm m})^{-1/2}\vec{\Pi}\right),\tag{3.7}$$

where $\vec{\Pi}=\varepsilon_0\frac{\partial\vec{A}}{\partial t}$ and from which Maxwell's equations become

$$i\frac{\partial\vec{\psi}_{\rm m}}{\partial t}=\Omega_{\rm m}\vec{\psi}_{\rm m}.\tag{3.8}$$

The classical phase space $(\vec{\Pi},\vec{A})$ has a natural Hilbert space structure, which in the complex representation takes the form

$$\mathscr{H}_{LP_{\rm m}}=\{\vec{\psi}_{\rm m}(\vec{x})|\,\langle\vec{\psi}_{\rm m}|\vec{\psi}'_{\rm m}\rangle_{LP}<\infty\},\tag{3.9}$$

with the same LP scalar product

$$\langle\vec{\psi}_{\rm m}|\vec{\psi}'_{\rm m}\rangle_{LP}=\int_{\mathbb{R}^3}d^3x\;\vec{\psi}^\star_{\rm m}(\vec{x})\cdot\vec{\psi}'_{\rm m}(\vec{x}).\tag{3.10}$$

We obtain here exactly the same structure that what we had before in the free field case. The only difference is hidden in $\Omega_{\rm m}$.
For the quantization, everything can then be run through without any differences, i.e., with a bosonic Fock space $\mathbb{F}^{\mathfrak{B}}(\mathscr{H}_{LP_{\rm m}})$ in which act bosonic creation-annihilation operators defined on elements of $\mathscr{H}_{LP_{\rm m}}$. Physical observables such as the electric field become operators whose forms are postulated through the correspondence principle. Finally, the quantum Hamiltonian is constructed as the generalization of $\Omega_{\rm m}$ to the full Fock space, i.e., $\hat{H}_{\rm m}=\mathrm{d}\Gamma(\hbar\Omega_{\rm m})$. The dynamics will thus automatically take into account the medium since all its information is included into $\Omega_{\rm m}$. In the following, we will drop the indices $_{\rm m}$ that refer to the medium construction in order to lighten the notations.

Remarks:

- A momentum representation can also be defined using an orthonormal basis $\{\vec{\varphi}_\kappa\}$ of eigenvectors of the medium frequency operator $\Omega_{\rm m}$. Beside the use of $\{\vec{\varphi}_\kappa\}$ instead of $\{\vec{\phi}_{\vec{k},\sigma}\}$, the construction is identical to what we did in Chapter 2, and both representations can also be related by a Hilbert space isomorphism. Just like in the vacuum case,

the momentum representation allows to diagonalize the Hamiltonian which reads

$$\hat{H} = \sum_{\kappa} \hbar\omega_\kappa \hat{B}^\dagger_{\vec{\varphi}_\kappa} \hat{B}_{\vec{\varphi}_\kappa}. \tag{3.11}$$

The sum over κ stands for a combination of sums and integrals over the multiple indices hidden in the notation κ and which reflect the degeneracy of the spectrum. This degeneracy will depend on the geometry of the considered medium and we thus use the abstract notation κ to be as general as possible.

- For the description of the fields inside a medium, the BB representation is less useful since the main aim was to construct a Lorentz invariant formulation which cannot be obtained in a medium that is by construction considered as non-relativistic.

3.2 Evolution of the photon states determined from the dynamics of the classical modes

We are going to show that the time evolution of photon states in Fock space, which is determined by the standard Schrödinger equation

$$i\hbar \frac{\partial |\Phi\rangle}{\partial t} = \hat{H} |\Phi\rangle, \qquad |\Phi\rangle \in \mathbb{F}^{\mathfrak{B}}(\mathcal{H}), \tag{3.12}$$

can be expressed in terms of the time evolution of the classical modes, determined by the classical wave equation, i.e., by Maxwell's equations. Here, $\hat{H}$ is the Hamiltonian of the system which can be equivalently written in momentum or position representations as discussed in Chapter 2. To prove the following formula, we will use the momentum representation since it diagonalizes $\hat{H}$ and makes the calculations easier.

(a) For a one-photon initial condition $|\Phi(t=0)\rangle = \hat{B}^\dagger_{\vec{\psi}(t=0)} |\varnothing\rangle$ the time evolution is

$$|\Phi(t)\rangle = \hat{B}^\dagger_{\vec{\psi}(t)} |\varnothing\rangle, \tag{3.13}$$

where $\vec{\psi}(t)$ is the solution of the classical wave equation (3.8) with initial condition $\vec{\psi}(t=0)$.

(b) For a two-photon initial condition $|\Phi(t=0)\rangle = \hat{B}^\dagger_{\vec{\psi}_1(t=0)} \hat{B}^\dagger_{\vec{\psi}_2(t=0)} |\varnothing\rangle$ the time evolution is

$$|\Phi(t)\rangle = \hat{B}^\dagger_{\vec{\psi}_1(t)} \hat{B}^\dagger_{\vec{\psi}_2(t)} |\varnothing\rangle, \tag{3.14}$$

where $\vec{\psi}_1(t)$ and $\vec{\psi}_2(t)$ are two solutions of the classical wave equation (3.8) for the corresponding initial conditions.

(c) In the general case of an N-photon initial condition $|\Phi(t=0)\rangle = \prod_{j=1}^{N} \hat{B}^\dagger_{\vec{\psi}_j(t=0)} |\varnothing\rangle$ the time evolution is

$$|\Phi(t)\rangle = \prod_{j=1}^{N} \hat{B}^\dagger_{\vec{\psi}_j(t)} |\varnothing\rangle, \tag{3.15}$$

where $\vec{\psi}_j(t)$ are the solutions of the classical equation (3.8) for the corresponding initial conditions.

Remark: The family of operators $\hat{B}^\dagger_{\vec{\psi}(t)}$ parametrized by time can be thought of as a time-dependent operator which can be written as

$$\hat{B}^\dagger_{\vec{\psi}(t)} = \hat{U}(t)\hat{B}^\dagger_{\vec{\psi}(t=0)}\hat{U}^\dagger(t), \tag{3.16}$$

where $\hat{U}(t) = \exp\left(-\frac{i}{\hbar}\hat{H}t\right)$ is the propagator in Fock space. This can be verified, e.g., by applying both sides to the vacuum state: Indeed, since

$$\hat{U}^\dagger(t)\,|\varnothing\rangle = \sum_{n=0}^{\infty}\left(\frac{i}{\hbar}t\right)^n\left(\sum_\kappa \hbar\omega_\kappa \hat{B}^\dagger_{\vec{\varphi}_\kappa}\hat{B}_{\vec{\varphi}_\kappa}\right)^n|\varnothing\rangle = |\varnothing\rangle\,, \tag{3.17}$$

we can write

$$\begin{aligned}\hat{U}(t)\hat{B}^\dagger_{\vec{\psi}(t=0)}\hat{U}^\dagger(t)\,|\varnothing\rangle &= \hat{U}(t)\hat{B}^\dagger_{\vec{\psi}(t=0)}\,|\varnothing\rangle &\text{(3.18a)}\\ &= \hat{U}(t)\,|\vec{\psi}(t=0)\rangle &\text{(3.18b)}\\ &= |\vec{\psi}(t)\rangle &\text{(3.18c)}\\ &= \hat{B}^\dagger_{\vec{\psi}(t)}\,|\varnothing\rangle\,. &\text{(3.18d)}\end{aligned}$$

We remark however that it is not the time evolution in the Heisenberg picture, which is given by a different expression [33, p.84]:

$$\left(\hat{B}^\dagger_{\vec{\psi}(t=0)}\right)^{\text{Heisenberg}}(t) = \hat{U}^\dagger(t)\hat{B}^\dagger_{\vec{\psi}(t=0)}\hat{U}(t) = \hat{B}^\dagger_{\vec{\psi}(-t)} \neq \hat{B}^\dagger_{\vec{\psi}(t)}. \tag{3.19}$$

3.2.1 Proof of the time evolution formulas

Although the proof of the general N-photon case given in **(c)** implies of course the results for the one- and two-photon cases, since it is notationally harder to read we will first give the proofs for the simplest particular cases.
We will use the relation

$$\hat{B}^\dagger_{\alpha\vec{\psi}_1+\beta\vec{\psi}_2} = \alpha\hat{B}^\dagger_{\vec{\psi}_1} + \beta\hat{B}^\dagger_{\vec{\psi}_2} \quad \text{for } \alpha,\beta\in\mathbb{C}, \tag{3.20}$$

which is a direct consequence of the definition of creation operators (2.7).

Proof of (a): We consider a state $|\Phi(t)\rangle$ as written in (3.13), and we verify that it fulfills the Schrödinger equation (3.12). We start by expressing the time evolution of the classical modes in terms of the eigenfunctions $\vec{\varphi}_\kappa$ of Ω

$$\vec{\psi}(t) = \sum_\kappa e^{-i\omega_\kappa t}\vec{\varphi}_\kappa\alpha_\kappa, \qquad \alpha_\kappa = \langle\vec{\varphi}_\kappa|\vec{\psi}(t=0)\rangle\,, \tag{3.21}$$

and

$$|\Phi(t)\rangle = \hat{B}^\dagger_{\vec{\psi}(t)}\,|\varnothing\rangle = \sum_\kappa e^{-i\omega_\kappa t}\alpha_\kappa\hat{B}^\dagger_{\vec{\varphi}_\kappa}\,|\varnothing\rangle\,. \tag{3.22}$$

With this representation we can rewrite the left-hand side of Schrödinger's equation as

$$i\hbar\frac{\partial}{\partial t}\,|\Phi(t)\rangle = \sum_\kappa \hbar\omega_\kappa\; e^{-i\omega_\kappa t}\alpha_\kappa\hat{B}^\dagger_{\vec{\varphi}_\kappa}|\varnothing\rangle. \tag{3.23}$$

The right-hand side can also be rewritten using (3.22) and the representation of the Hamiltonian (3.11); it yields

$$\hat{H}\,|\Phi(t)\rangle = \sum_{\kappa,\kappa'} \hbar\omega_{\kappa'} e^{-i\omega_\kappa t}\alpha_\kappa \hat{B}^\dagger_{\vec{\varphi}_{\kappa'}} \hat{B}_{\vec{\varphi}_{\kappa'}} \hat{B}^\dagger_{\vec{\varphi}_\kappa}\,|\varnothing\rangle \tag{3.24a}$$

$$= \sum_{\kappa,\kappa'} \hbar\omega_{\kappa'} e^{-i\omega_\kappa t}\alpha_\kappa \hat{B}^\dagger_{\vec{\varphi}_{\kappa'}} \left(\hat{B}^\dagger_{\vec{\varphi}_\kappa} \hat{B}_{\vec{\varphi}_{\kappa'}} + \delta_{\kappa,\kappa'}\right)|\varnothing\rangle \tag{3.24b}$$

$$= \sum_{\kappa} \hbar\omega_{\kappa} e^{-i\omega_\kappa t}\alpha_\kappa \hat{B}^\dagger_{\vec{\varphi}_\kappa}\,|\varnothing\rangle \tag{3.24c}$$

$$= i\hbar\frac{\partial}{\partial t}\,|\Phi(t)\rangle\,, \tag{3.24d}$$

where we have used the commutation relation $\hat{B}_{\vec{\varphi}_{\kappa'}} \hat{B}^\dagger_{\vec{\varphi}_\kappa} = \hat{B}^\dagger_{\vec{\varphi}_\kappa} \hat{B}_{\vec{\varphi}_{\kappa'}} + \delta_{\kappa,\kappa'}$, the fact that $\hat{B}_{\vec{\varphi}_{\kappa'}}\,|\varnothing\rangle = 0$ and (3.23), which completes the proof.

Proof of (b): We will use here notations which should help understanding the general N-photon case. We now consider a state $|\Phi(t)\rangle$ as written in (3.14), and we verify that it fulfills the Schrödinger equation (3.12). To do so, we expand the classical state functions in terms of eigenfunctions of Ω

$$\vec{\psi}_j(t) = \sum_{\kappa_j} e^{-i\omega_{\kappa_j} t}\vec{\varphi}_{\kappa_j}\alpha_{\kappa_j}, \qquad \alpha_{\kappa_j} = \langle\vec{\varphi}_{\kappa_j}|\vec{\psi}(t=0)\rangle\,, \qquad j = 1, 2, \tag{3.25}$$

which allows us to write

$$|\Phi(t)\rangle = \hat{B}^\dagger_{\vec{\psi}_1(t)} \hat{B}^\dagger_{\vec{\psi}_2(t)}\,|\varnothing\rangle = \prod_{j=1}^{2}\left(\sum_{\kappa_j} e^{-i\omega_{\kappa_j} t}\alpha_{\kappa_j}\hat{B}^\dagger_{\vec{\varphi}_{\kappa_j}}\right)|\varnothing\rangle \tag{3.26a}$$

$$= \sum_{\kappa_1,\kappa_2} e^{-i(\omega_{\kappa_1}+\omega_{\kappa_2})t}\alpha_{\kappa_1}\alpha_{\kappa_2}\hat{B}^\dagger_{\vec{\varphi}_{\kappa_1}} \hat{B}^\dagger_{\vec{\varphi}_{\kappa_2}}\,|\varnothing\rangle\,, \tag{3.26b}$$

and

$$i\hbar\frac{\partial}{\partial t}\,|\Phi(t)\rangle = \sum_{\kappa_1,\kappa_2} \hbar(\omega_{\kappa_1}+\omega_{\kappa_2}) e^{-i(\omega_{\kappa_1}+\omega_{\kappa_2})t}\alpha_{\kappa_1}\alpha_{\kappa_2}\hat{B}^\dagger_{\vec{\varphi}_{\kappa_1}} \hat{B}^\dagger_{\vec{\varphi}_{\kappa_2}}\,|\varnothing\rangle\,. \tag{3.27}$$

Applying the Hamiltonian (3.11) to (3.26) yields

$$\hat{H}\,|\Phi(t)\rangle = \sum_{\kappa'} \hbar\omega_{\kappa'} \hat{B}^\dagger_{\vec{\varphi}_{\kappa'}} \hat{B}_{\vec{\varphi}_{\kappa'}} \sum_{\kappa_1,\kappa_2} e^{-i(\omega_{\kappa_1}+\omega_{\kappa_2})t}\alpha_{\kappa_1}\alpha_{\kappa_2}\hat{B}^\dagger_{\vec{\varphi}_{\kappa_1}} \hat{B}^\dagger_{\vec{\varphi}_{\kappa_2}}\,|\varnothing\rangle \tag{3.28a}$$

$$= \sum_{\kappa_1,\kappa_2} e^{-i(\omega_{\kappa_1}+\omega_{\kappa_2})t}\alpha_{\kappa_1}\alpha_{\kappa_2} \sum_{\kappa'} \hbar\omega_{\kappa'} \hat{B}^\dagger_{\vec{\varphi}_{\kappa'}} \hat{B}_{\vec{\varphi}_{\kappa'}} \hat{B}^\dagger_{\vec{\varphi}_{\kappa_1}} \hat{B}^\dagger_{\vec{\varphi}_{\kappa_2}}\,|\varnothing\rangle\,. \tag{3.28b}$$

Using the commutation relations $\hat{B}_{\vec{\varphi}_{\kappa'}} \hat{B}^\dagger_{\vec{\varphi}_{\kappa_j}} = \hat{B}^\dagger_{\vec{\varphi}_{\kappa_j}} \hat{B}_{\vec{\varphi}_{\kappa'}} + \delta_{\kappa_j,\kappa'}$ and the fact that $\hat{B}_{\vec{\varphi}_{\kappa'}}\,|\varnothing\rangle = 0$ we can write

$$\hat{B}_{\vec{\varphi}_{\kappa'}} \hat{B}^\dagger_{\vec{\varphi}_{\kappa_1}} \hat{B}^\dagger_{\vec{\varphi}_{\kappa_2}}\,|\varnothing\rangle = \delta_{\kappa',\kappa_1}\hat{B}^\dagger_{\vec{\varphi}_{\kappa_2}}\,|\varnothing\rangle + \hat{B}^\dagger_{\vec{\varphi}_{\kappa_1}} \hat{B}_{\vec{\varphi}_{\kappa'}} \hat{B}^\dagger_{\vec{\varphi}_{\kappa_2}}\,|\varnothing\rangle \tag{3.29a}$$

$$= \delta_{\kappa',\kappa_1}\hat{B}^\dagger_{\vec{\varphi}_{\kappa_2}}\,|\varnothing\rangle + \delta_{\kappa',\kappa_2}\hat{B}^\dagger_{\vec{\varphi}_{\kappa_1}}\,|\varnothing\rangle + \hat{B}^\dagger_{\vec{\varphi}_{\kappa_1}} \hat{B}^\dagger_{\vec{\varphi}_{\kappa_2}} \hat{B}_{\vec{\varphi}_{\kappa'}}\,|\varnothing\rangle \tag{3.29b}$$

$$= \delta_{\kappa',\kappa_1}\hat{B}^\dagger_{\vec{\varphi}_{\kappa_2}}\,|\varnothing\rangle + \delta_{\kappa',\kappa_2}\hat{B}^\dagger_{\vec{\varphi}_{\kappa_1}}\,|\varnothing\rangle\,, \tag{3.29c}$$

and thus

$$\sum_{\kappa'} \hbar\omega_{\kappa'} \hat{B}^\dagger_{\vec{\varphi}_{\kappa'}} \hat{B}_{\vec{\varphi}_{\kappa'}} \hat{B}^\dagger_{\vec{\varphi}_{\kappa_1}} \hat{B}^\dagger_{\vec{\varphi}_{\kappa_2}} |\varnothing\rangle = \sum_{\kappa'} \hbar\omega_{\kappa'} \hat{B}^\dagger_{\vec{\varphi}_{\kappa'}} \left(\delta_{\kappa',\kappa_1} \hat{B}^\dagger_{\vec{\varphi}_{\kappa_2}} |\varnothing\rangle + \delta_{\kappa',\kappa_2} \hat{B}^\dagger_{\vec{\varphi}_{\kappa_1}} |\varnothing\rangle \right) \tag{3.30a}$$

$$= \hbar\omega_{\kappa_1} \hat{B}^\dagger_{\vec{\varphi}_{\kappa_1}} \hat{B}^\dagger_{\vec{\varphi}_{\kappa_2}} |\varnothing\rangle + \hbar\omega_{\kappa_2} \hat{B}^\dagger_{\vec{\varphi}_{\kappa_2}} \hat{B}^\dagger_{\vec{\varphi}_{\kappa_1}} |\varnothing\rangle \tag{3.30b}$$

$$= (\hbar\omega_{\kappa_1} + \hbar\omega_{\kappa_2}) \hat{B}^\dagger_{\vec{\varphi}_{\kappa_1}} \hat{B}^\dagger_{\vec{\varphi}_{\kappa_2}} |\varnothing\rangle , \tag{3.30c}$$

which inserted into (3.28) yields

$$\hat{H} |\Phi(t)\rangle = \sum_{\kappa_1,\kappa_2} e^{-i(\omega_{\kappa_1}+\omega_{\kappa_2})t} \alpha_{\kappa_1}\alpha_{\kappa_2} (\hbar\omega_{\kappa_1} + \hbar\omega_{\kappa_2}) \hat{B}^\dagger_{\vec{\varphi}_{\kappa_1}} \hat{B}^\dagger_{\vec{\varphi}_{\kappa_2}} |\varnothing\rangle \tag{3.31a}$$

$$= i\hbar \frac{\partial}{\partial t} |\Phi(t)\rangle . \tag{3.31b}$$

In the last equality we have used the relation (3.27), which completes the proof.

Proof of (c): The notationally more heavy proof for the general N-photon case can be performed in the same spirit and the detailed calculations are given in Appendix B.

3.2.2 Physical interpretation and application

In the preceding section, we have shown that the dynamics of any photon state is given by the associated classical dynamics of the pulse on which photons have been constructed. To fully understand the consequences of this property, let us focus first on the single-photon case: Such a state (and its time evolution) can be mathematically written as

$$|1_{\rm ph}(t)\rangle = \hat{B}^\dagger_{\vec{\eta}(t)} |\varnothing\rangle , \tag{3.32}$$

where $\vec{\eta}(t) \in \mathscr{H}_{LP}$ is a classical solution of Maxwell's equations, meaning that the photon is carried by $\vec{\eta}(t)$ for the whole dynamics as represented in Figure 3.1 (a)-(c). This result allows then to use the classical dynamics to analyze any single-photon propagation as we will illustrate later with the beam-splitter.
If we consider now a two-photon state, it is represented mathematically by

$$|2_{\rm ph}(t)\rangle = \hat{B}^\dagger_{\vec{\eta}_1(t)} \hat{B}^\dagger_{\vec{\eta}_2(t)} |\varnothing\rangle , \tag{3.33}$$

where $\vec{\eta}_{1,2}(t) \in \mathscr{H}_{LP}$ are two possibly different classical solutions of Maxwell's equations. The dynamics of each classical configuration governs then the propagation of the two-photon state. If $\vec{\eta}_1 = \vec{\eta}_2 \equiv \vec{\eta}$, we have thus a single-mode two-photon state

$$|2_{\rm ph}\rangle = \left(\hat{B}^\dagger_{\vec{\eta}(t)} \right)^2 |\varnothing\rangle , \tag{3.34}$$

carrying the two photons. Since the function $\vec{\eta}$ can be any classical solution of Maxwell's equation, one can choose a double-pulsed function like in Figure 3.1(c). However, as opposed to the two-photon state with two different classical functions, one cannot say that one photon is carried by one pulse and the second photon by the other. The state is to be interpreted as a global two-photon state which is carried by a single classical function which has a double-pulse shape. The difference between the two scenarios will also be illustrated later with the beam-splitter and the Hang-Ou-Mandel effect.

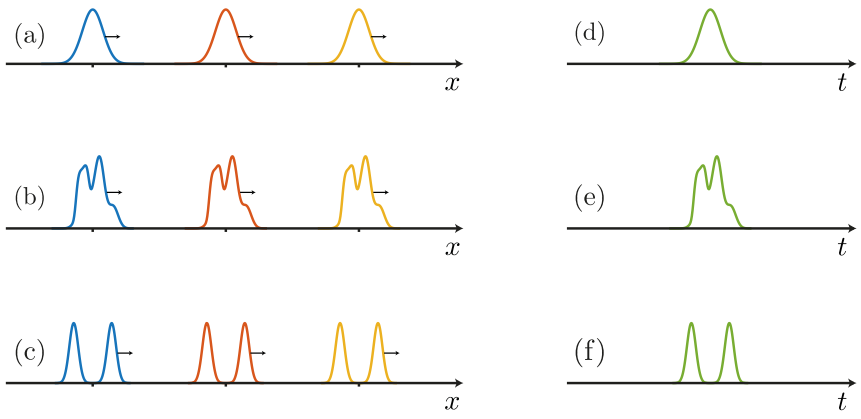

Figure 3.1: Sketch of the one-dimensional propagation of pulses of any shape. (a)-(c) Blue curves correspond to a fixed time t_1, red curves to a later time $t_2 > t_1$ and yellow curves to yet another time $t_3 > t_2$. All the pulses represented here propagate towards the positive x in a homogenous dielectric medium of optical index $n = \sqrt{\varepsilon}$ at the speed c/n. (d)-(f) The same pulses are represented as a temporal evolution seen from a fixed space point x_p.

3.2.2.1 Propagation in an optical fiber — Space-to-time mapping

In Figure 3.1 (a)-(c), we have represented the propagation in one-dimension of several pulses. This simple one dimensional model can be used, e.g., to describe the propagation in an optical fiber. The function representing the single-photon state in the fiber can thus be written as

$$\eta_\mathrm{fiber}(x,t) \equiv \eta_\mathrm{fiber}\left(x - \frac{c}{n}t\right), \tag{3.35}$$

where $n = \sqrt{\varepsilon}$ is the optical index of the fiber. Here, we see that the space and time coordinates are linked by the propagation and thus one or the other can be equivalently used to describe the state. Indeed, one can either choose particular times t_p and look at the pulse over the entire space as represented in Figure 3.1 (a)-(c), or look at the pulse from a given position x_p during the time interval $[0, +\infty)$ as represented in Figure 3.1 (d)-(f). Such mapping between space and time is a feature of propagating pulses that is extensively used experimentally since detectors are often fixed and one can only say when the photon is detected. Such space-to-time mapping is thus used to rebuild the spatial distribution of the state, as it is done, e.g., in [37]. It also justifies to qualify our formulation of the theory to be a "spatio-temporal description of photons". The key message behind these terms is the fact that we fully take into account the dynamics of photons which can in the end be equivalently considered as either a spatial or a temporal description.

3.2.2.2 Time-bin photon encoding

The theoretical construction and experimental production of photon states carried by pulses of any shapes, allows to encode information. Indeed, since Maxwell's equations are linear equations, any linear combination of solutions is still a solution, and one can

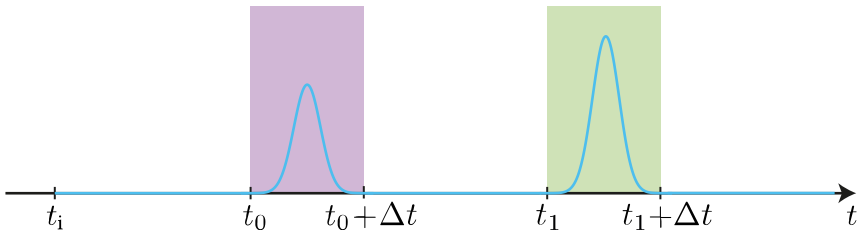

Figure 3.2: Schematic illustration of the definition of time-bins. t_i is the initial time corresponding, e.g., to the emission of the photon. The left violet rectangle corresponds to the first time-bin, i.e., if the detector clicks in the time interval $[t_0, t_0 + \Delta t]$, the photon is in the state $|0\rangle$. The right green rectangle corresponds to the second time-bin, i.e., if the detector clicks in the time interval $[t_1, t_1 + \Delta t]$, the photon is in the state $|1\rangle$. If one is able to repeatedly produce the same photon state, the statistics given by the time-bin detection allows to recover the parameter absolute value $|\alpha|$ and $|\beta|$. For time-bin encoding to be relevant and consistent, one should pay attention to have enough delay between the two bins, i.e., $t_1 - t_0 \gg \Delta t$. The blue trace gives an example of a time-bin encoded state for which $|\alpha| < |\beta|$.

construct single-photon states of the following form

$$|1_\mathrm{ph}(t)\rangle = \hat{B}^\dagger_{\alpha\vec{\eta}_1(t)+\beta\vec{\eta}_2(t)}\,|\varnothing\rangle \tag{3.36a}$$

$$= \alpha\hat{B}^\dagger_{\vec{\eta}_1(t)}\,|\varnothing\rangle + \beta\hat{B}^\dagger_{\vec{\eta}_2(t)}\,|\varnothing\rangle\,, \tag{3.36b}$$

where we have used the linearity of the creation operators and α, β are complex numbers such that $|\alpha|^2 + |\beta|^2 = 1$. Considering now that $\vec{\eta}_1$ and $\vec{\eta}_2$ are two identical normalized disjoint pulses, one can rewrite the single-photon state as

$$|1_\mathrm{ph}(t)\rangle = \alpha\,|\vec{\eta}_\mathrm{early}(t)\rangle + \beta\,|\vec{\eta}_\mathrm{late}(t)\rangle\,, \tag{3.37}$$

where $\vec{\eta}_\mathrm{early}$ and $\vec{\eta}_\mathrm{late}$ refer, respectively, to the first and second identical pulse, by chronological order of a hypothetic detection, and which we can represent using time as

$$|1_\mathrm{ph}(t)\rangle = \alpha\,|\eta_\mathrm{early}(t)\rangle + \beta\,|\eta_\mathrm{late}(t)\rangle\,. \tag{3.38}$$

Such notation is relevant for the propagation in 1D systems, e.g., in an optical fiber and is often used for quantum key distribution (QKD) protocols [91]. The so-called time-bin encoding is thus constructed by considering for instance a time interval Δt corresponding to the width of the pulses $\eta_\mathrm{early}(t)$ and $\eta_\mathrm{late}(t)$ and which defines two time-bins starting at t_0 and $t_1 > t_0$ as represented in Figure 3.2. The detector will thus click either in the time bin 0 corresponding to the late pulse or in the time bin 1 corresponding to the early pulse. The dimensionality of the full system is thus reduced to a state yielding two possible outcomes for a detection that one can therefore write simply as

$$|1_\mathrm{ph}\rangle = \alpha\,|0\rangle + \beta\,|1\rangle\,, \tag{3.39}$$

where $\langle 0|0\rangle = 1 = \langle 1|1\rangle$ and $\langle 0|1\rangle = 0$. The detection into one or the other time bin can thus be represented by the following operators

$$\mathbb{T}_0 = |0\rangle\langle 0|\,, \quad \mathbb{T}_1 = |1\rangle\langle 1|\,. \tag{3.40}$$

Such construction of both a qubit state (3.39) and of projective measurement operators show that one can use spatio-temporal properties of pulse-shaped photons to encode some information. This encoding method is called time-bin encoding and has been demonstrated experimentally using different sources of single-photon states such as trapped atoms/ions [92] or quantum dots [93, 94]. Practically, single-photon states carried by double-pulses can be produced using several techniques, e.g., directly through the shaping of the photon pulses [37, 95–99] or can be done for any single-pulse single-photon states using beam-splitters as we will describe in the next section. Furthermore, sources of entangled photon pairs like SPDC sources can generate time-bin entangled photons [100–102] of the following form

$$|2_{\text{ph}}\rangle = \alpha\,|01\rangle + \beta\,|10\rangle\,. \tag{3.41}$$

Although this construction seems to efficiently work in practice, we will see later in this chapter that the nonlocal property of single photons could be a technical limitation for the reliability of such scheme.

3.3 Photons through beam-splitters

3.3.1 One-photon state

In this section, we want to show that the description of photons through beam-splitters is fully determined by the classical dynamics of their associated pulses. We consider for simplicity, a single-pulse arriving on a $^{50}/_{50}$ beam-splitter at 45°.

3.3.1.1 Initial classical mode and its time evolution

The pulse at the initial time t_{i}, before it arrives at the beam splitter, is a classical mode. We define the following pulse shape function $\vec{S}(r_1, r_2, r_3, t; k)$, depending on three spatial arguments, r_1, r_2, r_3, a temporal variable t, and a wave number k,

$$\vec{S}(r_1, r_2, r_3, t; k) = \mathcal{N}\vec{e}_z\mathcal{E}(r_1 - ct)e^{i(kr_1-\omega t)}g(r_2, r_3) \tag{3.42}$$

where $\vec{e}_z = (0, 0, 1)$ is the linear polarization vector, $\omega = ck > 0$ is the carrier frequency, and $\mathcal{E}(r_1)$ is the pulse envelope in the direction of propagation. Here, $g(r_2, r_3)$ is the transverse profile, which we assume to be smaller than the beam splitter, and in the usual circumstances does not change significantly with the propagation. For the pulse envelope $\mathcal{E}(r_1)$ one can take, e.g., a sine squared function with a finite support, so that there is no ambiguity about when the process starts, or a Gaussian multiplied by a characteristic function to give it a finite support. The normalization constant $\mathcal{N}$ is chosen such that $\int_{\mathbb{R}^3} d^3r\ \vec{S}^\star \cdot \vec{S} = 1$.
With these assumptions, and as we discussed before, the propagation of the photon pulse can be reduced to a one dimensional propagation. The initial mode is chosen as

$$\vec{\psi}_i(\vec{x}) = \vec{S}(x, y, z; k, t = 0) = \vec{S}(x, t = 0), \tag{3.43}$$

where we introduce an abridged notation $\vec{S}(x, t)$, indicating only the first spatial argument of its direction of propagation and the time argument.

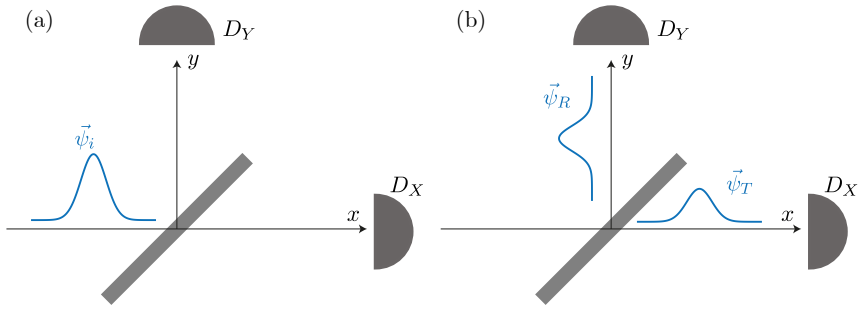

Figure 3.3: Schematic illustration of the partial transmission and reflection of a single-photon state through a $^{50}/_{50}$ beam-splitter. (a) Incoming pulse, (b) reflected and transmitted pulses. The dynamics of the single-photon state is the same as the classical dynamics of a pulse through a beam-splitters according to (3.13). D_X and D_Y represent detectors.

After crossing the beam splitter, the classical mode evolves into a reflected and a transmitted pulse as shown in Figure 3.3,

$$\vec{\psi}_i \xrightarrow{\text{B-S}} \vec{\psi}_R + \vec{\psi}_T, \tag{3.44a}$$

$$\vec{\psi}_R(\vec{x},t) = \tilde{r}\vec{S}(y-ct) = \tilde{r}\vec{Y}(y) \tag{3.44b}$$

$$\vec{\psi}_T(\vec{x},t) = \tilde{t}\vec{S}(x-ct) = \tilde{t}\vec{X}(x), \tag{3.44c}$$

where $\tilde{r}$ and $\tilde{t}$ are the reflection and transmission coefficients, respectively, which in general satisfy the relations $|\tilde{r}|^2 + |\tilde{t}|^2 = 1$ and $\tilde{r}^*\tilde{t} + \tilde{r}\tilde{t}^* = 0$. We have introduced the abridged notations $\vec{Y}(y), \vec{X}(x)$ to improve the readability of the construction below ($\vec{X}$: propagation along the x-axis; $\vec{Y}$: propagation along the y-axis).

3.3.1.2 Quantum dynamics of the one-photon state

We assume that the system is prepared with one photon on the initial mode, described in the Fock space by

$$|\vec{\psi}_i\rangle = \hat{B}^\dagger_{\vec{\psi}_i} |\varnothing\rangle . \tag{3.45}$$

The mode function must be normalized to use a probabilistic interpretation later on

$$\int_{\mathbb{R}^3} d^3x |\vec{\psi}_i(\vec{x})|^2 = 1, \tag{3.46}$$

which entails

$$\left[\hat{B}_{\vec{\psi}_i}, \hat{B}^\dagger_{\vec{\psi}_i}\right] = \langle\vec{\psi}_i|\vec{\psi}_i\rangle = \mathbb{1}. \tag{3.47}$$

After crossing the beam splitter, this one-photon initial state evolves according to the classical dynamics of the carrying pulse, i.e., according to (3.44) which yields

$$\hat{B}^\dagger_{\vec{\psi}_i} |\varnothing\rangle \xrightarrow{\text{B-S}} \hat{B}^\dagger_{\vec{\psi}_R+\vec{\psi}_T} |\varnothing\rangle . \tag{3.48}$$

The physical interpretation of the state at time t after the crossing of the beam-splitter is as follows: $|\vec{\psi}_R + \vec{\psi}_T\rangle$ is a one-photon state on the single classical mode $\vec{\psi}_R + \vec{\psi}_T$, which has two spatially disjoint components, one propagating in the x direction and the other one in the y direction, as represented by the classical pulses in Figure 3.3.

3.3.1.3 Alternative treatments of beam-splitters

In the quantum optics literature, beam-splitters are usually theoretically treated in a different way. The aim of this section is thus to illustrate some differences that exist and, in particular, explain why the construction of photon states directly defined on pulses of arbitrary shape, as we are using in this work, is also of interest in that context. We emphasize, however, that we do not intend to make a critical review of the literature; we only want to locate our approach within the most commonly used approaches that one can find in many textbooks.
First, we remark that the creation operator in (3.48) can be decomposed as the sum of two terms

$$\hat{B}^\dagger_{\vec{\psi}_R+\vec{\psi}_T} = \hat{B}^\dagger_{\vec{\psi}_R} + \hat{B}^\dagger_{\vec{\psi}_T}. \tag{3.49}$$

This property is a direct consequence of the definition (2.7), due to the linearity of the tensor product in each of its arguments. Since the time evolution of the classical modes is unitary, it implies that the norm of the states in Fock space is preserved, and also

$$\left[\hat{B}_{\vec{\psi}_R+\vec{\psi}_T}, \hat{B}^\dagger_{\vec{\psi}_R+\vec{\psi}_T}\right] = \mathbb{1}. \tag{3.50}$$

However, the separate terms in (3.49) satisfy the commutation relations

$$\left[\hat{B}_{\vec{\psi}_R}, \hat{B}^\dagger_{\vec{\psi}_R}\right] = \langle\vec{\psi}_R|\vec{\psi}_R\rangle = |\tilde{r}|^2 \neq \mathbb{1}, \tag{3.51a}$$

$$\left[\hat{B}_{\vec{\psi}_T}, \hat{B}^\dagger_{\vec{\psi}_T}\right] = \langle\vec{\psi}_T|\vec{\psi}_T\rangle = |\tilde{t}|^2 \neq \mathbb{1}. \tag{3.51b}$$

Thus, the separate creation operators cannot be "bosonic creation operators". This is sometimes presented as a major problem that needs to be corrected.
In order to analyze this question, we first make the link with the notation that is used conventionally in most of the literature, e.g., in [29, p. 511]:

$$\hat{B}_{\vec{\psi}_i} \to \hat{a}_1, \quad \hat{B}_{\vec{\psi}_R} \to \hat{a}_2, \quad \hat{B}_{\vec{\psi}_T} \to \hat{a}_3. \tag{3.52}$$

The proposed correction is to add a fourth port represented by an operator $\hat{a}_0$ that should correspond to "incoming fluctuations of the vacuum", represented by green dashed lines in Figure 3.4 (see, e.g., [28, p.432], [29, p.511 and p.640], [30, p.70], [31, p.138], [32, p.8 and p.229], [33, p.249 and footnote 1], [34, p.96 and p.123], [35, p.102],). The addition of this port is supposed to solve the problem, since instead of

$$\hat{a}_2 = \tilde{t}\hat{a}_1, \quad \hat{a}_3 = \tilde{r}\hat{a}_1, \tag{3.53}$$

its inclusion allows to construct modified operators

$$\hat{a}'_2 = \tilde{t}\hat{a}_1 + \tilde{r}\hat{a}_0, \quad \hat{a}'_3 = \tilde{r}\hat{a}_1 + \tilde{t}\hat{a}_0, \tag{3.54}$$

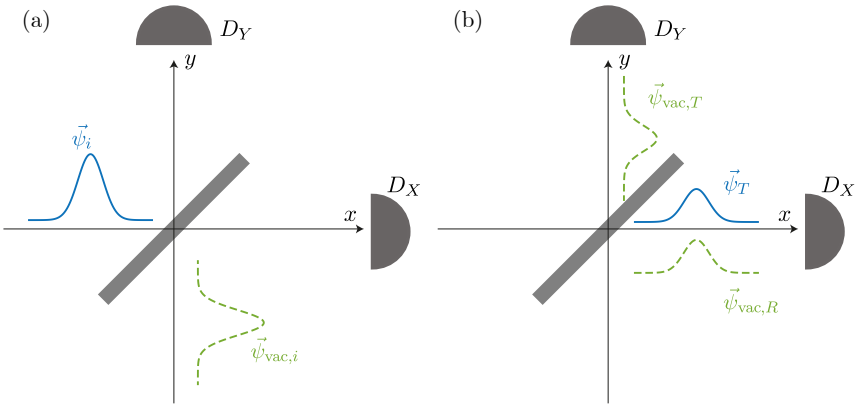

Figure 3.4: Schematic illustration of the description of beam-splitters which uses a fourth port representing the "incoming fluctuations of the vacuum". (a) Incoming pulses representing the initial state (in blue) and the vacuum fluctuations (dashed green curve). (b) Reflection and transmission of the initial pulse and the fluctuation pulse. Fluctuation pulses are drawn in dashed green lines since they do not have any meaning neither in the classical nor in the quantum theory.

that satisfy the bosonic commutation relations

$$\left[\hat{a}'_2, \hat{a}'^{\dagger}_2\right] = \mathbb{1}, \quad \left[\hat{a}'_3, \hat{a}'^{\dagger}_3\right] = \mathbb{1}, \tag{3.55}$$

since $|\tilde{r}|^2 + |\tilde{t}|^2 = 1$.
Although formally this seems to solve the "problem", yielding operators with apparently bosonic commutation relations, we have two criticisms of this construction:

- It is not a problem that the operators in (3.51) do not satisfy the commutation relation for bosons. The photon is not an excitation of the individual transmitted pulse nor of the reflected one. The photon is an excitation of the global mode $\vec{\psi}_R + \vec{\psi}_T$ and thus the bosonic nature of the photon is expressed by the global commutation relation (3.50). So in fact the commutation relations (3.51) are correct, and they do not pose any problem, since creation operators in Fock space are also well defined for unnormalized modes.

- The formal expression $\hat{a}_0^{\dagger}$ that would have to correspond to $\hat{B}^{\dagger}_{\mathrm{vac}}$ does not have any well-defined sense in the quantum field theory of light. There is no creation operator that could create "fluctuations of the vacuum". In Figure 3.4, the pulses drawn in dashed lines, which are supposed to refer to vacuum fluctuations, don't have any meaning. Creation operators can only add photons carried by classical modes, to the vacuum or to other states.

Our main conclusion from the analysis presented above is that vacuum fluctuations do not play any role in the transmission of a one-photon pulse through a beam splitter. Our explanation for the discrepancy sometimes found in the literature is that the notation $\hat{a}_1, \hat{a}_2, \hat{a}_3, \hat{a}_0$ is misleading and clearly insufficient for the description of the transmission of

a one-photon pulse through a beam splitter. One difficulty is that the operator $\hat{B}^\dagger_{\vec{\psi}_R+\vec{\psi}_T}$ has no natural representation in the conventional notation: it could maybe be noted as $\hat{a}^\dagger_{2+3}$, but it is not usually done. The notation also suggests that all operators that are denoted with $\hat{a}_j$ should satisfy the standard bosonic commutation relations, which is not well suited for the beam-splitter, as shown by equation (3.51). Another shortcoming of this notation is that it does not include the propagation in time: When one writes $\hat{a}_3 = \tilde{t}\hat{a}_1$, the operator $\hat{a}_1$ is not the incoming one, but implicitly it must be interpreted as the time evolution of the incoming one (which is not the evolution in the Heisenberg representation, as we remarked in (3.19)). All these difficulties disappear if one uses the more precise notation $\hat{B}^\dagger_{\vec{\psi}}$, which indicates on which classical mode a photon is created. With this notation it is immediately clear that it does not make sense to define a creation operator like $\hat{a}^\dagger_0$ that would create "fluctuations of the vacuum", since there is no $\vec{\psi}$ that can do that.

However, we emphasize that the above remarks do not mean that there are no quantum fluctuations in the one-photon pulse transmission through a beam splitter. The detector readings have quantum fluctuations that can be traced back to the fact that the state of the optical quantum field is not an eigenstate of the observable measured by the detector. Our point is only that the statement "vacuum fluctuations enter through the unused port" is not well defined within the theory and that it is unnecessary, since, without any such addition, the theory already gives a complete and consistent description of the process, including the fluctuations that will be manifest at the detectors. The fluctuations are a global feature of the quantum system, they are everywhere and delocalized, they do not enter through any particular port. The photon states and in particular the vacuum are global entities, they are not localized in any specific port. If the electromagnetic field is in a one-photon state, one cannot claim that it is in the vacuum state anywhere, in particular not in an "unused port". The fluctuations that may be measured in a particular detector, will be the ones determined by the one-photon state, and not by some partially localized vacuum.

In fact the model with four ports can describe a concrete physical situation, but only when an actual classical mode is injected into the fourth port, as we will see in the next section with the Hong-Ou-Mandel effect (HOM) [103, 104].

One should also note that other approaches using also four bosonic operators to describe beam-splitters exist but do not invoke vacuum fluctuations to justify them (see e.g., [79, 105, 106]). Instead, the beam-splitter is seen as a device which creates an interaction between four modes, each represented by their own creation-annihilation opertors. The passage of a single-photon state corresponds thus to the situation where three modes are in the vacuum state and one mode is in a one-quantum excited state. This model is therefore very close to what we have presented above, the major difference being that we do not use the concept of modes that would be located either before or after the beam-splitter but only consider propagating solutions of Maxwell's equations which include the beam-splitter in the dielectric function $\varepsilon(\vec{x})$. Our approach is thus a description within the entire Fock space while the other one is a model which treats only four modes in their respective tensorial Hilbert space. This difference in the dimensionality of the approaches is a good argument for the modal description, however, one should be very carefull when interpreting the results since the excitation of output modes is not strictly speaking a

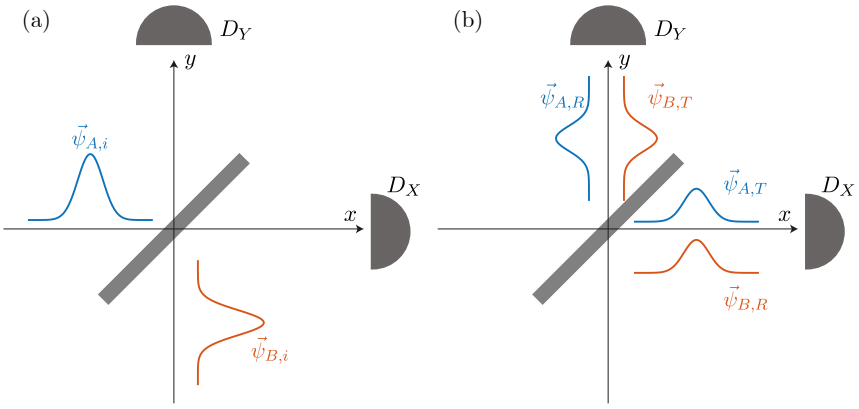

Figure 3.5: Schematic illustration of the HOM effect. (a) Two disjoint identical pulses impinge on the beam splitter at the same time. (b) Each of them produces reflected and transmitted pulses. D_X and D_Y represent detectors, located at the same distance from the beam-splitter.

photon. Indeed, in the situation where a single-photon passes through the beam splitter, the modal approach predicts a state of the form $|1\rangle_3 |0\rangle_4 + |0\rangle_3 |1\rangle_4$, where the indices referred to the output modes 3 and 4. Although this state is an entangled state of the two considered modes, it simply represents a single-photon.

3.3.2 Two-photon state: The Hong-Ou-Mandel effect

We consider two pulses arriving on a $^{50}/_{50}$ beam splitter at 45°: $\vec{\psi}_{A,i}$ moves horizontally in the x direction and $\vec{\psi}_{B,i}$ moves vertically in the y direction as it is shown in Figure 3.5 (a).

3.3.2.1 Initial classical modes and their time evolution

Each pulse at the initial time t_i (before the pulses arrive on the beam splitter) is a classical mode. We will use the pulse shape function $\vec{S}(r_1, r_2, r_3; k, t)$ defined in (3.42).
The initial modes A and B are chosen as

$$\vec{\psi}_{A,i}(\vec{x}) = \vec{S}(x, y, z, t = 0; k_A) = \vec{S}_A(x, t = 0), \tag{3.56a}$$
$$\vec{\psi}_{B,i}(\vec{x}) = \vec{S}(y, x, z, t = 0; k_B) = \vec{S}_B(y, t = 0), \tag{3.56b}$$

where we introduced an abridged notation $\vec{S}_A, \vec{S}_B$, indicating only the first spatial argument and the time argument.
After crossing the beam splitter, each classical mode evolves into a reflected and a transmitted pulse

$$\vec{\psi}_{A,i} \xrightarrow{\text{B-S}} \vec{\psi}_{A,R} + \vec{\psi}_{A,T}, \tag{3.57a}$$
$$\vec{\psi}_{B,i} \xrightarrow{\text{B-S}} \vec{\psi}_{B,R} + \vec{\psi}_{B,T}, \tag{3.57b}$$

where

$$\vec{\psi}_{A,R}(\vec{x},t) = \tilde{r}\vec{S}_A(y-ct,t) = \tilde{r}\vec{Y}_A(y), \tag{3.58a}$$
$$\vec{\psi}_{A,T}(\vec{x},t) = \tilde{t}\vec{S}_A(x-ct,t) = \tilde{t}\vec{X}_A(x), \tag{3.58b}$$
$$\vec{\psi}_{B,R}(\vec{x},t) = \tilde{r}\vec{S}_B(x-ct,t = \tilde{r}\vec{X}_B(x), \tag{3.58c}$$
$$\vec{\psi}_{B,T}(\vec{x},t) = \tilde{t}\vec{S}_B(y-ct,t) = \tilde{t}\vec{Y}_B(y), \tag{3.58d}$$

and $\tilde{r}$ and $\tilde{t}$ are still the reflection and transmission coefficients satisfying $|\tilde{r}|^2 + |\tilde{t}|^2 = 1$ and $\tilde{r}^*\tilde{t} + \tilde{r}\tilde{t}^* = 0$. For a $^{50}/_{50}$ beam splitter they satisfy furthermore

$$\tilde{t} = i\tilde{r}, \qquad \text{i.e., } \tilde{r}^2 + \tilde{t}^2 = 0. \tag{3.59}$$

We again introduce the abridged notations $\vec{Y}_A(y), \vec{X}_A(x)$ $\vec{Y}_B(y), \vec{X}_B(x)$ to improve the readability of the construction below ($\vec{X}$: propagation along the x-axis; $\vec{Y}$: propagation along the y-axis).

3.3.2.2 Quantum dynamics of the two-photon state

We assume that the system is prepared with one-photon on each mode. The two-photon state in the Fock space is thus

$$|\Phi_i\rangle = \hat{B}^\dagger_{\vec{\psi}_{A,i}} \hat{B}^\dagger_{\vec{\psi}_{B,i}} |\varnothing\rangle \tag{3.60a}$$
$$= \sqrt{2}\, |\vec{\psi}_{A,i} \otimes_S \vec{\psi}_{B,i}\rangle \tag{3.60b}$$
$$= \frac{1}{\sqrt{2}} |\vec{\psi}_{A,i} \otimes \vec{\psi}_{B,i} + \vec{\psi}_{B,i} \otimes \vec{\psi}_{A,i}\rangle\,. \tag{3.60c}$$

The mode functions must be normalized

$$\int d^3x |\vec{\psi}_{A,i}(\vec{x})|^2 = 1, \qquad \int d^3x |\vec{\psi}_{B,i}(\vec{x})|^2 = 1, \tag{3.61}$$

which entails

$$\left[\hat{B}_{\vec{\psi}_{A,i}}, \hat{B}^\dagger_{\vec{\psi}_{A,i}}\right] = \mathbb{1} = \left[\hat{B}_{\vec{\psi}_{B,i}}, \hat{B}^\dagger_{\vec{\psi}_{B,i}}\right], \tag{3.62a}$$
$$\left[\hat{B}_{\vec{\psi}_{A,i}}, \hat{B}^\dagger_{\vec{\psi}_{B,i}}\right] = \langle\vec{\psi}_{A,i}|\vec{\psi}_{B,i}\rangle = \int_{\mathbb{R}^3} d^3x\ \vec{\psi}^\star_{A,i}(\vec{x}) \cdot \vec{\psi}_{B,i}(\vec{x}) = 0, \tag{3.62b}$$

since the support of the two classical modes $\vec{\psi}_{A,i}(\vec{x})$ and $\vec{\psi}_{B,i}(\vec{x})$ is disjoint.
To obtain the time evolution after the beam splitter of the two-photon initial state, we apply the classical time evolution of each pulse

$$\vec{\psi}_{A,i} \otimes_S \vec{\psi}_{B,i} \xrightarrow{\text{B-S}} \left(\vec{\psi}_{A,R} + \vec{\psi}_{A,T}\right) \otimes_S \left(\vec{\psi}_{B,R} + \vec{\psi}_{B,T}\right) \tag{3.63a}$$
$$= \vec{\psi}_{A,R} \otimes_S \vec{\psi}_{B,R} + \vec{\psi}_{A,R} \otimes_S \vec{\psi}_{B,T} + \vec{\psi}_{A,T} \otimes_S \vec{\psi}_{B,R} + \vec{\psi}_{A,T} \otimes_S \vec{\psi}_{B,T}$$
$$= \tilde{r}\vec{Y}_A \otimes_S \tilde{r}\vec{X}_B + \tilde{r}\vec{Y}_A \otimes_S \tilde{t}\vec{Y}_B + \tilde{t}\vec{X}_A \otimes_S \tilde{r}\vec{X}_B + \tilde{t}\vec{X}_A \otimes_S \tilde{t}\vec{Y}_B$$
$$= \frac{1}{2}\Big[\tilde{r}^2\vec{Y}_A \otimes \vec{X}_B + \tilde{t}^2\vec{X}_A \otimes \vec{Y}_B + \tilde{r}\tilde{t}\left(\vec{Y}_A \otimes \vec{Y}_B + \vec{X}_A \otimes \vec{X}_B\right)$$
$$+\tilde{r}^2\vec{X}_B \otimes \vec{Y}_A + \tilde{t}^2\vec{Y}_B \otimes \vec{X}_A + \tilde{r}\tilde{t}\left(\vec{Y}_B \otimes \vec{Y}_A + \vec{X}_B \otimes \vec{X}_A\right)\Big]. \tag{3.63b}$$

In the degenerate Hong-Ou-Mandel effect the shapes of the two incoming classical modes are the same and they arrive at the same time at the beam splitter and at the detectors, which means that $\vec{Y}_A = \vec{Y}_B = \vec{Y}$ and $\vec{X}_A = \vec{X}_B = \vec{X}$. Therefore the final state after the beam-splitter can be deduced from (3.60), (3.63) and from the condition of identical modes, which yields

$$\Phi_f = \frac{\tilde{r}^2 + \tilde{t}^2}{\sqrt{2}} \left(\vec{X} \otimes \vec{Y} + \vec{Y} \otimes \vec{X} \right) + \sqrt{2}\, \tilde{r}\tilde{t} \left(\vec{Y} \otimes \vec{Y} + \vec{X} \otimes \vec{X} \right). \tag{3.64}$$

Since for a $^{50}/_{50}$ beam splitter $\tilde{r}^2 + \tilde{t}^2 = 0$, the final state for the degenerate Hong-Ou-Mandel effect can be written as

$$|\Phi_i\rangle = \sqrt{2}\, |\vec{\psi}_{A,i} \otimes_S \vec{\psi}_{B,i}\rangle \xrightarrow{\text{B-S}} |\Phi_f\rangle = \sqrt{2}\tilde{r}\tilde{t} \left(|\vec{Y} \otimes \vec{Y}\rangle + |\vec{X} \otimes \vec{X}\rangle \right). \tag{3.65}$$

From this expression, one can conclude that there will be no simultaneous detection of one photon in each detector, since the state does not contain terms of the form $|\vec{X} \otimes_S \vec{Y}\rangle$. In order to make this statement more precise we have to construct a model for the detectors, i.e., we have to write the observables that correspond to single and double detections.

3.3.2.3 Detection model to interpret the dynamics

A simple model for these observables can be constructed using the classical modes $\vec{X}$ and $\vec{Y}$. Following what we briefly introduced for the time-bin measurements (see equation 3.40), the observable corresponding to the detection of one photon in the considered mode shape in the detector D_X is

$$\hat{O}_{1X} = |\vec{X}\rangle \langle\vec{X}| \otimes \mathbb{1} + \mathbb{1} \otimes |\vec{X}\rangle \langle\vec{X}|, \tag{3.66}$$

and correspondingly in the detector D_Y

$$\hat{O}_{1Y} = |\vec{Y}\rangle \langle\vec{Y}| \otimes \mathbb{1} + \mathbb{1} \otimes |\vec{Y}\rangle \langle\vec{Y}|. \tag{3.67}$$

The major difference with the time-bin detection model is that here, we have an entangled state — similar to (3.41). The observable corresponding to the detection of two photons in D_X is

$$\hat{O}_{2XX} = |\vec{X}\rangle \langle\vec{X}| \otimes |\vec{X}\rangle \langle\vec{X}|, \tag{3.68}$$

and correspondingly for D_Y

$$\hat{O}_{2YY} = |\vec{Y}\rangle \langle\vec{Y}| \otimes |\vec{Y}\rangle \langle\vec{Y}|. \tag{3.69}$$

Finally, the observable corresponding to the detection of one photon in D_X and simultaneously one photon in D_Y is

$$\hat{O}_{2XY} = |\vec{Y}\rangle \langle\vec{Y}| \otimes |\vec{X}\rangle \langle\vec{X}| + |\vec{X}\rangle \langle\vec{X}| \otimes |\vec{Y}\rangle \langle\vec{Y}|. \tag{3.70}$$

Since $\hat{O}_{2XY}$ is a projector, the probability to observe simultaneously one photon in each detector in the final state $|\Phi_f\rangle$ is given by

$$\mathrm{P}(D_X \text{ and } D_Y) = \langle\Phi_f| \hat{O}_{2XY} |\Phi_f\rangle, \tag{3.71}$$

which we can compute using the expression (3.65) for $|\Phi_f\rangle$

$$\begin{aligned} \mathrm{P}(D_X \text{ and } D_Y) &= \langle\Phi_f|\,\hat{O}_{2XY}\,|\Phi_f\rangle \\ &= 2|\tilde{r}\tilde{t}|^2 \left\langle \vec{Y}\otimes\vec{Y} + \vec{X}\otimes\vec{X}\right| \Big(|\vec{Y}\rangle\,\langle\vec{Y}|\otimes|\vec{X}\rangle\,\langle\vec{X}| \Big) \left|\vec{Y}\otimes\vec{Y} + \vec{X}\otimes\vec{X}\right\rangle, \end{aligned} \tag{3.72}$$

and since

$$\Big(|\vec{Y}\rangle\,\langle\vec{Y}|\otimes|\vec{X}\rangle\,\langle\vec{X}| \Big)\,|\vec{Y}\otimes\vec{Y}\rangle = 0 = \Big(|\vec{Y}\rangle\,\langle\vec{Y}|\otimes|\vec{X}\rangle\,\langle\vec{X}| \Big)\,|\vec{X}\otimes\vec{X}\rangle\,, \tag{3.73}$$

we conclude that $\mathrm{P}(D_X \text{ and } D_Y) = 0$, namely, the probability for simultaneous detection of one photon in each detector is zero, which is the main characteristic of the Hong-Ou-Mandel effect.

3.3.2.4 Photons are not like classical waves nor like classical particles

We emphasize that the last equality of (3.63), and thus (3.64) and (3.65), are only true because photons are bosons (i.e., indistinguishable quanta) meaning that the effect of the bosonic symmetrization is essential for the HOM effect. In particular, the HOM effect is a purely quantum effect which does not appear with classical waves. Indeed the classical waves would arrive at the two detectors simultaneously — as one can see in Figure 3.5(b) with the dynamics of the classical pulses — and thus it is excluded that only one detector is activated. The event that for photons have probability zero, would have probability one for classical waves. The behavior of photons in the HOM effect is also completely different from that of classical particles. Indeed, for classical particles having 1/2 probability of transmission and 1/2 probability of reflection, the probability of detecting two particles in the detector D_X would be

$$\mathrm{P}(2 \text{ particles in } D_X) = \mathrm{P}(1 \text{ particle in } D_X) \times \mathrm{P}(1 \text{ particle in } D_X) = \frac{1}{2}\frac{1}{2} = \frac{1}{4}, \tag{3.74}$$

and similarly for D_Y

$$\mathrm{P}(2 \text{ particles in } D_Y) = \mathrm{P}(1 \text{ particle in } D_Y) \times \mathrm{P}(1 \text{ particle in } D_Y) = \frac{1}{2}\frac{1}{2} = \frac{1}{4}, \tag{3.75}$$

and by labeling the particles moving initially horizontally and vertically by X_i and Y_i, respectively, the probability of a joint detection would be

$$\begin{aligned} \mathrm{P}(1 \text{ particle in } D_X \text{ and } 1 \text{ particle in } D_Y) &= \mathrm{P}(\text{particle } Y_i \text{ in } D_Y \text{ and particle } X_i \text{ in } D_X) \\ &\quad + \mathrm{P}(\text{particle } Y_i \text{ in } D_X \text{ and particle } X_i \text{ in } D_Y) \\ &= \frac{1}{2}\frac{1}{2} + \frac{1}{2}\frac{1}{2} = \frac{1}{2}. \end{aligned} \tag{3.76}$$

It means that the event that has zero probability for photons has probability 1/2 for classical particles.

This example gives an illustration for the question on whether photons are particles or waves, or both. The answer is that they are neither particles nor waves in the classical sense. It is not that photons "behave sometimes like particles and sometimes like waves", as it was often stated in the early stages of the development of quantum mechanics. They are purely quantum entities, that have properties that do not exist in classical objects.

3.4 Local detection of single-photon states

We have seen in the preceding sections that the description of photon's dynamics cannot be fully understood by considering only the states, but requires to take into account the observables as well. So far, we have described several types of observables such as the electromagnetic fields and a quite simplistic model for a detection for the interpretation of the Hong-Ou-Mandel effect. In this section, we would like to introduce a more detailed model for the detection which should be relevant in some actual single-photon experiments.

3.4.1 Single-photon detectors

A single-photon detector should be an apparatus which informs of the presence of a photon, inside its volume of sensitivity $\mathcal{V}_\mathrm{d}$, at a given time τ. Ideally one would like the following properties:

- 100% of detection efficiency, i.e., it does not miss any photon;
- a dark count rate of zero, i.e., it does not give a signal when there is no photon;
- no dead time, i.e., it can detect a photon at any time, no matter if it has detected a photon before.

No such perfect detector exists but some are reasonably approaching these conditions to be used in experiments. One can cite for instance photomultipliers, single-photon avalanche photodiodes, quantum-dot field-effect transistor-based detectors, up-conversion single-photon detectors or superconducting nanowire single-photon detectors [107]. All of them rely on a current that is triggered when a photon is absorbed. To go into further details of the different processes that exist to detect a photon, one can look in [107] and refereces therein. In the following, we want to build a theoretical model that could represent some of these detectors. In a first approach, and to grasp the basic physics of photons, we will assume that the three conditions stated above about perfect detectors are true. We will rather focus on a fourth property that will allow us to probe interesting spatial properties of photons. We will consider detectors that have a finite volume $\mathcal{V}_\mathrm{d}$. This particularity, which one always deals with in a real experiment, brings questions about when the detection process starts and ends as illustrated in Figure 3.6. Keeping in mind that photons are always carried by classical pulsed functions, the detection is to be thought as a dynamical process.

3.4.2 Local observable for the detection

The fact that photons are carried by pulse-shaped classical functions, must influence the detection and one cannot ignore the different scenarios brought by the size of the considered photon pulses. In Figure 3.6, one can see that a detector cannot always probe photon pulses as a whole. To theoretically describe such situation, we need to use a local observable, i.e., a selfadjoint operator which depends on the position of the photon field.

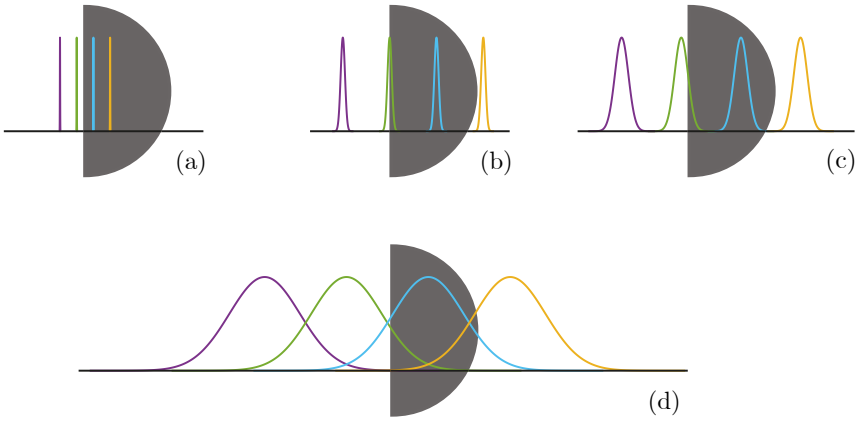

Figure 3.6: Sketch of the different scenarios possible for a photon state to pass through a detector. Photon states are represented by their associated classical pulses which propagate to the right and pass through the detector (in gray). The colors represent different times during the propagation of the pulse. (a) The photon pulse is so small compared to the detector size that it looks like a delta function. Consequently, it is either inside or outside the detector without any ambiguity. (b) The photon pulse is still small compare to the detector but some ambiguity can appear (green pulse). However, they are usually neglected since they correspond to a very short period of time, usually much shorter than the detector's time resolution. (c) Photon's size is comparable to that of the detector meaning that it can still be fully inside the detector but ambiguities on when does it come in and out become more important. (d) The photon pulse is bigger than the detector so it cannot be considered inside at any moment. This situation points out the need for a model of a local detection of photons.

Remarks:

- We note that a local observable is rather a physical than a mathematical consideration: an operator is said to be a local observable if it represents a physical measurement which can be made with an instrument well localized in space. We can assume that $\hat{\vec{E}}(\vec{x})$ and $\hat{\vec{B}}(\vec{x})$ are local since in practice they can be measured by instruments involving, e.g., localized charged particles or magnetic moments and thus possibly designed as small as required. Any operator that can be written as a point-wise function of $\hat{\vec{E}}(\vec{x})$ and $\hat{\vec{B}}(\vec{x})$ is thus considered to be a local observable too.
- To analyze the detection process in a rather simple way, we assume that the detector is placed far from any optical device like mirrors or beam-splitters. With this condition, the dielectric function in the surroundings of the detector can be considered as constant, and we therefore do not need to use the generalized quantization for inhomogeneous media anymore. Instead, we will work with the quantization in the vacuum, i.e., with a frequency operator $\Omega = c(-\Delta)^{-1/2}$, as well as with the BB representation. In practice, if the photon reaches the detector through a propagation in a homogenous dielectric medium of optical index $n > 1$, e.g., an optical fiber, one can still use the results we develop hereafter by replacing the vacuum speed of light c by its analog c/n.

The local observable we want to use in the context of single-photon detection is the electromagnetic energy density [38] represented by

$$\hat{\mathcal{E}}_{\mathrm{em}}(\vec{x}) = \frac{\varepsilon_0}{2} : \left(\hat{\vec{E}}^2(\vec{x}) + c^2\hat{\vec{B}}^2(\vec{x})\right) : , \tag{3.77}$$

where $: \cdot :$ stands for the normal ordering. This observable is a function of the position $\vec{x}$, but one can construct an more realistic model by integrating it over the detector volume $\mathcal{V}_{\mathrm{d}}$

$$\hat{\mathcal{E}}_{\mathrm{em},\mathcal{V}_{\mathrm{d}}} = \int_{\mathcal{V}_{\mathrm{d}}} d^3x \; \hat{\mathcal{E}}_{\mathrm{em}}(\vec{x}). \tag{3.78}$$

To analyze the response of a detector represented by such operators, we need to compute the mean values for a general single-photon state. We remark that $\hat{\mathcal{E}}_{\mathrm{em}}$ can be rewritten in terms of the RS vector

$$\hat{\mathcal{E}}_{\mathrm{em}}(\vec{x}) = \frac{\varepsilon_0}{2} : \left(\hat{\vec{E}} - ic\hat{\vec{B}}\right) \cdot \left(\hat{\vec{E}} + ic\hat{\vec{B}}\right) : \tag{3.79a}$$

$$= : \hat{\vec{F}}^{\dagger}_{RS}(\vec{x}) \cdot \hat{\vec{F}}_{RS}(\vec{x}) : , \tag{3.79b}$$

and we recall (equation 2.67c) that the quantized RS vector can be written as

$$\hat{\vec{F}}_{RS}(\vec{x}) = \int d^3k \left[\vec{g}_{\vec{k},+}(\vec{x})\hat{C}_{\vec{g}_{\vec{k},+}} + \vec{g}^{\star}_{\vec{k},-}(\vec{x})\hat{C}^{\dagger}_{\vec{g}_{\vec{k},-}}\right] \tag{3.80a}$$

$$= \hat{\vec{\mathbf{F}}}^{(h+)} + \hat{\vec{\mathbf{F}}}^{(h-)\dagger}. \tag{3.80b}$$

Since we have a quite compact expression for $\hat{\mathcal{E}}_{\mathrm{em}}$ in the BB representation, we write a general single-photon state as $|1_{\mathrm{ph}}\rangle = |\vec{F}\rangle = \hat{C}^{\dagger}_{\vec{F}}|\varnothing\rangle$ and the expectation value reads

$$\langle\hat{\mathcal{E}}_{\mathrm{em}}\rangle_{|1_{\mathrm{ph}}\rangle} = \langle\varnothing|\,\hat{C}_{\vec{F}} : \hat{\vec{F}}^{\dagger}_{RS}(\vec{x}) \cdot \hat{\vec{F}}_{RS}(\vec{x}) : \hat{C}^{\dagger}_{\vec{F}}\,|\varnothing\rangle\,. \tag{3.81}$$

Combining (3.79) and (3.80), the energy density operator can be written as

$$\hat{\mathcal{E}}_{\rm em}(\vec{x}) = \,:\vec{\hat{\mathbf{F}}}^{(h+)\dagger}\cdot\vec{\hat{\mathbf{F}}}^{(h+)} + \vec{\hat{\mathbf{F}}}^{(h-)}\cdot\vec{\hat{\mathbf{F}}}^{(h-)\dagger} + \vec{\hat{\mathbf{F}}}^{(h+)\dagger}\cdot\vec{\hat{\mathbf{F}}}^{(h-)\dagger} + \vec{\hat{\mathbf{F}}}^{(h-)}\cdot\vec{\hat{\mathbf{F}}}^{(h+)}:, \tag{3.82}$$

where one remarks that only the first two terms will contribute to mean values. Equation (3.81) transforms then into

$$\langle\hat{\mathcal{E}}_{\rm em}\rangle_{|1_{\rm ph}\rangle} = \langle\varnothing|\,\hat{C}_{\vec{F}}\vec{\hat{\mathbf{F}}}^{(h+)\dagger}\cdot\vec{\hat{\mathbf{F}}}^{(h+)}\hat{C}^{\dagger}_{\vec{F}}\,|\varnothing\rangle + \langle\varnothing|\,\hat{C}_{\vec{F}}\vec{\hat{\mathbf{F}}}^{(h-)\dagger}\cdot\vec{\hat{\mathbf{F}}}^{(h-)}\hat{C}^{\dagger}_{\vec{F}}\,|\varnothing\rangle \tag{3.83}$$

which can be computed using the following commutators

$$\begin{aligned}
\left[\vec{\hat{\mathbf{F}}}^{(h\pm)}(\vec{x}), \hat{C}^{\dagger}_{\vec{F}}\right] &= \int_{\mathbb{R}^3} d^3k\; \vec{g}_{\vec{k},\pm}(\vec{x})\left[\hat{C}_{\vec{g}_{\vec{k},\pm}}, \hat{C}^{\dagger}_{\vec{F}}\right] && \text{(3.84a)}\\
&= \int_{\mathbb{R}^3} d^3k \int_{\mathbb{R}^3} d^3k' \sum_{\lambda'} \langle\vec{g}_{\vec{k}',\lambda'}|\vec{F}\rangle_{BB}\,\vec{g}_{\vec{k},\pm}(\vec{x})\left[\hat{C}_{\vec{g}_{\vec{k},\pm}}, \hat{C}^{\dagger}_{\vec{g}_{\vec{k}',\lambda'}}\right] && \text{(3.84b)}\\
&= \int_{\mathbb{R}^3} d^3k\,\langle\vec{g}_{\vec{k},\pm}|\vec{F}\rangle_{BB}\,\vec{g}_{\vec{k},\pm}(\vec{x}) && \text{(3.84c)}\\
&= \vec{F}^{(h\pm)}(\vec{x}), && \text{(3.84d)}
\end{aligned}$$

and

$$\left[\hat{C}_{\vec{F}}, \vec{\hat{\mathbf{F}}}^{(h\pm)\dagger}(\vec{x})\right] = \left[\vec{\hat{\mathbf{F}}}^{(h\pm)}(\vec{x}), \hat{C}^{\dagger}_{\vec{F}}\right]^{\dagger} = \vec{F}^{(h\pm)\star}(\vec{x}). \tag{3.85}$$

We obtain thus [38]

$$\langle\hat{\mathcal{E}}_{\rm em}(\vec{x})\rangle_{|1_{\rm ph}\rangle} = \left|\vec{F}^{(h+)}(\vec{x})\right|^2 + \left|\vec{F}^{(h-)}(\vec{x})\right|^2. \tag{3.86}$$

In the LP representation, it is expressed as

$$\langle\hat{\mathcal{E}}_{\rm em}(\vec{x})\rangle_{|1_{\rm ph}\rangle} = \hbar\left|\Omega^{1/2}\vec{\psi}^{(h+)}(\vec{x})\right|^2 + \hbar\left|\Omega^{1/2}\vec{\psi}^{(h-)}(\vec{x})\right|^2, \tag{3.87}$$

and in the momentum representation

$$\langle\hat{\mathcal{E}}_{\rm em}(\vec{x})\rangle_{|1_{\rm ph}\rangle} = \hbar\left|\int d^3k\;\omega_{\vec{k}}^{1/2}\vec{\phi}_{\vec{k},+}(\vec{x})z(\vec{k},+)\right|^2 + \hbar\left|\int d^3k\;\omega_{\vec{k}}^{1/2}\vec{\phi}_{\vec{k},-}(\vec{x})z(\vec{k},-)\right|^2. \tag{3.88}$$

We remark that the splitting into helicity components of the field plays a central role in the model for local detection. In the following, we will use this property to discuss the nonlocal character of single-photon states.

3.4.3 Brief review on photon's nonlocality property

The question of the localization of single-quanta and in particular single photons has been a common theme throughout the development of quantum field theory. As in Chapter 2, we will again not use the concept of photon wavefunction to describe it since it usually carries the connotation of a Born probability rule, which is not well-adapted to photon detection.

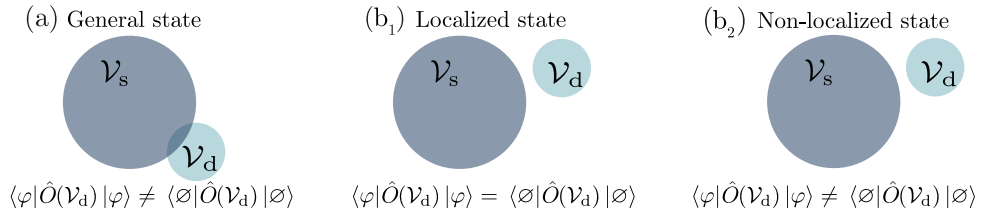

Figure 3.7: Sketch illustrating Knight's definition of a localized state. We consider a state $|\varphi\rangle$ with an associated localization volume $\mathcal{V}_\mathrm{s}$, and a detector $\hat{O}(\mathcal{V}_\mathrm{d})$ with finite volume $\mathcal{V}_\mathrm{d}$, which probes the state. Two situations can occur: (a) a general state where $\mathcal{V}_\mathrm{d} \cap \mathcal{V}_\mathrm{s} \neq \emptyset$ and the expectation value of $\hat{O}(\mathcal{V}_\mathrm{d})$ is not equal to that of the vacuum, or (b$_1$) a localized state where $\mathcal{V}_\mathrm{d} \cap \mathcal{V}_\mathrm{s} = \emptyset$ and the expectation value of $\hat{O}(\mathcal{V}_\mathrm{d})$ is equal to that of the vacuum for all observables $\hat{O}$. This means that the state cannot be "seen" outside its volume of localization by any localized detector. (b$_2$) A state is considered to be nonlocalized if it can be probed outside its apparent volume of localization by some observable $\hat{O}(\mathcal{V}_d)$, i.e., $\langle\varphi|\,\hat{O}(\mathcal{V}_\mathrm{d})\,|\varphi\rangle \neq \langle\varnothing|\,\hat{O}(\mathcal{V}_\mathrm{d})\,|\varnothing\rangle$ for $\mathcal{V}_\mathrm{d} \cap \mathcal{V}_\mathrm{s} = \emptyset$. In general, this means that for such extended states, there is no $\mathcal{V}_\mathrm{s}$ satisfying (a) and (b$_1$) for any $\hat{O}(\mathcal{V}_\mathrm{d})$.

We will rather use the combination of position space representations with suitable local observables to consider spatial localization properties of photons and discuss measurements that can be performed in actual experiments.
Before going through the state of the art regarding photon localization, we define the localization criterion that will be used thereafter, and following Knight [40]: We consider a state $|\varphi\rangle$, represented in a position representation in the Fock space of the considered quantum field theory. It is said to be a localized state if for any local observable $\hat{O}(\vec{x})$, the expectation value $\langle\varphi|\,\hat{O}(\vec{x})\,|\varphi\rangle$ is equal to that of the vacuum state outside a certain volume $\mathcal{V}_\mathrm{s}$ called the localization volume of the state. Mathematically it means that

$$\langle\varphi|\,\hat{O}(\vec{x})\,|\varphi\rangle \neq \langle\varnothing|\,\hat{O}(\vec{x})\,|\varnothing\rangle \quad \text{for } \vec{x} \in \mathcal{V}_\mathrm{s}, \tag{3.89}$$

and

$$\langle\varphi|\,\hat{O}(\vec{x})\,|\varphi\rangle = \langle\varnothing|\,\hat{O}(\vec{x})\,|\varnothing\rangle \quad \text{for } \vec{x} \notin \mathcal{V}_\mathrm{s}. \tag{3.90}$$

This property is illustrated in Figure 3.7. Consequently, a nonlocalized or nonlocalizable state would not respect this condition for at least one local observable, i.e., one can find a local observable for which $\langle\varphi|\,\hat{O}_\mathrm{s}(\vec{x})\,|\varphi\rangle \neq \langle\varnothing|\,\hat{O}_\mathrm{s}(\vec{x})\,|\varnothing\rangle$ for at least one $x \notin \mathcal{V}_\mathrm{s}$ as shown in Figure 3.7 (b$_2$).

Following this definition, Knight showed that for states composed of a finite number of quanta, a class of space- and time-dependent correlation functions of the Klein-Gordon field cannot be zero anywhere. Only states involving the superposition of infinitely many quanta, e.g., coherent states, can be spatially localized. This result was reformulated and extended by De Bièvre [90, 108] in terms of expectation values of Weyl unitary operators. In these type of approaches the main property that leads to nonlocality is the anti-local property of the frequency operator [109–111], where anti-locality means that if for some square-integrable field $\vec{v}(\vec{x})$ both $\vec{v} = 0$ and $\Omega\vec{v} = 0$ in some finite volume, then $\vec{v} = 0$

everywhere in $\mathbb{R}^3$ as we will precisely describe in Lemma 1. The main result one can extract from these works is that for any single-photon state and for any finite volume, there exists a local observable with support in that volume for which the expectation value in the single-photon state differs from the one in the vacuum.
In [112, 113], following the results of Knight, Licht characterized the whole set of strictly localized states by showing that they can be obtained by applying a partial isometry $\hat{W}^\dagger\hat{W} = \mathbb{1}$ on the vacuum $\hat{W}^\dagger |\varnothing\rangle$.
Białynicki-Birula showed that for two particular classes of single-photon states, the expectation value of the energy density cannot be zero in any finite volume. The two classes considered are states with a spherically uniform support [38], and states having either a magnetic or an electric localization property, defined in [39]. The argument in [38] was constructed using the Paley-Wiener theorem [114]: Single photons with an exponential radial falloff of the form $\exp(-Ar)$, $A > 0$, cannot exist, but weaker falloffs are allowed and an example corresponding to a falloff of the form $\exp(-A\sqrt{r})$ was given. In general, in order to fulfill the constraint from the Paley-Wiener theorem, a quasi exponential localization is possible with a falloff $\exp(-Ar^\gamma)$, where $\gamma < 1$. The advantage of the argument of [38] is that it provides a localization limit and gives a concrete example of a solution of Maxwell's equations approaching that limit. In [39] the authors introduced the notions of electrically and magnetically localized states and using a proof of the nonlocality of the helicity operator Λ, they showed that electrically or magnetically localized states cannot be considered as local if one uses the energy density observable.
We also mention [115, 116] where it was shown that there exist cylindrical functions for which a Gaussian falloff is possible in the waist plane only, making the localization, in these directions, stronger than the exponential limit shown in [38] but the nonlocality is transferred to the remaning direction. More recently in [117–119], some classes of strictly localized states — that are not single-photon states — were constructed so that they approach single-photon states as close as possible.
In an other line, Hegerfeldt [41,42] established some general properties of bosons: For states containing exclusively positive energies, if the state function has a finite support at a given time, the time evolution will spread it over all space at any later times (see also [120]). In a later work, concerning causality in Fermi's two-atom model [121], he showed that for positive bounded observables $0 \leq \hat{\mathcal{O}} \leq 1$, the expectation value $\langle\psi(t)|\,\hat{\mathcal{O}}\,|\psi(t)\rangle$ is either nonzero for almost all t or identically zero for all t. Some recent works have explored the possibility of constructing variations of quantum field theory involving negative energy states that could avoid Hegerfeldt's non locality [122–125].
In view of these results, the nonlocality of photons is considered as a well established property which however has not been fully characterized using an observable able to represent an actual detector used in experiment. This is what we will do in the next section by extending the proof of [39] using the energy density to all single-photon states.

3.4.4 Nonlocality of the energy density for single-photon states — Proof

In this section, we will show that all single-photon states cannot be localized in space. This is an extension of the works [38,39], and it has the advantage that it does not require the use of the time evolution compare to the results of Knigth and of Hegerfeldt. To do

so, we will use a property of the frequency operator Ω to demonstrate that the mean value of the local energy density observable (3.86) cannot be zero for any $\vec{x} \in \mathbb{R}^3$, i.e.,

$$\langle \hat{\mathcal{E}}_{\rm em}(\vec{x}) \rangle_{|1_{\rm ph}\rangle} \neq 0, \quad \forall \vec{x} \in \mathbb{R}^3. \tag{3.91}$$

We emphasize that the proof will be constructed to consider any single-photon state $|1_{\rm ph}\rangle$ and that the result is valid irrespective of the representation used to describe the photon since the isomorphisms $\mathcal{M}$ and $\mathcal{I}$ can be applied to switch from one representation to another. Having a proof that is true for any state is an improvement of Białynicki-Birula *et al* proof [38, 39] and does not contradict Knight's general theorem [40]. One advantage of our proof is that we explicitly find a local observable from which the nonlocalization character of photons can be seen. Moreover, as mentioned in Section 3.4.2, the local energy density observable is a relevant observable to describe actual detectors and thus the nonlocalizability of single photons is not a feature hidden in a hard-to-measure property of photons.
The result (3.91) is a consequence of the following Lemmas

Lemma 1: *For any field $\vec{g}(\vec{x})$ that is not identically zero, $\Omega\vec{g}$ and $\vec{g}$ cannot be both zero in any open set of $\mathbb{R}^3$* [109–111].

Lemma 2: *Fields of $\pm$ helicity, i.e., $\Lambda\vec{g}^{(h\lambda)}(\vec{x}) = \lambda\vec{g}^{(h\lambda)}(\vec{x})$, $\lambda = \pm$, have the property that either $\vec{g}^{(h\lambda)}$ is identically zero or $\vec{g}^{(h\lambda)} \neq 0$ in any open set of $\mathbb{R}^3$.*

A proof of Lemma 1 following the argument of [110] is given in Appendix D.
Lemma 2 can be shown directly as follows: Let $\vec{g}$ be a transverse field, $\vec{g} = \vec{g}^{(h+)} + \vec{g}^{(h-)}$. The helicity components are eigenfunctions of the helicity operator $\Lambda\vec{g}^{(h\pm)} = \pm\vec{g}^{(h\pm)}$. Using the definition of the helicity operator $\Lambda = c\Omega^{-1}\nabla\times$, we can reformulate this relation as

$$c\nabla \times \vec{g}^{(h\pm)} = \pm\Omega\vec{g}^{(h\pm)}. \tag{3.92}$$

Taking a given $\lambda = \pm$, if $\vec{g}^{(h\lambda)}$ is zero in an open set $\mathcal{S}$, then $\nabla \times \vec{g}^{(h\lambda)}$ is zero in the same set and finally (3.92) implies that $\Omega\vec{g}^{(h\lambda)}$ is also zero in $\mathcal{S}$, which by Lemma 1 implies that $\vec{g}^{(h\lambda)}$ is zero everywhere. We conclude that $\vec{g}^{(h\lambda)}$ is either identically zero or nonzero for any open set as stated in Lemma 2.
The central result (3.91) can thus be shown by taking $\vec{g}$ to be the BB representation $\vec{F}$ of any single-photon state which is transverse and thus can be decomposed as $\vec{F} = \vec{F}^{(h+)} + \vec{F}^{(h-)}$. We conclude then that $\vec{F}^{(h\pm)}$ is either identically zero or nonzero in any open set. Moreover, since (3.86) has two terms, even if one of them is identically zero, the other cannot be zero too since it would mean that the single-photon state itself is zero. This result is valid for any open set and therefore one can extend it to any point $\vec{x} \in \mathbb{R}^3$, which completes the proof.
Thus, since the zero-point energy has been removed using the normal ordering in (3.77), $\langle \hat{\mathcal{E}}_{\rm em}(\vec{x}) \rangle_{|1_{\rm ph}\rangle}$ is never equal to the vacuum mean value, preventing Knight's localization criterion to be fulfilled for any single-photon state.
In physical terms this means that if the electromagnetic field is prepared in a single-photon state, a detector, placed anywhere in space, which measures the energy in a finite volume,

has a nonzero probability of detecting the photon. The probability can be small but it is strictly nonzero.
The main advantage of our argument to show the nonlocality of single photons is that it does not require the time-evolution of the states. This is an important difference with the works of Knight using time-dependent correlation functions and of Hegerfeldt where locality is possible at initial time and nonlocality considered as a consequence of the time evolution. Also, we show in Appendix C that the result we have obtained for the energy density cannot be deduced from Knight's general theorem since the latter is not valid for equal-time correlation functions. Moreover, a strength of our result is that, while Knight or De Bièvre were showing that there always exists a local observable for which the expectation value differs from the vacuum one, we show that for the electromagnetic field, this local observable can always be the energy density. This result is an extension of the result of Białynicki-Birula et *al.* [39] since no assumptions on the type of single-photon states have been done.

3.4.5 Illustration of the nonlocality

The nonlocality brought by the splitting into helicity components can be illustrated through simple one-dimensional examples. We can compute the expectation value $\langle \hat{\mathcal{E}}_{\text{em}}(\vec{x}) \rangle$ for single-photon states representing three extreme cases: First we consider a state $|\psi^{LP}_{\text{comp}}\rangle = \hat{B}^{\dagger}_{\psi^{LP}_{\text{comp}}} |\varnothing\rangle$, where $\psi^{LP}_{\text{comp}} \in \mathcal{H}_{LP}$ is a function of compact support, i.e., $\psi^{LP}_{\text{comp}}(x) = 0$ outside an interval of size L; then we consider a state $|F^{BB}_{\text{comp}}\rangle = \hat{B}^{\dagger}_{F^{BB}_{\text{comp}}} |\varnothing\rangle$, where $F^{BB}_{\text{comp}} \in \mathcal{H}_{BB}$ is a function of compact support, i.e., $F^{BB}_{\text{comp}}(x) = 0$ outside an interval of size L, and finally a state $|\psi_{\text{ext}}\rangle = \hat{B}^{\dagger}_{\psi_{\text{ext}}} |\varnothing\rangle$, where $\psi_{\text{ext}} \in \mathcal{H}_{LP}$ is extended over all space, i.e., $\psi_{\text{ext}}(x) \neq 0$ for any $x \in \mathbb{R}$. To construct ψ_{ext}, we use the real fields $E_{\text{comp}}(x)$ and $A_{\text{comp}}(x)$ with support in the interval $[-L/2, L/2]$ of the form

$$E_{\text{comp}}(x) \propto \begin{cases} \sin^2(\frac{\pi}{L}x + \frac{\pi}{2}) & \text{if } x \in [-\frac{L}{2}, \frac{L}{2}], \\ 0 & \text{otherwise,} \end{cases} \tag{3.93a}$$

$$A_{\text{comp}}(x) \propto \begin{cases} \sin^2(\frac{\pi}{L}x + \frac{\pi}{2}) & \text{if } x \in [-\frac{L}{2}, \frac{L}{2}], \\ 0 & \text{otherwise,} \end{cases} \tag{3.93b}$$

and to build ψ^{LP}_{comp} we take the extended fields

$$E^{LP}_{\text{ext}}(x) = \Omega^{1/2} E_{\text{comp}}(x), \tag{3.94a}$$

$$A^{LP}_{\text{ext}}(x) = \Omega^{-1/2} A_{\text{comp}}(x). \tag{3.94b}$$

The resulting ψ^{LP}_{comp} and ψ_{ext} are represented by blue solid lines in Figure 3.8 (a),(d), and (b),(e), respectively. To construct a localized BB representation F^{BB}_{comp} we take the following fields

$$E^{BB}(x) = E_{\text{comp}}(x), \tag{3.95a}$$

$$A^{BB}(x) = \Omega^{-1} A_{\text{comp}}(x). \tag{3.95b}$$

The resulting localized BB representation is shown by the green dotted line in Figure 3.8 (c) and (f).

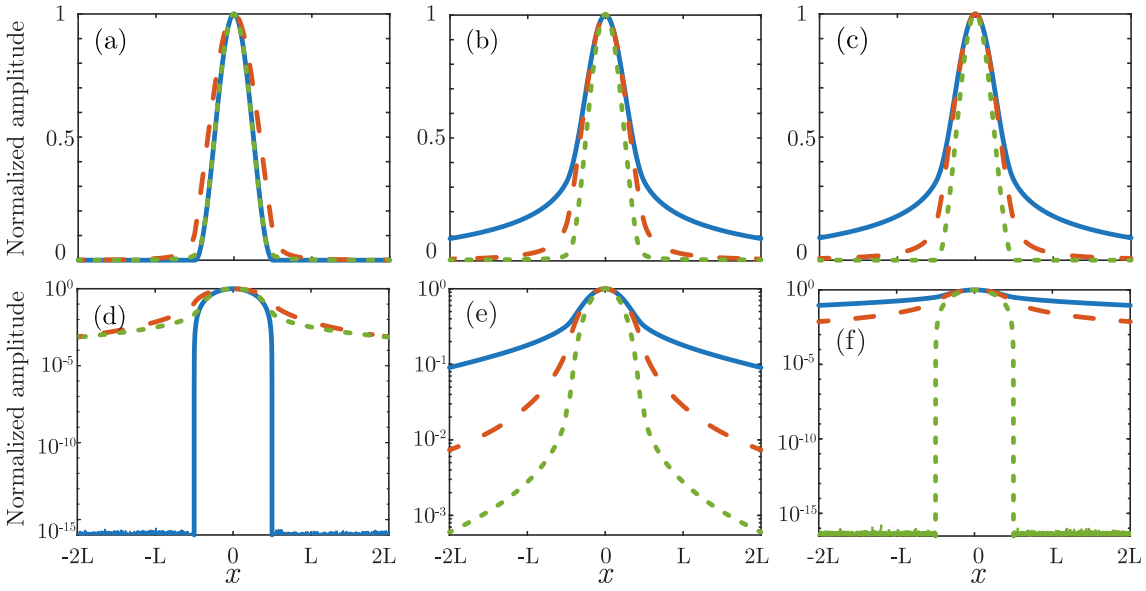

Figure 3.8: Illustration of the nonlocality of single-photon states for three extreme cases. (a) The blue solid line shows the LP representation of a single-photon state $|\psi^{LP}_{\text{comp}}\rangle$ with compact support and the green dotted line its BB representation. The red dashed line shows the expectation value of the energy density computed for that state. The compact support property of $|\psi^{LP}_{\text{comp}}\rangle$ is lost for both the BB representation and the energy. (b) The blue solid line shows the LP representation of an extended single-photon state $|\psi_{\text{ext}}\rangle$ and the green dotted line its BB representation. The red dashed line shows the expectation value of the energy density computed from that state. The extended property of $|\psi_{\text{ext}}\rangle$ is visible from both representations and for the energy. (c) The green dotted line shows the BB representation of a single-photon state $\left|F^{BB}_{\text{comp}}\right\rangle$ with compact support and the blue solid line its LP representation. The red dashed line shows the expectation value of the energy density computed for that state. The compact support property of $\left|F^{BB}_{\text{comp}}\right\rangle$ is lost for the LP representation and the energy. (d), (e), and (f) are the same plots as (a), (b), and (c), respectively, but with a logarithmic scale.

For these three examples, we compute the expectation value of the energy density operator and obtain the results displayed as the red dashed lines in Figure 3.8. In general one can see that the localization property of the LP or BB representation does not give any information for the localization of the energy density. Indeed, the compact support property of the states ψ^{LP}_{comp} and F^{BB}_{comp} is not preserved for the expectation value of the local energy — Figure 3.8 (a), (d), and (c), (f) — as expected. Moreover, a localized LP representation implies a nonlocalized BB representation and vice versa due to the form of the isomorphism $\mathcal{I}$. This is also illustrated in Figure 3.8 (a), (d), and (c), (f), where we have either a localized LP function and a nonlocalized BB function or a nonlocalized LP function and a localized BB function. The most general case is shown in Figure 3.8 (b) and (e), where neither the LP nor the BB representation is localized and so neither is the energy density.

3.4.6 Localization properties of other states of the quantum electromagnetic field

In the preceding sections, we have shown the nonlocal property of all single-photon states, and briefly discussed a direct impact this property could have on their production. In the present section, we would like to extend this proof to a general N-photon states and discuss the case of coherent states. Finally, we will show that one cannot see the nonlocal property of single-photon states using Glauber's photodetection theory.

3.4.6.1 N-photon states

To construct the most general N-photon state, one takes linear combinations of states constructed by applying N bosonic creation operator on the vacuum, for instance in the BB representation

$$|N_{\mathrm{ph}}\rangle = \left(\prod_{i=1}^{N} \hat{C}^{\dagger}_{\vec{F}_i}\right)|\varnothing\rangle\,, \tag{3.96}$$

where the functions $\vec{F}_i$ are elements of $\mathscr{H}_{BB}$. If one wants to describe an N-photon state carried by the same classical configuration $\vec{F}$, all the $\vec{F}_i$ are taken to be $\vec{F}$ and the N-photon state becomes

$$|N_{\vec{F}}\rangle = \left(\hat{C}^{\dagger}_{\vec{F}}\right)^{N}|\varnothing\rangle\,. \tag{3.97}$$

To analyze the locality of such states, we start with the particular case of a single classical configuration for simplicity. Indeed, the expectation value of the electromagnetic energy density can be computed in a similar way of what we did for the general single-photon state by using the generalization of the commutators (3.84) and (3.85)

$$\left[\vec{\hat{\mathbf{F}}}(\vec{x}), (\hat{C}^{\dagger}_{\vec{F}})^{N}\right] = N\vec{F}(\vec{x})(\hat{C}^{\dagger}_{\vec{F}})^{N-1}, \tag{3.98a}$$

$$\left[(\hat{C}_{\vec{F}})^{N}, \vec{\hat{\mathbf{F}}}^{\dagger}(\vec{x})\right] = N\vec{F}^{\star}(\vec{x})(\hat{C}_{\vec{F}})^{N-1}, \tag{3.98b}$$

which can be computed by induction for $N \geq 1$ using (3.84) and (3.85) as the base cases and the standard identity for commutators $[a, bc] = [a, b]c + b[a, c]$ for the induction steps. One has thus for the energy density

$$\langle\hat{\mathcal{E}}(\vec{x})\rangle_{|N_{\vec{F}}\rangle} = \sum_{\lambda=\pm}\left\langle N_{\vec{F}}\right|\vec{\hat{\mathbf{F}}}^{(h\lambda)\dagger}\cdot\vec{\hat{\mathbf{F}}}^{(h\lambda)}\left|N_{\vec{F}}\right\rangle \tag{3.99a}$$

$$= \sum_{\lambda=\pm}\langle\varnothing|\,(\hat{C}_{\vec{F}})^{N}\vec{\hat{\mathbf{F}}}^{(h\lambda)\dagger}\cdot\vec{\hat{\mathbf{F}}}^{(h\lambda)}(\hat{C}^{\dagger}_{\vec{F}})^{N}\,|\varnothing\rangle \tag{3.99b}$$

$$= N^2|\vec{F}^{(h+)}(\vec{x})|^2 + N^2|\vec{F}^{(h-)}(\vec{x})|^2. \tag{3.99c}$$

The result features a splitting into positive and negative helicity parts from which we conclude on the intrinsic nonlocality of the state.
For the most general N-photon state, the expression for the mean value of the energy density is much harder to compute but in fact one does not need to make the full calculation

to conclude on the nonlocality since

$$\langle \hat{\mathcal{E}}(\vec{x})\rangle_{|N\mathrm{ph}\rangle} = \sum_{\lambda=\pm} \langle N\mathrm{ph}| \hat{\vec{\mathbf{F}}}^{(h\lambda)\dagger} \cdot \hat{\vec{\mathbf{F}}}^{(h\lambda)} |N\mathrm{ph}\rangle \tag{3.100a}$$

$$= \sum_{\lambda=\pm} \langle \varnothing| \left(\prod_{i=1}^{N} \hat{C}_{\vec{F}_i}\right) \hat{\vec{\mathbf{F}}}^{(h\lambda)\dagger} \cdot \hat{\vec{\mathbf{F}}}^{(h\lambda)} \left(\prod_{j=1}^{N} \hat{C}^{\dagger}_{\vec{F}_j}\right) |\varnothing\rangle \tag{3.100b}$$

$$= N^2 \sum_{\lambda=\pm} \prod_{i,j=1}^{N} \vec{F}_i^{(h\lambda)\star}(\vec{x}) \cdot \vec{F}_j^{(h\lambda)}(\vec{x}) \langle (N-1)_{\vec{F}_i} | (N-1)_{\vec{F}_j} \rangle \tag{3.100c}$$

$$= N^2 \vec{\mathfrak{F}}^{(h+)} + N^2 \vec{\mathfrak{F}}^{(h-)}, \tag{3.100d}$$

where the functions $\vec{\mathfrak{F}}^{(h\lambda)}$ are

$$\vec{\mathfrak{F}}^{(h\lambda)} = \prod_{i,j=1}^{N} \vec{F}_i^{(h\lambda)\star}(\vec{x}) \cdot \vec{F}_j^{(h\lambda)}(\vec{x}) \langle (N-1)_{\vec{F}_i} | (N-1)_{\vec{F}_j} \rangle , \tag{3.101}$$

and are eigenfunctions of the helicity operator with eigenvalue λ. The fact that the result again can be written as a sum of functions with well-defined helicity, implies that the result we have explicitly shown for single-photon states, is valid here too. Consequently, the splitting into helicity part of the energy density allows to explicitly show that any photon state with a finite number of quanta is nonlocal. This result is in agreement with Knight's theorem but again is obtained without using the time-evolution of the states.

3.4.6.2 Coherent states

Coherent states are another class of states that are extensively used in quantum optics: for fundamental tests, e.g., the analysis of cat states [126], but also for application in particular the development of continuous variables quantum computing [127] and quantum key distribution [128–130]. The question of their localization property is thus interesting to address, especially in regard to the impact it could have for the application.
We recall their definition in terms of Weyl operators (also called displacement operators)

$$|\mathrm{coh}_{\vec{\eta}}\rangle = \hat{W}_{\vec{\eta}} |\varnothing\rangle = \exp\left(\hat{C}^{\dagger}_{\vec{\eta}} - \hat{C}_{\vec{\eta}}\right) |\varnothing\rangle \tag{3.102}$$

for any BB function $\vec{\eta} \in \mathscr{H}_{BB}$. They can also be expressed in terms of creation-annihilation operators as

$$|\mathrm{coh}_{\vec{\eta}}\rangle = e^{-\frac{1}{2}\langle\vec{\eta}|\vec{\eta}\rangle_{BB}} \sum_{n=0}^{\infty} \frac{1}{n!} \hat{C}^{\dagger}_{\vec{\eta}} |\varnothing\rangle . \tag{3.103}$$

More details and properties of coherent states are given in Appendix E. Regarding the localization properties, the expression (3.103) shows that a coherent state is a superposition of an infinite number of multicomponent states which, according to Knight's theorem, can be localized. To analyze this result from our model of local detection, we compute the mean value of the energy density and obtain

$$\langle \hat{\mathcal{E}}(\vec{x})\rangle_{|\mathrm{coh}_{\vec{\eta}}\rangle} = |\vec{\eta}^{(h+)}(\vec{x})|^2 + |\vec{\eta}^{(h-)}(\vec{x})|^2 + \vec{\eta}^{(h+)\star}(\vec{x}) \cdot \vec{\eta}^{(h-)\star}(\vec{x}) + \vec{\eta}^{(h-)}(\vec{x}) \cdot \vec{\eta}^{(h+)}(\vec{x})$$
$$= |\vec{\eta}_{RS}(\vec{x})|^2, \tag{3.104}$$

where the last term is the RS vector related to the BB vector by $\vec{\eta}_{RS} = \vec{\eta}^{(h+)} + \vec{\eta}^{(h-)\star}$ (see Chapter 2). The details of the calculations of the expectation value of the energy density are given in Appendix E. The question of localization of coherent states in our model for local detection can thus be answered by analyzing the RS vector for which we recall its expression in terms of the electromagnetic fields

$$\vec{\eta}_{RS}(\vec{x}) = \sqrt{\frac{\varepsilon_0}{2}} \left(\vec{E}(\vec{x}) + ic\vec{B}(\vec{x}) \right). \tag{3.105}$$

A localized RS vector is thus constructed by taking compactly supported electric and magnetic fields, i.e., $\vec{E}(\vec{x}) = \vec{B}(\vec{x}) = 0$ for all $\vec{x}$ outside a volume $\mathcal{V}_s$. As a consequence, coherent states can be localized but we emphasize that not all of them are localized. Indeed, if one construct a state with a compactly supported state function $\vec{\eta}$, the corresponding $\vec{\eta}_{RS}$ will not have a compact support so will not be the expectation value of the energy density for the associated coherent state. We also remark that all the localized coherent states are constructed with a delocalized state function $\vec{\eta} \in \mathscr{H}_{BB}$ since the relation between the RS and BB vectors involves the splitting into helicity parts. The same remark applies for the associated LP function due to the form of the isomorphism $\mathcal{I}$. This remark is another illustration of the irrelevance of the state functions alone to characterize localization properties. It is only through the analysis of both the states and the observables that one can address the question without ambiguity.
The local character of coherent states is not a surprising result since it is commonly accepted that they accurately represent what is emitted by a laser [33], which are able to produce extremely localized pulses as it is experimentally verified with the development of femtosecond pulses for instance.

3.4.7 Glauber's photodetection operator

In the quantum optics literature, another model of detection referred to as Glauber's photodetection theory [33] is often used to describe the detection of photons. It is built by considering an ideal apparatus of negligible size that has a frequency-independent photodetection probability. From this definition, it can be shown that the rate at which it detects photons is proportional to the expectation value of the following operator

$$\hat{G}_{ij}(\vec{x}) = \hat{E}_i^{(f-)}(\vec{x}) \hat{E}_j^{(f+)}(\vec{x}), \tag{3.106}$$

where the superscripts $^{(f\pm)}$ refer to the positive and negative frequency part of the electric field operator as it is defined in Appendix A and $i, j = 1, 2, 3$ refer to one particular component of $\hat{\vec{E}}$. Using this definition, $\hat{G}$ can be expressed in terms of the field operators for instance in the BB representation, as

$$\hat{G}_{ij}(\vec{x}) = \frac{1}{2\varepsilon_0} \hat{\mathbf{F}}_i^\dagger(\vec{x}) \hat{\mathbf{F}}_j(\vec{x}) \tag{3.107a}$$

$$= \frac{1}{4} \left(\hat{E}_i \hat{E}_j + c^2 \Lambda \hat{B}_i \Lambda \hat{B}_j + ic \hat{E}_i \Lambda \hat{B}_j - ic \Lambda \hat{B}_i \hat{E}_j \right). \tag{3.107b}$$

One can compute the expectation value of this observable for a general single-photon state using the commutators (3.84) and (3.85) and obtains [23]

$$\langle \hat{G}_{ij}(\vec{x}) \rangle_{|1_{\mathrm{ph}}\rangle} = \frac{1}{2\varepsilon_0} F_i^\star(\vec{x}) F_j(\vec{x}). \tag{3.108}$$

We remark that the result does not involve a splitting into helicity components and that therefore the nonlocality of photons is not visible for such a detection model. Indeed, to construct a function $\vec{F} \in \mathscr{H}_{BB}$ with localized components, one takes a localized field $\vec{v}$, i.e., $\vec{v}(\vec{x}) = 0$ outside a certain open set, which is also true for all the components. A corresponding localized BB vector is obtained by defining $\vec{F} = \nabla \times \vec{v}$, to ensure the transversality constraint. Since $\nabla\times$ does not affect the localization properties, all the components of $\vec{F}$ are localized too. The construction of a localized $\vec{F}$ have been illustrated in Figure 3.8 in a one dimensional example.
The fact that the nonlocality of single photons cannot be seen from the Glauber photodection theory is not surprising because $\hat{G}_{ij}(\vec{x})$ is not a local observable since it is not a point-wise combination of local electromagnetic observables as one can see in (3.107b) with the presence of the helicity operator Λ.

3.4.8 Nonlocality and causality

In view of the results for the nonlocality of single-photon states, one has to carefully interpret the consequences of this feature for the production of photons. The fact that the energy density is delocalized over the whole space for any time, raises the question about the possibility to produce perfect single photons through a processus that is localized in a finite volume. Indeed, if one considers a system, localized in a finite volume $\mathcal{V}_{\mathrm{p}}$, where a single-photon can be produced at a time t_{p}, the nonlocality tells us that the expectation value of the energy density will be instantaneously nonzero in any volume $\mathcal{V}_{\mathrm{d}}$ where a detector is placed. Consequently, the probability to detect the produced photon immediately after its production is nonzero, no matter what is the position of the detector. In particular, the causality requirements are explicitely not statisfied and we remind that the quantum field theory for the electromagnetic field is a relativistic theory as we have already discussed with its construction in the BB representation. A direct repercussion of this assessment is that perfect single-photon states cannot be produced by a physical process localized in a finite volume. One can expect that approximate single photons can be produced, as evidenced by the various experiments producing states with behaviors that are very close to single-photon state signatures, but they must be an infinite superposition of states with multiphoton contributions.
We note that the theory we have been constructing and analyzing so far does not predict the production of single-photon states since it is a free theory, without any interaction with matter[1], which is needed for the production of photons. The theory is thus perfectly consistent and for now, the existence of any photon state we have been using was always an assumption. The nonlocality of single-photon states is therefore not a failure of the theory which does not give any information about the production.

[1]The interaction with the propagating medium is in our case considered as a passive interaction meaning that it cannot produce nor destroy any photon.

In the next chapter, we will focus on the production of photons to complete our analysis of the nonlocality. We will see that the systems able to produce photon states in a localized volume in fact produce states with multiphoton components. It gives then a consistent result from a causality point of view. Besides this, the existence of experimental states with behaviors close to what we expect from single photons, is a clear indication that these multiphoton component must be small, not zero but small. The characterization of these components is an important theoretical inquiry especially with the current development of photon number resolving detectors [131–134]. Moreover, applications like time-bin encoding (see beginning of this chapter) seems to be working in practice [92, 100–102] even though the basic principles do not take into account the nonlocality.

4

Production of photons

To analyze some of the photon properties, as we have done in the preceding chapter, we have assumed that one can create photons in a reliable way. This chapter deals with that question and will address it by considering atoms as photon emitters.

To start, we consider the simplest process known to produce photons: spontaneous emission, and we look at the projection into the single-photon subspace of the dynamics. Within this approximation, we compute the energy density mean value of the emitted photon and show that it is nonlocal with an asymptotic radial decay of $1/r^6$ for distances far away from the atom. Then we consider the production of photons in a controlled way using a cavity quantum electrodynamics scheme in a perfect cavity. In that context, we discuss the importance of the rotating wave approximation which allows to predict perfect single-photon states. The validity of this approximation is thus analyzed, and we show using the Floquet theory that it is a relevant approximation in the adiabatic limit. Finally, as preliminary results, we introduce quasinormal modes as particular solutions of the wave equation with outgoing boundary conditions. By defining a dynamical function made of a spatially truncated quasinormal mode, we show that they can be used to describe the leakage of a photon from the cavity. We then introduce a heuristic quantum model by using a hybrid basis composed of quasinormal modes in the cavity, allowing to describe the system in a way similar to what is usually done for perfect cavities but including the leakage.
The first part of this Chapter has led to the article [4].

4.1 Spontaneous emission of a Hydrogen atom 80
4.1.1 Model 81
4.1.2 Weisskopf-Wigner equations 83
4.1.3 Spatial distribution of the energy density 85
4.1.4 Interpretation and multiphoton components 89
4.2 Photon production in perfect cavities 90
4.2.1 Hamiltonian and rotating wave approximation 90
4.2.2 Floquet theory and adiabatic theorem 93
4.2.3 Impact of the RWA on the production of single-photon states 94

4.3 Perspectives for further developments: open cavities 98
4.3.1 Normal modes vs quasinormal modes 100
4.3.2 Truncated quasinormal modes — Leakage of single photons 102
4.3.3 Quantum models using quasinormal modes 103
4.3.3.1 Hybrid basis 103
4.3.3.2 Interacting model 105
4.3.4 Summary on the perspectives 106

4.1 Spontaneous emission of a Hydrogen atom

The description of the spontaneous decay of a Hydrogen atom is a standard calculation that can be done using either the Weisskopf-Wigner theory [135–137] or time-dependent perturbation theory, e.g., with the Fermi golden rule [137]. These two approaches are usually applied to the Hydrogen atom approximated by a two-level system that is coupled to the quantized electromagnetic field in vacuum through a dipole coupling. These models are quite successful in describing the atomic decay, and allow to understand interesting experimental results like the Purcell effect. However, these approaches in general consider a dipole coupling between the field and the atom, taken as a two-level system, which prevents from computing the state of the emitted photons since there is a frequency Lamb shift given by a diverging intergral. The treatment of this divergence could be done by a renormalization procedure, as suggested in [138]. This problem was discussed, e.g., in [45–49, 139] and a way out was found by considering a minimal coupling instead of the dipole approximation, which provides an intrinsic ultraviolet cutoff function that avoids the need of a renormalization. Following the results of Moses [45, 46] (see also [49, 140]), we will alternatively use a model for spontaneous emission with a coupling of the form $\vec{\hat{p}} \cdot \vec{\hat{A}}$, which allows to compute the state of the emitted photon and we will then analyze its energy density distribution across space to characterize its falloff. We show that in this single-photon approximation, the mean energy density decreases as $1/r^6$ with the distance, which is quite far from the maximal quasi-exponential decrease rate established by Białynicki-Birula [38].

The usual intuition about spontaneous emission is that it produces pure single-photon states, without any multiphoton components. However, the result on the nonlocality of the energy density and the remark about causality we have discussed before indicate that this is an approximation. There must be a linear combination of n-photon components for arbitrarily high n. The weights of these components can be small, but they cannot be zero.

In what follows, we consider the spontaneous emission from the first excited state of a Hydrogen atom, making a single-photon approximation with the projection on the single-photon subspace. With this projection, we obtain a model of Weisskopf-Wigner type that is amenable to an explicit solution and to a description of the space-time properties of the produced single-photon state, as probed by the energy density expectation value. This approach is a first step towards a deeper characterization of such emission, where one should also include multiphoton components. It would give an information about the importance of these higher photon contributions for the emission to be causal. Some

results in this direction were obtained in [141, 142]. This second step, that we do not pursue in this work, would be an interesting theoretical analysis that one could hope to test experimentally with the current development of photon number resolving detectors [131–134].

4.1.1 Model

We consider a non-relativistic Hydrogen atom represented by a two-level system corresponding to the Lyman-α transition with ground state $|n_g = 1; j_g = 0; m_g = 0\rangle \equiv |g\rangle$ and excited state $|n_e = 2; j_e = 1; m_e = 0, \pm 1\rangle \equiv |e\rangle$. This transition is relevant since it can be prepared experimentally by applying, e.g., a π-pulse on the ground state with a linearly polarized laser light for $m_e = 0$ and a circularly polarized laser light for $m_e = \pm 1$. The wavefunctions associated to the ground and excited states are, respectively,

$$|g\rangle = \varphi_g(r, \vartheta, \varphi) = \frac{1}{\sqrt{\pi r_{\mathrm{B}}^3}} e^{-\frac{r}{r_{\mathrm{B}}}}, \tag{4.1a}$$

$$|e\rangle = \varphi_e(r, \vartheta, \varphi) = \beta_{m_e}(\vartheta, \varphi) \frac{r}{r_{\mathrm{B}}} e^{-\frac{r}{2r_{\mathrm{B}}}}. \tag{4.1b}$$

where $r_{\mathrm{B}} = \hbar/\alpha \mathfrak{m} c$ is the Bohr radius expressed here in terms of the fine structure constant α, the electron mass $\mathfrak{m}$ and the speed of light c. The functions $\beta_{m_e}(\vartheta, \varphi)$ depend on the choice that is made for $m_e = \{0, \pm 1\}$ and read

$$\beta_0(\vartheta, \varphi) = \frac{1}{4\sqrt{2\pi r_{\mathrm{B}}^3}} \cos\vartheta, \qquad \beta_{\pm 1}(\vartheta, \varphi) = \mp \frac{1}{8\sqrt{\pi r_{\mathrm{B}}^3}} \sin\vartheta \; e^{\pm i\varphi}, \tag{4.2}$$

The free Hamiltonian of the two-level atom can be expressed as

$$\hat{H}_{\mathrm{at}} = E_g \, |g\rangle \langle g| + E_e \, |e\rangle \langle e| \,, \tag{4.3}$$

where E_g and E_e are the energies of the ground and excited states, respectively. To describe the spontaneous emission, the two-level Hydrogen atom is interacting with the quantized electromagnetic field which we write using the basis $|k, J, M, \lambda\rangle \equiv \vec{\psi}^{(\lambda)}_{k,J,M}$ of helicity vector spherical harmonics as defined in (1.89):

$$\hat{H}_{\mathrm{em}} = \int_0^\infty dk \sum_{J,M} \sum_{\lambda = \pm} \hbar \omega_k \hat{B}^\dagger_{\vec{\psi}^{(\lambda)}_{k,J,M}} \hat{B}_{\vec{\psi}^{(\lambda)}_{k,J,M}}. \tag{4.4}$$

For the interaction part, and following [45], we take an operator of the form

$$\hat{H}_{\mathrm{int}} = -\frac{e}{\mathfrak{m}} \hat{\vec{p}} \cdot \hat{\vec{A}}(\vec{x}), \tag{4.5}$$

where $\hat{\vec{p}} = -i\hbar\nabla$ is the momentum operator of the electron and $\hat{\vec{A}}(\vec{x})$ is the vector potential in the Coulomb gauge and $-e$ the charge of the electron.

Remark: $\vec{\hat{A}}(\vec{x})$ acts on the whole tensor product space $\mathcal{H}_{\text{at}} \otimes \mathcal{H}_{\text{em}}$ with $\mathcal{H}_{\text{at}} = \mathbb{C}^2$ and $\mathcal{H}_{\text{em}} = \mathbb{F}(\mathscr{H})$. However, in the Coulomb gauge, $[\vec{p}, \vec{\hat{A}}(\vec{x})] = 0$ since for any state $|f\rangle \otimes |\vec{\phi}\rangle \equiv |f, \vec{\phi}\rangle \equiv |\varphi_f, \vec{\phi}\rangle$

$$-i\hbar\nabla \cdot \left(\vec{\hat{A}}(\vec{x}) \, |f, \vec{\phi}\rangle\right) = -i\hbar \left(\nabla \cdot \vec{\hat{A}}(\vec{x})\right) |f, \vec{\phi}\rangle - i\hbar \vec{\hat{A}}(\vec{x}) \cdot |\nabla\varphi_f, \vec{\phi}\rangle \tag{4.6a}$$

$$= -i\hbar \vec{\hat{A}}(\vec{x}) \cdot |\nabla\varphi_f, \vec{\phi}\rangle \tag{4.6b}$$

$$= \vec{\hat{A}}(\vec{x}) \cdot \vec{p} \, |f, \vec{\phi}\rangle \, . \tag{4.6c}$$

The resulting total Hamiltonian is finally

$$\hat{H} = \hat{H}_{\text{at}} + \hat{H}_{\text{em}} + \hat{H}_{\text{int}} \tag{4.7a}$$

$$= E_g \, |g\rangle \langle g| + E_e \, |e\rangle \langle e| + \int_0^\infty dk \sum_{J,M} \sum_{\lambda=\pm} \hbar\omega_k \hat{B}^\dagger_{\vec{\psi}^{(\lambda)}_{k,J,M}} \hat{B}_{\vec{\psi}^{(\lambda)}_{k,J,M}} - \frac{e}{\mathfrak{m}} \vec{\hat{p}} \cdot \vec{\hat{A}}(\vec{x}), \tag{4.7b}$$

where regarding the interaction, we have neglected the $\hat{A}^2$ term coming from the minimal coupling since it has been shown by Moses [45] (see also [48,140]) that taking an interaction of the form $\vec{\hat{p}} \cdot \vec{\hat{A}}$ is enough to have a consistent model allowing to compute the photon state. Moreover, the typical order of magnitude for the effects relating to the $\hat{A}^2$ term have been estimated to be much smaller than those from the $\vec{\hat{p}} \cdot \vec{\hat{A}}$ term [29].
In the following, since we are interested in the characterization of single photons, we project the system into the subspace generated by the vacuum and the single-photon states, which corresponds in the tensor product Hilbert space to the subspace generated by

$$\{|e; \varnothing\rangle \, , \, |g; \vec{\psi}^{(\lambda)}_{k,J,M}\rangle\},$$

i.e., the atom in its excited state and zero photons or the atom in its ground state and one photon. Within this subspace, the interaction coefficient takes the form [45]

$$\rho(k, J, M, \lambda) = -\frac{e}{\mathfrak{m}} \langle g; \vec{\psi}^{(\lambda)}_{k,J,M}| \, \vec{\hat{p}} \cdot \vec{\hat{A}}(\vec{x}) \, |e; \varnothing\rangle \tag{4.8a}$$

$$= \left(\frac{2}{3}\right)^{7/2} \sqrt{\frac{\alpha^5}{\pi}} \mathfrak{m}c^2 \frac{1}{\sqrt{k}} \frac{k/K}{\left[1 + \left(\frac{k}{K}\right)^2\right]^2} \delta_{J,1}\delta_{M,m_e} \tag{4.8b}$$

$$\equiv \rho(k)\delta_{J,1}\delta_{M,m_e}, \tag{4.8c}$$

where $K = 3/(2r_{\text{B}})$. A step-by-step derivation of this formula is given in Appendix F.

Remarks:

- We have chosen a slightly different convention for the global phases of the eigenfunctions $\vec{\psi}^{(\lambda)}_{k,J,M}$ than the one of [45]. Our convention has the advantage that ρ is real and independent of the helicity λ.
- It was shown in [45–47,49,140] that using the $\vec{p}\cdot\vec{A}$ interaction without making the electric dipole approximation, leads to a coupling $\rho(k)$ that does not diverge for $k \to \infty$. This

avoids the problem encountered with the dipole approximation that the frequency shift for the photons in the solution of the Weisskopf-Wigner equation was divergent.

4.1.2 Weisskopf-Wigner equations

If one considers a general state in such subspace

$$|\Psi\rangle = c_0 \,|e;\varnothing\rangle + \int_0^\infty dk \sum_{J,M,\lambda} c_{k,J,M,\lambda} \,|g;\vec{\psi}^{(\lambda)}_{k,J,M}\rangle \,, \tag{4.9}$$

the standard Schrödinger equation gives a set of coupled equations for the coefficients

$$i\hbar\dot{c}_0(t) = E_e c_0(t) + \int_0^\infty dk \sum_{\lambda=\pm} \rho(k) c_{k,J=1,M=m_e,\lambda}(t), \tag{4.10a}$$

$$i\hbar\dot{c}_{k,J\neq1,M\neq m_e,\lambda}(t) = (E_g + \hbar\omega_k)\, c_{k,J\neq1,M\neq m_e,\lambda}(t), \tag{4.10b}$$

$$i\hbar\dot{c}_{k,J=1,M=m_e,\lambda}(t) = \rho(k)c_0(t) + (E_g + \hbar\omega_k)\, c_{k,J=1,M=m_e,\lambda}(t), \tag{4.10c}$$

from which we extract first the solution for the coefficients

$$c_{k,J\neq1,M\neq m_e,\lambda}(t) = e^{-i(E_g/\hbar+\omega_k)} c_{k,J\neq1,M\neq m_e,\lambda}(t=0). \tag{4.11}$$

In order to study spontaneous emission, we consider the following initial condition

$$c_0(t=0) = 1, \tag{4.12a}$$

$$c_{k,J,M,\lambda}(t=0) = 0, \quad \text{for any } k, J, M \text{ and } \lambda, \tag{4.12b}$$

implying directly

$$c_{k,J\neq1,M\neq m_e,\lambda}(t) = 0, \quad \text{for all } t. \tag{4.13}$$

The set of equation is thus reduced to

$$i\hbar\dot{c}_0(t) = E_e c_0(t) + \int_0^\infty dk \sum_{\lambda=\pm} \rho(k) c_{k,\lambda}(t), \tag{4.14a}$$

$$i\hbar\dot{c}_{k,\lambda}(t) = \rho(k)c_0(t) + (E_g + \hbar\omega_k)\, c_{k,\lambda}(t), \tag{4.14b}$$

where we have introduced the shorter notation $c_{k,J=1,M=m_e,\lambda} \equiv c_{k,\lambda}$. This set of equations is actually composed of three equations if one considers both helicities

$$i\hbar\dot{c}_0(t) = E_e c_0(t) + \int_0^\infty dk\rho(k) \left(c_{k,+}(t) + c_{k,-}(t)\right), \tag{4.15a}$$

$$i\hbar\dot{c}_{k,+}(t) = \rho(k)c_0(t) + (E_g + \hbar\omega_k)\, c_{k,+}(t), \tag{4.15b}$$

$$i\hbar\dot{c}_{k,-}(t) = \rho(k)c_0(t) + (E_g + \hbar\omega_k)\, c_{k,-}(t). \tag{4.15c}$$

Since $\rho(k)$ is λ-independent, the last two equations are also λ-independent and thus $c_{k,+}(t) = c_{k,-}(t)$ for all t and one can define $d_k(t)/\sqrt{2} = c_{k,\lambda}(t)$, to rewrite the set of dynamical equations as

$$i\dot{c}_0(t) = \omega_\mathrm{a} c_0(t) + \int_0^\infty dk \frac{\sqrt{2}}{\hbar}\rho(k) d_k(t), \tag{4.16a}$$

$$i\dot{d}_k(t) = \frac{\sqrt{2}}{\hbar}\rho(k)c_0(t) + \omega_k d_k(t), \tag{4.16b}$$

and then in terms of $\omega_k = ck$

$$i\dot{c}_0(t) = \omega_{\rm a} c_0(t) + \int_0^\infty d\omega_k \tilde{\rho}(\omega_k) D_{\omega_k}(t), \tag{4.17a}$$

$$i\dot{D}_k(t) = \tilde{\rho}(\omega_k) c_0(t) + \omega_k D_k(t), \tag{4.17b}$$

where

$$\tilde{\rho}(\omega_k) = \sqrt{\frac{2}{c\hbar^2}} \rho(\omega_k), \tag{4.18}$$

and we have set $E_g = 0$, $E_e - E_g = \hbar\omega_{\rm a}$ and

$$D_{\omega_k} = d_{\omega_k}/\sqrt{c}. \tag{4.19}$$

One can then write the set of equations (4.17) in a matrix form

$$i \begin{bmatrix} \dot{c}_0 \\ \dot{D}_{\omega_k} \end{bmatrix} = \begin{bmatrix} \omega_{\rm a} & \langle\tilde{\rho}|\cdot\rangle \\ \tilde{\rho} & \omega_k \end{bmatrix} \begin{bmatrix} c_0 \\ D_{\omega_k} \end{bmatrix}, \tag{4.20}$$

which is the Friedrichs-Lee formulation [143, 144]. We remark that the choice of the prefactors in the variables D_{ω_k} and $\tilde{\rho}(\omega_k)$ is made in order to obtain a formulation very close to the notations used in [136, Section 17.3], where the solution of the model is given as

$$c_0(t) = \int_0^\infty d\omega \; g(\omega) e^{-i\omega t}, \tag{4.21a}$$

$$D_{\omega_k}(t) = -ie^{-i\omega_k t} \tilde{\rho}(\omega_k) \int_0^t dt' \; e^{i\omega_k t'} c_0(t'), \tag{4.21b}$$

with

$$g(\omega) = \frac{1}{2\pi} \frac{\Gamma(\omega)}{(\omega - \omega_e - \Delta(\omega))^2 + \frac{\Gamma(\omega)^2}{4}}, \tag{4.22}$$

and

$$\Gamma(\omega) = 2\pi |\tilde{\rho}(\omega)|^2, \tag{4.23a}$$

$$\Delta(\omega) = \mathrm{pv} \int_0^\infty d\omega_k \; \frac{|\tilde{\rho}(\omega_k)|^2}{\omega - \omega_k}. \tag{4.23b}$$

Equations (4.21), (4.22) and (4.23) give the exact solution of the Weisskopf-Wigner model in terms of integrals, provided that the coupling is weak enough to guarantee that the spectrum is absolutely continuous. A derivation of these results is given in Appendix G for any model which can be written like (4.20).
To have a concrete expression of these parameters, we express the coupling function in terms of $\omega_k = ck$

$$\tilde{\rho}(k) = \tilde{\rho}(\omega_k/c) = \left(\frac{2}{3}\right)^{7/2} \sqrt{\frac{2\alpha^5}{\pi\hbar^2}} \mathfrak{m}c^2 \frac{1}{\sqrt{\omega_k}} \frac{\omega_k/(cK)}{\left[1 + \left(\frac{\omega_k}{cK}\right)^2\right]^2} \equiv \tilde{\rho}(\omega_k). \tag{4.24}$$

In the weak coupling regime $g(\omega)$ has a high peak centered at $\omega = \omega_\mathrm{a}$ and one can thus make the following approximation [136]

$$g(\omega) \simeq g_\mathrm{w}(\omega) = \frac{1}{2\pi} \frac{\Gamma(\omega_\mathrm{a})}{(\omega - \omega_\mathrm{a} - \Delta(\omega_\mathrm{a}))^2 + \frac{\Gamma(\omega_\mathrm{a})^2}{4}} \tag{4.25a}$$

$$= \frac{1}{2\pi} \frac{\Gamma_\mathrm{a}}{(\omega - \omega_\mathrm{a} - \Delta_\mathrm{a})^2 + \frac{\Gamma_\mathrm{a}^2}{4}}, \tag{4.25b}$$

which allows to express $c_0(t)$ as

$$c_0(t) \simeq \int_0^\infty d\omega \; g_\mathrm{w}(\omega) e^{-i\omega t} = e^{-\frac{\Gamma_\mathrm{a}}{2}t} e^{-i(\omega_\mathrm{a}+\Delta_\mathrm{a})t}, \tag{4.26}$$

yielding a result essentially equivalent to the Weisskopf-Wigner approximation. From this, one can compute

$$D_{\omega_k}(t) = -ie^{-i\omega_k t}\tilde{\rho}(\omega_k) \int_0^t dt' \; e^{i\omega_k t'} c_0(t') \tag{4.27a}$$

$$\simeq -ie^{-i\omega_k t}\tilde{\rho}(\omega_k) \int_0^t dt' \; e^{-\frac{\Gamma_\mathrm{a}}{2}t'} e^{-i(\omega_\mathrm{a}-\omega_k+\Delta_\mathrm{a})t'} \tag{4.27b}$$

$$= -i \frac{\tilde{\rho}(\omega_k)}{\frac{\Gamma_\mathrm{a}}{2} + i(\omega_\mathrm{a} - \omega_k + \Delta_\mathrm{a})} \left(e^{-i\omega_k t} - e^{-i(\omega_\mathrm{a}+\Delta_\mathrm{a})t} e^{-\frac{\Gamma_\mathrm{a}}{2}t} \right). \tag{4.27c}$$

4.1.3 Spatial distribution of the energy density

Using the preceding results, we are going to express the state of the photon that is spontaneously emitted by the Lyman-α transition of the Hydrogen atom in the single photon approximation, and then compute the expectation value of the electromagnetic energy density to characterize the nonlocality of such photons. We consider here only the photon part of the state, i.e.,

$$\vec{\psi}_\mathrm{ph}(r, \vartheta, \varphi) = \int_0^\infty dk \sum_{\lambda=\pm} c_{k,\lambda}(t) \vec{\psi}_k^{(\lambda)}(r, \vartheta, \varphi) \tag{4.28a}$$

$$= \int_0^\infty dk \frac{d_k(t)}{\sqrt{2}} \left(\vec{\psi}_k^{(+)}(r, \vartheta, \varphi) + \vec{\psi}_k^{(-)}(r, \vartheta, \varphi) \right), \tag{4.28b}$$

where we use the abridged notation $\vec{\psi}_k^{(\lambda)} \equiv \vec{\psi}_{k,J=1,M=m_e}^{(\lambda)}$. The positive and negative helicity parts of the state can be written as

$$\vec{\psi}_\mathrm{ph}^{(h\pm)}(r, \vartheta, \varphi) = \int_0^\infty dk \frac{d_k(t)}{\sqrt{2}} \vec{\psi}_k^{(\pm)}(r, \vartheta, \varphi). \tag{4.29}$$

To compute the mean value, one further needs

$$\Omega^{1/2} \vec{\psi}_\mathrm{ph}^{(h\lambda)}(r, \vartheta, \varphi) = \int_0^\infty dk \frac{d_k(t)}{\sqrt{2}} \Omega^{1/2} \vec{\psi}_k^{(\lambda)}(r, \vartheta, \varphi) = \int_0^\infty dk \sqrt{\frac{\omega_k}{2}} d_k(t) \vec{\psi}_k^{(\lambda)}(r, \vartheta, \varphi), \tag{4.30}$$

and

$$\left|\Omega^{1/2}\vec{\psi}^{(h\lambda)}_{\rm ph}(r,\vartheta,\varphi)\right|^2 = \left|\int_0^\infty dk\sqrt{\frac{\omega_k}{2}}d_k(t)\vec{\psi}^{(\lambda)}_k(r,\vartheta,\varphi)\right|^2. \tag{4.31}$$

To be able to compute these terms, we need to insert the functions $\vec{\psi}^{(\lambda)}_k(r,\vartheta,\varphi)$ which according to (1.89) read

$$\vec{\psi}^{(\lambda)}_k(r,\vartheta,\varphi) = \frac{i}{\sqrt{\pi}}k\left[\sqrt{\frac{2}{3}}j_0(kr)\vec{Y}^0_{1,m_e}(\vartheta,\varphi) - \sqrt{\frac{1}{3}}j_2(kr)\vec{Y}^2_{1,m_e}(\vartheta,\varphi) - i\lambda j_1(kr)\vec{Y}^1_{1,m_e}(\vartheta,\varphi)\right]. \tag{4.32}$$

The integral in (4.30) becomes thus

$$\begin{aligned}\Omega^{1/2}\vec{\psi}^{(h\lambda)}_{\rm ph}(r,\vartheta,\varphi) &= \frac{i}{\sqrt{\pi}}\int_0^\infty dk\sqrt{\frac{\omega_k}{2}}d_k(t)k\left[\sqrt{\frac{2}{3}}j_0(kr)\vec{Y}^0_{1,m_e} - \frac{1}{\sqrt{3}}j_2(kr)\vec{Y}^2_{1,m_e} - \right.\\ &\qquad\left. i\lambda j_1(kr)\vec{Y}^1_{1,m_e}\right] &\text{(4.33a)}\\ &= F_0(r,t)\vec{Y}^0_{1,m_e} + F_1(r,t)\vec{Y}^1_{1,m_e} + F_2(r,t)\vec{Y}^2_{1,m_e} &\text{(4.33b)}\\ &= \sum_{L=0}^{2}F_L(r,t)\vec{Y}^L_{1,m_e}(\vartheta,\varphi), &\text{(4.33c)}\end{aligned}$$

where we have defined

$$\begin{aligned}F_0(r,t) &= \frac{i}{\sqrt{3\pi}}\int_0^\infty dk\sqrt{\omega_k}d_k(t)kj_0(kr), &\text{(4.34a)}\\ F_1(r,t) &= \frac{\lambda}{\sqrt{2\pi}}\int_0^\infty dk\sqrt{\omega_k}d_k(t)kj_1(kr), &\text{(4.34b)}\\ F_2(r,t) &= -\frac{i}{\sqrt{6\pi}}\int_0^\infty dk\sqrt{\omega_k}d_k(t)kj_2(kr). &\text{(4.34c)}\end{aligned}$$

Equation (4.31) can thus be written as

$$\left|\Omega^{1/2}\vec{\psi}^{(h\lambda)}_{\rm ph}(\vec{x})\right|^2 = \sum_{L=0}^{2}\sum_{L'=0}^{2}F^\star_L(r,t)F_{L'}(r,t)\vec{Y}^{L\star}_{1,m_e}\cdot\vec{Y}^{L'}_{1,m_e}, \tag{4.35}$$

and to go further into the calculation, we need to express the integrals F_L which are proportional to

$$\begin{aligned}F_L(r,t) &\propto \int_0^\infty dk\sqrt{\omega_k}kd_k(t)j_L(kr) &\text{(4.36a)}\\ &= \int_0^\infty dk\ ck^{3/2}D_k(t)j_L(kr). &\text{(4.36b)}\end{aligned}$$

We then insert (4.27) to obtain

$$F_L(r,t) \propto -i\left(\frac{2}{3}\right)^{7/2}\sqrt{\frac{2c\alpha^5}{\pi\hbar^2}}\mathfrak{m}c^2\int_0^\infty dk\frac{kj_L(kr)}{\tilde{\Gamma}_{\rm a}+i(\Omega_{\rm a}-k)}\frac{k/K}{\left[1+\left(\frac{k}{K}\right)^2\right]^2}\left(e^{-i\omega_k t}-e^{-i(\Omega_{\rm a}-i\tilde{\Gamma}_{\rm a})t}\right), \tag{4.37}$$

with the abridged notations

$$\tilde{\Gamma}_{\rm a} = \frac{\Gamma_{\rm a}}{2}, \quad \Omega_{\rm a} = \omega_{\rm a} + \Delta_{\rm a}. \tag{4.38}$$

To analyze the asymptotic behavior $r \to +\infty$ of the F_L functions, we express them in terms of the dimensionless parameters

$$A = \frac{\tilde{\Gamma}_{\rm a}}{cK} = \frac{\Gamma_{\rm a}}{2cK}, \quad B = \frac{\Omega_{\rm a}}{cK} = \frac{\omega_{\rm a} + \Delta_{\rm a}}{cK}, \tag{4.39a}$$

$$p = cKt, \quad q = \frac{k}{K}, \quad r' = Kr, \tag{4.39b}$$

as

$$F_L(r,t) \propto -i \left(\frac{2}{3}\right)^{7/2} \sqrt{\frac{2\alpha^5 K^2}{\pi c \hbar^2}} \mathfrak{m} c^2 \int_0^\infty dq \frac{q^2}{A + i(B-q)} \frac{j_L(qr')}{[1+q^2]^2} \left(e^{-iqp} - e^{-i(\Omega_{\rm a} - i\tilde{\Gamma}_{\rm a})t}\right). \tag{4.40}$$

We also express the spherical Bessel functions in terms of qr'

$$j_0(kr) = \frac{\sin(kr)}{kr} = \frac{\sin(qr')}{qr'}, \tag{4.41a}$$

$$j_1(kr) = \frac{\sin(kr)}{k^2 r^2} - \frac{\cos(kr)}{kr} = \frac{\sin(qr')}{q^2 r'^2} - \frac{\cos(qr')}{qr'}, \tag{4.41b}$$

$$j_2(kr) = \frac{3}{kr} j_1(kr) - j_0(kr) = \frac{3}{qr'} j_1(qr') - j_0(qr'), \tag{4.41c}$$

and we perform an asymptotic analysis for $r' \to \infty$. The details of the calculations are given in Appendix H where we show that $F_1(r',t)$ is the leading term with the following behavior

$$F_1(r',t) \underset{r' \to \infty}{\sim} -i\lambda \left(\frac{2}{3}\right)^{5/2} \sqrt{\frac{\alpha^5}{c}} \frac{\mathfrak{m} c^2}{\pi \hbar r_{\rm B}} \mathcal{T}(t) \frac{1}{r'^3}. \tag{4.42}$$

Here, $\mathcal{T}(t)$ is a dimensionless function of time which reads

$$\mathcal{T}(t) = \frac{1}{A+iB} \left(1 - e^{-i(\Omega_{\rm a} - i\tilde{\Gamma}_{\rm a})t} - 2icKt + i\frac{1 - e^{-i(\Omega_{\rm a} - i\tilde{\Gamma}_{\rm a})t}}{A+iB}\right). \tag{4.43}$$

In view of this result, the sum (4.35) can be rewritten in the asymptotic limit as

$$\left|\Omega^{1/2} \vec{\psi}_{\rm ph}^{(h\lambda)}(\vec{x})\right|^2 \underset{r' \to \infty}{\sim} |F_1(r',t)|^2 \vec{Y}^{1\star}_{1,m_e} \cdot \vec{Y}^1_{1,m_e} \tag{4.44a}$$

$$= \left(\frac{2}{3}\right)^5 \frac{\alpha^5 \mathfrak{m}^2 c^3}{\pi^2 \hbar^2 r_{\rm B}^2} |\mathcal{T}(t)|^2 \frac{1}{r'^6} \vec{Y}^{1\star}_{1,m_e} \cdot \vec{Y}^1_{1,m_e}, \tag{4.44b}$$

where we have discarded the terms which decrease faster than $1/r'^6$.
We need now to compute the angular part for which we have to pick different values of m_e. We start with $m_e = 0$, meaning, e.g., that the atom has been prepared in the first

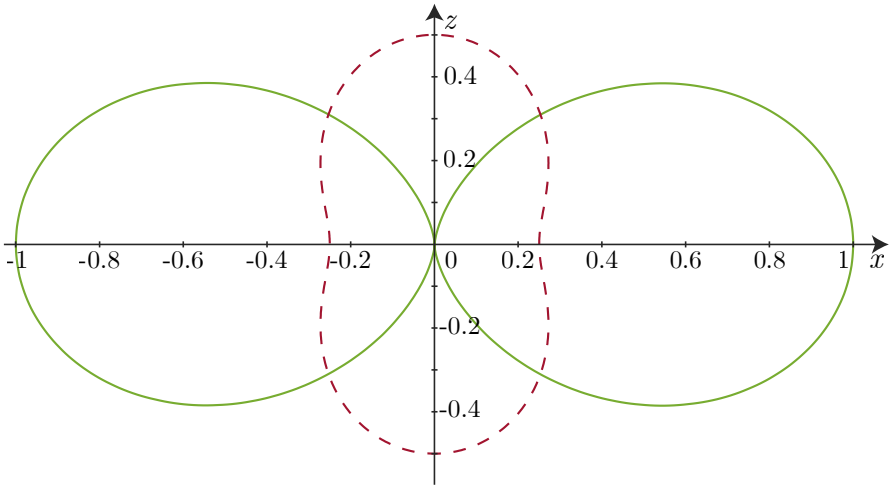

Figure 4.1: Plot of the angular distribution $\gamma_{|m_e|}(\vartheta)$ of the photon state emitted by spontaneous emission of the Lyman-α transition of a Hydrogen atom, obtained in the asymptotic limit of large distances. The green solid line is the distribution for an excited state with $m_e = 0$. The red dashed line is the distribution for an excited state with $|m_e| = 1$.

excited state using a linearly polarized light. In this case, the vector spherical harmonic and its scalar product with itself are

$$\vec{Y}^1_{1,0} = i\sqrt{\frac{3}{8\pi}}\begin{pmatrix} -\sin\vartheta\sin\varphi \\ \sin\vartheta\cos\varphi \\ 0 \end{pmatrix}, \quad \vec{Y}^{1\star}_{1,0}\cdot\vec{Y}^1_{1,0} = \frac{3}{8\pi}\sin^2\vartheta, \tag{4.45}$$

yielding for the asymptotics

$$\left|\Omega^{1/2}\vec{\psi}^{(h\lambda)}_{\rm ph}(\vec{x})\right|^2 \underset{r'\to\infty}{\sim} \left(\frac{2}{3}\right)^4 \frac{\alpha^5 m^2c^3}{4\pi^3\hbar^2 r_{\rm B}}|\mathcal{T}(t)|^2\gamma_0(\vartheta)\frac{1}{r'^6}. \tag{4.46}$$

The angular distribution $\gamma_0(\vartheta) = \sin^2\vartheta$ is represented by the green solid curve in Figure 4.1. The other two possibilities, $m_e = \pm 1$ yield the following vector spherical harmonics and corresponding scalar products with themselves

$$\vec{Y}^1_{1,\pm1} = -\sqrt{\frac{3}{16\pi}}\begin{pmatrix} \pm\cos\vartheta \\ i\cos\vartheta \\ \sin\vartheta\ e^{\pm i\varphi} \end{pmatrix}, \quad \vec{Y}^{1\star}_{1,\pm1}\cdot\vec{Y}^1_{1,\pm1} = \frac{3}{16\pi}\left(1+\cos^2\vartheta\right), \tag{4.47}$$

which give asymptotics of the form

$$\left|\Omega^{1/2}\vec{\psi}^{(h\lambda)}_{\rm ph}(\vec{x})\right|^2 \underset{r'\to\infty}{\sim} \left(\frac{2}{3}\right)^4 \frac{\alpha^5 \mathfrak{m}^2c^3}{4\pi^3\hbar^2 r_{\rm B}}|\mathcal{T}(t)|^2\gamma_1(\vartheta)\frac{1}{r'^6}. \tag{4.48}$$

The angular distribution $\gamma_1(\vartheta) = (1+\cos^2\vartheta)/4$ is represented by the red dashed curve in Figure 4.1.

To summarize the results, one reinstates the original variables so that the positive and negative helicity parts of the energy density mean value read

$$\left|\Omega^{1/2}\vec{\psi}_{\mathrm{ph}}^{(h\pm)}(\vec{x})\right|^2 = \left(\frac{2}{3}\right)^{10} \frac{\mathfrak{m}^2 c^3 r_{\mathrm{B}}^4 \alpha^5}{4\pi^3\hbar^2} \gamma_{|m_e|}(\vartheta)|\mathcal{T}(t)|^2 \frac{1}{r^6} + o\left(\frac{1}{r^6}\right). \tag{4.49}$$

We remark that the result does not depend on the helicity, thus the full energy density mean value of the spontaneously emitted photon, in the asymptotic limit of large distances, is twice this result multiplied by $\hbar$

$$\langle\hat{\mathcal{E}}_{\mathrm{em}}\rangle_{|1_{\mathrm{ph}}\rangle} = \left(\frac{2}{3}\right)^{10} \frac{\mathfrak{m}^2 c^3 r_{\mathrm{B}}^4 \alpha^5}{2\pi^3\hbar} \gamma_{|m_e|}(\vartheta)|\mathcal{T}(t)|^2 \frac{1}{r^6} + o\left(\frac{1}{r^6}\right). \tag{4.50}$$

4.1.4 Interpretation and multiphoton components

As we explained in the beginning of this section, the model we use to describe spontaneous emission does not predict the production of single-photon states only but also multiphoton components. Our calculation however only takes into account single photons since we looked at the interaction by projecting into the single-photon subspace. The resulting asymptotic distribution of the energy density mean value for distances far from the atom yields a decrease which scale like $1/r^6$. This behavior, which is far from the quasi-exponential limit derived in [38], illustrates the fact that one should consider higher photon number components without which the emission would not be causal. Indeed, at any fixed time t there would be a non-zero probability of detecting the photon with an instrument located at an arbitrary distance r from the source, in particular one could take $r > ct$, where c is the speed of light. This was already stated in [141] in an analysis of the energy density for spontaneous emission within a second order perturbation theory, but without a characterization of the decrease of its mean value. Similar calculations with asymptotics of the energy density for near and far fields up to second order in perturbation theory were also performed in [142, Section 7.2] but for the dressed atomic ground state only.

The non causality of the spontaneous emission of single-photon states by a non-relativistic Hydrogen atom was also analyzed in [145–149]. In this series of articles, a representation of the state, that is essentially equivalent (up to a global phase) to the BB representation, is used to look at the emitted single-photon state in the near-, mid- and far-field regions as well as within multiple time regimes such as the Zeno regime for very short times, the Fermi regime for short times and the Weisskopf-Wigner regime for long times. The model used for this analysis is of Weisskopf-Wigner type with a full coupling of the form (4.8). However, no local observables are introduced to probe the nonlocality as we have done with the energy density, and the nonlocality is analyzed only through the properties of the state functions. This is a major limitation as we already discussed in Section 3.4.3 since a state can be found with a compact support while its expectation value for a local observable is not (see Figure 3.8).

Another remark was made in [150] concerning the nonlocality of the atomic wave functions. Indeed, eigenfunctions of the Hydrogen atom (4.1) decrease exponentially in the radial

variable meaning that they are nonzero everywhere. Based on this remark, the emission of photons cannot be expected to be local but should at least have an exponential tail. This effect has been described as a "blurring of the light cone" and should be of the same order as the quasiexponential decrease limit of [38]. However, the algebraic decrease that we found cannot be solely justified by the nonlocality of the atomic part and is thus mostly a feature coming from photon's properties.
In view of these remarks, an open question that should be addressed is the determination of the weights of the n-photon components in concrete emission processes, like spontaneous emission or in the production of photons at demand by the different techniques that are being developed experimentally.

4.2 Photon production in perfect cavities

In practice, to produce on demand single photons from individual atoms, one needs to have a very good control of the light-matter interaction. To do so, cavities are often used to enhance the light-matter coupling for some particular atomic transitions. The atom can be described by a 2- or 3-level system as we have discussed in Chapter 1, which allows to drastically reduce the dimensionality of the problem. Moreover, if the cavity is considered to be perfect, i.e., the mirrors are 100% reflective, only a set of discrete electromagnetic modes exist in the cavity and will be available to be populated by the produced photons. Therefore, instead of describing a system composed of a large number of energy levels interacting with a continuum of electromagnetic configurations, one needs to deal with two or three energy levels interacting with a few quantum electromagnetic modes. This huge simplification of the problem justifies this approach, even though perfect cavities do not exist in practice. Conversely, since calculations are often very heavy when cavities are far from perfect, it also justifies why experimental techniques have been extensively used to construct cavities that are close to perfect, i.e., with high quality factor Q.
Due to the theoretical results on the nonlocality of single-photon states, and to the experimental progress for the construction of on-demand single-photon sources, we want in this section to analyze the models that are used to describe these experiments. Indeed, we want to give a theoretical insight into the importance of the multiphoton components that are predicted by certain models but which can also be removed with some approximations, like the rotating wave approximation (RWA). The validity of this approximation is thus a central question that we want to analyze in the following.

4.2.1 Hamiltonian and rotating wave approximation

To analyze the possible production of single photons in a perfect cavity, we consider a model in which a 2-level system interacts with the quantized electromagnetic field of a perfect cavity and an external laser field described classically. In a cavity, the quantum description of the electromagnetic field we have been using so far is still valid. The difference will come from the classical electromagnetic configurations on which photons are created. Since the emitter is a 2-level atom $\{|e\rangle, |g\rangle\}$, we can select one cavity mode which has a frequency ω_{c} that is the closest to the 2-level transition $\omega_{\mathrm{a}} = (E_e - E_g)/\hbar$, where $E_{e,g}$ are the respective energies of the excited and ground states. The Hamiltonians

of the two isolated subsystems are thus

$$\hat{H}_{\rm at} = E_e \left|e\right\rangle \left\langle e\right| + E_g \left|g\right\rangle \left\langle g\right|, \tag{4.51a}$$

$$\hat{H}_{\rm c} = \hbar\omega_{\rm c} \hat{B}^{\dagger}_{\vec{\zeta}} \hat{B}_{\vec{\zeta}} = \hbar\omega_{\rm c} \hat{a}^{\dagger}\hat{a}, \tag{4.51b}$$

where $\vec{\zeta}(\vec{x})$ is the resonant cavity mode chosen to be real. Since the cavity will be described only with one mode, we have also introduced the single-mode creation-annihilation operators $\hat{a} = i\hat{B}_{\vec{\zeta}}$ and $\hat{a}^{\dagger} = -i\hat{B}^{\dagger}_{\vec{\zeta}}$, which is the standard choice in the cavity quantum electrodynamics (cQED) literature. Here, $\hat{H}_{\rm at}$ acts on the atomic Hilbert space $\mathbb{C}^2$ and $\hat{H}_{\rm c}$ on the single-mode bosonic Fock space $\mathcal{F} = \{\left|n\right\rangle, n \in \mathbb{N}\}$, where n is interpreted as the number of photons in the cavity.
The interaction Hamiltonian can be split into two parts: the full quantum part which describes the interaction between the atom and the cavity, and the semi-classical part which describes the interaction between the quantum atom and the classical laser field. In order to start with the simplest model possible, we consider a dipole coupling and to justify this choice in our context, we recall (see Chapter 1) that the dipole coupling arises from the long wavelength approximation which is relevant if one chooses a cavity mode with a resonant wavelength $\lambda_{\rm c} = {}^{2\pi c}/_{\omega_{\rm c}}$ large compared to the typical atomic dimensions, i.e., $\lambda_{\rm c} \gg r_{\rm B}$. Cavity QED experiments are in general performed in the infrared or visible domain so that typical wavelengths are of the order of $10^{-5}{\rm m} \gg r_{\rm B} \simeq 10^{-10}{\rm m}$.
The interaction Hamiltonian reads thus

$$\hat{H}_{\rm int} = -\left\langle e\right| \vec{\hat{d}} \cdot \vec{E}(\vec{x}_{\rm at}, t) \left|g\right\rangle \left(\left|e\right\rangle \left\langle g\right| + \left|g\right\rangle \left\langle e\right|\right) - \left\langle e\right| \vec{\hat{d}} \cdot \vec{\hat{E}}_{\rm c}(\vec{x}_{\rm at}, t) \left|g\right\rangle \left(\left|e\right\rangle \left\langle g\right| + \left|g\right\rangle \left\langle e\right|\right), \tag{4.52}$$

where $\vec{E}(\vec{x}_{\rm at}, t)$ is the classical electric field created by the control laser and $\vec{\hat{E}}_{\rm c}(\vec{x}_{\rm at}, t)$ is the cavity quantized electric field. The time dependence of the quantized field has been added to account for the motion of the atom inside the cavity. This motion is not always needed to have a control scheme able to produce photons but it is anyway unavoidable practically. The semi-classical first term in (4.52) is identical to what we had in Chapter 1 and it can thus be reformulated in the same way. The second full quantum term however needs the expression of the quantized electric field in terms of the cavity-mode creation-annihilation operators which is

$$\vec{\hat{E}}_{\rm c}(\vec{x}_{\rm at}, t) = \sqrt{\frac{\hbar\omega_{\rm c}}{2\varepsilon_0}} \vec{\zeta}(\vec{x}_{at}, t) \left(\hat{a} + \hat{a}^{\dagger}\right). \tag{4.53}$$

The interaction Hamiltonian can thus be rewritten as

$$\hat{H}_{\rm int} = \frac{\hbar\Omega_{eg}(t)}{2} \left(e^{i\omega_{\rm L}t} + e^{-i\omega_{\rm L}t}\right) \left(\left|e\right\rangle \left\langle g\right| + \left|g\right\rangle \left\langle e\right|\right) + \hbar G(t) \left(\hat{a} + \hat{a}^{\dagger}\right) \left(\left|e\right\rangle \left\langle g\right| + \left|g\right\rangle \left\langle e\right|\right) \tag{4.54a}$$

$$= \frac{\hbar\Omega_{eg}(t)}{2} \begin{pmatrix} 0 & e^{i\omega_{\rm L}t} + e^{-i\omega_{\rm L}t} \\ e^{i\omega_{\rm L}t} + e^{-i\omega_{\rm L}t} & 0 \end{pmatrix} + \hbar G(t) \begin{pmatrix} 0 & \hat{a} + \hat{a}^{\dagger} \\ \hat{a} + \hat{a}^{\dagger} & 0 \end{pmatrix}, \tag{4.54b}$$

and the full Hamiltonian as

$$\hat{H} = \hbar \begin{pmatrix} \hat{a}^\dagger \hat{a} & 0 \\ 0 & \omega_\mathrm{a} + \hat{a}^\dagger \hat{a} \end{pmatrix} + \hbar G(t) \begin{pmatrix} 0 & \hat{a} + \hat{a}^\dagger \\ \hat{a} + \hat{a}^\dagger & 0 \end{pmatrix} + \frac{\hbar \Omega_{eg}(t)}{2} \begin{pmatrix} 0 & e^{i\omega_\mathrm{L} t} + e^{-i\omega_\mathrm{L} t} \\ e^{i\omega_\mathrm{L} t} + e^{-i\omega_\mathrm{L} t} & 0 \end{pmatrix} \tag{4.55}$$

where we have set the zero of energy $E_g = 0$ and the Rabi frequency $G(t) = \sqrt{\frac{\omega_\mathrm{c}}{2\hbar\varepsilon_0}} \vec{\zeta}(t) \cdot \vec{d}$. This Hamiltonian is general and is usually simplified by applying the rotating wave approximation (RWA) as introduced in Chapter 1 for the semi-classical interaction. We want now to explain why such approximation is relevant for the quantum interaction too. To do so, we consider the Hamiltonian (4.55) wihtout the classical control, i.e., $\Omega_{eg}(t) = 0$ for all t and with a constant cavity coupling $G(t) \equiv G$ for all t. We obtain the Rabi Hamiltonian

$$\hat{H}_\mathrm{Rabi} = \hbar\omega_\mathrm{at} |e\rangle\langle e| + \hbar\omega_\mathrm{c} \hat{a}^\dagger \hat{a} + \hbar G \left(\hat{a} + \hat{a}^\dagger\right) (|e\rangle\langle g| + |g\rangle\langle e|) \tag{4.56a}$$

$$= \hat{H}_0 + \hat{W}, \tag{4.56b}$$

where $\hat{H}_0 = \hbar\omega_\mathrm{a} |e\rangle\langle e| + \hbar\omega_\mathrm{c} \hat{a}^\dagger \hat{a}$ and $\hat{W} = \hbar G \left(\hat{a} + \hat{a}^\dagger\right) (|e\rangle\langle g| + |g\rangle\langle e|)$. To decide which interaction terms produce resonances, we treat the Rabi Hamiltonian perturbatively, considering $\hat{H}_0$ as the unperturbed part where the set $\{|g;n\rangle, |e;n\rangle\}$ is a basis of eigenstates with eigenvalues

$$\hat{H}_0 |g;n\rangle = n\hbar\omega_\mathrm{c} |g;n\rangle = E_{g,n} |g;n\rangle, \tag{4.57a}$$

$$\hat{H}_0 |e;n\rangle = (\hbar\omega_\mathrm{a} + n\hbar\omega_\mathrm{c}) |g;n\rangle = E_{e,n} |e;n\rangle. \tag{4.57b}$$

Time-independent perturbation theory allows to compute the corrections to these eigenstates and eigenenergies for the perturbation $\hat{W}$. We obtain up to second order for the energies

$$E_{g,n}^\mathrm{corr.} = E_{g,n} + \langle g;n| \hat{W} |g;n\rangle + \sum_{s=g,e} \sum_{m \neq n} \frac{|\langle s,m| \hat{W} |s,n\rangle|^2}{E_{s,n} - E_{s,m}} \tag{4.58a}$$

$$= E_{g,n} + \frac{|\langle e;n-1| \hbar G |e\rangle\langle g| \hat{a} |g;n\rangle|^2}{E_{g,n} - E_{e,n-1}} + \frac{|\langle e;n+1| \hbar G |e\rangle\langle g| \hat{a}^\dagger |g;n\rangle|^2}{E_{g,n} - E_{e,n+1}} \tag{4.58b}$$

$$= E_{g,n} - \frac{n\hbar G^2}{\omega_\mathrm{a} - \omega_\mathrm{c}} - \frac{(n+1)\hbar G^2}{\omega_\mathrm{a} + \omega_\mathrm{c}}, \tag{4.58c}$$

and

$$E_{e,n}^\mathrm{corr.} = E_{e,n} + \langle e;n| \hat{W} |e;n\rangle + \sum_{s=g,e} \sum_{m \neq n} \frac{|\langle s,m| \hat{W} |s,n\rangle|^2}{E_{s,n} - E_{s,m}} \tag{4.59a}$$

$$= E_{e,n} + \frac{|\langle g;n+1| \hbar G |g\rangle\langle e| \hat{a}^\dagger |e;n\rangle|^2}{E_{e,n} - E_{g,n+1}} + \frac{|\langle g;n-1| \hbar G |g\rangle\langle e| \hat{a} |e;n\rangle|^2}{E_{e,n} - E_{g,n-1}} \tag{4.59b}$$

$$= E_{e,n} + \frac{(n+1)\hbar G^2}{\omega_\mathrm{a} - \omega_\mathrm{c}} + \frac{n\hbar G^2}{\omega_\mathrm{a} + \omega_\mathrm{c}}. \tag{4.59c}$$

The corrected states up to the first order are

$$|g;n\rangle^{\text{corr.}} = |g;n\rangle + \sum_{s=g,e}\sum_{m\neq n}\frac{\langle s;m|\,\hat{W}\,|s;n\rangle}{E_{s,n}-E_{s,m}}\,|s;m\rangle \tag{4.60a}$$

$$= |g;n\rangle - \frac{G\sqrt{n}}{\omega_{\text{a}}-\omega_{\text{c}}}\,|e;n-1\rangle - \frac{G\sqrt{n+1}}{\omega_{\text{a}}+\omega_{\text{c}}}\,|e;n+1\rangle\,, \tag{4.60b}$$

and

$$|e;n\rangle^{\text{corr.}} = |e;n\rangle + \sum_{s=g,e}\sum_{m\neq n}\frac{\langle s;m|\,\hat{W}\,|s;n\rangle}{E_{s,n}-E_{s,m}}\,|s;m\rangle \tag{4.61a}$$

$$= |e;n\rangle + \frac{G\sqrt{n+1}}{\omega_{\text{a}}-\omega_{\text{c}}}\,|g;n+1\rangle + \frac{G\sqrt{n}}{\omega_{\text{a}}+\omega_{\text{c}}}\,|g;n-1\rangle\,. \tag{4.61b}$$

We see that corrections come with different amplitudes due to the denominators of the form $\omega_{\text{a}}-\omega_{\text{c}}\simeq 0$ and $\omega_{\text{a}}+\omega_{\text{c}}\gg 1$. One can thus trace back to the resonant and non resonant contributions in $\hat{W}$

$$\hat{W} = \hat{W}_{\text{res.}} + \hat{W}_{\text{nres.}}\,, \tag{4.62a}$$

$$\hat{W}_{\text{res.}} = \hbar G\hat{a}\,|e\rangle\langle g| + \hbar G\hat{a}^\dagger\,|g\rangle\langle e|\,,\quad \hat{W}_{\text{nres.}} = \hbar G\hat{a}^\dagger\,|e\rangle\langle g| + \hbar G\hat{a}\,|g\rangle\langle e|\,, \tag{4.62b}$$

and the quantum RWA consists in neglecting $\hat{W}_{\text{nres.}}$. The Rabi Hamiltonian in the RWA becomes thus

$$\hat{H}_{\text{JC}} = \hbar\omega_{\text{a}}\,|e\rangle\langle e| + \hbar\omega_{\text{c}}\hat{a}^\dagger\hat{a} + \hbar G\left(\hat{a}\,|e\rangle\langle g| + \hat{a}^\dagger\,|g\rangle\langle e|\right), \tag{4.63}$$

known as the Jaynes-Cummings (JC) Hamiltonian. The particularity of the JC Hamiltonian is that it drives only transitions of the form $|g;n\rangle \leftrightarrow |e;n-1\rangle$ and thus if one manages to prepare the system in the state $|e;0\rangle$, the dynamics will automatically couple it to $|g;1\rangle$ and the production of single photons in that context seems to be quite straightforward. Applying the RWA for both interactions in (4.55), we obtain

$$\hat{H}_{\text{rwa}} = \hbar\begin{pmatrix}\hat{a}^\dagger\hat{a} & 0\\ 0 & \omega_{\text{a}}+\hat{a}^\dagger\hat{a}\end{pmatrix} + \hbar G(t)\begin{pmatrix}0 & \hat{a}\\ \hat{a}^\dagger & 0\end{pmatrix} + \frac{\hbar\Omega_{eg}(t)}{2}\begin{pmatrix}0 & e^{-i\omega_{\text{L}}t}\\ e^{i\omega_{\text{L}}t} & 0\end{pmatrix}. \tag{4.64}$$

4.2.2 Floquet theory and adiabatic theorem

The RWA allows to construct Hamiltonians able to produce perfect single-photon states provided that one brings the atom to its excited state. However, in sight of the results we have shown regarding the nonlocality of single photons, we want to analyze the validity of this approximation not only through the basic estimation of the contribution of non resonant terms, but also on the impact of these terms when one applies the control scheme. For that, we will compare what path the state follows in the adiabatic limit considering both the RWA Hamiltonian (4.64) and the general one (4.55) [50, 151].

The aim of the Floquet formalism is to simplify the resolution of systems with a time-dependent Hamiltonian for which the dynamics is given by Schrödinger's equations of the form

$$i\hbar\frac{\partial\left|\phi(t)\right\rangle}{\partial t}=\hat{H}(t;\theta)\left|\phi(t)\right\rangle, \tag{4.65}$$

where $\theta=\omega t$. The idea is to work in an enlarged Hilbert space $\mathcal{K}=\mathcal{H}\otimes\mathcal{S}$, where $\mathcal{S}=L^2(\mathbb{S}^1,\mathrm{d}\theta/2\pi)$ is the space of square integrable functions of the variable θ on the circle $\mathbb{S}^1$ of length 2π generated by the basis $\{e^{il\theta}\}_{l\in\mathbb{Z}}$, and $\mathcal{H}$ is the Hilbert space of the system. The parameter l will represent the relative number of photons with respect to the large mean number $\bar{l}$ of the classical field. In the Floquet space, the dynamics is given by

$$i\hbar\frac{\partial\left|\psi(t)\right\rangle}{\partial t}=\hat{K}(t;\theta)\left|\psi(t)\right\rangle, \tag{4.66}$$

with the Floquet Hamiltonian

$$\hat{K}(t;\theta)=-i\hbar\omega\frac{\partial}{\partial\theta}+\hat{H}(t;\theta). \tag{4.67}$$

The relation between $|\psi\rangle$ and $|\phi\rangle$ is given by the following: if $|\psi(t;\theta)\rangle$ is a solution of (4.66) with initial condition $|\psi(t_0;\theta)\rangle=|\phi_0\rangle\otimes\mathbb{1}_{\mathcal{S}}$ where $\mathbb{1}_{\mathcal{S}}$ is the function $f(\theta)=1$ in $\mathcal{S}$, then $|\phi(t)\rangle=|\psi(t;\omega t)\rangle$. A more detailed review of the Floquet theory is given in [50].
The second ingredient we will be using to analyze the production of photons in a cavity, is the adiabatic approximation which rests on the following adiabatic theorem as stated originally by Born and Fock [51]:
A physical system remains in its instantaneous eigenstate if a given perturbation is acting on it slowly enough and if there is a gap between the eigenvalue and the rest of the Hamiltonian's spectrum.
In our case, it means that for slow-enough variations of the coupling constants $G(t)$ and $\Omega_{eg}(t)$, the dynamics will follow the instantaneous eigenstates where the spectrum has gaps.

4.2.3 Impact of the RWA on the production of single-photon states

Using the Floquet formalism and the adiabatic theorem, we want now to analyze the impact of the RWA on the controlled production of single photons by a 2-level atom. Indeed, as we have briefly stated before, the RWA Hamiltonian drives only transitions of the form $|g;n+1\rangle\leftrightarrow|e;n\rangle$, i.e., if one manages to put the system in the state $|e;0\rangle$, it will eventually be transferred to the state $|g;1\rangle$ — without controls, the system oscillates between the two states, but using an appropriate control scheme, one can force the system to be completely transferred to $|g;1\rangle$ — and a perfect single-photon state would be created in the cavity. However, without the RWA, transitions of the form $|g;n\rangle\leftrightarrow|e;n+1\rangle$ are also driven and even if the system is put in the state $|e,0\rangle$, it will be resonantly coupled to $|g,1\rangle$ which itself is non resonantly coupled to $|e,2\rangle$, yielding photon states with arbitrarily high photon component — in agreement with causality requirements. The production of perfect single-photon states[1] in a cavity is thus related to the validity of the RWA, which

[1]By perfect single-photon states, we mean states that approach ideal single-photon states as much as wanted. Since the production scheme we are considering here is a local process, we know that causality

we will analyze from the adiabatic point of view to justify the use of the approximation in that regime.
We start with the full Hamiltonian (4.55)

$$\hat{H} = \hbar \begin{pmatrix} \hat{a}^\dagger \hat{a} & 0 \\ 0 & \omega_{\rm a} + \hat{a}^\dagger \hat{a} \end{pmatrix} + \hbar G(t) \begin{pmatrix} 0 & \hat{a} + \hat{a}^\dagger \\ \hat{a} + \hat{a}^\dagger & 0 \end{pmatrix} + \frac{\hbar \Omega_{eg}(t)}{2} \begin{pmatrix} 0 & e^{i\omega_{\rm L} t} + e^{-i\omega_{\rm L} t} \\ e^{i\omega_{\rm L} t} + e^{-i\omega_{\rm L} t} & 0 \end{pmatrix} \tag{4.68a}$$

$$= \hat{H}_{\rm rwa} + \hat{V}, \tag{4.68b}$$

where $\hat{H}_{\rm rwa}$ is given by (4.64) and the non resonant coupling Hamiltonian $\hat{V}$ is

$$\hat{V} = \hbar G(t) \begin{pmatrix} 0 & \hat{a}^\dagger \\ \hat{a} & 0 \end{pmatrix} + \frac{\hbar \Omega_{eg}(t)}{2} \begin{pmatrix} 0 & e^{i\omega_{\rm L} t} \\ e^{-i\omega_{\rm L} t} & 0 \end{pmatrix}. \tag{4.69}$$

We construct now the Floquet Hamiltonian

$$\hat{K}(t, \theta) = -i\hbar\omega_{\rm L} \frac{\partial}{\partial \theta} + \hat{H}(t; \theta) \tag{4.70a}$$

$$= -i\hbar\omega_{\rm L} \frac{\partial}{\partial \theta} + \hat{H}_{\rm rwa} + \hat{V} \tag{4.70b}$$

$$= \hat{K}_{\rm rwa} + \hat{V}, \tag{4.70c}$$

with $\theta = \omega_{\rm L} t$. Following the procedure presented in [151], we apply the resonant transformation

$$\hat{R} = \begin{pmatrix} e^{-i\theta} & 0 \\ 0 & 1 \end{pmatrix}, \tag{4.71}$$

which yields

$$\hat{K}'_{\rm rwa} = \hat{R}^\dagger \hat{K}_{\rm rwa} \hat{R} = \hbar \begin{pmatrix} \omega_C \hat{a}^\dagger \hat{a} + \Delta_{\rm L} - i\omega_{\rm L} \frac{\partial}{\partial \theta} & \frac{\Omega_{eg}(t)}{2} + G(t) \hat{a} e^{i\theta} \\ \frac{\Omega_{eg}(t)}{2} + G(t) \hat{a}^\dagger e^{-i\theta} & \omega_{\rm c} \hat{a}^\dagger \hat{a} - i\omega_{\rm L} \frac{\partial}{\partial \theta} \end{pmatrix}, \tag{4.72}$$

and

$$\hat{V}' = R^\dagger \hat{V} R = \hbar \begin{pmatrix} 0 & G(t) \hat{a}^\dagger e^{i\theta} + \frac{\Omega_{eg}(t)}{2} e^{2i\theta} \\ G(t) \hat{a} e^{-i\theta} + \frac{\Omega_{eg}(t)}{2} e^{-2i\theta} & \end{pmatrix}. \tag{4.73}$$

To further simplify the Hamiltonian, we use the phase representation of the creation-annihilation operators [152, 153]

$$\hat{a} \to e^{-i\varphi} \sqrt{-i \frac{\partial}{\partial \varphi}}, \quad \hat{a}^\dagger \to \sqrt{-i \frac{\partial}{\partial \varphi}} e^{i\varphi}, \quad \hat{a}^\dagger \hat{a} \to -i \frac{\partial}{\partial \varphi}, \tag{4.74}$$

where $\varphi \in [0, 2\pi]$. The phase representation corresponds to a mapping of the single-mode bosonic Fock space $\mathcal{F}$ onto the positive restriction of $\mathcal{S}$, i.e., generated by the basis

prevents to produce a perfect single-photon state. We also emphasize that the theory does not predict such a state that would contradict causality but it is only through particular approximations that such states arise.

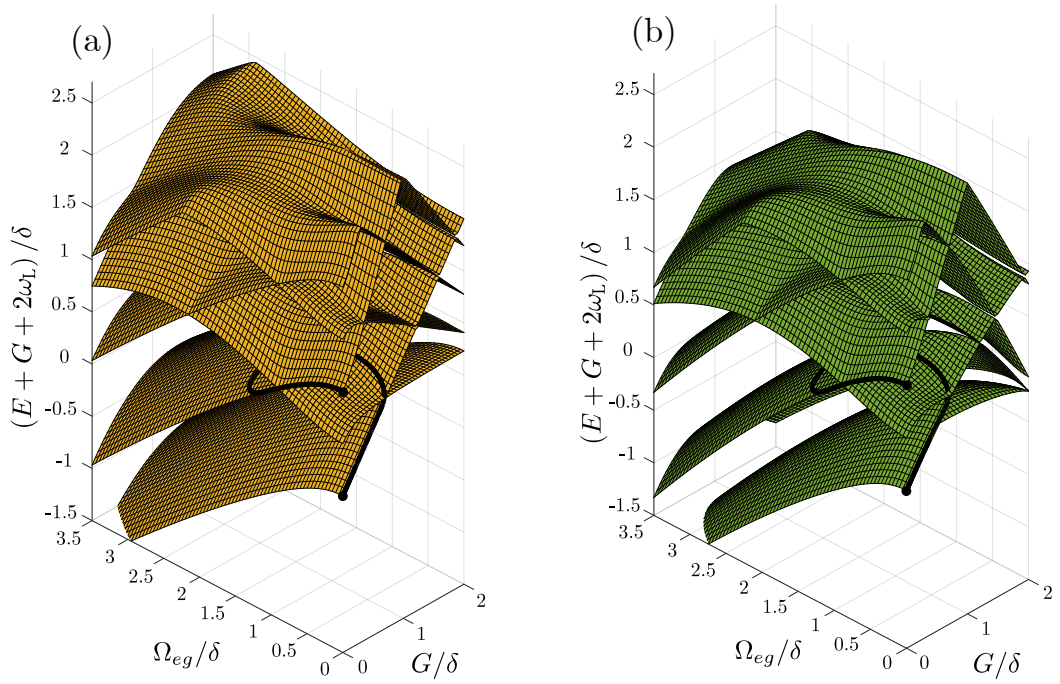

Figure 4.2: Plot of the first five eigenenergy surfaces of the Floquet Hamiltonians. From bottom to top, the surfaces correspond, respectively, to the states $\{|g,0\rangle, |e,0\rangle, |g,1\rangle, |e,1\rangle, |g,2\rangle\}$. (a) has been computed with the RWA, i.e., with the Hamilotnian $\hat{K}'_{\text{rwa}}$ (4.72). (b) has been computed without the RWA, i.e., with the Hamiltonian $\hat{K}'$ (4.77). For both cases, we have used the following parameters: $\Delta_{\text{L}} = \Delta_{\text{c}} = \delta/2$ and $\omega_{\text{L}} = 3\delta$. The black lines correspond to the adiabatic path that the system follows if it is driven with the pulse sequence shown in Figure 4.3; it brings thus the system from $|g,0\rangle$ to $|g,1\rangle$, i.e., it allows to produce a single-photon state in the cavity. The key result shown by this path is that the non resonant terms do not impact the production of single photons since the topology of the energy surfaces are unchanged. In both plots, the term $G + 2\omega_{\text{L}}$ has been added to the energies for clarity of the display.

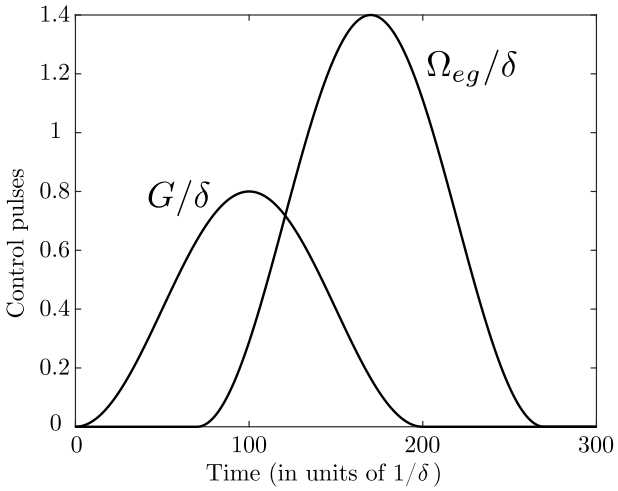

Figure 4.3: Pulse sequence that can be used to produce a photon in the cavity, i.e., manipulating the system from the initial state $|g,0\rangle$ to the final state $|g,1\rangle$. Both pulses have a full width at half maximum — also called interaction time — of $T_{\text{int}} = 100/\delta$, The amplitude of the normalized controls $G(t)$ and $\Omega_{eg}(t)$ are, respectively, 0.8δ and 1.4δ. The time delay between the two pulses is $\tau = 70/\delta$.

$\{e^{il\theta}\}_{l\in\mathbb{N}}$, to ensure that $-i\partial/\partial\varphi$ is positive. This mapping combined with the change of variables

$$\zeta = \varphi - \theta, \quad \eta = \theta, \tag{4.75a}$$

$$\frac{\partial}{\partial\varphi} = \frac{\partial}{\partial\zeta}, \quad \frac{\partial}{\partial\theta} = \frac{\partial}{\partial\eta} - \frac{\partial}{\partial\zeta}, \tag{4.75b}$$

allow to define the new operators

$$\hat{b} = e^{-i\zeta}\sqrt{-i\frac{\partial}{\partial\zeta}}, \quad \hat{b}^\dagger = \sqrt{-i\frac{\partial}{\partial\zeta}}e^{i\zeta}, \tag{4.76}$$

which can formally be interpreted as the exchange of a photon between the laser and the cavity. One can then rewrite the full Hamiltonian as

$$\begin{aligned}\hat{K}' = -i\hbar\omega_{\text{L}}\frac{\partial}{\partial\eta} + \hbar\begin{pmatrix}\delta\hat{b}^\dagger\hat{b} + \Delta_{\text{L}} & \frac{\Omega(t)}{2} + G(t)\hat{b} \\ \frac{\Omega(t)}{2} + G(t)\hat{b}^\dagger & \delta\hat{b}^\dagger\hat{b}\end{pmatrix} + \\ \hbar\begin{pmatrix}0 & G(t)\hat{b}^\dagger e^{2i\eta} + \frac{\Omega(t)}{2}e^{2i\eta} \\ G(t)\hat{b}e^{-2i\eta} + \frac{\Omega(t)}{2}e^{-2i\eta} & 0\end{pmatrix},\end{aligned} \tag{4.77}$$

where $\delta = \omega_{\text{C}} - \omega_{\text{L}}$ and $\Delta_{\text{L}} = \omega_{\text{a}} - \omega_{\text{L}}$. We see that the second term is independent of the Floquet parameter η and can thus be diagonalized by considering time as a parameter. It gives the results presented in [151] that we extend here for a non resonant coupling (third term in (4.77)) to compare the adiabatic control with and without the RWA. To do so, we numerically diagonalize the Floquet Hamiltonian and we obtain the eigenenergy

surfaces shown in Figure 4.2 where we see that the non resonant terms do not change the topology of the surfaces, meaning that in the adiabatic limit, one can equivalently bring the system from the initial state $|g,0\rangle$ to $|e,1\rangle$ by following the paths shown by the black line. It corresponds to the adiabatic following of the system with the counterintuitive pulse sequence shown in Figure 4.3 which is similar to the STIRAP configuration but for a 2-level system. The key point in the adiabatic following here is that the crossings between the different energy surfaces only happen when one of the controls is zero. In that case, the adiabatic theorem predicts that the dynamics follows diabatically the crossing [151]. In general, the typical dynamics to bring the system from zero photon to one photon in the cavity is thus a mix of an adiabatic following around the intersections and of a diabatic evolution through the intersections of the energy surfaces.
This result shows that in the adiabatic limit, the states produced by such controls are very close to single-photon states and that multiphoton components are expected to be small. From this analysis, we can expect that on-demand single-photon sources using an adiabatic process should create photons that are very close to perfect single-photon states, e.g., [37, 95–98]. The contribution of the multiphoton components is thus given by the correction terms to the adiabatic evolution which scale as $1/\tau$ where τ is the typical duration of the control pulses [154]. As expected for an adiabatic process, one can thus reduce the multiphoton components as much as needed by increasing the duration of the driven pulses. Smaller corrections can even be obtained using superadiabatic techniques [155].

4.3 Perspectives for further developments: open cavities

In the preceding section, we have considered the standard cQED scheme where one cavity mode is coupled to a two-level system. The major hypothesis behind this model is to have a cavity of high finesse, i.e., with very low transmission towards the outside and where the different sustained modes are well-separated in frequency. These two conditions ensure that the outside can be neglected and that the inside can be described with a single-mode. This model and its generalizations to three-level systems and few cavity modes have been extensively used to analyze cavity experiments in general [156, 157]. However, the use of cavities to produce single-photon states as well as the developments of plasmonic resonances to enhance the light-matter coupling [158,159], have revealed the need of cQED models in which the outside environment must be taken into account.
Several theoretical approaches have been developed to analyze this question, and they can be separated into two main categories. A first technique is to describe the same system for which decay parameters are added — usually empirically. The Hamiltonian of the resulting lossy system is then non-Hermitian, and one should treat it within the framework of Lindblad master equations. A second technique consists in including the description of the outside environment into the quantum model, so that the full system remains conservative and can thus still be described within the standard quantum framework of Hermitian systems. The two major difficulties associated to these models are that the non-Hermitian approach uses phenomenological parameters to introduce the leakage, while the Hermitian approach drastically increases the dimensionality of the problem. Bypassing these issues is still a current topic of research and one can refer to the following articles [160–162] and references therein to get a more detailed overview of the state of

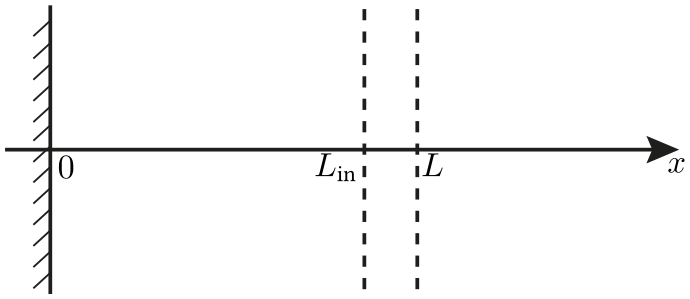

Figure 4.4: Sketch of the one-dimensional open cavity we analyze in this section. A perfect mirror is placed at $x = 0$ and a partially reflective mirror lies in $[L_{\text{in}}, L]$. The associated dielectric function is given in (4.78).

the art.

We want now to present, as a set of preliminary results which should be further developed in a near future, how one can use the concept of quasinormal modes (QNM) [163, 164] to describe the production of photons inside an open cavity. QNMs (also called resonant states) have been extensively used in scattering problems which appear in many branches of physics [52, 165–168]. They have already proved to be very useful for computational purposes in plasmonics for instance where they allow to reduce the number of modes that must be taken into account to obtain a convergence of the results [56, 60].

In the rest of this section, we will introduce our approach to use these QNMs as a tool for the quantum dynamics of photons in an open cavity. We note that some works have already tried to construct models using QNMs to describe photons in cavities [52–54, 60, 169–172] but the approach we will introduce hereafter will be different since we will not attempt to quantize the QNMs as one would do with normal modes, but we will take benefit from the importance of the classical dynamics in the quantum model to incorporate only some of the features of QNMs in our description.

Before getting into the details of QNMs, we first introduce the cavity system we will be considering in the following. An open cavity is a cavity for which at least one mirror is not fully reflective. For simplicity, we choose a one-dimensional cavity which has a perfect mirror located in $x = 0$ and a partially reflective mirror whose right extremity is located in $x = L$ as illustrated in Figure 4.4. We take into account the thickness of the partially reflecting mirror to be as general as possible. The dielectric function of such a system has the following form

$$\varepsilon(x) = \begin{cases} 1 & \text{for } x \in (0, L_{\text{in}}), \\ m(x) & \text{for } x \in (L_{\text{in}}, L), \\ n_{\text{out}}^2 & \text{for } x \in (L, +\infty), \end{cases} \tag{4.78}$$

where $n_{\text{out}} > 1$ is the optical index of the outside material into which the photon will propagate and $m(x)$ can be a piecewise constant function to represent mirrors made of dielectric stacks [173]. We assume here that the inside of the cavity is in the vacuum but the formalism could be further generalized by considering an optical index n_{int} for the inside without much difficulties.

The classical electromagnetic description of such a system is governed by the one dimen-

sional wave equation

$$\frac{\partial^2\phi(x,t)}{\partial t^2} - \frac{c^2}{\varepsilon(x)}\frac{\partial^2\phi(x,t)}{\partial x^2} = 0, \tag{4.79}$$

written here for a general field $\phi(x,t)$. The decomposition of the solutions $\phi(x,t)$ into a set of modes, is the standard technique to analyze perfect cavities, and it is with a similar objective that the QNMs are defined as we will show in the next section.

4.3.1 Normal modes vs quasinormal modes

We recall that a normal mode — in the context of the wave equation (4.79) in $[0,L]$ — is an eigenfunction of the positive operator $-\frac{c^2}{\varepsilon(x)}\frac{\partial^2}{\partial x^2}$ with its boundary conditions, i.e., it is a function f_i satisfying

$$-\frac{c^2}{\varepsilon(x)}\frac{\partial^2}{\partial x^2}f_i(x) = \omega_i^2 f_i(x), \tag{4.80a}$$

$$f_i(x=0) = 0 = f_i(x=L), \tag{4.80b}$$

where ω_i^2 is real. Consequently, if one takes such a mode as initial condition for (4.79), the system has a harmonic evolution

$$\phi(x,t) = e^{-i\omega_i t} f_i(x), \quad \omega_i > 0. \tag{4.81}$$

They are called normal modes because $\{f_i\}_{i\in\mathbb{N}}$ is an orthonormal basis of $L^2([0,L])$ meaning that any $g \in L^2([0,L])$ can be written as

$$g(x) = \sum_i \alpha_i f_i(x) = \sum_i \langle f_i|g\rangle\, f_i(x), \tag{4.82}$$

and solutions of the wave equation can thus also be written as linear combinations of normal modes

$$\phi(x,t) = \sum_i \alpha_i f_i(x) e^{-i\omega_i t}. \tag{4.83}$$

The power of such a representation is that it makes the dynamical part of the problem much easier since the modes have a harmonic evolution. All the properties of the system are thus contained in this modal decomposition.

The concept of quasinormal modes arises if one wants to follow a similar procedure but considering the wave equation over $[0,+\infty)$. Indeed, in this situation, the boundary conditions for the cavity change since we need to allow waves escaping from $[0,L]$. The quasinormal mode is thus a function f_j satisfying

$$-\frac{c^2}{\varepsilon(x)}\frac{\partial^2}{\partial x^2}f_j(x) = \omega_j^2 f_j(x), \tag{4.84a}$$

$$f_j(x=0) = 0, \tag{4.84b}$$

$$f_j(x \geq L) = e^{i\omega_j \frac{n_{\text{out}}}{c} x}. \tag{4.84c}$$

The last equation is known as the Sommerfeld outgoing boundary condition because it yields a solution of (4.79) for $x \geq L$ that is a wave propagating towards positive x. This change of boundary conditions modifies the nature of the operator $-\frac{c^2}{\varepsilon(x)}\frac{\partial^2}{\partial x^2}$ which has now complex eigenvalues $\omega_j^2 \in \mathbb{C}$. We define ω_j as the particular square root for which $\omega_j^r = \mathrm{Re}(\omega_j) > 0$ to obtain outgoing waves propagating in the correct direction. A particularity of the QNM eigenfrequencies is that they always have negative imaginary parts, i.e.,

$$\omega_j = \omega_j^r - i|\omega_j^i|\,, \tag{4.85}$$

with $\omega_j^i = \mathrm{Im}(\omega_j)$. The negativity of the imaginary part leads to the divergence of QNMs when $x \to +\infty$ since for $x \geq L$

$$|f_j| = |e^{i\omega_j \frac{n_{\mathrm{out}}}{c}x}| = |e^{i\omega_j^r \frac{n_{\mathrm{out}}}{c}x} e^{|\omega_j^i|\frac{n_{\mathrm{out}}}{c}x}| = e^{|\omega_j^i|\frac{n_{\mathrm{out}}}{c}x} \underset{x\to\infty}{\longrightarrow} +\infty. \tag{4.86}$$

This exponential divergence prevents from using QNMs as a basis — even generalized — of $L^2([0,+\infty))$ which is the major drawback of these functions. From the dynamical point of view, however, taking a QNM as initial condition for the wave equation yields the following solution

$$\phi(x,t) = e^{-i\omega_j t} f_j(x) = e^{-i\omega_j^r t} f_j(x) e^{-|\omega_j^i|t}. \tag{4.87}$$

We see that the real part of the quasinormal mode eigenfrequency is responsible for the usual harmonic evolution while the imaginary part is a damping parameter. Physically, a QNM represents thus a solution with a damped oscillation in $[0, L]$, arising from the natural leakage towards $[L, +\infty)$ of the solution. Such behavior is what is observed in any actual resonator like cavities and it is the reason why QNMs are promising tools for the description of open systems and already proved to be useful for calculations with systems where the losses are large like in plasmonics for instance.
Additionally, at least in one dimension, QNMs can be used as a basis inside the cavity, i.e., any function $g \in L^2([0, L])$ can be written as

$$g(x) = \sum_j \alpha_j f_j(x) = \sum_j \langle\langle f_j | g \rangle\rangle f_j(x), \tag{4.88}$$

where $\langle\langle \cdot | \cdot \rangle\rangle$ stands for the bilinear form as defined in [52, 53, 55] that one should use to construct the decomposition in place of the standard scalar product. This point is a key ingredient for applications of QNMs and has been discussed in several works [52, 53, 55, 174–176]. In the following, we will assume that it is true for our system and that the decomposition (4.88) is valid with an appropriate bilinear form like the one given in [52][2]. With this assumption, and similarly to what is done for normal modes, any solution of the wave equation inside the cavity can be written as

$$\phi(x,t) = \sum_j \alpha_j f_j(x) e^{-i\omega_j^r t} e^{-|\omega_j^i|t}, \tag{4.89}$$

where we explicitly see the decay with time of the solution.

[2] In [52], one sufficient condition given for the completeness of the set of QNMs in the cavity, is that the dielectric function $\varepsilon(x)$ has a discontinuity at $x = L$. In our model for open cavities, this is always true and could thus justify that the QNMs are a basis in $[0, L]$

In our context, and in view of the natural leakage property of QNMs, we would like to use them to describe how a photon leaks out from the cavity. Indeed, the combination of damped oscillation and propagation towards the outside is what one expects for a photon produced in the cavity. However, due to their diverging property, the QNMs cannot be used directly for the quantum model outside the cavity. In the following, we want to introduce a way out for this issue using spatially truncated QNMs.

4.3.2 Truncated quasinormal modes — Leakage of single photons

We start in this section by considering photons without their sources since we know from Chapter 3 that the propagation is given by the classical solutions of Maxwell's equations. Therefore, in order to describe the leakage of a single-photon from the cavity, we construct a truncated QNM of the form

$$\tilde{f}_j(x) = \begin{cases} f_j(x) & \text{for } x \leq L, \\ 0 & \text{for } x > L, \end{cases} \tag{4.90a}$$

$$= f_j(x)\chi_{[0,L]}. \tag{4.90b}$$

The notation $\chi_{[a,b]}$ stands for the characteristic function over the interval $[a,b]$, i.e., a function that is one on this interval and zero everywhere else. If we choose $\tilde{f}_j$ as initial condition for the wave equation (4.79), we obtain the following solution

$$\tilde{\phi}_j(x,t) = \begin{cases} f_j(x)e^{-i\omega_j t} & \text{for } x \leq L, \\ f_j(L)e^{-i\omega_j\left(\frac{n_{\text{out}}}{c}(L-x)+t\right)} & \text{for } L < x \leq L + ct/n_{\text{out}}, \\ 0 & \text{otherwise}, \end{cases} \tag{4.91a}$$

$$= f_j(x)e^{-i\omega_j t}\chi_{[0,L]} + f_j(L)e^{-i\omega_j\left(\frac{n_{\text{out}}}{c}(L-x)+t\right)}\chi_{[L,L+ct/n_{\text{out}}]}, \tag{4.91b}$$

which splits into two parts: inside the cavity the QNM keeps its standard time evolution, namely oscillation at the real frequency ω_j^r and damping due to the imaginary part ω_j^i; in the causal set $[L, L+ct/n_{\text{out}}]$ the discontinuity of the truncated QNM propagates towards positive x at the speed of light. The function $\tilde{\phi}_j(x,t)$ has thus a time-dependent support $[0, L+ct/n_{\text{out}}]$ which tends toward the full half-line for infinite time. This solution $\tilde{\phi}_j(x,t)$, obtained with a truncated QNM as initial condition, is by construction not divergent since it is smooth and has a finite support $[0, L+ct/n_{\text{out}}]$ for any time t. One can indeed compute its norm as

$$\|\tilde{\phi}_j(t)\|^2 = \int_0^\infty dx|\tilde{\phi}_j(x,t)|^2 \tag{4.92a}$$

$$= \int_0^L dx|f_j(x)e^{-i\omega_j t}|^2 + \int_L^{L+ct/n_{\text{out}}} dx|f_j(L)e^{-i\omega_j\left(\frac{n_{\text{out}}}{c}(L-x)+t\right)}|^2 < \infty \tag{4.92b}$$

$$= \int_0^L dx|f_j(x)|^2 e^{-2|\omega_j^i|t} + \frac{|f_j(L)|^2}{2|\omega_j^i|}\left(1 - e^{-2|\omega_j^i|t}\right). \tag{4.92c}$$

Additionally, the norm must be constant in time since we integrate over the full space $[0, +\infty)$ and the system is by construction lossless. Thus

$$\|\tilde{\phi}_j(t)\|^2 = \|\tilde{\phi}_j(x, t=0)\|^2 = \int_0^L dx|f_j(x)|^2 \equiv \mathcal{N}_j, \tag{4.93}$$

which combined with (4.92c) leads to

$$\mathcal{N}_j = \frac{|f_j(L)|^2}{2|\omega_j^i|}. \tag{4.94}$$

We can then define a normalized truncated QNM solution of the wave equation

$$\tilde{\phi}_j^{\mathrm{n}}(x,t) = \mathcal{N}_j^{-1/2}\tilde{\phi}_j(x,t), \tag{4.95}$$

which fulfills all the requirements to represent a photon state in the BB or LP representation. For instance, for $t = 0$, the LP representation of the states gives the following single-photon state

$$|\tilde{\phi}_j^{\mathrm{n}}\rangle = \hat{B}^\dagger_{\tilde{\phi}_j^{\mathrm{n}}}|\varnothing\rangle, \tag{4.96}$$

with its associated time evolution

$$|\tilde{\phi}_j^{\mathrm{n}}(t)\rangle = \hat{B}^\dagger_{\tilde{\phi}_j^{\mathrm{n}}(t)}|\varnothing\rangle \tag{4.97a}$$

$$= e^{-i\omega_j t}\hat{B}^\dagger_{f_j\chi_{[0,L]}}|\varnothing\rangle + f_j(L)e^{-i\omega_j(\frac{n_{\mathrm{out}}}{c}L+t)}\hat{B}^\dagger_{e^{i\omega_j\frac{n_{\mathrm{out}}}{c}x}\chi_{[L,L+ct/n_{\mathrm{out}}]}}|\varnothing\rangle, \tag{4.97b}$$

which can be interpreted as the superposition of a single-photon with damped oscillations inside the cavity and a plane wave like single-photon propagating outside the cavity. The time-dependent factors give a smooth transition between the two extreme cases: oscillating single-photon only in the cavity and propagating single-photon only in the outside.

4.3.3 Quantum models using quasinormal modes

Given the interesting properties of QNMs, we would like to use them not only as classical solutions onto which photon states can be created, but also to express the whole quantum field theory and its interaction with matter. In this section, we will sketch some preliminary ideas in this direction with first a procedure that could allow to use QNMs as a basis to represent any quantum observable and then the construction of a heuristic model that consists of one QNM interacting with a two-level system in order to describe the production of single photons in open cavities.

4.3.3.1 Hybrid basis

We have seen that QNMs can be used as a basis for the inside of the cavity $[0, L]$. This result is a key tool towards the description of open cavities since the field inside the cavity can thus be expressed in terms of modes that eventually leak out to the exterior. However, to have the full picture of the processes, one cannot restrict the description to the interior only, since it would yield a non-Hermitian system for which the standard construction of the quantum theory cannot be used. Instead, one needs a basis able to represent the quantum theory over the full half-line $[0, +\infty)$.
To do so, we want to construct a hybrid basis composed of QNMs for the inside and of any other basis for the outside. We start with the set of QNMs $\{f_j\}$ and with a plane wave

basis $\{\phi_k\}$ of $L^2([L,+\infty))$, $\phi_k = \exp(ikx)$ with $k \in \mathbb{R}$. From these two bases we construct a hybrid basis over the full half-line, composed of the functions defined as

$$\varphi_{j,k}(x) = f_j(x)\chi_{[0,L]} + \phi_k(x)\chi_{[L,+\infty)}, \tag{4.98}$$

from which any $\mathfrak{g} \in L^2([0,+\infty))$ can be decomposed as

$$\mathfrak{g}(x) = \sum_j \alpha_j f_j(x)\chi_{[0,L]} + \int_{\mathbb{R}} dk\ \beta_k \phi_k(x)\chi_{[L,+\infty)} \tag{4.99a}$$

$$= \int_{\mathbb{R}} dk \sum_j \gamma_{j,k}\varphi_{j,k}(x), \tag{4.99b}$$

with $\alpha_j = \langle\langle f_j|\mathfrak{g}\rangle\rangle$, $\beta_k = \langle\phi_k|\mathfrak{g}\rangle$ and $\gamma_{j,k} = \alpha_j\chi_{[0,L]} + \beta_k\chi_{[L,+\infty)}$. The set $\{\varphi_{j,k}\}$ is a basis since it has been constructed from two separated bases on disjoint intervals. It can then represent any function and in particular the one dimensional LP representation

$$\psi(x) = \sqrt{\frac{\varepsilon_0}{2\hbar}}\left(\Omega^{1/2}A(x) - i\Omega^{-1/2}E(x)\right) \tag{4.100a}$$

$$= \sum_j \alpha_j f_j(x)\chi_{[0,L]} + \int_{\mathbb{R}} dk\ \beta_k\phi_k(x)\chi_{[L,+\infty)} \tag{4.100b}$$

$$= \int_{\mathbb{R}} dk \sum_j \gamma_{j,k}\varphi_{j,k}(x). \tag{4.100c}$$

Following the quantization procedure presented in Chapter 2, we apply the correspondence principle

$$\text{Quantization map:} \qquad \psi(x) \mapsto \int_{\mathbb{R}} dk \sum_j \varphi_{j,k}(x)\hat{B}_{\varphi_{j,k}} = \hat{\Psi}(x), \tag{4.101a}$$

$$\psi^\star(x) \mapsto \int_{\mathbb{R}} dk \sum_j \varphi^\star_{j,k}(x)\hat{B}^\dagger_{\varphi_{j,k}} = \hat{\Psi}^\dagger(x), \tag{4.101b}$$

defining the bosonic creation-annihilation operators as well as the field operators acting on the bosonic Fock space. They are the key tools to express the electromagnetic observables as

$$\hat{A}(x) = \sqrt{\frac{\hbar}{2\varepsilon_0}}\Omega^{-1/2}\left(\hat{\Psi}(x) + \hat{\Psi}^\dagger(x)\right) = \sqrt{\frac{\hbar}{2\varepsilon_0}}\int_{\mathbb{R}} dk \sum_j \Omega^{-1/2}\left(\varphi_{j,k}(x)\hat{B}_{\varphi_{j,k}} + \varphi^\star_{j,k}(x)\hat{B}^\dagger_{\varphi_{j,k}}\right), \tag{4.102a}$$

$$\hat{E}(x) = i\sqrt{\frac{\hbar}{2\varepsilon_0}}\Omega^{1/2}\left(\hat{\Psi}(x) - \hat{\Psi}^\dagger(x)\right) = i\sqrt{\frac{\hbar}{2\varepsilon_0}}\int_{\mathbb{R}} dk \sum_j \Omega^{1/2}\left(\varphi_{j,k}(x)\hat{B}_{\varphi_{j,k}} - \varphi^\star_{j,k}(x)\hat{B}^\star_{\varphi_{j,k}}\right), \tag{4.102b}$$

and the energy as

$$\hat{H} = \hbar\int_{\mathbb{R}} dx\ \hat{\Psi}^\dagger(x)\Omega\hat{\Psi}(x) \tag{4.103a}$$

$$= \hbar\int_{\mathbb{R}} dk \int_{\mathbb{R}} dk' \sum_{j,j'} \langle\varphi_{j,k}|\,\Omega\,|\varphi_{j',k'}\rangle\,\hat{B}^\dagger_{\varphi_{j,k}}\hat{B}_{\varphi_{j',k'}}. \tag{4.103b}$$

We emphasize that the expressions for the quantum observables cannot be further simplified since the functions $\varphi_{j,n}$ are not eigenfunctions of Ω and $\Omega^{\pm 1/2}$.
However, the advantage of the formulation in terms of the basis functions $\varphi_{j,n}$ is that we can easily split the observable according to the inside and outside part of the cavity. The electric field, e.g., can be expressed as

$$\hat{E}(x) = i\sqrt{\frac{\hbar}{2\varepsilon_0}} \int_{\mathbb{R}} dk \sum_j \Omega^{1/2} \left(f_j(x)\chi_{[0,L]} + \phi_k(x)\chi_{[L,+\infty)} \right) \hat{B}_{f_j(x)\chi_{[0,L]}+\phi_k(x)\chi_{[L,+\infty)}} + \text{h.c.} \tag{4.104a}$$

$$= i\sqrt{\frac{\hbar}{2\varepsilon_0}} \sum_j \Omega^{1/2} f_j(x)\chi_{[0,L]} \hat{B}_{f_j\chi_{[0,L]}} + i\sqrt{\frac{\hbar}{2\varepsilon_0}} \int_{\mathbb{R}} dk\ \Omega^{1/2}\phi_k(x)\chi_{[L,+\infty)} \hat{B}_{\phi_k\chi_{[L,+\infty)}} + \text{h.c.} \tag{4.104b}$$

$$= \hat{E}_{\text{in}}(x) + \hat{E}_{\text{out}}(x). \tag{4.104c}$$

The interest of such a splitting will become clear when constructing a model for the interaction of an atom in an open cavity since only the inside part of the electric field will be used in that context. However we emphasize that, due to the antilocality of $\Omega^{1/2}$ discussed in Chapter 3, in general $\hat{E}_{\text{in}}(x) \neq 0$ for $x \in [0, +\infty)$ and $\hat{E}_{\text{out}}(x) \neq 0$ for $x \in [0, L]$.

4.3.3.2 Interacting model

Combining the quantum construction using QNMs and the model for production of single photons in perfect cavity, we want to construct a model for the production of single photons in open cavities. We start with the interaction part of the Hamiltonian for which we consider that the atom is coupled to only one QNM f_j, meaning that $\omega_j^r \simeq \omega_{\text{a}}$. The electric field at the position x_{at} inside the cavity — where the interaction takes place — is given by

$$\hat{E}(x_{\text{at}}) = i\sqrt{\frac{\hbar}{2\varepsilon_0}}\Omega^{1/2} f_j(x_{\text{at}}) \hat{B}_{f_j\chi_{[0,L]}} + i\sqrt{\frac{\hbar}{2\varepsilon_0}} \int_{\mathbb{R}} dk\ \Omega^{1/2}\phi_k(x_{\text{at}})\chi_{[L,+\infty)} \hat{B}_{\phi_k\chi_{[L,+\infty)}} + \text{h.c.}. \tag{4.105}$$

We emphasize again that the second term here is a priori nonzero due to the nonlocality arising with $\Omega^{1/2}$. However, since it is applied on a function with compact support over $[0, +\infty)$ one can argue that its contribution will be small in the cavity and can be neglected compare to the first term. We obtain then

$$\hat{E}(x_{\text{at}}) \simeq i\sqrt{\frac{\hbar}{2\varepsilon_0}}\Omega^{1/2} \left(f_j(x_{\text{at}}) \hat{B}_{f_j\chi_{[0,L]}} - f_j^\star(x_{\text{at}}) \hat{B}^\dagger_{f_j\chi_{[0,L]}} \right). \tag{4.106}$$

Using this approximate expression for the electric field operator, we construct an effective interaction Hamiltonian in the RWA as

$$\hat{H}_{\text{int}}^{\text{eff.}} = id\sqrt{\frac{\hbar}{2\varepsilon_0}}\Omega^{1/2} \left(f_j(x_{\text{at}}) \hat{B}_{f_j\chi_{[0,L]}} |e\rangle\langle g| - f_j^\star(x_{\text{at}}) \hat{B}^\dagger_{f_j\chi_{[0,L]}} |g\rangle\langle e| \right). \tag{4.107}$$

It looks very similar to what we had for the perfect cavity case (4.63) but here, the interaction is expressed in terms of creation-annihilation operators defined on a truncated QNM which satisfies the outgoing boundary condition. We can thus expect the dynamics to produce photon states with a natural propagation towards the outside. The rest of the Hamiltonian is given by the free contributions: for the atom $\hat{H}_{\text{at}} = E_e \left|e\right\rangle \left\langle e\right| + E_g \left|g\right\rangle \left\langle g\right|$ and for the field

$$\hat{H}_{\text{elm}} = \hbar \int_{\mathbb{R}} dk \int_{\mathbb{R}} dk' \left\langle \varphi_{j,k} \right| \Omega \left| \varphi_{j,k'} \right\rangle \hat{B}^{\dagger}_{\varphi_{j,k}} \hat{B}_{\varphi_{j,k'}}. \tag{4.108}$$

The free Hamiltonian of the field could in principle be further simplified by splitting it into a bright part and a dark part following the procedure given in [177]. The advantage of such procedure would be to extract all the basis functions that are needed to represent the chosen propagating QNM with index j. The rest of the sum would thus be decoupled from the dynamics and could be removed. For instance, if one splits the basis ϕ_k according to the sign of $k = \pm|k|$, all the functions for negative k should be in the dark part since they correspond to waves propagating towards the left and thus are not needed to describe the outgoing photon. Another important task that one should consider to perform some calculations with this model, is the action of the operators Ω and $\Omega^{1/2}$ on the hybrid basis functions $\varphi_{j,k}$.

4.3.4 Summary on the perspectives

To conclude on the perspective section, we want to make a brief overview of what we expect to obtain with the models using QNMs, and rapidly explain why our approach is different from what exists already in the literature.
Regarding the use of a truncated QNM function to describe the dynamics of a photon state, the formalism we have used does not introduce anything new. Indeed, we have only constructed a function that is a valid classical configuration to be used in the Fock space formalism for representing a photon and its dynamics. The key point in this construction, is that the truncated QNM is not divergent but still fulfills the outgoing condition. Similar approaches have been developed in the literature, e.g., in [60, 178–180] where QNMs are also used only in the resonant structure and regularized for the outside to avoid the divergence. In [60, 178, 179], the regularization for the outside is done using the Green function of the outside in a way very close to what we did here but for 3D. In [180] QNMs outside the resonant structure are regularized by taking advantage of the dispersion properties of the dielectric function as well as causality conditions. The major difference of these approaches with our construction, is that they never use the regularized QNMs as a state function representing the dynamics of a leaky photon, but they rather use them to express the classical Green function of the system.
Regarding the construction of the quantum model, everything is based on the property that QNMs are a basis inside the cavity. This result is claimed in several works [52, 53, 55, 60] and is used to obtain relevant results. A mathematical proof in one-dimension also points in this direction [174–176]. Assuming that it is true, and using the truncated QNMs construction, we were able to construct a hybrid basis into which any square integrable function can be represented. Consequently, the quantum field theory of light in an open cavity can be expressed in terms of QNMs that naturally propagate the photons towards the outside. Then, by applying the standard single-mode approximation and a coupling

of the RWA form, we obtained a model similar to the JC model but for an open cavity. To validate our result, we will need to make detailed calculations to see whether this construction predicts behaviors that are observed in practice for open cavities. A first step could be to look at the time evolution of the system for an initial condition of the form $|e, 0\rangle$, i.e., atom in its excited state and no photon in the cavity, for which we expect to observe Rabi oscillations with a damping in time. A second step would be to add some control parameters like we did in the perfect cavity case to force the system to go from $|0, g\rangle$ to $|1, g\rangle$ which by construction of the model is a one-photon state propagating towards the outside and thus would perfectly represent an on-demand single-photon experiment that uses single atom/ions in cavities.
In the literature, several attempts to quantize the electromagnetic field using QNMs have been made [60, 179, 181, 182]. In [181, 182], the quantization is performed by considering the outside as a bath and using the non-positive bilinear form $\langle\langle\cdot|\cdot\rangle\rangle$ in place of a scalar product for the Hilbert space. In [60, 179], the construction in terms of regularized QNMs is used to quantize the field by splitting the electromagnetic field observable into two parts: the one which can be written in terms of the regularized QNMs, and the rest. The first part is then quantized while the other is forgotten since should not contribute to the dynamics. Another important difference with our approach is that they formulate the quantization in terms of Green functions while we used a canonical quantization with a correspondence principle. This last difference could be of major importance when considering the quantization in a dispersive and dissipative media, e.g., in plasmonics, since the quantization using Green functions brings intrinsic problems for finite size structures [183, 184].

Conclusion and outlook

In this thesis, we have shown that the description of photons and in particular single photons, should not only be done in momentum space. Even though the latter often allows to make explicit calculations, it can also restrain our ability to interpret the obtained results. This is why having an explicit relation between the equivalent momentum and position formulations, as we introduced in Chapter 2, gives the possibility to take advantage of both representations to maximize our understanding of the theory. On top of this, there exists several equivalent formulations within the momentum and position representations that we also related with explicit isomorphisms. This diversity for the description of the same theory is a nice feature one can take benefit from in order to simplify the problems to analyze. It also demonstrates the robustness of the general quantization procedure that we used to construct all these equivalent representations which in the end arise simply from different Hamiltonian formulations of the same Maxwell equations. Other formulations are of course conceivable and a systematic procedure close to the so-called Glauber extraction rule [24,146] could be developed as a generator of equivalent representations of the quantum theory of the electromagnetic field.

One advantage of the position space representations is illustrated when it comes to computing the dynamics of photons. Indeed, we have shown that the time evolution of any free photon state is given by the dynamics predicted by the associated classical Maxwell equations. Therefore, the position space formulation in terms of pulses provides an easy picture of how a photon state evolves with time since it is the standard propagation of the associated classical pulse onto which the photon has been defined. This picture can even be kept for the propagation of photons inside linear inhomogeneous dielectric media like lenses, beam-splitters or optical fibers, by generalizing the position space quantization in free space to this particular interacting situation in a rather simple way. To illustrate the efficiency of this model, we discussed the passage of a pulse-shaped single-photon through a beam-splitter as well as the Hong-Ou-Mandel effect, and obtained results in agreement with the known experimental observations.

The description of photons in terms of pulses in position space, also unveils the importance of their spatial distribution when it comes to detection processes. In fact, as it is

sometimes the case in experiments, photons can be carried by pulses that cannot fit inside the finite volume of the detector. The process of detection should thus be considered as a local operation meaning that the detector does not probe photons as a whole but it probes their spatial distribution. To address this issue, we have used a model for the local detection using the energy density operator which we consider to be a relevant observable to represent detectors, e.g., superconducting nanowires. To analyze this model, we have computed the mean value of this observable for several states of the quantum electromagnetic field: general single- and N-photon states as well as coherent states. These results have led us to conclude that any state with a finite number of excitation, i.e., N-photon states and in particular single-photon states, are intrinsically nonlocal meaning that there is no localization volume outside which the expectation value of the energy density coincides with the value obtained for the vacuum state. This result was already known and demonstrated using several techniques, but we showed it for an explicit observable which can represent concrete detectors, and without using the time evolution of the states. It means that the intrinsic nonlocality is present at any time and is not only a consequence of the dynamics. A direct effect of this nonlocal character of single-photon states is that one cannot produce a perfect single-photon state in a finite volume due to causality restrictions. States produced in a finite volume are expected to have an infinite number of multiphoton components. Regarding the experiments that aim to produce on-demand single-photon states, and which provides experimental tests of their claim using the Hanbury-Brown-Twiss effect, we expect these multiphoton components to be quite small but they definitely cannot be zero. A characterization of their contribution is a difficult task both theoretically and experimentally but it is certainly an open question that could be answered by a combination of theoretical calculations characterizing the exact state emitted by those sources, and of the experimental measurement of the multiphoton contributions using, e.g., photon number resolving detectors.

The production of photons has been analyzed in the last part of this work, where we have computed the spatial distribution of the state produced by spontaneous emission of a Hydrogen atom in the single-photon approximation. All the calculations have been performed in the subspace of single-photon states meaning that we did not analyze the contributions from multiphoton components, even though the model does predict some, in agreement with the causality restrictions we have stated before. Within this approximation, we characterized the decrease of the energy density for large distances and we found an asymptotic of $1/r^6$ behavior which is far from the quasi-exponential mathematical limit established in the literature. It illustrates the nonlocality and shows that depending on the method of production, the single-photon approximation is not always sufficient. To be closer to the description of actual on-demand single-photon sources, we have also analyzed the production in a perfect cavity by considering a model with a two-level atom interacting with a single-mode bosonic field, as it is customary in cavity quantum electrodynamics. The key point for the production of single-photon states in such model is related to the validity of the rotating wave approximation (RWA). Indeed, the Jaynes-Cummings model that includes the RWA predicts the production of perfect single-photon states while the Rabi model which is the version without the RWA predicts the appearance of an infinite number of excitations. By considering the interaction between the atom and the cavity as a control parameter and by applying another control through the interaction with a

classical laser field, we have analyzed using the Floquet theory, the impact of the RWA in the adiabatic limit. We found through a topological argument that within this limit, the non resonant terms that appear in the Rabi model, do not prevent to control the system dynamics to the target state interpreted as one photon in the cavity and atom in its ground state, i.e., production of a perfect single-photon state as it is done with the RWA. If the process is adiabatic, the same controls applied to both models, yield the same final states. This result justifies the efficiency of on-demand single-photon sources using adiabatic processes to produce states that are close to perfect single-photon states. The error will be given by the validity of the adiabatic approximation, i.e., first order correction terms will be of order $1/\tau$, for τ the interaction time of the adiabatic — i.e., slow — process. Smaller correction can even be obtained using superadiabatic techniques.

As preliminary results, we have also presented a line to follow in order to describe the production of photons in open cavities. To do so, we have used, in a one-dimensional model, the concept of quasinormal modes (QNMs) that are functions with outgoing properties, i.e., they are constructed to naturally propagate outside the cavity. Using a state function composed of a truncated QNM, we have shown that the dynamical leakage of a photon from the cavity can be described without changing the formulation of the quantum theory. Moreover, by introducing a hybrid basis made of the direct sum between truncated QNMs inside the cavity with a standard basis truncated for the outside, quantum observables like the total energy and the electric field operators can be expressed in a natural way. Using this technique, we have constructed a heuristic model similar to the one we have used for perfect cavities but that will automatically include the leakage of the emitted photons towards the outside. The construction of such model is a promising result from which we could in principle describe the dynamics of open systems like cavities without introducing empirical parameters for the coupling with the environment. Indeed, all the information for the leakage is included in the QNMs for which several techniques have been developed to compute them for many different systems. A natural continuation of this work is thus to compute actual dynamics predicted by this model to check whether it yields expected properties, e.g., damped Rabi oscillations. A second step could be to generalize the procedure introduced briefly here to more complex systems like 3D cavities or plasmonic resonators.

A

Positive and negative frequency parts of a field

In this work, we extensively use the notion of helicity and the associated splitting into positive and negative helicity parts one can apply to transverse fields. However, this concept is not to be confused with that of positive and negative frequency parts of a time-dependent field. In this appendix, we will explain in details the latter and show why the two concepts do not coincide in general but only in some particular cases, which could be misleading in our context.

Definition and properties

In this section, we consider a complex time-dependent field $f(t)$ with well-defined time-frequency Fourier transforms, i.e.,

$$f(t) = \frac{1}{2\pi} \int_{-\infty}^{+\infty} d\omega \ \tilde{f}(\omega) e^{-i\omega t}, \tag{A.1a}$$

$$\tilde{f}(\omega) = \int_{-\infty}^{+\infty} dt \ f(t) e^{i\omega t}. \tag{A.1b}$$

The positive frequency part — also referred to as the analytic signal — of $f(t)$ is defined by

$$f^{(f+)}(t) = \frac{1}{2\pi} \int_{0}^{+\infty} d\omega \ \tilde{f}(\omega) e^{-i\omega t}, \tag{A.2}$$

and the negative frequency part by

$$f^{(f-)}(t) = \frac{1}{2\pi} \int_{-\infty}^{0} d\omega \ \tilde{f}(\omega) e^{-i\omega t}. \tag{A.3}$$

The total field is thus the sum of its positive and negative frequency parts

$$f(t) = f^{(f+)}(t) + f^{(f-)}(t). \tag{A.4}$$

Remark: If $f(t)$ is real, $\tilde{f}(\omega) = \left(\tilde{f}(-\omega)\right)^\star$ and the corresponding positive/negative frequency parts are complex and fulfill

$$f^{(f-)}(t) = \left(f^{(f+)}(t)\right)^\star. \tag{A.5}$$

Positive and negative frequency parts of electromagnetic fields

The separation of the positive and negative parts have been widely used in classical electrodynamics. In quantum optics they also play a role, but it is extended in some ways that we will describe in this section. The main point is that one wants to separate the operators representing the observables for the electric field, the magnetic field and the vector potential. In the Heisenberg representation the observables are time-dependent and one can use the definitions of the preceding section. But one would like to make the separation also in the Schrödinger representation, where they do not have any time-dependence. We define for real classical time-independent electromagnetic quantities

$$\vec{E}(\vec{x}) = \vec{E}^{(f+)}(\vec{x}) + \vec{E}^{(f-)}(\vec{x}), \tag{A.6a}$$

$$\vec{B}(\vec{x}) = \vec{B}^{(f+)}(\vec{x}) + \vec{B}^{(f-)}(\vec{x}), \tag{A.6b}$$

$$\vec{A}(\vec{x}) = \vec{A}^{(f+)}(\vec{x}) + \vec{A}^{(f-)}(\vec{x}). \tag{A.6c}$$

To analyze these separations, we use the Landau-Peierls (LP) complex representation

$$\vec{\psi} = \sqrt{\frac{\varepsilon_0}{2\hbar}}\left(\Omega^{1/2}\vec{A} - i\Omega^{-1/2}\vec{E}\right), \tag{A.7}$$

in terms of which the electromagnetic fields can be expressed as

$$\vec{A}(\vec{x}) = \sqrt{\frac{\hbar}{2\varepsilon_0}}\Omega^{-1/2}\left(\vec{\psi}(\vec{x})) + \vec{\psi}^\star(\vec{x})\right), \tag{A.8a}$$

$$\vec{E}(\vec{x}) = i\sqrt{\frac{\hbar}{2\varepsilon_0}}\Omega^{1/2}\left(\vec{\psi}(\vec{x})) - \vec{\psi}^\star(\vec{x})\right). \tag{A.8b}$$

Maxwell's equations written in terms of the LP field are

$$i\frac{\partial\vec{\psi}}{\partial t} = \Omega\vec{\psi}, \quad \nabla\cdot\vec{\psi} = 0, \tag{A.9}$$

and solutions can be written as

$$\vec{\psi}(\vec{x},t) = e^{-i\Omega t}\vec{\psi}(\vec{x},t=0) \tag{A.10a}$$

$$= \int_{\mathbb{R}^3} d^3k \sum_{\lambda=\pm} \vec{\phi}_{\vec{k},\lambda} e^{-i\omega_{\vec{k}}t}\,\langle\vec{\phi}_{\vec{k},\lambda}|\vec{\psi}(t=0)\rangle_{LP}\,, \tag{A.10b}$$

for any initial condition $\vec{\psi}(\vec{x},t=0)$ satisfying $\nabla\cdot\vec{\psi}(\vec{x},t=0) = 0$. Since Ω is a positive operator, its eigenvalues $\omega_{\vec{k}}$ are positive and thus $\vec{\psi}$ has zero negative frequency part

$$\vec{\psi}^{(f+)}(\vec{x},t) = \vec{\psi}(\vec{x},t), \quad \vec{\psi}^{(f-)}(\vec{x},t) = 0. \tag{A.11}$$

We extend this result to the initial time and one can then define the positive and negative frequency parts of the time-independent electromagnetic quantities as

$$\vec{A}^{(f+)}(\vec{x}) = \sqrt{\frac{\hbar}{2\varepsilon_0}}\Omega^{-1/2}\vec{\psi}(\vec{x}), \quad \vec{A}^{(f-)}(\vec{x}) = \sqrt{\frac{\hbar}{2\varepsilon_0}}\Omega^{-1/2}\vec{\psi}^{\star}(\vec{x}), \tag{A.12a}$$

$$\vec{E}^{(f+)}(\vec{x}) = i\sqrt{\frac{\hbar}{2\varepsilon_0}}\Omega^{1/2}\vec{\psi}(\vec{x}), \quad \vec{E}^{(f-)}(\vec{x}) = -i\sqrt{\frac{\hbar}{2\varepsilon_0}}\Omega^{1/2}\vec{\psi}^{\star}(\vec{x}). \tag{A.12b}$$

They can also be expressed in terms of the real electromagnetic quantities as

$$\vec{A}^{(f+)}(\vec{x}) = \frac{1}{2}\left(\vec{A}(\vec{x}) - i\Omega^{-1}\vec{E}(\vec{x})\right), \quad \vec{A}^{(f-)}(\vec{x}) = \frac{1}{2}\left(\vec{A}(\vec{x}) + i\Omega^{-1}\vec{E}(\vec{x})\right), \tag{A.13a}$$

$$\vec{E}^{(f+)}(\vec{x}) = \frac{1}{2}\left(\vec{E}(\vec{x}) + i\Omega\vec{A}(\vec{x})\right), \quad \vec{E}^{(f-)}(\vec{x}) = \frac{1}{2}\left(\vec{E}(\vec{x}) - i\Omega\vec{A}(\vec{x})\right). \tag{A.13b}$$

Remarks:

- The positive frequency part of $\vec{E}$ is in fact proportional to the Białynicki-Birula (BB) vector (2.53) since $\Omega\vec{A} = c\nabla\times\Lambda\vec{A} = c\Lambda\vec{B}$, which gives

$$\vec{E}^{(f+)} = \frac{1}{2}\left(\vec{E} + ic\Lambda\vec{B}\right) = \frac{1}{\sqrt{2\varepsilon_0}}\vec{F}. \tag{A.14}$$

  In the same time it shows that, just like the LP field, the BB vector has zero negative frequency part. This result arises from the fact that the generator of their dynamics Ω is a positive operator.

- The Riemann-Silberstien (RS) vector

$$\vec{F}_{RS} = \sqrt{\frac{\varepsilon_0}{2}}\left(\vec{E} + ic\vec{B}\right), \tag{A.15}$$

  has the property that the concept of positive/negative frequency parts coincides with the concept of positive/negative helicity parts. Indeed, the splitting into helicity parts reads

$$\vec{F}^{(h\pm)}_{RS} = \mathbb{P}^{(h\pm)}\vec{F}_{RS} \tag{A.16a}$$

$$= \mathbb{P}^{(h\pm)}\int_{\mathbb{R}^3} d^3k \sum_{\lambda=\pm} \vec{\phi}_{\vec{k},\lambda}\,\langle\vec{\phi}_{\vec{k},\lambda}|\vec{F}_{RS}\rangle_{LP} \tag{A.16b}$$

$$= \int_{\mathbb{R}^3} d^3k\ \vec{\phi}_{\vec{k},\pm}\,\langle\vec{\phi}_{\vec{k},\pm}|\vec{F}_{RS}\rangle_{LP}\,, \tag{A.16c}$$

  while the splitting into frequency parts can be deduced in a similar way as for the LP field starting with Maxwell's equations for the RS vector

$$i\frac{\partial\vec{F}_{RS}}{\partial t} = c\nabla\times\vec{F}_{RS}, \quad \nabla\cdot\vec{F}_{RS} = 0. \tag{A.17}$$

The solutions for an initial transverse field $\vec{F}_{RS}(\vec{x}, t=0)$ can be written as

$$\vec{F}_{RS}(\vec{x},t) = e^{-ic\nabla\times t}\vec{F}_{RS}(\vec{x},t=0) \tag{A.18a}$$

$$= \int_{\mathbb{R}^3} d^3k \sum_{\lambda=\pm} \vec{\phi}_{\vec{k},\lambda} e^{-i\lambda\omega_{\vec{k}}t} \langle \vec{\phi}_{\vec{k},\lambda} | \vec{F}_{RS}(t=0)\rangle_{LP} \tag{A.18b}$$

$$= \int_{\mathbb{R}^3} d^3k \ \vec{\phi}_{\vec{k},+} e^{-i\omega_{\vec{k}}t} \langle \vec{\phi}_{\vec{k},+} | \vec{F}_{RS}(t=0)\rangle_{LP} + \int_{\mathbb{R}^3} d^3k \ \vec{\phi}_{\vec{k},-} e^{i\omega_{\vec{k}}t} \langle \vec{\phi}_{\vec{k},-} | \vec{F}_{RS}(t=0)\rangle_{LP}\,, \tag{A.18c}$$

from which we identify at $t=0$

$$\vec{F}^{(f\pm)}_{RS} = \int_{\mathbb{R}^3} d^3k \ \vec{\phi}_{\vec{k},\pm} \langle \vec{\phi}_{\vec{k},\pm} | \vec{F}_{RS}(t=0)\rangle_{LP} = \vec{F}^{(h\pm)}_{RS}. \tag{A.19}$$

This special property of the RS vector has led to some misleadingness in the literature. Indeed, to construct the BB 6-component spinor from the RS vector (see equation (2.54)), one can use equivalently the splitting into frequency parts as it was done originally in [21], or the splitting into helicity parts as we have chosen to do in this work. Our choice is justified by the fact that it is the splitting into helicity parts that is needed to construct the isomorphism between the BB representation and the LP representation (see Chapter 2).

Positive and negative frequency parts in the quantum model

The concept of positive and negative frequency parts, as described in the preceding section, can be extended to the quantum electromagnetic field operators, even in the Schrödinger representation. Indeed, one starts with the LP field operator which by analogy with its classical counterpart has zero negative frequency part and thus

$$\hat{\vec{\Psi}}^{(f+)}(\vec{x}) = \hat{\vec{\Psi}}(\vec{x}) = \int_{\mathbb{R}^3} d^3k \sum_{\lambda=\pm} \vec{\phi}_{\vec{k},\lambda}(\vec{x}) \hat{B}_{\vec{\phi}_{\vec{k},\lambda}}\,. \tag{A.20}$$

Positive and negative parts of the electromagnetic field operators are thus directly

$$\hat{\vec{A}}^{(f+)} = \sqrt{\frac{\hbar}{2\varepsilon_0}}\Omega^{-1/2} \int_{\mathbb{R}^3} d^3k \sum_{\lambda=\pm} \vec{\phi}_{\vec{k},\lambda} \hat{B}_{\vec{\phi}_{\vec{k},\lambda}}, \quad \hat{\vec{A}}^{(f-)} = \sqrt{\frac{\hbar}{2\varepsilon_0}}\Omega^{-1/2} \int_{\mathbb{R}^3} d^3k \sum_{\lambda=\pm} \vec{\phi}^{\star}_{\vec{k},\lambda} \hat{B}^{\dagger}_{\vec{\phi}_{\vec{k},\lambda}}, \tag{A.21a}$$

$$\hat{\vec{E}}^{(f+)} = i\sqrt{\frac{\hbar}{2\varepsilon_0}}\Omega^{1/2} \int_{\mathbb{R}^3} d^3k \sum_{\lambda=\pm} \vec{\phi}_{\vec{k},\lambda} \hat{B}_{\vec{\phi}_{\vec{k},\lambda}}, \quad \hat{\vec{E}}^{(f-)} = -i\sqrt{\frac{\hbar}{2\varepsilon_0}}\Omega^{1/2} \int_{\mathbb{R}^3} d^3k \sum_{\lambda=\pm} \vec{\phi}^{\star}_{\vec{k},\lambda} \hat{B}^{\dagger}_{\vec{\phi}_{\vec{k},\lambda}}. \tag{A.21b}$$

In view of these results, and especially in the Scrödinger picture where the concept of positive and negative frequency is not natural, this separation is also called creation and annihilation splitting of the operators, where positive frequencies corresponds to annihilation operators and negative frequencies to creation operators.

B

Time evolution of a general N-photon state

In this appendix, we want to show the result of Chapter 3 about the time evolution of a general N-photon state of the form

$$|\Phi(t=0)\rangle = \prod_{j=1}^{N} \hat{B}^{\dagger}_{\vec{\psi}_j(t=0)} |\varnothing\rangle \,, \tag{B.1}$$

where $\vec{\psi}_j(t=0)$ are the initial conditions in the Landau-Peierls (LP) representation (see (2.13) and (3.7) for vacuum and medium cases). Just like for the one- and two-photon cases which have been shown in Chapter 3, the time evolution of such state is given by (see point **(c)** in Section 3.2)

$$|\Phi(t)\rangle = \prod_{j=1}^{N} \hat{B}^{\dagger}_{\vec{\psi}_j(t)} |\varnothing\rangle \,. \tag{B.2}$$

To do so, we first expand the state function $\vec{\psi}_j$ in terms of the eigenfunctions of Ω

$$\vec{\psi}_j(t) = \sum_{\kappa_j} e^{-i\omega_{\kappa_j} t} \vec{\varphi}_{\kappa_j} \alpha_{\kappa_j}, \qquad \alpha_{\kappa_j} = \langle \vec{\varphi}_{\kappa_j} | \vec{\psi}(t=0) \rangle \,, \qquad j = 1, \dots N, \tag{B.3}$$

which allows us to write the full N-photon state as

$$|\Phi(t)\rangle = \prod_{j=1}^{N} \hat{B}^{\dagger}_{\vec{\psi}_j(t)} |\varnothing\rangle = \prod_{j=1}^{N} \left(\sum_{\kappa_j} e^{-i\omega_{\kappa_j} t} \alpha_{\kappa_j} \hat{B}^{\dagger}_{\vec{\varphi}_{\kappa_j}} \right) |\varnothing\rangle \tag{B.4a}$$

$$= \left(\sum_{\kappa_1} e^{-i\omega_{\kappa_1} t} \, \alpha_{\kappa_1} \hat{B}^{\dagger}_{\vec{\varphi}_{\kappa_1}} \right) \dots \left(\sum_{\kappa_N} e^{-i\omega_{\kappa_N} t} \alpha_{\kappa_N} \hat{B}^{\dagger}_{\vec{\varphi}_{\kappa_N}} \right) |\varnothing\rangle \tag{B.4b}$$

$$= \sum_{\kappa_1, \dots, \kappa_N} e^{-i \sum_{j=1}^{N} \omega_{\kappa_j} t} \left(\prod_{j'} \alpha_{\kappa_{j'}} \right) \left(\prod_{j''} \hat{B}^{\dagger}_{\vec{\varphi}_{\kappa_{j''}}} \right) |\varnothing\rangle \,. \tag{B.4c}$$

We want to check now that this state fulfills Schrödinger's equation, i.e.,

$$i\hbar\frac{\partial}{\partial t}\left|\Phi(t)\right\rangle = \hat{H}\left|\Phi(t)\right\rangle, \tag{B.5}$$

and we compute first the left-hand side

$$i\hbar\frac{\partial}{\partial t}|\Phi(t)\rangle = \sum_{\kappa_1,\ldots,\kappa_N}\left(\sum_j \hbar\omega_{\kappa_j}\right) e^{-i\sum_j \omega_{\kappa_j}t}\prod_{j'}\alpha_{\kappa_{j'}}\prod_{j''}\hat{B}^\dagger_{\vec{\varphi}_{\kappa_{j''}}}\left|\varnothing\right\rangle. \tag{B.6}$$

The right-hand side is obtained by applying the Hamiltonian written in momentum representation

$$\hat{H} = \sum_\kappa \hbar\omega_\kappa \hat{B}^\dagger_{\vec{\varphi}_\kappa}\hat{B}_{\vec{\varphi}_{\kappa'}} \tag{B.7}$$

to (B.4), which yields

$$\hat{H}\left|\Phi(t)\right\rangle = \sum_\kappa \hbar\omega_\kappa \hat{B}^\dagger_{\vec{\varphi}_\kappa}\hat{B}_{\vec{\varphi}_\kappa}\sum_{\kappa_1,\ldots,\kappa_N} e^{-i\sum_{j=1}^N \omega_{\kappa_j}t}\left(\prod_{j'}\alpha_{\kappa_{j'}}\right)\left(\prod_{j''}\hat{B}^\dagger_{\vec{\varphi}_{\kappa_{j''}}}\right)\left|\varnothing\right\rangle \tag{B.8a}$$

$$= \sum_{\kappa_1,\ldots,\kappa_N} e^{-i\sum_j \omega_{\kappa_j}t}\prod_{j'}\alpha_{\kappa'_j}\sum_\kappa \hbar\omega_\kappa \hat{B}^\dagger_{\vec{\varphi}_\kappa}\hat{B}_{\vec{\varphi}_\kappa}\prod_{j''}\hat{B}^\dagger_{\vec{\varphi}_{\kappa_{j''}}}\left|\varnothing\right\rangle. \tag{B.8b}$$

Using the commutation relations $\hat{B}_{\vec{\varphi}_\kappa}\hat{B}^\dagger_{\vec{\varphi}_{\kappa_j}} = \hat{B}^\dagger_{\vec{\varphi}_{\kappa_j}}\hat{B}_{\vec{\varphi}_\kappa} + \delta_{\kappa_j,\kappa}$ one can show by recursion that

$$\hat{B}_{\vec{\varphi}_\kappa}\prod_{j=1}^N \hat{B}^\dagger_{\vec{\varphi}_{\kappa_j}} = \sum_{j=1}^N \delta_{\kappa,\kappa_j}\prod_{j'\neq j}\hat{B}^\dagger_{\vec{\varphi}_{\kappa_{j'}}} + \prod_{j=1}^N \hat{B}^\dagger_{\vec{\varphi}_{\kappa_j}}\hat{B}_{\vec{\varphi}_\kappa}. \tag{B.9}$$

Indeed, in (3.29b) we have shown that it is true for $N = 2$. If we assume now that it is true for N, the following relations show that it is true also for $N+1$:

$$\hat{B}_{\vec{\varphi}_\kappa}\prod_{j=1}^{N+1}\hat{B}^\dagger_{\vec{\varphi}_{\kappa_j}} = \left(\sum_{j=1}^N \delta_{\kappa,\kappa_j}\prod_{j'\neq j}\hat{B}^\dagger_{\vec{\varphi}_{\kappa_{j'}}} + \prod_{j=1}^N \hat{B}^\dagger_{\vec{\varphi}_{\kappa_j}}\hat{B}_{\vec{\varphi}_\kappa}\right)\hat{B}^\dagger_{\vec{\varphi}_{\kappa_{N+1}}} \tag{B.10a}$$

$$= \sum_{j=1}^N \delta_{\kappa,\kappa_j}\prod_{j'\neq j}\hat{B}^\dagger_{\vec{\varphi}_{\kappa_{j'}}}\hat{B}^\dagger_{\vec{\varphi}_{\kappa_{N+1}}} + \prod_{j=1}^N \hat{B}^\dagger_{\vec{\varphi}_{\kappa_j}}\left(\hat{B}_{\vec{\varphi}_\kappa}\hat{B}^\dagger_{\vec{\varphi}_{\kappa_{N+1}}}\right) \tag{B.10b}$$

$$= \sum_{j=1}^N \delta_{\kappa,\kappa_j}\prod_{j'\neq j}\hat{B}^\dagger_{\vec{\varphi}_{\kappa_{j'}}}\hat{B}^\dagger_{\vec{\varphi}_{\kappa_{N+1}}} + \prod_{j=1}^N \hat{B}^\dagger_{\vec{\varphi}_{\kappa_j}}\left(\delta_{\kappa,\kappa_{N+1}} + \hat{B}^\dagger_{\vec{\varphi}_{\kappa_{N+1}}}\hat{B}_{\vec{\varphi}_\kappa}\right) \tag{B.10c}$$

$$= \sum_{j=1}^N \delta_{\kappa,\kappa_j}\prod_{j'\neq j}\hat{B}^\dagger_{\vec{\varphi}_{\kappa_{j'}}}\hat{B}^\dagger_{\vec{\varphi}_{\kappa_{N+1}}} + \prod_{j=1}^N \hat{B}^\dagger_{\vec{\varphi}_{\kappa_j}}\delta_{\kappa,\kappa_{N+1}} + \prod_{j=1}^{N+1}\hat{B}^\dagger_{\vec{\varphi}_{\kappa_j}}\hat{B}_{\vec{\varphi}_\kappa} \tag{B.10d}$$

$$= \sum_{j=1}^{N+1}\delta_{\kappa,\kappa_j}\prod_{j'\neq j}\hat{B}^\dagger_{\vec{\varphi}_{\kappa_{j'}}} + \prod_{j=1}^{N+1}\hat{B}^\dagger_{\vec{\varphi}_{\kappa_j}}\hat{B}_{\vec{\varphi}_\kappa}. \tag{B.10e}$$

Thus, using the fact that $\hat{B}_{\vec{\varphi}_\kappa} |\varnothing\rangle = 0$ we have

$$\hat{B}_{\vec{\varphi}_\kappa} \prod_j \hat{B}^\dagger_{\vec{\varphi}_{\kappa_j}} |\varnothing\rangle = \sum_j \delta_{\kappa,\kappa_j} \prod_{j' \neq j} \hat{B}^\dagger_{\vec{\varphi}_{\kappa_{j'}}} |\varnothing\rangle \,, \tag{B.11}$$

and further

$$\sum_\kappa \hbar\omega_\kappa \hat{B}^\dagger_{\vec{\varphi}_\kappa} \hat{B}_{\vec{\varphi}_\kappa} \prod_j \hat{B}^\dagger_{\vec{\varphi}_{\kappa_j}} |\varnothing\rangle = \sum_\kappa \hbar\omega_\kappa \hat{B}^\dagger_{\vec{\varphi}_\kappa} \sum_j \delta_{\kappa,\kappa_j} \prod_{j' \neq j} \hat{B}^\dagger_{\vec{\varphi}_{\kappa_{j'}}} |\varnothing\rangle \tag{B.12a}$$

$$= \sum_j \sum_\kappa \hbar\omega_\kappa \hat{B}^\dagger_{\vec{\varphi}_\kappa} \delta_{\kappa,\kappa_j} \prod_{j' \neq j} \hat{B}^\dagger_{\vec{\varphi}_{\kappa_{j'}}} |\varnothing\rangle \tag{B.12b}$$

$$= \sum_j \hbar\omega_{\kappa_j} \hat{B}^\dagger_{\vec{\varphi}_{\kappa_j}} \prod_{j' \neq j} \hat{B}^\dagger_{\vec{\varphi}_{\kappa_{j'}}} |\varnothing\rangle \tag{B.12c}$$

$$= \left(\sum_j \hbar\omega_{\kappa_j} \right) \prod_{\text{all } j'} \hat{B}^\dagger_{\vec{\varphi}_{\kappa_{j'}}} |\varnothing\rangle \,. \tag{B.12d}$$

Finally inserting (B.12d) into (B.8b) we obtain

$$\hat{H} |\Phi(t)\rangle = \sum_{\kappa_1,\ldots,\kappa_N} e^{-i\sum_i \omega_{\kappa_i} t} \prod_j \alpha_{\kappa_j} \sum_\kappa \hbar\omega_\kappa \hat{B}^\dagger_{\vec{\varphi}_\kappa} \hat{B}_{\vec{\varphi}_\kappa} \prod_{j'} \hat{B}^\dagger_{\vec{\varphi}_{\kappa_{j'}}} |\varnothing\rangle \tag{B.13a}$$

$$= \sum_{\kappa_1,\ldots,\kappa_N} e^{-i\sum_i \omega_{\kappa_i} t} \prod_j \alpha_{\kappa_j} \left(\sum_{j'} \hbar\omega_{\kappa_{j'}} \right) \prod_{j''} \hat{B}^\dagger_{\vec{\varphi}_{\kappa_{j''}}} |\varnothing\rangle \tag{B.13b}$$

$$= i\hbar \frac{\partial}{\partial t} |\Phi(t)\rangle \,, \tag{B.13c}$$

where in the last equality we have used the relation (B.6), which completes the proof.

C

Knight's theorem and equal-time correlation functions

The goal of this appendix is to show that one cannot deduce the nonlocality of the energy density expectation value from the nonlocality of the time-dependent correlation functions used by Knight [40]. To do so, we will give as counterexamples, states for which equal-time correlation functions of $\vec{A}$ or $\vec{E}$ are local in the sense defined by Knigth [40] (see Chapter 3). This example is inspired by the work of Białynicki-Birula *et al.* [39]. Since we are interested in photons, we adapt Knight's construction for the scalar Klein-Gordon equation to the electromagnetic case but a similar argument can be made for massive scalar fields.
We start with a state $|\vec{\psi}_{\vec{A}}\rangle = \hat{B}^{\dagger}_{\vec{\psi}_{\vec{A}}} |\varnothing\rangle$ with the properties

$$\left[\hat{B}_{\vec{\psi}_{\vec{A}}}, \hat{B}^{\dagger}_{\vec{\psi}_{\vec{A}}}\right] = \mathbb{1}, \tag{C.1a}$$

$$\left[\vec{\hat{A}}(\vec{x}_j, t_0), \hat{B}^{\dagger}_{\vec{\psi}_{\vec{A}}}\right] = 0 \quad \text{for all } \vec{x}_j \notin \mathcal{R}, \tag{C.1b}$$

where $\mathcal{R}$ is an open set of $\mathbb{R}^3$ and t_0 a given time which we take as zero in the following without loss of generality. The mean value of the equal-time correlation function of the potential vector outside $\mathcal{R}$ for a state with such properties is thus

$$\langle\vec{\psi}_{\vec{A}}| \vec{\hat{A}}(\vec{x}_1) \dots \vec{\hat{A}}(\vec{x}_M) |\vec{\psi}_{\vec{A}}\rangle = \langle\varnothing| \hat{B}_{\vec{\psi}_{\vec{A}}} \vec{\hat{A}}(\vec{x}_1) \dots \vec{\hat{A}}(\vec{x}_M) \hat{B}^{\dagger}_{\vec{\psi}_{\vec{A}}} |\varnothing\rangle \tag{C.2a}$$

$$= \langle\varnothing| \hat{B}_{\vec{\psi}_{\vec{A}}} \hat{B}^{\dagger}_{\vec{\psi}_{\vec{A}}} \vec{\hat{A}}(\vec{x}_1) \dots \vec{\hat{A}}(\vec{x}_M) |\varnothing\rangle \tag{C.2b}$$

$$= \langle\varnothing| \left(\mathbb{1} + \hat{B}^{\dagger}_{\vec{\psi}_{\vec{A}}} \hat{B}_{\vec{\psi}_{\vec{A}}}\right) \vec{\hat{A}}(\vec{x}_1) \dots \vec{\hat{A}}(\vec{x}_M) |\varnothing\rangle \tag{C.2c}$$

$$= \langle\varnothing| \vec{\hat{A}}(\vec{x}_1) \dots \vec{\hat{A}}(\vec{x}_M) |\varnothing\rangle . \tag{C.2d}$$

This calculation shows that outside $\mathcal{R}$, the mean value is that of the vacuum. The key point of this result is to construct a state $|\vec{\psi}_{\vec{A}}\rangle$ with the properties (C.1). To do so, one

remarks that the commutator (C.1b) can be written as

$$\left[\hat{\vec{A}}(\vec{x}_j), \hat{B}^\dagger_{\vec{\psi}_{\vec{A}}}\right] = \sqrt{\frac{\hbar}{2\varepsilon_0}} \int_{\mathbb{R}^3} d^3k \sum_{\lambda=\pm} \omega_{\vec{k}}^{-1/2} \vec{\phi}_{\vec{k},\sigma}(\vec{x}_j) \left[\hat{B}_{\vec{\phi}_{\vec{k},\sigma}}, \hat{B}^\dagger_{\vec{\psi}_{\vec{A}}}\right] \tag{C.3a}$$

$$= \sqrt{\frac{\hbar}{2\varepsilon_0}} \Omega^{-1/2} \int_{\mathbb{R}^3} d^3k \sum_{\lambda=\pm} \vec{\phi}_{\vec{k},\sigma}(\vec{x}_j) \langle \vec{\phi}_{\vec{k},\sigma} | \vec{\psi}_{\vec{A}} \rangle \tag{C.3b}$$

$$= \sqrt{\frac{\hbar}{2\varepsilon_0}} \Omega^{-1/2} \vec{\psi}_{\vec{A}}(\vec{x}_j), \tag{C.3c}$$

which is zero outside $\mathcal{R}$ if one takes a function $\vec{\xi}_{\vec{A}}$ with compact support in $\mathcal{R}$, i.e., $\vec{\xi}_{\vec{A}}(\vec{x}_j) = 0$ for all $\vec{x}_j \notin \mathcal{R}$ and defines $\vec{\psi}_{\vec{A}} = \Omega^{1/2} \vec{\xi}_{\vec{A}}$.

A similar construction can be done for $\vec{\hat{E}}$ where one has

$$\left[\hat{B}_{\vec{\psi}_{\vec{E}}}, \hat{B}^\dagger_{\vec{\psi}_{\vec{E}}}\right] = \mathbb{1}, \tag{C.4a}$$

$$\left[\vec{\hat{E}}(\vec{x}_j, t_0), \hat{B}^\dagger_{\vec{\psi}_{\vec{E}}}\right] = 0 \quad \text{for all } \vec{x}_j \notin \mathcal{T}, \tag{C.4b}$$

which gives for the correlation function

$$\langle \vec{\psi}_{\vec{E}} | \, \vec{\hat{E}}(\vec{x}_1) \dots \vec{\hat{E}}(\vec{x}_M) \, | \vec{\psi}_{\vec{E}} \rangle = \langle \varnothing | \, \hat{B}_{\vec{\psi}_{\vec{E}}} \vec{\hat{E}}(\vec{x}_1) \dots \vec{\hat{E}}(\vec{x}_M) \hat{B}^\dagger_{\vec{\psi}_{\vec{E}}} \, | \varnothing \rangle \tag{C.5a}$$

$$= \langle \varnothing | \, \hat{B}_{\vec{\psi}_{\vec{E}}} \hat{B}^\dagger_{\vec{\psi}_{\vec{E}}} \vec{\hat{E}}(\vec{x}_1) \dots \vec{\hat{E}}(\vec{x}_M) \, | \varnothing \rangle \tag{C.5b}$$

$$= \langle \varnothing | \left(\mathbb{1} + \hat{B}^\dagger_{\vec{\psi}_{\vec{E}}} \hat{B}_{\vec{\psi}_{\vec{E}}} \right) \vec{\hat{E}}(\vec{x}_1) \dots \vec{\hat{E}}(\vec{x}_M) \, | \varnothing \rangle \tag{C.5c}$$

$$= \langle \varnothing | \, \vec{\hat{E}}(\vec{x}_1) \dots \vec{\hat{E}}(\vec{x}_M) \, | \varnothing \rangle \, . \tag{C.5d}$$

To construct the state $|\vec{\psi}_{\vec{E}}\rangle$, we use the expression of the commutator

$$\left[\vec{\hat{E}}(\vec{x}_j), \hat{B}^\dagger_{\vec{\psi}_{\vec{E}}}\right] = i\sqrt{\frac{\hbar}{2\varepsilon_0}} \int_{\mathbb{R}^3} d^3k \sum_{\sigma=\pm} \omega_{\vec{k}}^{1/2} \vec{\phi}_{\vec{k},\sigma}(\vec{x}_j) \left[\hat{B}_{\vec{\phi}_{\vec{k},\sigma}}, \hat{B}^\dagger_{\vec{\psi}_{\vec{E}}}\right] \tag{C.6a}$$

$$= i\sqrt{\frac{\hbar}{2\varepsilon_0}} \Omega^{1/2} \int_{\mathbb{R}^3} d^3k \sum_{\sigma=\pm} \vec{\phi}_{\vec{k},\sigma}(\vec{x}_j) \langle \vec{\phi}_{\vec{k},\sigma} | \vec{\psi}_{\vec{E}} \rangle \tag{C.6b}$$

$$= i\sqrt{\frac{\hbar}{2\varepsilon_0}} \Omega^{1/2} \vec{\psi}_{\vec{E}}(\vec{x}_j), \tag{C.6c}$$

and define $\vec{\psi}_{\vec{E}} = \Omega^{-1/2} \vec{\xi}_{\vec{E}}$, where $\vec{\xi}_{\vec{E}}$ is a function with compact support in $\mathcal{T}$, i.e., $\vec{\xi}_{\vec{E}}(\vec{x}_j) = 0$ for all $\vec{x}_j \notin \mathcal{T}$.

Remark: The construction for $\vec{\hat{B}}$ can be deduced from that for $\vec{\hat{A}}$ by using $\vec{\hat{B}} = \nabla \times \vec{\hat{A}}$ which gives for the commutator

$$\left[\vec{\hat{B}}(\vec{x}_j), \hat{B}^\dagger_{\vec{\psi}_{\vec{B}}}\right] = \sqrt{\frac{\hbar}{2\varepsilon_0}} \nabla \times \Omega^{-1/2} \vec{\psi}_{\vec{B}}(\vec{x}_j). \tag{C.7}$$

We take then simply $\vec{\psi}_{\vec{B}} = \vec{\psi}_{\vec{A}} = \Omega^{1/2}\vec{\xi}_{\vec{A}}$ since $\nabla \times \vec{\xi}_{\vec{A}}$ also has compact support in $\mathcal{R} \subset \mathbb{R}^3$.

These two examples show, as it was already said by Knight [40], that the theorem does not apply for equal-time correlation functions. As a consequence, the non locality of the energy density, which is a time-independent operator, cannot be deduced from Knight's theorem and one needs to use another approach to show the nonlocality, e.g., what we have done in Chapter 3.

D

Anti-locality of the frequency operator — Proof of Lemma 1

We provide in this appendix, a proof of the Lemma 1 used to show the nonlocality of photons in Section 3.4.4. This result was shown in [109–111] and we will sketch here the argument of [110]. We recall the statement:

Lemma 1: *For any field $\vec{v}(\vec{x})$ that is not identically zero, $\Omega\vec{v}$ and $\vec{v}$ cannot be both zero in any open set of $\mathbb{R}^3$.*

To show the Lemma, we will show an equivalent formulation that is: if $\vec{v}$ and $\Omega\vec{v}$ are both equal to zero in some open set $\mathcal{S}$, it implies that $\vec{v}(\vec{x}) = 0$ everywhere.

Since Ω is positive and selfadjoint, the operators $U(t) = \exp(i\Omega t)$, $t \in (-\infty, +\infty)$ define a one-parameter family of unitary operators. The field defined as $\vec{u}(\vec{x}, t) = U(t)\vec{v}(\vec{x})$ satisfies the wave equation

$$\frac{\partial^2 \vec{u}}{\partial t^2} = -\Omega^2 \vec{u}, \tag{D.1}$$

with initial conditions

$$\vec{u}(\vec{x}, t = 0) = \vec{v}(\vec{x}), \tag{D.2a}$$

$$\frac{\partial \vec{u}}{\partial t}(\vec{x}, t = 0) = i\Omega\vec{v}(\vec{x}). \tag{D.2b}$$

Since the solutions of the wave equation propagate with a finite speed c, the property of the initial conditions to be zero, i.e., $\vec{v}(\vec{x}) = 0$ in a set $\mathcal{S}$, implies that there is a $t_0 > 0$ and a nonempty open subset $\mathcal{S}_0 \subset \mathcal{S}$ such that $\vec{u}(\vec{x}, t) = 0$ for all $\vec{x} \in \mathcal{S}_0$ and $0 \leq t < t_0$. Thus, for any $\mathcal{C}^\infty$ field $\vec{\varphi}(\vec{x})$ with compact support in $\mathcal{S}_0$,

$$\langle \vec{\varphi} | \vec{u}(\cdot, t) \rangle = \int_{\mathbb{R}^3} d^3x \; \vec{\varphi}(\vec{x})^\star \cdot \vec{u}(\vec{x}, t) = 0 \tag{D.3}$$

for $0 \leq t < t_0$. We now consider the continuation of the variable t into the upper complex half-plane and define the function

$$f(z) = \langle \vec{\varphi} | e^{i\Omega z} \vec{v} \rangle \,, \tag{D.4}$$

for $\operatorname{Im} z \geq 0$ that has the following properties [110]:

(i) $f(z)$ is holomorphic for $\operatorname{Im} z > 0$, and continuous for $\operatorname{Im} z \geq 0$;

(ii) $f(t) = \langle \vec{\varphi} | \vec{u}(\cdot, t) \rangle$ when $t \in \mathbb{R}$, and $f(t) \in \mathbb{R}$ for $t \in (0, t_0)$;

(iii) $f(t) = 0$ for $0 \leq t < t_0$.

We remark that for $t > t_0$, $f(t)$ is not necessarily zero nor real. The main steps of a proof that $f(z)$ is holomorphic in the upper half plane, by showing the existence of the derivative df/dz, can be summarized as follows: $\vec{v}$ can be developed in the basis $\vec{\phi}_{\vec{k},\sigma}$ of continuum eigenfunctions of the Laplacian $\vec{v} = \int_{\mathbb{R}^3} d^3k \sum_\sigma \alpha_{\vec{k},\sigma} \vec{\phi}_{\vec{k},\sigma}$. We can then write

$$\frac{d}{dz} f(z) = \frac{d}{dz} \int_{\mathcal{S}_0} d^3x \; \vec{\varphi}^\star \cdot e^{i\Omega z} \vec{v} \tag{D.5a}$$

$$= \int_{\mathcal{S}_0} d^3x \; \vec{\varphi}^\star \cdot e^{i\Omega z} i\Omega \vec{v} \tag{D.5b}$$

$$= \int_{\mathcal{S}_0} d^3x \int_{\mathbb{R}^3} d^3k \sum_\sigma \vec{\varphi}^\star \cdot \vec{\phi}_{\vec{k},\sigma} \alpha_{\vec{k},\sigma} i\omega_{\vec{k}} e^{i\omega_{\vec{k}} z}. \tag{D.5c}$$

The derivative can be brought inside the integral by the Weierstrass M-test and the Lebesgue dominated convergence theorem, because the integral converges absolutely since $e^{i\Omega z}$ is a contractive semi-group [185]. The existence of the derivative is then obtained by exchanging the two integrals by the Fubini-Tonelli theorem: Writing z as $z = z_r + iz_i$, one obtains

$$\begin{aligned} \left| \frac{d}{dz} f(z) \right| &\leq \int_{\mathcal{S}_0} d^3x \int_{\mathbb{R}^3} d^3k \sum_\sigma |\vec{\varphi}^\star \cdot \vec{\phi}_{\vec{k},\sigma}| \, |\alpha_{\vec{k},\sigma}| \, \omega_{\vec{k}} e^{-\omega_{\vec{k}} z_i} \\ &= \int_{\mathbb{R}^3} d^3k \sum_\sigma |\alpha_{\vec{k},\sigma}| \, \omega_{\vec{k}} e^{-\omega_{\vec{k}} z_i} \int_{\mathcal{S}_0} d^3x |\vec{\varphi}^\star \cdot \vec{\phi}_{\vec{k},\sigma}| \\ &\leq C \int_{\mathbb{R}^3} d^3k \sum_\sigma |\alpha_{\vec{k},\sigma}| \, \omega_{\vec{k}} e^{-\omega_{\vec{k}} z_i} < \infty, \end{aligned} \tag{D.6a}$$

where C is a constant. The last integral is finite for $z_i > 0$, which completes the argument for the existence of df/dz.

We will now use the Schwarz reflection principle [186, p.75], which in the present context can be formulated as follows: If $f_+(z)$ satisfies the following properties:

(S-i) $f_+(z)$ is holomorphic in the open upper complex rectangle $D_+ = \{\operatorname{Im} z > 0, \operatorname{Re} z \in (0, t_0)\}$;

(S-ii) $f_+(z)$ continuous in $D_+ \cup (0, t_0)$;

(S-iii) $f_+(t)$ is real in the interval $t \in (0, t_0)$;

then $f_+(z)$ can be continued holomorphically through the interval $(0, t_0)$ to the lower rectangle $D_- = \{\operatorname{Im} z \leq 0, \operatorname{Re} z \in (0, t_0)\}$, by defining

$$f_+(z) = \begin{cases} f_+(z) & \text{for } z \in D_+, \\ [f_+(z^\star)]^\star & \text{for } z \in D_-. \end{cases} \tag{D.7}$$

This defines thus a holomorphic function $f_+(z)$ in the whole open set $D_+ \cup D_- = \{\mathrm{Re}\, z \in (0, t_0)\}$, which includes the interval $(0, t_0)$.
By applying the Schwarz reflection principle to the function $f(z)$ that we combine with the properties (i) and (ii), it shows that $f(z)$ is analytic in the union of the open upper half plane and D_-. Property (iii) states that $f(z) = 0$ in the interval $z \in (0, t_0)$, which implies that $f(z) = 0$ in the whole region where f is holomorphic, in particular in the whole open upper half-plane $\mathrm{Im}\, z > 0$. Since, according to (i), $f(z)$ is continuous for $\mathrm{Im}\, z \geq 0$, this implies that $f(z) = 0$ for $\mathrm{Im}\, z \geq 0$. In particular, $f(t) : \langle \vec{\varphi} | \vec{u}(\cdot, t) \rangle = 0$ for $-\infty < t < \infty$. Since $\vec{\varphi}$ is an arbitrary function, this implies that $\vec{u}(\vec{x}, t) = 0$ for $-\infty < t < \infty$ and $\vec{x} \in \mathcal{S}_0$. The unique continuation theorem for solutions $\vec{u}(\vec{x}, t)$ of the wave equation, proven, e.g., in [187], states that if $\vec{u}(\vec{x}, t) = 0$ for an open set for all $-\infty < t < \infty$, then $\vec{u}(\vec{x}, t) = 0$ everywhere. In particular, for $t = 0$ this implies that

$$\vec{u}(\vec{x}, t = 0) = \vec{v}(\vec{x}) = 0, \quad \text{for all } \vec{x} \in \mathbb{R}^3, \tag{D.8}$$

which completes the proof.

E

Coherent states

Coherent states, also called quasi-classical states, are states that were originally constructed for the standard one-dimensional quantum harmonic oscillator in order to analyze the classical limit of the quantum theory. One can also define them for the quantum theory of the electromagnetic field as we will do in this appendix. They are interesting states of the field since it is commonly accepted that lasers produce coherent states [33].

Definition

We start by defining for any BB function $\vec{\eta} \in \mathscr{H}_{BB}$ the following Weyl operator

$$\hat{W}_{\vec{\eta}} = \exp\Big(\hat{C}^\dagger_{\vec{\eta}} - \hat{C}_{\vec{\eta}}\Big) \tag{E.1a}$$

$$= e^{-\frac{1}{2}\langle\vec{\eta}|\vec{\eta}\rangle_{BB}} \exp\Big(\hat{C}^\dagger_{\vec{\eta}}\Big) \exp\Big(-\hat{C}_{\vec{\eta}}\Big), \tag{E.1b}$$

which is unitary, i.e., $\hat{W}^{-1}_{\vec{\eta}} = \hat{W}^\dagger_{\vec{\eta}}$, and where we have used the Baker-Hausdorff-Campbell formula as well as the commutation relation $[\hat{C}_{\vec{\eta}}, \hat{C}^\dagger_{\vec{\eta}}] = \langle\vec{\eta}|\vec{\eta}\rangle_{BB}$ to obtain the second expression. We note that $\hat{W}_{\vec{\eta}}$ is a generalization of the displacement operator traditionally used for the construction of coherent states for the quantum harmonic oscillator. An equivalent formulation can be done in the LP representation by applying the isomorphism

$$\mathcal{I}^{-1}\hat{W}_{\vec{\eta}}\mathcal{I} = \exp\Big(\mathcal{I}^{-1}\hat{B}^\dagger_{\vec{\eta}}\mathcal{I} - \mathcal{I}^{-1}\hat{B}_{\vec{\eta}}\mathcal{I}\Big) \tag{E.2a}$$

$$= \exp\Big(\hat{C}^\dagger_{\mathcal{I}^{-1}\vec{\eta}} - \hat{C}_{\mathcal{I}^{-1}\vec{\eta}}\Big) = \hat{W}_{\mathcal{I}^{-1}\vec{\eta}}. \tag{E.2b}$$

A coherent state, described in position space representation, is thus obtained by applying a Weyl operator to the vacuum state as

$$|\mathrm{coh}_{\vec{\eta}}\rangle = \hat{W}_{\vec{\eta}}\,|\varnothing\rangle\,. \tag{E.3}$$

This construction is general in the sense that no constraints about the normalization of $\vec{\eta}$ are required. However, one can express the same coherent state in terms of a normalized

BB function $\vec{\xi}$ related to $\vec{\eta}$ by $\vec{\eta} = \alpha\vec{\xi}$, for $\alpha \in \mathbb{C}$, as

$$|\mathrm{coh}_{\vec{\eta}}\rangle = |\mathrm{coh}_{\alpha\vec{\xi}}\rangle = \hat{W}_{\alpha\vec{\xi}}|\varnothing\rangle = \exp\Big(\hat{C}^{\dagger}_{\alpha\vec{\xi}} - \hat{C}_{\alpha\vec{\xi}}\Big)|\varnothing\rangle = \exp\Big(\alpha\hat{C}^{\dagger}_{\vec{\xi}} - \alpha^{\star}\hat{C}_{\vec{\xi}}\Big)|\varnothing\rangle\,. \tag{E.4}$$

The last expression shows the close relation between the construction we are doing here using Weyl operators and the standard quantum harmonic oscillator construction using the displacement operator. We remark that a coherent state is always normalized, no matter the normalization of the state function since

$$\langle \mathrm{coh}_{\vec{\eta}}|\mathrm{coh}_{\vec{\eta}}\rangle = \langle\varnothing|\,\hat{W}^{\dagger}_{\vec{\eta}}\hat{W}_{\vec{\eta}}\,|\varnothing\rangle = \langle\varnothing|\varnothing\rangle = 1. \tag{E.5}$$

By decomposing the exponential in (E.1a), one can also express coherent states in terms of bosonic creation-annihilation operators as

$$|\mathrm{coh}_{\vec{\eta}}\rangle = e^{-\frac{1}{2}\langle\vec{\eta}|\vec{\eta}\rangle_{BB}}\sum_{n=0}^{\infty}\frac{1}{n!}\hat{C}^{\dagger}_{\vec{\eta}}|\varnothing\rangle\,, \tag{E.6}$$

and this is the representation we will use in the following.

Energy density

We have used in Chapter 3 the expectation value of the energy density operator for a coherent state $|\mathrm{coh}_{\vec{\eta}}\rangle$ which yields

$$\begin{aligned}\langle\hat{\mathcal{E}}(\vec{x})\rangle_{|\mathrm{coh}_{\vec{\eta}}\rangle} &= |\vec{\eta}^{(h+)}(\vec{x})|^2 + |\vec{\eta}^{(h-)}(\vec{x})|^2 + \vec{\eta}^{(h+)\star}(\vec{x})\cdot\vec{\eta}^{(h-)\star}(\vec{x}) + \vec{\eta}^{(h-)}(\vec{x})\cdot\vec{\eta}^{(h+)}(\vec{x})\\ &= |\vec{\eta}_{RS}(\vec{x})|^2,\end{aligned} \tag{E.7}$$

where $\vec{\eta}_{RS} = \vec{\eta}^{(h+)} + \vec{\eta}^{(h-)\star}$ is the Riemann-Silberstein vector (see Chapter 2). In this section, we aim at showing this result. We recall that the energy density operator can be expressed in terms of the BB field operators (3.82) as

$$\hat{\mathcal{E}}_{\mathrm{em}}(\vec{x}) = \vec{\hat{\mathbf{F}}}^{(h+)\dagger}\cdot\vec{\hat{\mathbf{F}}}^{(h+)} + \vec{\hat{\mathbf{F}}}^{(h-)\dagger}\cdot\vec{\hat{\mathbf{F}}}^{(h-)} + \vec{\hat{\mathbf{F}}}^{(h-)\dagger}\cdot\vec{\hat{\mathbf{F}}}^{(h+)\dagger} + \vec{\hat{\mathbf{F}}}^{(h+)}\cdot\vec{\hat{\mathbf{F}}}^{(h-)}, \tag{E.8}$$

and to compute the mean value, one has to compute four terms:

$$T_1 = \langle\varnothing|\,\hat{W}^{\dagger}_{\vec{\eta}}\vec{\hat{\mathbf{F}}}^{(h+)\dagger}\cdot\vec{\hat{\mathbf{F}}}^{(h+)}\hat{W}_{\vec{\eta}}\,|\varnothing\rangle\,, \tag{E.9a}$$

$$T_2 = \langle\varnothing|\,\hat{W}^{\dagger}_{\vec{\eta}}\vec{\hat{\mathbf{F}}}^{(h-)\dagger}\cdot\vec{\hat{\mathbf{F}}}^{(h-)}\hat{W}_{\vec{\eta}}\,|\varnothing\rangle\,, \tag{E.9b}$$

$$T_3 = \langle\varnothing|\,\hat{W}^{\dagger}_{\vec{\eta}}\vec{\hat{\mathbf{F}}}^{(h+)\dagger}\cdot\vec{\hat{\mathbf{F}}}^{(h-)\dagger}\hat{W}_{\vec{\eta}}\,|\varnothing\rangle\,, \tag{E.9c}$$

$$T_4 = \langle\varnothing|\,\hat{W}^{\dagger}_{\vec{\eta}}\vec{\hat{\mathbf{F}}}^{(h-)}\cdot\vec{\hat{\mathbf{F}}}^{(h-)}\hat{W}_{\vec{\eta}}\,|\varnothing\rangle\,. \tag{E.9d}$$

We will use the extension of the commutation relation used in Chapter 3 and its complex conjugate

$$\Big[\vec{\hat{\mathbf{F}}}, (\hat{C}^{\dagger}_{\vec{\eta}})^n\Big] = n\vec{\eta}(\vec{x})(\hat{C}^{\dagger}_{\vec{\eta}})^{n-1}, \qquad \text{for } n \geq 1, \tag{E.10a}$$

$$\Big[(\hat{C}_{\vec{\eta}})^n, \vec{\hat{\mathbf{F}}}^{\dagger},\Big] = n\vec{\eta}^{\star}(\vec{x})(\hat{C}_{\vec{\eta}})^{n-1}, \quad \text{for } n \geq 1. \tag{E.10b}$$

It can be proved by induction by remarking that (3.84) is the base case $n = 1$, and by propagating it to $n+1$ with the commutator identity $[a, bc] = [a, b]c + b[a, c]$

$$\left[\vec{\hat{\mathbf{F}}}, (\hat{C}^\dagger_{\vec{\eta}})^{n+1}\right] = \left[\vec{\hat{\mathbf{F}}}, (\hat{C}^\dagger_{\vec{\eta}})^{n}\right] \hat{C}^\dagger_{\vec{\eta}} + (\hat{C}^\dagger_{\vec{\eta}})^{n} \left[\vec{\hat{\mathbf{F}}}, \hat{C}^\dagger_{\vec{\eta}}\right] \tag{E.11a}$$

$$= n\vec{\eta}(\vec{x})(\hat{C}^\dagger_{\vec{\eta}})^{n} + \vec{\eta}(\vec{x})(\hat{C}^\dagger_{\vec{\eta}})^{n} \tag{E.11b}$$

$$= (n+1)\vec{\eta}(\vec{x})(\hat{C}^\dagger_{\vec{\eta}})^{n}. \tag{E.11c}$$

This commutation relation can be expressed for any positive/negative helicity part of the field operator since

$$\left[\vec{\hat{\mathbf{F}}}^{(h\pm)}, (\hat{C}^\dagger_{\vec{\eta}})^{n+1}\right] = \mathbb{P}^{(h\pm)} \left[\vec{\hat{\mathbf{F}}}, (\hat{C}^\dagger_{\vec{\eta}})^{n+1}\right] = n\vec{\eta}^{(h\pm)}(\vec{x})(\hat{C}^\dagger_{\vec{\eta}})^{n-1}. \tag{E.12}$$

We compute then

$$T_1 = e^{-\langle\vec{\eta}|\vec{\eta}\rangle} \sum_{n,m} \frac{1}{n!m!} \langle\varnothing| (\hat{C}_{\vec{\eta}})^{n} \vec{\hat{\mathbf{F}}}^{(h+)\dagger} \cdot \vec{\hat{\mathbf{F}}}^{(h+)} (\hat{C}^\dagger_{\vec{\eta}})^{m} |\varnothing\rangle \tag{E.13a}$$

$$= e^{-\langle\vec{\eta}|\vec{\eta}\rangle} \sum_{n,m} \frac{1}{n!m!} \langle\varnothing| n\vec{\eta}^{(h+)\star}(\vec{x}) \cdot (\hat{C}_{\vec{\eta}})^{n-1} \vec{\hat{\mathbf{F}}}^{(h+)} (\hat{C}^\dagger_{\vec{\eta}})^{m} |\varnothing\rangle \tag{E.13b}$$

$$= e^{-\langle\vec{\eta}|\vec{\eta}\rangle} \sum_{n,m} \frac{\vec{\eta}^{(h+)\star}(\vec{x})}{(n-1)!m!} \cdot \langle\varnothing| (\hat{C}_{\vec{\eta}})^{n-1} m\vec{\eta}^{(h+)}(\vec{x}) (\hat{C}^\dagger_{\vec{\eta}})^{m-1} |\varnothing\rangle \tag{E.13c}$$

$$= e^{-\langle\vec{\eta}|\vec{\eta}\rangle} \sum_{n,m} \frac{\left|\vec{\eta}^{(h+)}(\vec{x})\right|^2}{(n-1)!(m-1)!} \langle\varnothing| (\hat{C}_{\vec{\eta}})^{n-1} (\hat{C}^\dagger_{\vec{\eta}})^{m-1} |\varnothing\rangle \tag{E.13d}$$

$$= \left|\vec{\eta}^{(h+)}(\vec{x})\right|^2 \langle \mathrm{coh}_{\vec{\eta}} | \mathrm{coh}_{\vec{\eta}} \rangle = \left|\vec{\eta}^{(h+)}(\vec{x})\right|^2, \tag{E.13e}$$

and following the same procedure we obtain the three other terms

$$T_2 = \left|\vec{\eta}^{(h-)}(\vec{x})\right|^2, \tag{E.14a}$$

$$T_3 = \vec{\eta}^{(h+)\star}(\vec{x}) \cdot \vec{\eta}^{(h-)\star}(\vec{x}) \tag{E.14b}$$

$$T_4 = \vec{\eta}^{(h-)}(\vec{x}) \cdot \vec{\eta}^{(h+)}(\vec{x}). \tag{E.14c}$$

The mean value of the energy density is then the sum of the four terms

$$\langle \hat{\mathcal{E}}_{\mathrm{em}}(\vec{x}) \rangle_{|\mathrm{coh}_{\vec{\eta}}\rangle} = \left|\vec{\eta}^{(h+)}(\vec{x})\right|^2 + \left|\vec{\eta}^{(h-)}(\vec{x})\right|^2 + \vec{\eta}^{(h+)\star}(\vec{x}) \cdot \vec{\eta}^{(h-)\star}(\vec{x}) + \vec{\eta}^{(h-)}(\vec{x}) \cdot \vec{\eta}^{(h+)}(\vec{x}). \tag{E.15}$$

To be able to analyze its localization property, we express the result in terms of the RS vector (2.43) by reminding its relation with the BB vector: $\vec{\eta}^{(h+)} = \vec{\eta}^{(h+)}_{RS}$ and $\vec{\eta}^{(h-)} = \vec{\eta}^{(h-)\star}_{RS}$. It gives for the energy density

$$\begin{aligned} \langle \hat{\mathcal{E}}_{\mathrm{em}}(\vec{x}) \rangle_{|\mathrm{coh}_{\vec{\eta}}\rangle} &= \left|\vec{\eta}^{(h+)}_{RS}(\vec{x})\right|^2 + \left|\vec{\eta}^{(h-)}_{RS}(\vec{x})\right|^2 + \vec{\eta}^{(h+)\star}_{RS}(\vec{x}) \cdot \vec{\eta}^{(h-)}_{RS}(\vec{x}) + \vec{\eta}^{(h-)\star}_{RS}(\vec{x}) \cdot \vec{\eta}^{(h+)}_{RS}(\vec{x}) \\ &= \left|\vec{\eta}_{RS}(\vec{x})\right|^2. \end{aligned} \tag{E.16}$$

F

Coupling coefficient for the single-photon spontaneous emission

To compute the spontaneously emitted photon produced by the Lyman-α transition of a Hydrogen atom, we have used in Chapter 4 the coupling function (4.8)

$$\rho(k,J,M,\lambda) = -\frac{e}{\mathfrak{m}} \langle g; \vec{\psi}^{(\lambda)}_{k,J,M} | \, \vec{\hat{p}} \cdot \vec{\hat{A}}(\vec{x}) \, | e; \varnothing \rangle \tag{F.1a}$$

$$= \left(\frac{2}{3}\right)^{7/2} \sqrt{\frac{\alpha^5}{\pi}} \mathfrak{m}c^2 \frac{1}{\sqrt{k}} \frac{k/K}{\left[1+\left(\frac{k}{K}\right)^2\right]^2} \delta_{J,1}\delta_{M,m_e} \tag{F.1b}$$

$$\equiv \rho(k)\delta_{J,1}\delta_{M,m_e}. \tag{F.1c}$$

In this appendix, we aim at deriving this coupling, i.e., computing the matrix element

$$\mathcal{M} = \langle g; \vec{\psi}^{(\lambda)}_{k,J,M} | \, \vec{\hat{p}} \cdot \vec{\hat{A}}(\vec{x}) \, | e; \varnothing \rangle \, , \tag{F.2}$$

where $|g\rangle \equiv |\varphi_g\rangle = \varphi_{n=1,l=0,m=0}(r,\vartheta,\varphi)$ and $|e\rangle \equiv |\varphi_e\rangle = \varphi_{n=2,l=1,m=0,\pm1}(r,\vartheta,\varphi)$ as introduced for the Hydrogen atom in Chapter 1.
Following the remark from Chapter 4 equations (4.6), and choosing $\vec{\psi}^{(\lambda)}_{k,J,M}$ as the basis $\vec{\phi}_\kappa$ to represent $\vec{\hat{A}}$, we have first

$$\mathcal{M} = \langle g; \vec{\psi}^{(\lambda)}_{k,J,M} | \sqrt{\frac{\hbar}{2\varepsilon_0}} \sum_\kappa \omega_\kappa^{-1/2} \vec{\phi}^\star_\kappa \cdot \, | -i\hbar\nabla\varphi_e; \vec{\phi}_\kappa \rangle \tag{F.3a}$$

$$= -i\hbar\sqrt{\frac{\hbar}{2\varepsilon_0}} \sum_\kappa \omega_\kappa^{-1/2} \langle g; \vec{\psi}^{(\lambda)}_{k,J,M} | \vec{\phi}^\star_\kappa \cdot \nabla\varphi_e; \vec{\phi}_\kappa \rangle \tag{F.3b}$$

$$= -i\hbar\sqrt{\frac{\hbar}{2\varepsilon_0}} \sum_\kappa \omega_\kappa^{-1/2} \langle \varphi_g | \vec{\phi}^\star_\kappa \cdot \nabla\varphi_e \rangle_{\text{at}} \, \langle \vec{\psi}^{(\lambda)}_{k,J,M} | \vec{\phi}_\kappa \rangle_{\text{em}} \tag{F.3c}$$

$$= -i\hbar\sqrt{\frac{\hbar}{2\varepsilon_0}} \omega_k^{-1/2} \langle \varphi_g | \vec{\psi}^{(\lambda)\star}_{k,J,M} \cdot \nabla\varphi_e \rangle_{\text{at}} \, , \tag{F.3d}$$

and now we want to compute the atomic scalar product

$$I = \langle\varphi_g|\vec{\psi}^{(\lambda)\star}_{k,J,M}\cdot\nabla\varphi_e\rangle_{\rm at} = \int_{\mathbb{R}^3} d^3x\ \varphi_g(\vec{x})\vec{\psi}^{(\lambda)\star}_{k,J,M}(\vec{x})\cdot\nabla\varphi_e(\vec{x}) \tag{F.4a}$$

$$= \sum_{j=1}^{3}\int_{\mathbb{R}^3} d^3x\ \varphi_g(\vec{x})\psi^{(\lambda)(j)\star}_{k,J,M}(\vec{x})\frac{\partial\varphi_e(\vec{x})}{\partial x_j} = -\sum_{j=1}^{3}\int_{\mathbb{R}^3} d^3x\frac{\partial}{\partial x_j}\left(\varphi_g\psi^{(\lambda)(j)\star}_{k,J,M}\right)\varphi_e(\vec{x}) \tag{F.4b}$$

$$= -\sum_{j=1}^{3}\int_{\mathbb{R}^3} d^3x\left(\frac{\partial\varphi_g}{\partial x_j}\psi^{(\lambda)(j)\star}_{k,J,M} + \varphi_g\frac{\partial\psi^{(\lambda)(j)\star}_{k,J,M}}{\partial x_j}\right)\varphi_e(\vec{x}) \tag{F.4c}$$

$$= -\int_{\mathbb{R}^3} d^3x\left(\nabla(\varphi_g)\cdot\vec{\psi}^{(\lambda)\star}_{k,J,M} + \varphi_g\nabla\cdot\vec{\psi}^{(\lambda)\star}_{k,J,M}\right)\varphi_e(\vec{x}) = -\int_{\mathbb{R}^3} d^3x\nabla(\varphi_g)\cdot\vec{\psi}^{(\lambda)\star}_{k,J,M}\varphi_e(\vec{x}), \tag{F.4d}$$

where we have performed an integration by part in (F.4b) and used the transversality of the helicity vector harmonics in (F.4d). To go further into the calculation, we use the identity $\nabla f(r) = df/dr\ \vec{n}$ where $\vec{n} = \vec{x}/r$ to compute

$$\nabla\varphi_g = \frac{d\varphi_g}{dr}\vec{n} = -\frac{1}{r_{\rm B}}\varphi_g\vec{n}, \tag{F.5}$$

and thus

$$\nabla\varphi_g\cdot\vec{\psi}^{(\lambda)\star}_{k,J,M} = -\frac{1}{r_{\rm B}}\varphi_g\vec{n}\cdot\vec{\psi}^{(\lambda)\star}_{k,J,M} \tag{F.6a}$$

$$= \frac{i}{\sqrt{\pi}r_{\rm B}}\frac{\sqrt{J(J+1)}}{2J+1}k\Big(j_{J-1}(kr) + j_{J+1}(kr)\Big)\varphi_g(r)Y^{\star}_{J,M}(\vartheta,\varphi), \tag{F.6b}$$

where we have used the relations [74, p.219]

$$\vec{n}\cdot\vec{Y}^{J}_{J,M} = 0, \quad \vec{n}\cdot\vec{Y}^{J+1}_{J,M} = -\sqrt{\frac{J+1}{2J+1}}Y_{J,M}, \quad \vec{n}\cdot\vec{Y}^{J-1}_{J,M} = \sqrt{\frac{J}{2J+1}}Y_{J,M}. \tag{F.7}$$

The integral I becomes then

$$I = \frac{-ik}{\sqrt{\pi}r_{\rm B}}\frac{\sqrt{J(J+1)}}{2J+1}\int_{\mathbb{R}^3} d^3x\ \varphi_g(\vec{x})\varphi_e(\vec{x})\Big(j_{J-1}(kr) + j_{J+1}(kr)\Big)Y^{\star}_{J,M}(\vartheta,\varphi), \tag{F.8}$$

which can be simplified by expressing the product $\varphi_g\varphi_e$ for the different values $m_e = 0, \pm 1$:

$$\varphi_g(\vec{x})\varphi_e(\vec{x}) \equiv \varphi_{n=1,l=0,m=0}(r,\vartheta,\varphi)\varphi_{n=2,l=1,m=m_e}(r,\vartheta,\varphi) \tag{F.9a}$$

$$= \frac{1}{\sqrt{24\pi}}\frac{r}{r_{\rm B}^4}e^{-\frac{3r}{2r_{\rm B}}}Y_{1,m_e}(\vartheta,\varphi) \tag{F.9b}$$

$$= R_{2,1}(r)Y_{1,m_e}(\vartheta,\varphi), \tag{F.9c}$$

where we have used the expression of the spherical harmonics

$$Y_{1,0}(\vartheta,\varphi) = \sqrt{\frac{3}{4\pi}}\cos\vartheta, \quad Y_{1,\pm1}(\vartheta,\varphi) = \mp\sqrt{\frac{3}{8\pi}}\sin\vartheta e^{\pm i\varphi}. \tag{F.10}$$

Radial and angular parts of I are independent and we arrive at

$$I = \frac{-ik}{\sqrt{\pi} r_{\mathrm{B}}} \frac{\sqrt{J(J+1)}}{2J+1} \int_0^\infty dr\ r^2 R_{2,1}(r) \Big(j_{J-1}(kr) + j_{J+1}(kr) \Big) \times \int_0^\pi d\vartheta \sin\vartheta \int_0^{2\pi} d\varphi\ Y^\star_{J,M} Y_{1,m_e} \tag{F.11a}$$

$$= \frac{-ik}{\sqrt{\pi} r_{\mathrm{B}}} \frac{\sqrt{2}}{3} \int_0^\infty dr\ r^2 R_{2,1}(r) \Big(j_0(kr) + j_2(kr) \Big) \delta_{J,1} \delta_{M,m_e} \tag{F.11b}$$

$$= \frac{-ik}{\sqrt{\pi} r_{\mathrm{B}}} \frac{\sqrt{2}}{3} \delta_{J,1} \delta_{M,m_e} I_r(k). \tag{F.11c}$$

It remains thus only the radial integral $I_r(k)$ which we compute using the spherical Bessel functions of the form

$$j_0(kr) = \frac{\sin(kr)}{kr}, \quad j_2(kr) = \left(\frac{3}{(kr)^2} - 1 \right) \frac{\sin(kr)}{kr} - 3 \frac{\cos(kr)}{(kr)^2}, \tag{F.12}$$

and thus

$$I_r(k) = \frac{1}{\sqrt{24\pi}} \int_0^\infty dr\ \frac{r^3}{r_{\mathrm{B}}^4} \left(3 \frac{\sin(kr)}{(kr)^3} - 3 \frac{\cos(kr)}{(kr)^2} \right) e^{-\frac{3r}{2r_{\mathrm{B}}}} \tag{F.13a}$$

$$= \frac{3}{\sqrt{24\pi} r_{\mathrm{B}}^4} \int_0^\infty dr \left(\frac{\sin(kr)}{k^3} - r \frac{\cos(kr)}{k^2} \right) e^{-\frac{3r}{2r_{\mathrm{B}}}} \tag{F.13b}$$

$$= I_{r,s} + I_{r,c}. \tag{F.13c}$$

We compute now the two terms and for simplicity we introduce the notation $K = 3/2r_{\mathrm{B}}$:

$$I_{r,s} = \frac{3}{\sqrt{24\pi} r_{\mathrm{B}}^4} \frac{1}{k^3} \int_0^\infty dr\ \sin(kr) e^{-Kr} \tag{F.14a}$$

$$= \frac{3}{2i\sqrt{24\pi} r_{\mathrm{B}}^4} \frac{1}{k^3} \left[\frac{e^{(ik-K)r}}{ik-K} + \frac{e^{-(ik+K)r}}{ik+K} \right]_0^\infty \tag{F.14b}$$

$$= \frac{3}{2i\sqrt{24\pi} r_{\mathrm{B}}^4} \frac{1}{k^3} \left(\frac{-1}{ik-K} - \frac{1}{ik+K} \right) = \frac{3}{\sqrt{24\pi} r_{\mathrm{B}}^4} \frac{1}{k^2} \frac{1}{k^2+K^2}, \tag{F.14c}$$

and

$$I_{r,c} = -\frac{3}{\sqrt{24\pi} r_{\mathrm{B}}^4} \frac{1}{k^2} \int_0^\infty dr\ r \cos(kr) e^{-Kr} \tag{F.15a}$$

$$= \frac{3}{2\sqrt{24\pi} r_{\mathrm{B}}^4} \frac{1}{k^2} \left[\frac{e^{(ik-K)r}}{(ik-K)^2} + \frac{e^{(ik+K)r}}{(ik+K)^2} \right]_0^\infty \tag{F.15b}$$

$$= \frac{3}{2\sqrt{24\pi} r_{\mathrm{B}}^4} \frac{1}{k^2} \left(\frac{-1}{(ik-K)^2} - \frac{1}{(ik+K)^2} \right) = \frac{3}{\sqrt{24\pi} r_{\mathrm{B}}^4} \frac{1}{k^2} \frac{k^2-K^2}{(k^2+K^2)^2}, \tag{F.15c}$$

which allow to calculate

$$I_r(k) = \frac{3}{\sqrt{24\pi} r_{\mathrm{B}}^4} \frac{2}{(k^2+K^2)^2} = \frac{6}{K^4 \sqrt{24\pi} r_{\mathrm{B}}^4} \frac{1}{\left[1 + \left(\frac{k}{K}\right)\right]^2} = \left(\frac{2}{3} \right)^4 \frac{3}{\sqrt{6\pi}} \frac{1}{\left[1 + \left(\frac{k}{K}\right)\right]^2}. \tag{F.16}$$

We finally gather all the results to express the coupling function $\rho(k, J, M, \lambda)$ as

$$\rho(k, J, M, \lambda) = -\frac{e}{\mathfrak{m}}\mathcal{M} = i\sqrt{\frac{\hbar^3 e^2}{2\varepsilon_0 \mathfrak{m}^2 \omega_k}} I = \sqrt{\frac{\hbar^3 e^2}{\pi\varepsilon_0 \mathfrak{m}^2 \omega_k}} \frac{k}{3r_\mathrm{B}} \delta_{J,1}\delta_{M,m_e} I_r(k) \tag{F.17a}$$

$$= \left(\frac{2}{3}\right)^{7/2} \sqrt{\frac{\alpha^5}{\pi}} \mathfrak{m}c^2 \frac{1}{\sqrt{k}} \frac{k/K}{\left[1 + \left(\frac{k}{K}\right)^2\right]^2} \delta_{J,1}\delta_{M,m_e}, \tag{F.17b}$$

where we have used the relations

$$\alpha = \frac{e^2}{4\pi\varepsilon_0 \hbar c}, \quad r_\mathrm{B} = \frac{\hbar}{\alpha \mathfrak{m} c}, \tag{F.18}$$

to reach the final result.

G

Solution of the Friedrichs model

The aim of this appendix is to obtain the solution of the Friedrichs model we have used in Section 4.1.2. We will mostly reproduce and demonstrate results from [136, Section 17.3]. We start thus with the Hamiltonian from (4.20) written as

$$\hat{H} = \begin{pmatrix} \omega_{\mathrm{a}} & \langle\tilde{\rho}|\cdot\rangle \\ \tilde{\rho} & \omega_k \end{pmatrix}, \tag{G.1}$$

where $\hbar\omega_{\mathrm{a}}$ is the energy of the excited state, $\omega_k > 0$ is the continuous spectrum, $\tilde{\rho} \in L^2$ is the real coupling function and $\langle\tilde{\rho}|f\rangle = \int_0^\infty d\omega\tilde{\rho}^\star(\omega)f(\omega)$. Our goal, is to look for a solution of the Schrödinger-like equation

$$i\frac{\partial}{\partial t}|\psi\rangle = \hat{H}|\psi\rangle, \tag{G.2}$$

where $|\psi\rangle = \begin{pmatrix} u & v(\omega_k) \end{pmatrix}^T$, i.e., a solution of the system

$$i\frac{\partial u}{\partial t} = \omega_{\mathrm{a}} + \langle\tilde{\rho}|v\rangle, \tag{G.3a}$$

$$i\frac{\partial v(\omega_k)}{\partial t} = \tilde{\rho}(\omega_k)u + \omega_k v(\omega_k), \tag{G.3b}$$

with an initial state $|\psi_0\rangle = \begin{pmatrix} 1 & 0 \end{pmatrix}^T$ to analyze the spontaneous emission. In this situation, we remark that the second equation can be integrated formally as a function of $u(t)$

$$v(\omega_k, t) = -ie^{-i\omega_k t}\tilde{\rho}(\omega_k)\int_0^t dt' e^{i\omega_k t'}u(t'), \tag{G.4}$$

meaning that the problem is reduced to finding $u(t)$. To do so, we consider a basis set $\{|\psi_\nu\rangle\}$ of eigenfunctions of $\hat{H}$, i.e., $\hat{H}|\psi_\nu\rangle = \nu|\psi_\nu\rangle$, with $\nu \in [0, \infty)$ which we will use to compute $u(t)$ expressed as

$$u(t) = \langle\psi_0| e^{-i\hat{H}t}|\psi_0\rangle. \tag{G.5}$$

We rewrite this equation using the spectral decomposition of $\hat{H}$ and $|\psi_0\rangle$

$$\hat{H} = \int_0^\infty d\nu \ \nu \, |\psi_\nu\rangle \langle\psi_\nu| \,, \tag{G.6a}$$

$$|\psi_0\rangle = \int_0^\infty d\nu \ \ |\psi_\nu\rangle \langle\psi_\nu|\psi_0\rangle \,, \tag{G.6b}$$

and obtain

$$u(t) = \int_0^\infty d\nu |\langle\psi_0|\psi_\nu\rangle|^2 e^{-i\nu t} = \int_0^\infty d\nu \ g(\nu) e^{-i\nu t}. \tag{G.7}$$

We propose now to compute the function $g(\nu)$ using the resolvent operator $\hat{R}(z) = (z - \hat{H})^{-1}$, $z \in \mathbb{C}$, which can be written using the continuous eigenstates as

$$\hat{R}(z) = \int_0^\infty d\nu' \frac{1}{z - \nu'} \, |\psi_{\nu'}\rangle \langle\psi_{\nu'}| \,. \tag{G.8}$$

By taking the limit of zero imaginary part of $z = \nu + i\epsilon$, and using the identity [64, Chapter 8]

$$\frac{1}{\nu - \nu' \pm i0^+} = \mathrm{pv}\left(\frac{1}{\nu - \nu'}\right) \mp i\pi\delta(\nu - \nu'), \tag{G.9}$$

where ν is the pole and ν' the integrated variable, we arrive at

$$\hat{R}(\nu \pm i0^+) = \int_0^\infty d\nu' \frac{1}{\nu - \nu' \pm i0^+} \, |\psi_{\nu'}\rangle \langle\psi_{\nu'}| \tag{G.10a}$$

$$= \int_0^\infty d\nu' \left[\mathrm{pv}\left(\frac{1}{\nu - \nu'}\right) \mp i\pi\delta(\nu - \nu')\right] |\psi_{\nu'}\rangle \langle\psi_{\nu'}| \,, \tag{G.10b}$$

and then

$$\hat{R}(\nu + i0^+) - \hat{R}(\nu - i0^+) = -2i\pi \, |\psi_\nu\rangle \langle\psi_\nu| \,. \tag{G.11}$$

One can apply the resolvent operator on the initial state, yielding a state $|\eta\rangle$

$$|\eta\rangle = (z - \hat{H})^{-1} \, |\psi_0\rangle \,, \tag{G.12}$$

which can be written as

$$|\eta\rangle = \begin{pmatrix} a \\ b(\omega_k) \end{pmatrix}. \tag{G.13}$$

By inverting the definition of $|\eta\rangle$, one obtains

$$|\psi_0\rangle = (z - \hat{H}) \, |\eta\rangle = \begin{pmatrix} z - \omega_\mathrm{a} & -\langle\tilde{\rho}|\cdot\rangle \\ -\tilde{\rho}(\omega_k) & z - \omega_k \end{pmatrix} \begin{pmatrix} a \\ b(\omega_k) \end{pmatrix} = \begin{pmatrix} 1 \\ 0 \end{pmatrix}, \tag{G.14}$$

from which a and $b(\omega_k)$ can be expressed as

$$b(\omega_k) = \frac{\tilde{\rho}(\omega_k)}{z - \omega_k} a, \tag{G.15a}$$

$$a = \left[z - \omega_\mathrm{a} - \langle\tilde{\rho}| \frac{\tilde{\rho}}{z - \omega_k} \rangle\right]^{-1} = \langle\psi_0| \, \hat{R}(z) \, |\psi_0\rangle \equiv R_0(z). \tag{G.15b}$$

Using the decomposition of the resolvent (G.8), one can then write

$$R_0(z) = \langle\psi_0|\,\hat{R}(z)\,|\psi_0\rangle \tag{G.16a}$$

$$= \int_0^\infty d\nu' \frac{1}{z-\nu'} |\langle\psi_0|\psi_{\nu'}\rangle|^{\,2} = \int_0^\infty d\nu' \frac{g(\nu')}{z-\nu'}, \tag{G.16b}$$

from which we can express $g(\nu)$ by using (G.11)

$$g(\nu) = -\frac{1}{2i\pi}\left(R_0(\nu+i0^+) - R_0(\nu-i0^+)\right). \tag{G.17}$$

To compute $g(\nu)$ we need thus to combine the results from (G.15b) and (G.17). As an intermediary step, we express the scalar product from (G.15b) as

$$\langle\tilde{\rho}|\frac{\tilde{\rho}}{\nu-\omega_k\pm i0^+}\rangle = \int_0^\infty d\omega_k \frac{|\tilde{\rho}(\omega_k)|^2}{\nu-\omega_k\pm i0^+} \tag{G.18a}$$

$$= \int_0^\infty d\omega_k |\tilde{\rho}(\omega_k)|^2 \left[\mathrm{pv}\left(\frac{1}{\nu-\omega_k}\right) \mp i\pi\delta(\nu-\omega_k)\right] \tag{G.18b}$$

$$= \mathrm{pv}\int_0^\infty d\omega_k \frac{|\tilde{\rho}(\omega_k)|^2}{\nu-\omega_k} \mp i\pi|\tilde{\rho}(\nu)|^2 \tag{G.18c}$$

$$= \Delta(\nu) \mp i\frac{\Gamma(\nu)}{2}, \tag{G.18d}$$

where

$$\Delta(\nu) = \mathrm{pv}\int_0^\infty d\omega_k \frac{|\tilde{\rho}(\omega_k)|^2}{\nu-\omega_k}, \tag{G.19a}$$

$$\Gamma(\nu) = 2\pi|\tilde{\rho}(\nu)|^2. \tag{G.19b}$$

By combining (G.15b), (G.17) and (G.18), we compute $g(\nu)$ as

$$g(\nu) = -\frac{1}{2i\pi}\left[\frac{1}{\nu-\omega_\mathrm{a}+i0^+-\Delta(\nu)+i\frac{\Gamma(\nu)}{2}} - \frac{1}{\nu-\omega_\mathrm{a}-i0^+-\Delta(\nu)-i\frac{\Gamma(\nu)}{2}}\right] \tag{G.20a}$$

$$= -\frac{1}{2i\pi}\frac{-2i0^+ - i\Gamma(\nu)}{(\nu-\omega_\mathrm{a}-\Delta(\nu)+i(0^+ + \frac{\Gamma(\nu)}{2}))(\nu-\omega_\mathrm{a}-\Delta(\nu)-i(0^+ + \frac{\Gamma(\nu)}{2}))} \tag{G.20b}$$

$$= \frac{1}{2\pi}\frac{\Gamma(\nu)}{(\nu-\omega_\mathrm{a}-\Delta(\nu))^2 + \frac{\Gamma(\nu)^2}{4}}, \tag{G.20c}$$

where every term involving 0^+ vanishes by applying the limit.

H

Asymptotic behavior of the radial integrals for spontaneous emission

In this appendix, we want to compute the asymptotic behavior of the radial integrals that appear in the calculation of the energy density of a spontaneously emitted photon from the Lyman-α transition of a Hydrogen atom. The integrals have the following forms

$$F_0(r,t) = \left(\frac{2}{3}\right)^3 \sqrt{\frac{\alpha^5}{c}} \frac{\mathfrak{m}c^2}{\pi\hbar r_\mathrm{B}} \int_0^\infty dq \frac{e^{-iqp} - e^{-i(\Omega_\mathrm{a} - i\tilde{\Gamma}_\mathrm{a})t}}{A + i(B-q)} \frac{q^2}{(1+q^2)^2} j_0(qr'), \tag{H.1a}$$

$$F_1(r,t) = -i\lambda \left(\frac{2}{3}\right)^{5/2} \sqrt{\frac{\alpha^5}{c}} \frac{\mathfrak{m}c^2}{\pi\hbar r_\mathrm{B}} \int_0^\infty dq \frac{e^{-iqp} - e^{-i(\Omega_\mathrm{a} - i\tilde{\Gamma}_\mathrm{a})t}}{A + i(B-q)} \frac{q^2}{(1+q^2)^2} j_1(qr'), \tag{H.1b}$$

$$F_2(r,t) = -\left(\frac{2}{3}\right)^3 \sqrt{\frac{\alpha^5}{2c}} \frac{\mathfrak{m}c^2}{\pi\hbar r_\mathrm{B}} \int_0^\infty dq \frac{e^{-iqp} - e^{-i(\Omega_\mathrm{a} - i\tilde{\Gamma}_\mathrm{a})t}}{A + i(B-q)} \frac{q^2}{(1+q^2)^2} \left(\frac{3}{qr'} j_1(qr') - j_0(qr')\right), \tag{H.1c}$$

where

$$A = \frac{\tilde{\Gamma}_\mathrm{a}}{cK} = \frac{\Gamma_\mathrm{a}}{2cK}, \quad B = \frac{\Omega_\mathrm{a}}{cK} = \frac{\omega_\mathrm{a} + \Delta_\mathrm{a}}{cK}, \tag{H.2a}$$

$$q = \frac{k}{K}, \quad p = cKt, \quad r' = Kr. \tag{H.2b}$$

To obtain the asymptotic behavior of the F_L integrals, and due to the expression of the spherical Bessel functions

$$j_0(qr') = \frac{\sin(qr')}{qr'}, \quad j_1(qr') = \frac{\sin(qr')}{q^2 r'^2} - \frac{\cos(qr')}{qr'}, \tag{H.3}$$

one needs to analyze integrals of the form

$$\int_0^\infty dq R(q) \sin\big(qr'\big), \quad \int_0^\infty dq R(q) \cos\big(qr'\big). \tag{H.4}$$

Here, $R(q)$ is a function with the properties that for some $N_s \geq 0$ even or $N_c \geq 0$ odd,

$$\left.\frac{d^n R(q)}{dq^n}\right|_{q=0} = \begin{cases} 0 & \text{for } n < N_{c,s},\ n \text{ same parity as } N_{c,s}, \\ \text{cst} \neq 0 & \text{for } n = N_{c,s},\ n \text{ same parity as } N_{c,s}, \end{cases} \tag{H.5a}$$

$$\lim_{q\to\infty} \frac{d^n R(q)}{dq^n} = 0, \tag{H.5b}$$

and

$$\int_0^\infty dq \left|\frac{d^n R(q)}{dq^n}\right| < \infty, \quad \text{for all } n < N_{c,s}. \tag{H.6}$$

The indices c, s, are needed to treat the cosine and sine integrals in (H.4), respectively. Using these properties and some integrations by parts the sine integral becomes

$$\int_0^\infty dq R(q)\sin(qr') = -\frac{1}{r'}\left[R(q)\cos(qr')\right]_0^\infty + \frac{1}{r'}\int_0^\infty dq \frac{dR(q)}{dq}\cos(qr') \tag{H.7a}$$

$$= \frac{1}{r'}R(0) - \frac{1}{r'}\int_0^\infty dq \frac{dR(q)}{dq}\cos(qr') \tag{H.7b}$$

$$= \frac{1}{r'}R(0) + o\left(\frac{1}{r'}\right). \tag{H.7c}$$

The last equality is obtained by the Riemann-Lebesgue lemma [64] which states that

$$\left|\int_0^\infty dq \frac{dR(q)}{dq}\cos(qr')\right| \underset{r'\to+\infty}{\longrightarrow} 0, \tag{H.8}$$

if $\int_0^\infty dq\left|\frac{dR(q)}{dq}\right| < \infty$, which is true according to (H.6). Therefore, the first term of (H.7c) gives the asymptotics for large r' if $N_s = 0$, otherwise, one has to iterate the integration by parts as

$$\int_0^\infty dq R(q)\sin(qr') = \frac{1}{r'^2}\left[\frac{dR}{dq}\sin(qr')\right]_0^\infty - \frac{1}{r'^2}\int_0^\infty dq \frac{d^2R(q)}{dq^2}\sin(qr') \tag{H.9a}$$

$$= -\frac{1}{r'^2}\int_0^\infty dq \frac{d^2R(q)}{dq^2}\sin(qr') \tag{H.9b}$$

$$= \frac{1}{r'^3}\left[\frac{d^2R}{dq^2}\cos(qr')\right]_0^\infty + \frac{1}{r'^3}\int_0^\infty dq \frac{d^3R(q)}{dq^3}\cos(qr') \tag{H.9c}$$

$$= \frac{1}{r'^3}\left.\frac{d^2R}{dq^2}\right|_{q=0} + \frac{1}{r'^3}\int_0^\infty dq \frac{d^3R(q)}{dq^3}\cos(qr') \tag{H.9d}$$

$$= \frac{1}{r'^3}\left.\frac{d^2R}{dq^2}\right|_{q=0} + o\left(\frac{1}{r'^3}\right), \tag{H.9e}$$

and again, the first term gives the asymptotics by the Riemann-Lebesgue lemma if $N_s = 2$. Otherwise, the same process can be continued until one reaches N_s. A similar process can be done for the cosine integral and gives after one step

$$\int_0^\infty dq R(q)\cos(qr') = -\frac{1}{r'^2}\left.\frac{dR}{dq}\right|_{q=0} + \frac{1}{r'^2}\int_0^\infty dq \frac{d^2R(q)}{dq^2}\cos(qr') \tag{H.10a}$$

$$= -\frac{1}{r'^2}\left.\frac{dR}{dq}\right|_{q=0} + o\left(\frac{1}{r'^2}\right), \tag{H.10b}$$

by the Riemann-Lebesgue lemma. This step is enough if $N_c = 1$ but others can be performed if not.
To apply this technique, we now need the concrete form of the functions $R(q)$ and thus we rewrite the F_L integrals as

$$F_0 = \left(\frac{2}{3}\right)^3 \sqrt{\frac{\alpha^5}{c}} \frac{\mathfrak{m}c^2}{\pi\hbar r_\mathrm{B}} \frac{1}{r'} \int_0^\infty dq \left(R_+^{(1)}(q) + R_-^{(1)}(q)\right) \sin\big(qr'\big), \tag{H.11a}$$

$$F_1 = -i\lambda \left(\frac{2}{3}\right)^{5/2} \sqrt{\frac{\alpha^5}{c}} \frac{\mathfrak{m}c^2}{\pi\hbar r_\mathrm{B}} \left\{ \frac{1}{r'^2} \int_0^\infty dq \left(R_+^{(0)}(q) + R_-^{(0)}(q)\right) \sin\big(qr'\big) - \frac{1}{r'} \int_0^\infty dq \left(R_+^{(1)}(q) + R_-^{(1)}(q)\right) \cos\big(qr'\big) \right\}, \tag{H.11b}$$

where the R functions are

$$R_+^{(1)}(q) = \frac{e^{-iqp}}{A + i(B-q)} \frac{q}{(1+q^2)^2}, \qquad R_-^{(1)}(q) = -\frac{e^{-i(\Omega_\mathrm{a} - i\tilde{\Gamma}_\mathrm{a})t}}{A + i(B-q)} \frac{q}{(1+q^2)^2}, \tag{H.12a}$$

$$R_+^{(0)}(q) = \frac{e^{-iqp}}{A + i(B-q)} \frac{1}{(1+q^2)^2}, \qquad R_-^{(0)}(q) = -\frac{e^{-i(\Omega_\mathrm{a} - i\tilde{\Gamma}_\mathrm{a})t}}{A + i(B-q)} \frac{1}{(1+q^2)^2}. \tag{H.12b}$$

The integral F_2 can be deduced rapidly from the other two as we will discuss later. The asymptotics for F_0 and F_1 can be computed using the iterative process and we obtain

$$F_0(r,t) \underset{r'\to\infty}{\sim} \left(\frac{2}{3}\right)^3 \sqrt{\frac{\alpha^5}{c}} \frac{\mathfrak{m}c^2}{\pi\hbar r_\mathrm{B}} \frac{1}{r'^4} \left(\left.\frac{d^2 R_+^{(1)}}{dq^2}\right|_{q=0} + \left.\frac{d^2 R_-^{(1)}}{dq^2}\right|_{q=0} \right), \tag{H.13a}$$

$$F_1(r,t) \underset{r'\to\infty}{\sim} -i\lambda \left(\frac{2}{3}\right)^{5/2} \sqrt{\frac{\alpha^5}{c}} \frac{\mathfrak{m}c^2}{\pi\hbar r_\mathrm{B}} \frac{1}{r'^3} \left(R_+^{(0)}(0) + R_-^{(0)}(0) + \left.\frac{d^2 R_+^{(1)}}{dq^2}\right|_{q=0} + \left.\frac{d^2 R_-^{(1)}}{dq^2}\right|_{q=0} \right), \tag{H.13b}$$

which can be further simplified using

$$R_+^{(0)}(q=0) = \frac{1}{A+iB}, \qquad R_-^{(0)}(q=0) = -\frac{e^{-i(\Omega_\mathrm{a} - i\tilde{\Gamma}_\mathrm{a})t}}{A+iB}, \tag{H.14a}$$

$$\left.\frac{d^2 R_+^{(1)}}{dq^2}\right|_{q=0} = \frac{i}{(A+iB)^2} - \frac{ip}{A+iB}, \qquad \left.\frac{d^2 R_-^{(1)}}{dq^2}\right|_{q=0} = -i\frac{e^{-i(\Omega_\mathrm{a} - i\tilde{\Gamma}_\mathrm{a})t}}{(A+iB)^2}. \tag{H.14b}$$

Since $F_0 \sim F_1/r'$, we compute only F_1 which will dominate for large r'. We obtain then the result used in Section 4.1.3 by inserting (H.14) in (H.13b)

$$F_1(r',t) \underset{r'\to\infty}{\sim} -i\lambda \left(\frac{2}{3}\right)^{5/2} \sqrt{\frac{\alpha^5}{c}} \frac{\mathfrak{m}c^2}{\pi\hbar r_\mathrm{B}} \mathcal{T}(t) \frac{1}{r'^3}, \tag{H.15}$$

where the dimensionless function of time reads

$$\mathcal{T}(t) = \frac{1}{A+iB} \left(1 - e^{-i(\Omega_\mathrm{a} - i\tilde{\Gamma}_\mathrm{a})t} - 2icKt + i\frac{1 - e^{-i(\Omega_\mathrm{a} - i\tilde{\Gamma}_\mathrm{a})t}}{A+iB} \right). \tag{H.16}$$

Regarding F_2 we recall its expression

$$F_2(r,t) = -\left(\frac{2}{3}\right)^3 \sqrt{\frac{\alpha^5}{2c}} \frac{\mathfrak{m}c^2}{\pi\hbar r_{\mathrm{B}}} \int_0^\infty dq \frac{e^{-iqp} - e^{-i(\Omega_{\mathrm{a}} - i\tilde{\Gamma}_{\mathrm{a}})t}}{A + i(B-q)} \frac{q^2}{(1+q^2)^2} \left(\frac{3}{qr'} j_1(qr') - j_0(qr')\right), \tag{H.17}$$

from which we see that the term involving j_0 will behave as F_0 and can thus be neglected. For the term involving j_1, one has to be more cautious since it does not have the same form as what we had for F_1. It yields

$$F_2(r',t) \underset{r'\to\infty}{\sim} -\left(\frac{2}{3}\right)^2 \sqrt{\frac{2\alpha^5}{c}} \frac{\mathfrak{m}c^2}{\pi\hbar r_{\mathrm{B}}} \frac{1}{r'} \int_0^\infty dq \frac{e^{-iqp} - e^{-i(\Omega_{\mathrm{a}} - i\tilde{\Gamma}_{\mathrm{a}})t}}{A + i(B-q)} \frac{q}{(1+q^2)^2} j_1(qr') \tag{H.18a}$$

$$= -\left(\frac{2}{3}\right)^2 \sqrt{\frac{2\alpha^5}{c}} \frac{\mathfrak{m}c^2}{\pi\hbar r_{\mathrm{B}}} \left\{ \frac{1}{r'^3} \int_0^\infty dq \frac{e^{-iqp} - e^{-i(\Omega_{\mathrm{a}} - i\tilde{\Gamma}_{\mathrm{a}})t}}{A + i(B-q)} \frac{1}{q\,(1+q^2)^2} \sin\!\big(qr'\big) \right.$$

$$\left. -\frac{1}{r'^2} \int_0^\infty dq \frac{e^{-iqp} - e^{-i(\Omega_{\mathrm{a}} - i\tilde{\Gamma}_{\mathrm{a}})t}}{A + i(B-q)} \frac{1}{(1+q^2)^2} \cos\!\big(qr'\big) \right\}, \tag{H.18b}$$

from which one can already see that F_2 will decrease faster than F_1. Indeed, the first term scales like $1/r'^3$ before making the iterative process to analyze the integral. Moreover, the function of q to integrate does not yield a constant when $q \to 0$ meaning that the iterative process must be done more than one time. Thus, this term will decrease faster than $1/r'^3$ and can be neglected. The second term involves a cosine for which the first iterative step (H.10) already scales as $1/r'^2$, so that the full term would scale like $1/r'^4$, decreasing faster than F_1.

Bibliography

[1] M. Federico, V. Dorier, S. Guérin, and H. R. Jauslin. Space-time propagation of photon pulses in dielectric media, illustrations with beam splitters. *Journal of Physics B: Atomic, Molecular and Optical Physics*, 55(17):174002, 2022. (pages 1, 2, 47).

[2] M. Federico and H. R. Jauslin. Isomorphism between the Białynicki-Birula and the Landau-Peierls Fock space quantization of the electromagnetic field in position representation. *Journal of Physics A: Mathematical and Theoretical*, 56(23):235302, 2023. (pages 1, 27).

[3] M. Federico and H. R. Jauslin. Nonlocality of the energy density for all single-photon states. *Physical Review A*, 108(4):043720, 2023. (pages 1, 47).

[4] M. Federico and H. R. Jauslin. Nonlocality of the energy density of a spontaneously emitted single-photon from a hydrogen atom. *arXiv:2403.13622v1*, 2024. (pages 1, 79).

[5] B. W. Shore. *Our Changing Views of Photons: A Tutorial Memoir*. Oxford University Press, 2020. (page 1).

[6] M. Planck. Zur theorie des gesetzes der energieverteilung im normalspektrum. *Verhandlungen der Deutschen Physikalischen Gesellschaft*, 2:237–245, 1900. (page 1).

[7] A. Einstein. Über einen die erzeugung und verwandlung des lichtes betreffenden heuristischen gesichtspunkt. *Annalen der physik*, 322(6):132–148, 1905. (page 1).

[8] A. Einstein. Die Plancksche theorie der strahlung und die theorie der spezifischen wärme. *Annalen der Physik*, 327(1):180–190, 1907. (page 1).

[9] P. A. M. Dirac. *The Principles of Quantum Mechanics*. Clarendon Press, Oxford, 4th edition edition, 1989. (page 1).

[10] J. F. Clauser. Experimental limitations to the validity of semiclassical radiation theories. *Physical Review A*, 6(1):49–54, 1972. (page 1).

[11] J. F. Clauser. Experimental distinction between the quantum and classical field-theoretic predictions for the photoelectric effect. *Physical Review D*, 9(4):853–860, 1974. (page 1).

[12] P. Grangier, G. Roger, and A. Aspect. Experimental evidence for a photon anti-correlation effect on a beam splitter: A new light on single-photon interferences. *Europhysics Letters (EPL)*, 1(4):173–179, 1986. (page 1).

[13] R. Ghosh and L. Mandel. Observation of nonclassical effects in the interference of two photons. *Physical Review Letters*, 59(17):1903–1905, 1987. (page 1).

[14] R. J. Glauber and M. Lewenstein. Quantum optics of dielectric media. *Physical Review A*, 43(1):467–491, 1991. (pages 2, 48).

[15] L. Landau and R. Peierls. Quantenelectrodynamik im konfigurationsraum. *Zeitschrift für Physik*, 62:188–198, 1930. (pages 2, 31).

[16] T. D. Newton and E. P. Wigner. Localized states for elementary systems. *Reviews of Modern Physics*, 21(3):400–406, 1949. (page 2).

[17] L. Mandel. Configuration-space photon number operators in quantum optics. *Physical Review*, 144(4):1071–1077, 1966. (page 2).

[18] R. J. Cook. Photon dynamics. *Physical Review A*, 25(4):2164–2167, 1982. (pages 2, 31).

[19] R. J. Cook. Lorentz covariance of photon dynamics. *Physical Review A*, 26(5):2754–2760, 1982. (pages 2, 31).

[20] J. E. Sipe. Photon wave functions. *Physical Review A*, 52(3):1875–1883, 1995. (pages 2, 40).

[21] I. Białynicki-Birula. Photon wave function. In E. Wolf, editor, *Progress in Optics*. Elsevier, 1996. (pages 2, 3, 36, 38, 39, 39, 39, 40, 40, 42, 45, 116).

[22] M. Hawton. Photon wave functions in a localized coordinate space basis. *Physical Review A*, 59(5):3223–3227, 1999. (page 2).

[23] O. Keller. On the theory of spatial localization of photons. *Physics Reports*, 411(1-3):1–232, 2005. (pages 2, 40, 77).

[24] B. J. Smith and M. G. Raymer. Photon wave functions, wave-packet quantization of light, and coherence theory. *New Journal of Physics*, 9(11):414–414, 2007. (pages 2, 40, 109).

[25] I. Białynicki-Birula and Z. Białynicka-Birula. The role of the Riemann-Silberstein vector in classical and quantum theories of electromagnetism. *Journal of Physics A: Mathematical and Theoretical*, 46(5):053001, 2013. (pages 2, 3, 36, 39, 40, 42).

[26] O. Keller. *Light: The Physics of the Photon*. Taylor & Francis, 2014. (pages 2, 40).

[27] M. K. H. Kiessling and A. S. Tahvildar-Zadeh. On the quantum-mechanics of a single photon. *Journal of Mathematical Physics*, 59(11), 2018. (page 2).

[28] G. Grynberg, A. Aspect, and C. Fabre. *Introduction to Quantum Optics*. Cambridge University Press, 2010. (pages 3, 3, 16, 32, 58).

[29] L. Mandel and E. Wolf. *Optical Coherence and Quantum Optics*. Cambridge University Press, 1995. (pages 3, 29, 32, 36, 58, 58, 82).

[30] U. Leonhardt. *Measuring the Quantum State of Light*. Cambridge University Press, 1997. (pages 3, 58).

[31] C. Gerry and P. Knight. *Introductory Quantum Optics*. Cambridge University Press, 2005. (pages 3, 32, 36, 58).

[32] W. Vogel and D.G. Welsch. *Quantum Optics*. Wiley-VCH, 2006. (pages 3, 32, 58).

[33] J. C. Garrison and R. Y. Chiao. *Quantum Optics*. Oxford University Press, 2008. (pages 3, 29, 32, 36, 51, 58, 76, 76, 129).

[34] U. Leonhardt. *Essential Quantum Optics*. Cambridge Univ. Press, 2010. Literaturverz. S. 262 - 273. (pages 3, 32, 58).

[35] H. A. Bachor. *A guide to experiments in quantum optics*. (New York: Wiley), 2019. (pages 3, 58).

[36] G. S. Buller and R. J. Collins. Single-photon generation and detection. *Measurement Science and Technology*, 21(1):012002, 2009. (page 3).

[37] P. B. R. Nisbet-Jones, J. Dilley, D. Ljunggren, and A. Kuhn. Highly efficient source for indistinguishable single photons of controlled shape. *New Journal of Physics*, 13(10):103036, 2011. (pages 3, 54, 56, 98).

[38] I. Białynicki-Birula. Exponential localization of photons. *Physical Review Letters*, 80(24):5247–5250, 1998. (pages 3, 36, 40, 42, 42, 67, 68, 70, 70, 70, 70, 70, 71, 80, 89, 90).

[39] I. Białynicki-Birula and Z. Białynicka-Birula. Why photons cannot be sharply localized. *Physical Review A*, 79(3):032112, 2009. (pages 3, 70, 70, 70, 70, 71, 72, 121).

[40] J. M. Knight. Strict localization in quantum field theory. *Journal of Mathematical Physics*, 2(4):459–471, 1961. (pages 3, 69, 71, 121, 121, 123).

[41] G. C. Hegerfeldt. Remark on causality and particle localization. *Physical Review D*, 10(10):3320–3321, 1974. (pages 3, 70).

[42] G. C. Hegerfeldt and S. N. M. Ruijsenaars. Remarks on causality, localization, and spreading of wave packets. *Physical Review D*, 22(2):377–384, 1980. (pages 3, 70).

[43] G. C. Hegerfeldt. Causality problems for Fermi's two-atom system. *Physical Review Letters*, 72(5):596–599, 1994. (page 3).

[44] G. C. Hegerfeldt. Causality, particle localization and positivity of the energy. In *Irreversibility and Causality Semigroups and Rigged Hilbert Spaces*, pages 238–245. Springer Berlin Heidelberg, 1998. (page 3).

[45] H. E. Moses. Photon wave functions and the exact electromagnetic matrix elements for hydrogenic atoms. *Physical Review A*, 8(4):1710–1721, 1973. (pages 4, 25, 80, 80, 81, 82, 82, 82, 82).

[46] H. E. Moses. Derivation of the dipole approximation from the exact transition probabilities for hydrogen atoms. *Physical Review A*, 11(6):2196–2197, 1975. (pages 4, 80, 80, 82).

[47] H. E. Moses. Exact electromagnetic matrix elements and selection rules for relativistic hydrogenic atoms. *Physical Review A*, 11(1):387–389, 1975. (pages 4, 80, 82).

[48] E. Grimm and V. Ernst. Bound photons in the lowest order weisskopf-wigner theory. *Zeitschrift für Physik A Atoms and Nuclei*, 274(4):293–303, 1975. (pages 4, 80, 82).

[49] J. Seke and W. N. Herfort. Deviations from exponential decay in the case of spontaneous emission from a two-level atom. *Physical Review A*, 38(2):833–840, 1988. (pages 4, 80, 80, 82).

[50] S. Guérin and H. R. Jauslin. Control of quantum dynamics by laser pulses: Adiabatic floquet theory, 2003. (pages 4, 20, 93, 94).

[51] M. Born and V. Fock. Beweis des adiabatensatzes. *Zeitschrift für Physik*, 51(3-4):165–180, 1928. (pages 4, 94).

[52] P. T. Leung, S. Y. Liu, and K. Young. Completeness and orthogonality of quasinormal modes in leaky optical cavities. *Physical Review A*, 49(4):3057–3067, 1994. (pages 4, 99, 99, 101, 101, 101, 101, 106).

[53] P. T. Leung, S. Y. Liu, and K. Young. Completeness and time-independent perturbation of the quasinormal modes of an absorptive and leaky cavity. *Physical Review A*, 49(5):3982–3989, 1994. (pages 4, 99, 101, 101, 106).

[54] P. T. Leung, S. Y. Liu, S. S. Tong, and K. Young. Time-independent perturbation theory for quasinormal modes in leaky optical cavities. *Physical Review A*, 49(4):3068–3073, 1994. (pages 4, 99).

[55] E. S. C. Ching, P. T. Leung, A. Maassen van den Brink, W. M. Suen, S. S. Tong, and K. Young. Quasinormal-mode expansion for waves in open systems. *Reviews of Modern Physics*, 70(4):1545–1554, oct 1998. (pages 4, 101, 101, 106).

[56] C. Sauvan, J. P. Hugonin, I. S. Maksymov, and P. Lalanne. Theory of the spontaneous optical emission of nanosize photonic and plasmon resonators. *Physical Review Letters*, 110(23):237401, 2013. (pages 4, 99).

[57] R. C. Ge, P. T. Kristensen, J. F. Young, and S. Hughes. Quasinormal mode approach to modelling light-emission and propagation in nanoplasmonics. *New Journal of Physics*, 16(11):113048, 2014. (page 4).

[58] P. T. Kristensen, R. C. Ge, and S. Hughes. Normalization of quasinormal modes in leaky optical cavities and plasmonic resonators. *Physical Review A*, 92(5):053810, 2015. (page 4).

[59] P. Lalanne, W. Yan, K. Vynck, C. Sauvan, and J. P. Hugonin. Light interaction with photonic and plasmonic resonances. *Laser &amp: Photonics Reviews*, 12(5), 2018. (page 4).

[60] S. Franke, S. Hughes, M. K. Dezfouli, P. T. Kristensen, K. Busch, A. Knorr, and M. Richter. Quantization of quasinormal modes for open cavities and plasmonic cavity quantum electrodynamics. *Physical Review Letters*, 122(21):213901, 2019. (pages 4, 99, 99, 106, 106, 106, 107, 107).

[61] P. T. Kristensen, K. Herrmann, F. Intravaia, and K. Busch. Modeling electromagnetic resonators using quasinormal modes. *Advances in Optics and Photonics*, 12(3):612, 2020. (page 4).

[62] C. Sauvan. Quasinormal modes expansions for nanoresonators made of absorbing dielectric materials: study of the role of static modes. *Optics Express*, 29(6):8268, 2021. (page 4).

[63] C. Sauvan, T. Wu, R. Zarouf, E. A. Muljarov, and P. Lalanne. Normalization, orthogonality, and completeness of quasinormal modes of open systems: the case of electromagnetism [invited]. *Optics Express*, 30(5):6846, 2022. (page 4).

[64] W. Appel. *Mathematics for Physics and Physicists*. Princeton University Press, 2007. (pages 9, 138, 142).

[65] A. Dereux. *Physique de l'État Solide*. Unpublished lecture notes at Université de Bourgogne, 2017. (page 10).

[66] C. Cohen-Tannoudji, B. Diu, and F. Laloe. *Quantum Mechanics*, volume 1. Wiley-Interscience, 2006. (page 14).

[67] C. Cohen-Tannoudji, J. Dupont-Roc, and G. Grynberg. *Photons and Atoms: Introduction to Quantum Electrodynamics*. VCH PUBN, 1997. (pages 16, 32, 36, 37).

[68] D. A. Steck. *Quantum and Atom Optics*. Available online at `http://steck.us/teaching`, 2023. revision 0.13.21. (page 17).

[69] H. R. Jauslin, S. Guérin, and S. Thomas. Quantum averaging for driven systems with resonances. *Physica A: Statistical Mechanics and its Applications*, 279(1-4):432–442, 2000. (page 20).

[70] E. M. Stein. *Singular Integrals and Differentiability Properties of Functions (Pms-30), Volume 30*. Princeton Univ Press, 1971. (page 23).

[71] N. S. Landkof. *Foundations of Modern Potential Theory*. Springer Berlin Heidelberg, 2011. (page 23).

[72] M. Kwaśnicki. Ten equivalent definitions of the fractional Laplace operator. *Fractional Calculus and Applied Analysis*, 20(1):7–51, 2017. (page 23).

[73] A. Lischke, G. Pang, M. Gulian, F. Song, C. Glusa, X. Zheng, Z. Mao, W. Cai, M. M. Meerschaert, M. Ainsworth, and G. Em Karniadakis. What is the fractional Laplacian ? A comparative review with new results. *Journal of Computational Physics*, 404:109009, 2020. (page 23).

[74] D. A. Varshalovich. *Quantum Theory of Angular Momentum*. World Scientific Pub., 1988. (pages 25, 134).

[75] L. Dai, M. Kamionkowski, and D. Jeong. Total angular momentum waves for scalar, vector, and tensor fields. *Physical Review D*, 86(12):125013, 2012. (page 25).

[76] F. A. Berezin. *The Method of Second Quantization*. Academic Press, 1966. (page 28).

[77] R. Honegger and A. Rieckers. *Photons in Fock Space and Beyond*, volume 1. World Scientific, 2014. (pages 28, 44, 44).

[78] W. Pauli. The connection between spin and statistics. *Physical Review*, 58(8):716–722, 1940. (page 28).

[79] R. Loudon. *The Quantum Theory of Light*. Oxford University Press, 2000. (pages 29, 32, 36, 60).

[80] C. Fabre and N. Treps. Modes and states in quantum optics. *Reviews of Modern Physics*, 92(3):035005, 2020. (page 29).

[81] H. Goldstein, C. P. Poole, and J. L. Safko. *Classical Mechanics (3rd Edition)*. Addison Wesley, 2002. (page 30).

[82] W. Greiner. *Field quantization*. Springer, 1996. (page 30).

[83] C. Cohen-Tannoudji, B. Diu, and F. Laloe. *Quantum Mechanics*, volume 2. Wiley-Interscience, 2006. (page 30).

[84] J. D. Jackson. *Classical Electrodynamics*. John Wiley & Sons Inc, 3rd edition, 1999. (page 37).

[85] L. Silberstein. Elektromagnetische grundgleichungen in bivektorieller behandlung. *Annalen der Physik*, 327(3):579–586, 1907. (page 37).

[86] I. Białynicki-Birula and Z. Białynicka-Birula. Uncertainty relation for photons. *Physical Review Letters*, 108(14):140401, 2012. (page 42).

[87] I. Białynicki-Birula and Z. Białynicka-Birula. Heisenberg uncertainty relations for photons. *Physical Review A*, 86(2):022118, 2012. (page 42).

[88] I. Białynicki-Birula and Z. Białynicka-Birula. Quantum-mechanical description of optical beams. *Journal of Optics*, 19(12):125201, 2017. (page 42).

[89] I. Białynicki-Birula and Z. Białynicka-Birula. Beams of electromagnetic radiation carrying angular momentum: The Riemann-Silberstein vector and the classical-quantum correspondence. *Optics Communications*, 264(2):342–351, 2006. (page 42).

[90] S. De Bièvre. Local states of free bose fields. In *Large Coulomb Systems*, pages 15–61. Springer Berlin Heidelberg, 2006. (pages 44, 69).

[91] J. Brendel, N. Gisin, W. Tittel, and H. Zbinden. Pulsed energy-time entangled twin-photon source for quantum communication. *Physical Review Letters*, 82(12):2594–2597, 1999. (page 55).

[92] T. Ward and M. Keller. Generation of time-bin-encoded photons in an ion-cavity system. *New Journal of Physics*, 24(12):123028, 2022. (pages 56, 78).

[93] H. Jayakumar, A. Predojević, T. Kauten, T. Huber, G. S. Solomon, and G. Weihs. Time-bin entangled photons from a quantum dot. *Nature Communications*, 5(1), 2014. (page 56).

[94] L. Yu, C. M. Natarajan, T. Horikiri, C. Langrock, J. S. Pelc, M. G. Tanner, E. Abe, S. Maier, C. Schneider, S. Höfling, M. Kamp, R. H. Hadfield, M. M. Fejer, and Y. Yamamoto. Two-photon interference at telecom wavelengths for time-bin-encoded single photons from quantum-dot spin qubits. *Nature Communications*, 6(1), 2015. (page 56).

[95] A. Kuhn, M. Hennrich, and G. Rempe. Deterministic single-photon source for distributed quantum networking. *Physical Review Letters*, 89(6):067901, 2002. (pages 56, 98).

[96] M. Keller, B. Lange, K. Hayasaka, W. Lange, and H. Walther. Continuous generation of single photons with controlled waveform in an ion-trap cavity system. *Nature*, 431(7012):1075–1078, 2004. (pages 56, 98).

[97] J. McKeever, A. Boca, A. D. Boozer, R. Miller, J. R. Buck, A. Kuzmich, and H. J. Kimble. Deterministic generation of single photons from one atom trapped in a cavity. *Science*, 303(5666):1992–1994, 2004. (pages 56, 98).

[98] P. Farrera, G. Heinze, B. Albrecht, M. Ho, M. Chávez, C. Teo, N. Sangouard, and H. De Riedmatten. Generation of single photons with highly tunable wave shape from a cold atomic ensemble. *Nature Communications*, 7(1), 2016. (pages 56, 98).

[99] E. N. Knall, C. M. Knaut, R. Bekenstein, D. R. Assumpcao, P. L. Stroganov, W. Gong, Y. Q. Huan, P.-J. Stas, B. Machielse, M. Chalupnik, D. Levonian, A. Suleymanzade, R. Riedinger, H. Park, M. Lončar, M. K. Bhaskar, and M. D. Lukin.

Efficient source of shaped single photons based on an integrated diamond nanophotonic system. *Physical Review Letters*, 129(5):053603, 2022. (page 56).

[100] J. Brendel, E. Mohler, and W. Martienssen. Time-resolved dual-beam two-photon interferences with high visibility. *Physical Review Letters*, 66(9):1142–1145, mar 1991. (pages 56, 78).

[101] Y. H. Shih, A. V. Sergienko, and M. H. Rubin. Einstein-Podolsky-Rosen state for space-time variables in a two-photon interference experiment. *Physical Review A*, 47(2):1288–1293, 1993. (pages 56, 78).

[102] I. Marcikic, H. de Riedmatten, W. Tittel, V. Scarani, H. Zbinden, and N. Gisin. Time-bin entangled qubits for quantum communication created by femtosecond pulses. *Physical Review A*, 66(6):062308, 2002. (pages 56, 78).

[103] C. K. Hong, Z. Y. Ou, and L. Mandel. Measurement of subpicosecond time intervals between two photons by interference. *Physical Review Letters*, 59(18):2044–2046, 1987. (page 60).

[104] F. Bouchard, A. Sit, Y. Zhang, R. Fickler, F. M. Miatto, Y Yao, F. Sciarrino, and E. Karimi. Two-photon interference: the Hong-Ou-Mandel effect. *Reports on Progress in Physics*, 84:012402, 2021. (page 60).

[105] S. Haroche and J. M. Raimond. *Exploring the quantum : atoms, cavities, and photons*. Oxford University Press, 2013. (page 60).

[106] A. Serafini. *Quantum Continuous Variables A Primer of Theoretical Methods*. Taylor & Francis Group, 2023. (page 60).

[107] M. D. Eisaman, J. Fan, A. Migdall, and S. V. Polyakov. Invited review article: Single-photon sources and detectors. *Review of Scientific Instruments*, 82(7):071101, 2011. (page 65, 65).

[108] S. De Bièvre. Where's that quantum ? In *Contributions in Mathematical Physics*, pages 123–146. Hindustan Book Agency, 2007. (page 69).

[109] I. E. Segal and R. W. Goodman. Anti-locality of certain Lorentz-invariant operators. *Journal of Mathematics and Mechanics*, 14(4):629–638, 1965. (pages 69, 71, 125).

[110] K. Masuda. Anti-locality of the one-half power of elliptic differential operators. *Publications of the Research Institute for Mathematical Sciences*, 8(1):207–210, 1972. (pages 69, 71, 71, 125, 125, 126).

[111] M. Murata. Anti-locality of certain functions of the Laplace operator. *Journal of the Mathematical Society of Japan*, 25(4), 1973. (pages 69, 71, 125).

[112] A. L. Licht. Strict localization. *Journal of Mathematical Physics*, 4(11):1443–1447, 1963. (page 70).

[113] A. L. Licht. Local states. *Journal of Mathematical Physics*, 7(9):1656–1669, 1966. (page 70).

[114] R. C. Paley and N. Wiener. *Fourier Transforms in the Complex Domain*. American Mathematical Society, New York, 1934. (page 70).

[115] P. Saari, M. Menert, and H. Valtna. Photon localization barrier can be overcome. *Optics Communications*, 246(4-6):445–450, 2005. (page 70).

[116] P. Saari. Photon localization revisited. In *Quantum Optics and Laser Experiments*. InTech, 2012. (page 70).

[117] J. Gulla and J. Skaar. Approaching single-photon pulses. *Physical Review Letters*, 126(7):073601, 2021. (page 70).

[118] K. Ryen, J. Gulla, and J. Skaar. Strictly localized three-dimensional states close to single photons. *International Journal of Theoretical Physics*, 61(5), 2022. (page 70).

[119] J. Gulla, K. Ryen, and J. Skaar. Limits for realizing single photons. *arXiv:2109.06472v2*, 2023. (page 70).

[120] E. Karpov, G. Ordonez, T. Petrosky, I. Prigogine, and G. Pronko. Causality, delocalization, and positivity of energy. *Physical Review A*, 62(1):012103, 2000. (page 70).

[121] G. C. Hegerfeldt. Problems about causality in fermi's two-atom model and possible resolutions. 1997. (page 70).

[122] A. Mostafazadeh and F. Zamani. Quantum mechanics of Klein-Gordon fields i: Hilbert space, localized states, and chiral symmetry. *Annals of Physics*, 321(9):2183–2209, 2006. (page 70).

[123] H. Babaei and A. Mostafazadeh. Quantum mechanics of a photon. *Journal of Mathematical Physics*, 58(8):082302, 2017. (page 70).

[124] D. Hodgson, J. Southall, R. Purdy, and A. Beige. Local photons. *Frontiers in Photonics*, 3, 2022. (page 70).

[125] M. Hawton. Validation of classical modeling of single-photon pulse propagation. *Physical Review A*, 107(1):013711, 2023. (page 70).

[126] M. Brune, S. Haroche, J. M. Raimond, L. Davidovich, and N. Zagury. Manipulation of photons in a cavity by dispersive atom-field coupling: Quantum-nondemolition measurements and generation of "Schrödinger cat" states. *Physical Review A*, 45(7):5193–5214, 1992. (page 75).

[127] S. L. Braunstein and P. Van Loock. Quantum information with continuous variables. *Reviews of Modern Physics*, 77(2):513–577, 2005. (page 75).

[128] T. C. Ralph. Continuous variable quantum cryptography. *Physical Review A*, 61(1):010303, 1999. (page 75).

[129] E. Diamanti and A. Leverrier. Distributing secret keys with quantum continuous variables: Principle, security and implementations. *Entropy*, 17(12):6072–6092, 2015. (page 75).

[130] S. Pirandola, U. L. Andersen, L. Banchi, M. Berta, D. Bunandar, R. Colbeck, D. Englund, T. Gehring, C. Lupo, C. Ottaviani, J. L. Pereira, M. Razavi, J. Shamsul Shaari, M. Tomamichel, V. C. Usenko, G. Vallone, P. Villoresi, and P. Wallden. Advances in quantum cryptography. *Advances in Optics and Photonics*, 12(4):1012, 2020. (page 75).

[131] A. J. Miller, S. Woo Nam, J. M. Martinis, and A. V. Sergienko. Demonstration of a low-noise near-infrared photon counter with multiphoton discrimination. *Applied Physics Letters*, 83(4):791–793, 2003. (pages 78, 81).

[132] L. A. Morais, T. Weinhold, M. P. de Almeida, J. Combes, A. Lita, T. Gerrits, S. W. Nam, A. G. White, and G. Gillett. Precisely determining photon-number in real-time. 2020. (pages 78, 81).

[133] A. N. Vetlugin, F. Martinelli, S. Dong, and C. Soci. Photon number resolution without optical mode multiplication. *Nanophotonics*, 12(3):505–519, 2023. (pages 78, 81).

[134] C. Fabre. *Quantum Processes and Measurement*. Cambridge University Press, 2023. (pages 78, 81).

[135] V. Weisskopf and E. Wigner. Berechnung der natürlichen linienbreite auf grund der diracschen lichttheorie. *Zeitschrift für Physik*, 63(1-2):54–73, 1930. (page 80).

[136] H. Spohn. *Dynamics of Charged Particles and Their Radiation Field*. Cambridge University Press, 2009. (pages 80, 84, 85, 137).

[137] L. Novotny and B. Hecht. *Principles of Nano-Optics*. Cambridge University Press, 2012. (page 80, 80).

[138] J. Dereziński and R. Früboes. Renormalization of the Friedrichs Hamiltonian. *Reports on Mathematical Physics*, 50(3):433–438, December 2002. (page 80).

[139] E. Grimm and V. Ernst. On the existence of Weisskopf-Wigner type theories. *Journal of Physics A: Mathematical, Nuclear and General*, 7(13):1664–1675, September 1974. (page 80).

[140] V. Ernst. A composition law for solutions of Weisskopf-Wigner theories. *Journal of Physics A: Mathematical and General*, 8(1):76–94, 1975. (pages 80, 82, 82).

[141] G. Compagno, R. Passante, and F. Persico. Virtual photons, causality and atomic dynamics in spontaneous emission. *Journal of Modern Optics*, 37(8):1377–1382, 1990. (pages 81, 89).

[142] G. Compagno, R. Passante, and F. Persico. *Atom-Field Interactions and Dressed Atoms*. Cambridge University Press, 1995. (pages 81, 89).

[143] K. O. Friedrichs. On the perturbation of continuous spectra. *Communications on Pure and Applied Mathematics*, 1(4):361–406, 1948. (page 84).

[144] T. D. Lee. Some special examples in renormalizable field theory. *Physical Review*, 95(5):1329–1334, 1954. (page 84).

[145] V. Debierre, I. Goessens, E. Brainis, and T. Durt. Fermi's golden rule beyond the Zeno regime. *Physical Review A*, 92(2):023825, 2015. (page 89).

[146] V. Debierre and T. Durt. Apparent deviations from causality in spontaneous light emission by atomic hydrogen in the mid- and far-field regions. *Physical Review A*, 93(2):023847, 2016. (pages 89, 109).

[147] V. Debierre, T. Durt, A. Nicolet, and F. Zolla. Spontaneous light emission by atomic hydrogen: Fermi's golden rule without cheating. *Physics Letters A*, 379(40-41):2577–2585, 2015. (page 89).

[148] V. Debierre, B. Stout, and T. Durt. Non-classical properties of the e.m. near field of an atom in spontaneous light emission. 2018. (page 89).

[149] M. L. Lei and V. Debierre. Short-time emission of higher-angular-momentum photons by atomic transitions. *Journal of Physics B: Atomic, Molecular and Optical Physics*, 54(2):025002, 2021. (page 89).

[150] M. I. Shirokov. Signal velocity in quantum electrodynamics. *Soviet Physics Uspekhi*, 21(4):345–358, 1978. (page 89).

[151] M. Amniat-Talab, S. Lagrange, S. Guérin, and H. R. Jauslin. Generation of multiphoton fock states by bichromatic adiabatic passage: Topological analysis. *Physical Review A*, 70(1):013807, 2004. (pages 93, 95, 97, 98).

[152] I. Białynicki-Birula and Z. Białynicka-Birula. Quantum electrodynamics of intense photon beams. new approximation method. *Physical Review A*, 14(3):1101–1108, 1976. (page 95).

[153] S. Guérin, F. Monti, J. M. Dupont, and H. R. Jauslin. On the relation between cavity-dressed states, Floquet states, RWA and semiclassical models. *Journal of Physics A: Mathematical and General*, 30(20):7193–7215, 1997. (page 95).

[154] A. Messiah. *Quantum Mechanics*. Dover Publications, Incorporated, 2014. (page 98).

[155] A. Joye and C. E. Pfister. Superadiabatic evolution and adiabatic transition probability between two nondegenerate levels isolated in the spectrum. *Journal of Mathematical Physics*, 34(2):454–479, 1993. (page 98).

[156] R Miller, T E Northup, K M Birnbaum, A Boca, A D Boozer, and H J Kimble. Trapped atoms in cavity QED: coupling quantized light and matter. *Journal of Physics B: Atomic, Molecular and Optical Physics*, 38(9):S551–S565, 2005. (page 98).

[157] A. Kuhn. Cavity induced interfacing of atoms and light. In *Engineering the Atom-Photon Interaction*, pages 3–38. Springer International Publishing, 2015. (page 98).

[158] P. Törmä and W. L. Barnes. Strong coupling between surface plasmon polaritons and emitters: a review. *Reports on Progress in Physics*, 78(1):013901, 2014. (page 98).

[159] D. G. Baranov, B. Munkhbat, E. Zhukova, A. Bisht, A. Canales, B. Rousseaux, G. Johansson, T. J. Antosiewicz, and T. Shegai. Ultrastrong coupling between nanoparticle plasmons and cavity photons at ambient conditions. *Nature Communications*, 11(1), 2020. (page 98).

[160] D. Dzsotjan, B. Rousseaux, H. R. Jauslin, G. Colas des Francs, C. Couteau, and S. Guérin. Mode-selective quantization and multimodal effective models for spherically layered systems. *Physical Review A*, 94(2):023818, 2016. (page 98).

[161] J. Feist, A. I. Fernández-Domínguez, and F. J. García-Vidal. Macroscopic QED for quantum nanophotonics: emitter-centered modes as a minimal basis for multiemitter problems. *Nanophotonics*, 10(1):477–489, 2020. (page 98).

[162] A. Saharyan, B. Rousseaux, Z. Kis, S. Stryzhenko, and S. Guérin. Propagating single photons from an open cavity: Description from universal quantization. *Physical Review Research*, 5(3):033056, 2023. (page 98).

[163] M. Zworski. Resonances in physics and geometry. *Notices of the American Mathematical Society*, 46(3):319, 1999. (page 99).

[164] S. Dyatlov and M. Zworski. *Mathematical Theory of Scattering Resonances*. American Mathematical Society, 2019. (page 99).

[165] H. P. Nollert. Quasinormal modes: the characteristic "sound" of black holes and neutron stars. *Classical and Quantum Gravity*, 16(12):R159–R216, 1999. (page 99).

[166] O. Civitarese and M. Gadella. Physical and mathematical aspects of gamow states. *Physics Reports*, 396(2):41–113, 2004. (page 99).

[167] G. García-Calderón. Theory of resonant states: An exact analytical approach for open quantum systems. In *Unstable States in the Continuous Spectra, Part I: Analysis, Concepts, Methods, and Results*, pages 407–455. Elsevier, 2010. (page 99).

[168] S Both and T Weiss. Resonant states and their role in nanophotonics. *Semiconductor Science and Technology*, 37(1):013002, 2021. (page 99).

[169] P. T. Leung, W. M. Suen, C. P. Sun, and K. Young. Waves in open systems via a biorthogonal basis. *Physical Review E*, 57(5):6101–6104, 1998. (page 99).

[170] A. Settimi, S. Severini, N. Mattiucci, C. Sibilia, M. Centini, G. D'Aguanno, M. Bertolotti, M. Scalora, M. Bloemer, and C. M. Bowden. Quasinormal-mode description of waves in one-dimensional photonic crystals. *Physical Review E*, 68(2):026614, 2003. (page 99).

[171] S. Severini, A. Settimi, C. Sibilia, M. Bertolotti, A. Napoli, and A. Messina. Quantum counter-propagation in open optical cavities via the quasi-normal-mode approach. *Laser Physics*, 16(6):911–920, 2006. (page 99).

[172] M. Kamandar D. and S. Hughes. Regularized quasinormal modes for plasmonic resonators and open cavities. *Physical Review B*, 97(11):115302, 2018. (page 99).

[173] A. Saharyan, J. R. Álvarez, T. H. Doherty, A. Kuhn, and S. Guérin. Light-matter interaction in open cavities with dielectric stacks. *Applied Physics Letters*, 118(15), 2021. (page 99).

[174] M. A. Shubov. Basis property of eigenfunctions of nonselfadjoint operator pencils generated by the equation of nonhomogeneous damped string. *Integral Equations and Operator Theory*, 25(3):289–328, 1996. (pages 101, 106).

[175] M. A. Shubov. Nonselfadjoint operators generated by the equation of a nonhomogeneous damped string. *Transactions of the American Mathematical Society*, 349(11):4481–4499, 1997. (pages 101, 106).

[176] M. A. Shubov. The riesz basis property of the system of root vectors for the equation of a nonhomogeneous damped string: Transformation operators method. *Methods and Applications of Analysis*, 6(4):571–592, 1999. (pages 101, 106).

[177] A. Castellini, H. R. Jauslin, B. Rousseaux, D. Dzsotjan, G. Colas des Francs, A. Messina, and S. Guérin. Quantum plasmonics with multi-emitters: application to stimulated raman adiabatic passage. *The European Physical Journal D*, 72(12), 2018. (page 106).

[178] J. Ren, S. Franke, A. Knorr, M. Richter, and S. Hughes. Near-field to far-field transformations of optical quasinormal modes and efficient calculation of quantized quasinormal modes for open cavities and plasmonic resonators. *Physical Review B*, 101(20):205402, 2020. (page 106, 106).

[179] S. Franke, M. Richter, J. Ren, A. Knorr, and S. Hughes. Quantized quasinormal-mode description of nonlinear cavity-QED effects from coupled resonators with a fano-like resonance. *Physical Review Research*, 2(3):033456, 2020. (pages 106, 106, 107, 107).

[180] M. I. Abdelrahman and B. Gralak. Completeness and divergence-free behavior of the quasi-normal modes using causality principle. *OSA Continuum*, 1(2):340, 2018. (page 106, 106).

[181] K. C. Ho, P. T. Leung, Alec Maassen van den Brink, and K. Young. Second quantization of open systems using quasinormal modes. *Physical Review E*, 58(3):2965–2978, 1998. (page 107, 107).

[182] S. Severini, A. Settimi, C. Sibilia, M. Bertolotti, A. Napoli, and A. Messina. Second quantization and atomic spontaneous emission inside one-dimensional photonic crystals via a quasinormal-modes approach. *Physical Review E*, 70(5):056614, 2004. (page 107, 107).

[183] V. Dorier, J. Lampart, S. Guérin, and H. R. Jauslin. Canonical quantization for quantum plasmonics with finite nanostructures. *Physical Review A*, 100(4):042111, 2019. (page 107).

[184] V. Dorier, S. Guérin, and H. R. Jauslin. Critical review of quantum plasmonic models for finite-size media. *Nanophotonics*, 9(12):3899–3907, 2020. (page 107).

[185] E. Talvila. Necessary and sufficient conditions for differentiating under the integral sign. *The American Mathematical Monthly*, 108(6):544–548, 2001. (page 126).

[186] H. Cartan. *Elementary theory of analytic functions of one or several complex variables*. Addison-Wesley Educational Publishers Inc, 1963. (page 126).

[187] K. Masuda. A unique continuation theorem for solutions of the Schrödinger equations. *Proceedings of the Japan Academy, Series A, Mathematical Sciences*, 43(5), 1967. (page 127).